Canonical and noncanonical action of thyroid hormone receptor α in the cardiovascular system

Inaugural-Dissertation

zur

Erlangung des Doktorgrades

doctor rerum naturalium

(Dr. rer. nat.)

der Fakultät für

Biologie

an der

Universität Duisburg-Essen

vorgelegt von

Daniela Geist

aus Schlitz

Juni 2020

Die der vorliegenden Arbeit zugrundeliegenden Experimente wurden am Universitätsklinikum Essen in der Klinik für Endokrinologie, Diabetes und Stoffwechsel, sowie im Institut für Pathophysiologie, durchgeführt.

1. Gutachter: Prof. Dr. Lars Möller
2. Gutachter: Prof. Dr. Joachim Fandrey
3. Gutachter: Prof. Dr. Lutz Schomburg

Vorsitzender des Prüfungsausschusses: Prof. Dr. Dirk Hermann

Tag der mündlichen Prüfung: 10. Dezember 2020

DOI: 10.17185/duepublico/73911
URN: urn:nbn:de:hbz:464-20220127-104706-2

Zusammenfassung

Schilddrüsenhormone sind essentiell für die Entwicklung und Regulation des Herz-Kreislaufsystems und spielen eine wichtige Rolle in der Kontrolle des arteriellen Blutdrucks, der Herzfrequenz und Körpertemperatur sowie in der Entstehung von Herzhypertrophie. Sie wirken über Schilddrüsenhormon Rezeptoren (TR) α und β, wobei TRα der vorherrschende Rezeptor im Herz-Kreislauf-System ist. TRs sind Kernrezeptoren, welche in der Lage sind, die Expression von Zielgenen zu steuern (kanonischer Signalweg) und zytoplasmatische Signalwege zu aktivieren und dadurch schnelle Effekte zu vermitteln (nichtkanonischer Signalweg). Durch den Vergleich von Wildtyp (WT) und TRα-Knockout ($TR\alpha^0$) Mäusen und einem Maus Modell, in welchem nur der nichtkanonische Signalweg vorhanden ist ($TR\alpha^{GS}$), konnten relevante Schilddrüsenhormoneffekte im Herz-Kreislauf-System dem kanonischen oder nichtkanonischen Signalweg zugeschrieben werden.

Um aufzuklären, wie Schilddrüsenhormone den Blutdruck beeinflussen können, wurden *ex vivo* Mausarterien untersucht, wobei sich zeigte, dass die von Triiodthyronin (T_3) verursachte Vasodilatation eine rapide Folge der nichtkanonischen TRα Signalübertragung ist. Diese Beobachtung wurde zudem mittels *in vivo* Blutdruckmessungen, bei denen die Injektion von T_3 innerhalb von Sekunden zur rapiden Blutdrucksenkung geführt hat, bestätigt. Als zugrundeliegende Prozesse konnten die Aktivierung der endothelialen Stickoxidsynthase (eNOS) und Phosphoinositid-3-Kinase (PI3K) im Endothel identifiziert werden. Weitere Charakterisierungen zeigten, dass T_3-induzierte Vasodilation in verschiedenen Gefäßentitäten auftritt und unverändert in hypo- aber nicht hyperthyreoten Tieren erhalten bleibt.

Schilddrüsenüberfunktionen können in Mensch und Maus zur Herzhypertrophie führen, wobei die Verdickung des Herzmuskels auf lange Sicht die Herzfunktion verschlechtert. Um herauszufinden, welcher Rezeptor, TRα oder TRβ, und welche Art der Signalübertragung die Herzhypertrophie vermittelt, wurden eu- und hyperthyreote TR^{WT}, $TR\alpha^0$-, $TR\beta^-$ und $TR\alpha^{GS}$ Mäuse mittels Echokardiografie untersucht. Mithilfe dieser Messungen konnte die Herzwanddicke bestimmt werden, welche in allen Mausstämmen mit Ausnahme von $TR\alpha^0$ Tieren unter T_3-Behandlung zunahm. Diese Beobachtung wurde anhand finaler Herzgewichte bestätigt und zeigte, dass die kardiale Hypertrophie eine Folge der nichtkanonischen TRα Signalübertragung ist. Durch die Analyse der Kardiomyozytengröße wurde gezeigt, dass die

Zunahme des Herzgewichts eine Folge von Kardiomyozytenwachstum ist. Jedoch konnten bei der Analyse möglicher Signalwege noch keine Erklärung für die wichtigsten Mediatoren in diesem Prozess gefunden werden.

Abnormale Herzfrequenzen sind ein häufig beobachtetes Symptom in Patienten, die unter Schilddrüsenfehlfunktionen leiden. Die Einflüsse dieser Fehlfunktionen und die Beteiligung von TRs in der Regulation der Herzfrequenz wurden in dieser Studie mithilfe von *in vivo* Messungen aufgeklärt. Da bei einer Vielzahl von Messmethoden Anästhesie oder stressinduzierende Handhabung von Versuchstieren die resultierenden Daten verfälschen können, wurde zum Ausschluss dieser Faktoren ein Radiotelemetrieansatz gewählt. Durch den Vergleich von eu-, hypo- und hyperthyreoten $TR\alpha^{WT}$, $TR\alpha^{0}$- und $TR\alpha^{GS}$ Mäusen konnte festgestellt werden, dass in Schilddrüsenfunktionsstörungen sowohl die circadiane als auch langfristige Regulation der Herzfrequenz über den kanonischen TRα Signalweg reguliert werden. Zudem konnten in dieser Messung die Kernkörpertemperatur und Bewegungsaktivität aufgezeichnet werden. Hier hat sich herausgestellt, dass die circadiane Regulation der Temperatur über den kanonischen TRα Signalweg reguliert ist. Allerdings blieb die langfristige Adaption der Körpertemperatur in Schilddrüsenfunktionsstörungen in $TR\alpha^{0}$- und $TR\alpha^{GS}$-Mäusen erhalten, was nahelegt, dass diese Anpassung über andere TR Isoformen oder Mechanism reguliert ist. Der Vergleich der Bewegungsaktivität von eu-, hypo- und hyperthyreoten Mäusen hat gezeigt, dass $TR\alpha^{0}$- und $TR\alpha^{GS}$-Mäusen geringfügige Änderungen im Vergleich zu Wildtyp Mäusen aufwiesen. Diese Beobachtung liefert Hinweise für einen kanonischen TRα Effekt.

Zusammenfassend liefert diese Studie Hinweise darauf, dass sowohl der kanonische als auch der nichtkanonische Signalweg eine physiologische Relevanz für das Herz-Kreislauf-System haben. Durch den Vergleich von Wildtyp, $TR\alpha^{0}$ und $TR\alpha^{GS}$-Mäuse konnten kanonische und nichtkanonische Effekte *in vivo* identifiziert werden. Diese Ergebnisse tragen zu einem neuen Verständnis der TH/TR Wirkung im Herz-Kreislaufsystem bei, legen ein therapeutisches Potential für TR- und Signalweg-spezifische Anwendungen nahe und liefern eine Grundlage für weiterführende Untersuchungen.

Abstract

Thyroid hormones (TH) are crucial for the regulation of cardiovascular functions, such as arterial blood pressure and heart rate, and play a major role in the development of cardiac hypertrophy and regulation of body temperature. They act via TH receptors (TRs) α and β, with TRα being the predominant receptor in the cardiovascular system. TRs are nuclear receptors, which are able to regulate TH target gene expression (canonical signalling) and mediate rapid TH effects by activating cytoplasmic pathways (noncanonical signalling). By comparing wildtype (WT), TR knockout ($TR\alpha^0$) mice, and mutant mice in which only noncanonical signalling is present ($TR\alpha^{GS}$) we were able to categorise TH effects in the cardiovascular system.

To identify the underlying mechanisms in blood pressure regulation, mouse arteries were examined *ex vivo*, which revealed that triiodothyronine (T_3)-dependent rapid vasodilation was a consequence of noncanonical TRα signalling. This observation was further confirmed by *in vivo* blood pressure measurements, where T_3 injections caused strong decrease of arterial pressure within seconds. The activations of endothelial nitric oxide synthase (eNOS) and phosphoinositide 3-kinase (PI3K) in the endothelium were identified as the underlying processes. Further characterisations revealed that T_3-induced vasodilation occurs in different artery entities and remains unaltered in arteries from hypo- but not hyperthyroid animals.

Hyperthyroidism can lead to cardiac hypertrophy in humans and mice which can worsen cardiac function if left untreated. Therefore, our aim was to determine which receptor, TRα or TRβ, and which mode of signalling, mediates cardiac hypertrophy. Consequently, we examined eu- and hyperthyroid TR^{WT}, $TR\alpha^0$-, $TR\beta^-$ und $TR\alpha^{GS}$ mice *via* echocardiography. These measurements were used to determine heart wall thickness, which increased in all mouse strains with the exception of $TR\alpha^0$ mice under T_3 treatment. This observation was further confirmed when final heart weights were compared *ex vivo*, which indicates that cardiac hypertrophy is a consequence of noncanonical TRα signalling. However, the analysis of possible pathways did not yet yield an explanation for key mediators in this process and requires further examination. Analysis of cardiomyocyte size showed that the observed cardiac growth is a result of cardiomyocyte growth.

Abnormal heart rates are a commonly observed symptom in patients suffering from thyroid dysfunction. In order to clarify the effects of these malfunctions and the involvement of TRs in heart rate regulation, *in vivo* measurements were carried out in this study. Since anaesthesia and

stress-inducing handling of animals can influence resulting measurements in many methods, we chose a radio telemetry approach to exclude those factors from our study. The comparison of eu-, hypo- and hyperthyroid $TR\alpha^{WT}$, $TR\alpha^{0}$- und $TR\alpha^{GS}$ mice showed that circadian and long-term adaptation of heart rates during thyroid dysfunctions is regulated by canonical TRα signalling. In addition, core body temperature and locomotor activity were measured using radio telemetry. Here, we observed that circadian rhythm of body temperature is controlled by canonical TRα signalling. However, long-term adaptation in $TR\alpha^{0}$- and $TR\alpha^{GS}$ did not differ from controls suggesting that other TR isoforms and mechanisms might be involved. The comparison of locomotor activity in eu-, hypo- and hyperthyroid mice demonstrated minor differences between wildype and $TR\alpha^{0}$ and $TR\alpha^{GS}$ mice, respectively. This observation suggests that canonical TRα action has an impact on locomotor activity control.

In conclusion, this study provides evidence that both, canonical and noncanonical TR signalling, are physiologically relevant in the cardiovascular system. By comparing wildtype, $TR\alpha^{0}$ and $TR\alpha^{GS}$ mice we were able to identify canonical and noncanonical TR effects *in vivo*. These results contribute to a new understanding of TH/TR action in the cardiovascular system, put forward a therapeutic potential for TR- and pathway-specific applications and provide a basis for further investigations.

Abbreviations and Acronyms

µL	Microliter
µm	Micrometer
µM	Micromolar
AKT (PKB)	Protein kinase B
ANOVA	Analysis of variance
ATP	Adenosine triphosphate
AV node	Atrioventricular node
BAT	Brown adipose tissue
bpm	Beats per minute
BSA	Bovine serum albumin
BW	Body weight
CA	Carbachol
$CaCl_2$	Calcium chloride
cGMP	Cyclic guanosine monophosphate
CNS	Central nervous system
CO	Cardiac output
CO_2	Carbon dioxide
CoA	Coactivator
CoR	Corepressor
CRC	Concentration response curve
DBD	DNA-binding domain
DIO	Deiodinase
DIT	Diiodotyrosine
DMSO	Dimethyl sulfoxide
DNA	Deoxyribonucleic acid
ECG	Electrocardiogram/Electrocardiography
EDTA	Ethylenediaminetetraacetic acid
ELISA	Enzyme-linked Immunosorbent Assay
eNOS	Endothelial nitric oxide synthase

EtOH	Ethanol
ERK	Extracellular-signal regulated kinase
fT_3	Free thyronine
fT_4	Free thyroxine
GAPDH	Glycerin aldehyde phosphate dehydrogenase
GC-1	Sobetirome
GMC	German Mouse Clinic
GS	Glycine and serine
HPT-axis	Hypothalamic-pituitary-thyroid axis
IGF-1	Insulin-like growth factor 1
IVC	Individually ventilated cages
IVS	Interventricular septum
KCl	Potassium chloride
KHB	Krebs Henseleit Buffer
KO	Knockout
L	Liter
LA/LV	Left atrium/ventricle
LBD	Ligand-binding domain
LID	Low-iodine diet
L-NAME	N(G)-Nitro-L-arginine methyl ester
LVID	Left ventricular inner diameter
LVM	Left ventricular mass
LVPW	Left ventricular posterior wall
MAPK	Mitogen-activated protein kinase
MCT8/10	Monocarboxylate transporter 8/10
MIT	Monoiodotyrosine
mL	Milliliter
mM	Millimolar
mN	Millinewton
MMI	Methimazole
mRNA	Messenger RNA
MOPS	3-(N-morpholino)propanesulfonic acid

mTOR	Mammalian target of rapamycine
NaOH	Sodium hydroxide
$NaVO_4$	Sodium orthovanadate
NCoR	Nuclear corepressor
NcoA-1	Nuclear receptor coactivator 1
LAT1/LAT2	Large neutral amino acid transporters 1/2
NES	Nuclear export sequence
NIS	Sodium iodine symporter
NLS	Nuclear localisation sequence
NO	Nitric oxide
NE	Norepinephrine bitartrate
O_2	Oxygen
OATP1C1	Organic anion transporter polypeptides 1C1
PBS	Phosphate buffered saline
PCR	Polymerase chain reaction
PI3K	Phosphatidylinositol 3 kinase
PI2P	Phosphatidylinositol 2 phosphate
PI3P	Phosphatidylinositol 3 phosphate
PKA/PKC/PKG	Protein kinase A/C/G
qRT-PCR	Quantitative reverse transcriptase PCR
RA/RV	Right atrium/ventricle
RNA	Ribonucleic acid
rpm	Revolutions per min
rT_3	Reverse thyronine
RTH	Resistance to thyroid hormone
RXR	Retinoid X receptor
SA node	Sinoatrial node
SD	Standard deviation
SDS	Sodium dodecyl sulfate
SEM	Standard error of the mean
SERCA	Sarcoplasmic/endoplasmic reticulum calcium ATPase
SNP	Sodium nitroprusside

SRC1	Steroid coactivator family
SVR	Systemic vascular resistance
T_3	Triiodothyronine
T_4	Thyroxine
TAE	TRIS-Acetate-EDTA Buffer
TBG	Thyroxine-binding globulin
TBS-T	Tris-buffered saline
Tg	Thyroglobulin
TH	Thyroid hormone
TPO	Thyroid peroxidase
TR	Thyroid hormone receptor
TRE	Thyroid hormone response element
TRH	Thyrotropin releasing hormone
TRα/β	Thyroid hormone receptor α/β
TSH	Thyroid stimulating hormone (thyrotropin)
TT_3	Total thyronine
TT_4	Total thyroxine
TTR	Transthyretin
UPC1	Uncoupling protein 1
VSMC	Vascular smooth muscle cells
WT	Wildtype

Nomenclature of mouse models	
$TR\alpha^{GS}$	TRα GS mutant (*knock-in*)
$TR\beta^{GS}$	TRβ GS mutant (*knock-in*)
TR^{GS}	TRα *and* TRβ GS mutant (*knock-in*)
$TR\alpha^{0}$	TRα KO (*knockout*)
$TR\beta^{-}$	TRβ KO (*knockout*)
TR^{KO}	TRα *and* TRβ KO (*knockout*)

Introduction

Thyroid hormones

Thyroid hormone synthesis and secretion

The thyroid hormones (TH) T_3 (3,5,3'-triiodothyronine, thyronine) and T_4 (3,5,3',5'-tetraiodothyroxine; thyroxine) play an essential role in embryonic organ development and maintenance in adulthood (Brix, Fuhrer, and Biebermann 2011). They are produced in the thyroid gland, a butterfly shaped organ located beneath the larynx on the trachea, and consists of two lobes connected by the *isthmus glandularis thyroidae* (Figure 1a). TH production takes place in the lumen of the thyroid follicles, which are formed by thyrocytes (Figure 1b, c).

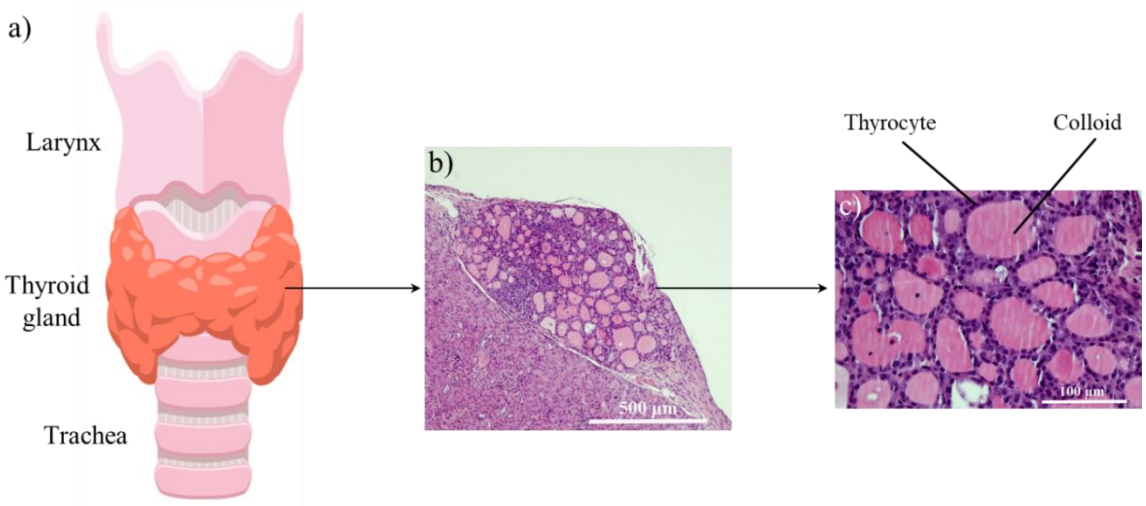

Figure 1: Anatomy and morphology of the thyroid gland. *a) The thyroid gland is located beneath the larynx surrounding the trachea and consists of two lobes. b-c) Connective tissue divides the tissue into lobules consisting of 20-40 round hollow follicles of varying size. Follicles are lined by a single layer of follicular cells containing thyroglobulin colloid and are connected to a capillary network, and thus blood flow.*

The prohormone thyroxine (T_4) as well as triiodothyronine (T_3), which is considered to be the 'active' hormone, are released into the blood stream *via* the TH-specific transporters mono carboxylate transporter 8 (MCT8) and 10 (MCT10) (Galton 2017). In humans, the thyroidal secretion ratio of T_4/T_3 is 14:1, whereas it is only 5.7:1 in rats (Pilo *et al.* 1990; Wiersinga *et al.* 2012). In order to produce TH, sufficient amounts of iodide need to be absorbed and carried into the thyroid gland where it actively gets concentrated across the basolateral plasma membrane of

thyrocytes by the sodium iodide symporter (NIS) (iodine trapping) (Andros and Wollman 1967; Pitt-Rivers and Trotter 1953; Wolff 1960). Iodide gets activated to iodine by oxidation and subsequently transported into the thyroid follicles by the chloride/iodine transporter pendrin and Ca^{2+}-dependent channel anoctamin (Twyffels *et al.* 2014; Royaux *et al.* 2000; Yoshida *et al.* 2002). Thyroid peroxidase (TPO) and thyroglobulin (Tg) are produced at the thyrocyte endoplasmatic reticulum and secreted into the follicular lumen. Here, the initial iodination of Tg by TPO results in the formation of monoiodotyrosine (MIT) and diiodotyrosine (DIT), which are then coupled to T_4 (two DIT molecules) or T_3 (one MIT and DIT molecule each) (Yokoyama and Taurog 1988; Alquier *et al.* 1989; Ohtaki *et al.* 1982). This formation is catalysed by H_2O_2, which is generated by the NADPH oxidase DUOX at the apical membrane (Dupuy *et al.* 1999; Carvalho and Dupuy 2013). When the thyroid gland is stimulated by thyroid stimulating hormone (TSH), Tg gets endocytosed and combined with a lysosome where Tg is digested by cathepsins B, L, D and exopeptidases, and T_4 and T_3 get released into the circulation (Miot *et al.* 2000; Dunn, Myers, and Dunn 1996; Dunn, Crutchfield, and Dunn 1991; Jordans *et al.* 2009).

The hypothalamus-pituitary-thyroid axis

TH production is tightly regulated by the hypothalamus-pituitary-thyroid axis (HPT axis), which determines the amount of available TH by a classical negative feedback-system (Figure 2). Low TH levels are sensed by the hypothalamus and result in the production and release of the tripeptide amide thyrotropin-releasing hormone (TRH). Through binding to the TRH receptor in the anterior lobe of the pituitary, TRH stimulates the release of pre-synthesised TSH as well as the increased production of both TSH subunits (Reichlin 1989). TSH can then activate TSH receptors of the thyrocytes in the thyroid gland, which results in increased expression of TH synthesis key components such as NIS, Tg and TPO, and ultimately the synthesis and secretion of T_4 and T_3 (Miot *et al.* 2000). TH are released into the blood stream and transported to target organs and cause a negative feedback effect on the hypothalamus and pituitary (Ortiga-Carvalho *et al.* 2016; Fekete and Lechan 2014; Chiamolera and Wondisford 2009).

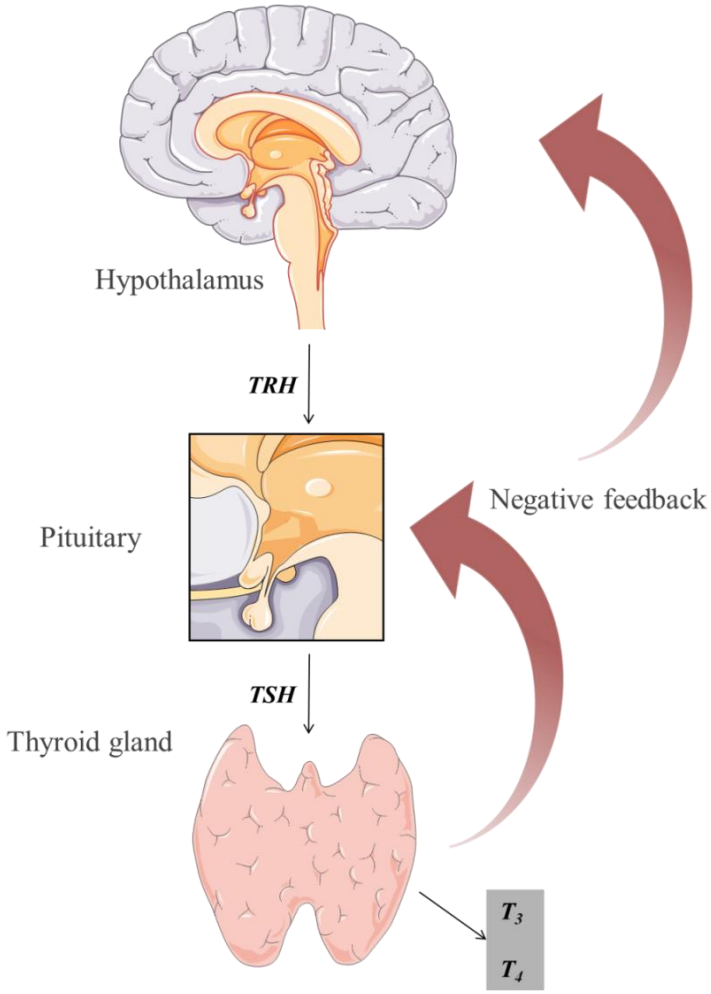

Figure 2: Regulation of thyroid hormone production *via* the hypothalamus-pituitary-thyroid gland axis. *When the hypothalamus senses low levels of TH, it responds by producing and releasing thyrotropin-releasing hormone (TRH). TRH is transported to the anterior pituitary gland and stimulates the production of thyroid-stimulating-hormone (TSH). TSH binds to the TSH receptor on thyrocytes causing the thyroid to produce and release T_3 and T_4. TH production is reduced when high concentrations of circulating T_3/T_4 are sensed by the hypothalamus and pituitary (negative feedback control).*

Thyroid hormone transport and metabolism

Based on their lipophilic nature TH require specialised carrier proteins such as thyroxine-binding globulin (TBG), transthyretin (TTR) and albumin to get transported through the blood stream (Schussler 2000). With more than 99% of TH bound to those proteins, only a minor fraction of < 0.5% of TH circulate in the blood unbound and can be taken up by target cells where TH are transported across the lipid bilayer of cell membranes *via* TH-specific transporters (Figure 3). The main TH transporters are MCT8 and MCT10 as well as organic anion transporter polypeptides 1C1 (OATP1C1) and large neutral amino acid transporters 1 (LAT1) and LAT2 (Bernal, Guadano-Ferraz, and Morte 2015; Kinne *et al.* 2015; Pizzagalli *et al.* 2002). Although T_3

is considered to be the active form of TH, 80% of the daily produced and secreted portion is T_4 (Schimmel and Utiger 1977). Inside the cells TH availability is controlled by the activity of selenoproteins, termed iodothyronine deiodinases, which activate and inactivate intracellular TH (Bianco *et al.* 2002). There are three different deiodinases (DIO1, 2, 3), which are differently expressed in organs and tissues and facilitate dissimilar reactions in the process of TH activation and inactivation (Figure 4). In humans and rodents, DIO1 is mainly expressed in the liver, kidneys and thyroid gland, where it appears to be responsible for T_4 to T_3 conversion by outer ring deiodination. Hepatic DIO1 majorly contributes to peripheral T_3 availability by deiodinating T_4 (Peeters and Visser 2000; O'Mara *et al.* 1993). DIO2 can be found in the central nervous system (CNS), pituitary, brown adipose (BAT) tissue and skeletal muscle and has been shown to exert adaptive changes in thyroid dysfunctions in order to maintain T_3 levels despite altered T_4/T_3 availability (Yen 2001).

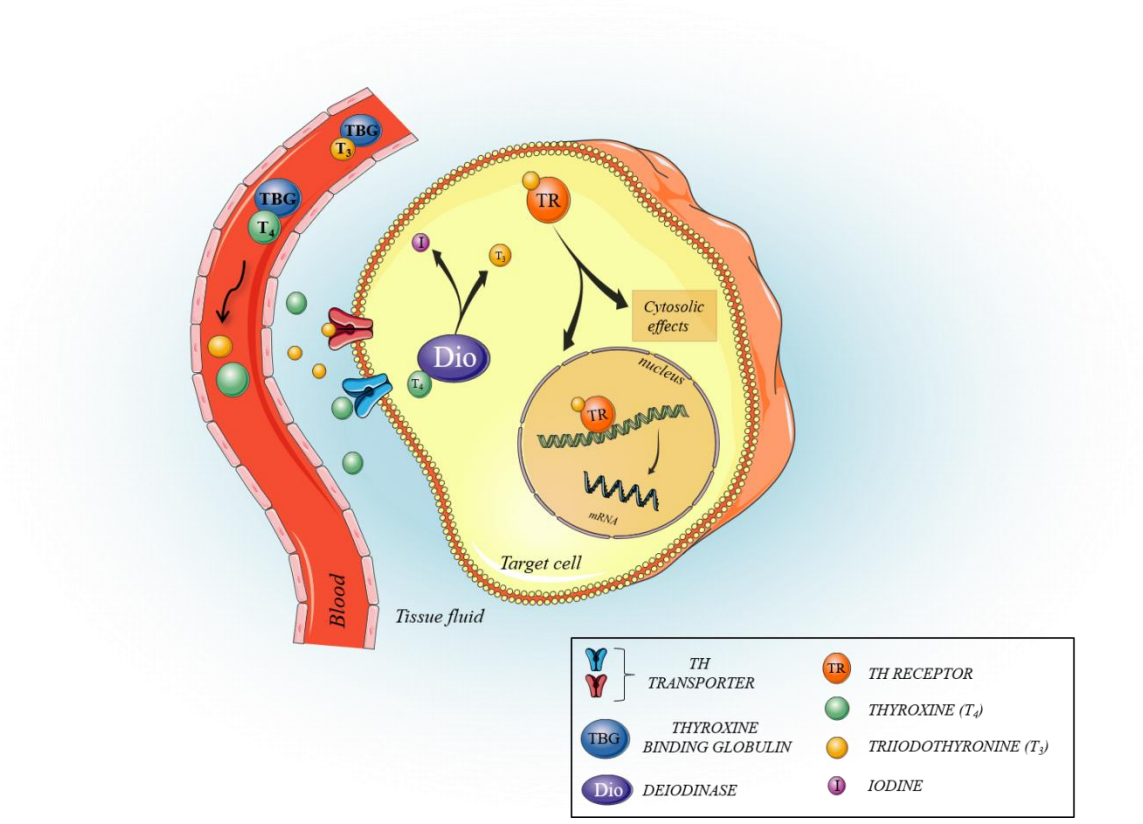

Figure 3: TH transport, activation and signalling in target cells. *The majority of TH in the blood is bound to plasma proteins such as thyroxine-binding globulin (TBG), transthyretin (TTR), or albumin. TH are actively transported into the cells via specific TH transporters. Within the target cell TH are activated by deiodinases and can then either exhibit cytoplasmic actions or regulate gene expression.*

Additionally, studies in DIO2 knockout mice have shown that DIO2 is important in the pituitary and hypothalamus negative feedback (Schneider *et al.* 2001; Galton *et al.* 2009). Finally, DIO3 activity has been observed in brain, skin, liver, intestine, placenta as well as pregnant rat uterus, and it appears to play a role in regulating local and systemic TH activity by converting and thus inactivating T_3 to rT_3 (Bianco and Kim 2006; Huang *et al.* 2000; Gereben *et al.* 2008). By clearing plasma T_3 it keeps developing organs from being exposed to undue levels of active TH (Tu *et al.* 1999). Activated TH can ultimately bind to TH receptors and exert their action *via* different signalling pathways.

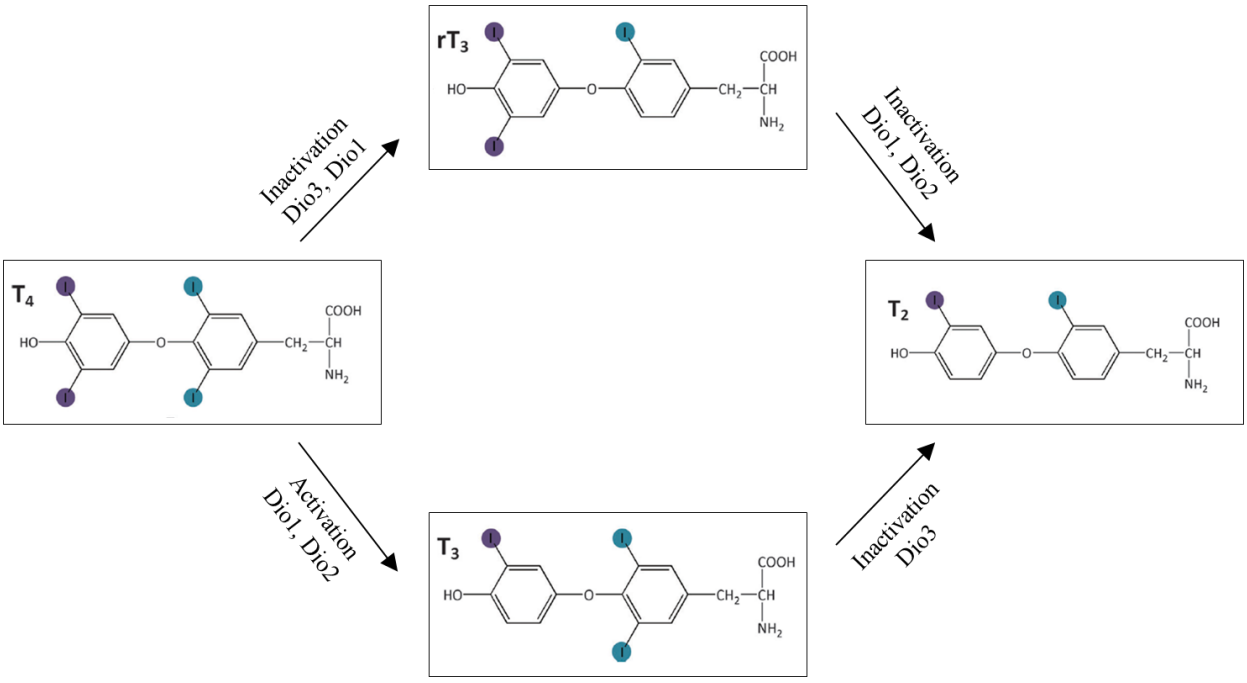

Figure 4: Scheme of thyroid hormone metabolism and deiodinase-dependent activation/inactivation. *Deiodinases (DIO) DIO1 and DIO2 activate 3,5,3‘,5‘-tetraiodothyronine (thyroxine; T_4) by converting it to 3,5,3‘-triiodothyronine (thyronine; T_3). Alternatively, T_4 can get inactivated by conversion into 3,3‘,5‘-triiodothyronine (reverse thyronine; rT_3) by DIO1 or DIO3. T_3 gets inactivated by DIO3 whereas rT_3 is deactivated into 3,3‘-diiodothyronine (T_2) by DIO1 or DIO2 (Roman, Jitaru, and Barbante 2014).*

Thyroid hormone receptors

History of thyroid hormone receptors

TH and thyroid diseases have been discovered early in medical history. How those small, relatively simple molecules elicit such a diversity of biological actions, though, has long been unknown (Evans 1988). Early research reported biological actions of TH such as stimulation of growth, acceleration of metamorphosis and metabolism regulation. However, conflicting mechanisms have been proposed to explain those actions. Nevertheless, increasing evidence in the 1960s and 70s lead to the assumption that TH can regulate target gene expression (Tata *et al.* 1963; Tata 1960). First evidence for the existence of TRs was given when Oppenheimer and Samuels used radiolabelled TH and thus demonstrated specific nuclear binding sites in T_3-sensitive tissues (Oppenheimer *et al.* 1972; Samuels and Tsai 1973). Additionally, it became apparent that TRs showed strong homology to steroid hormone receptors, and in the following years, it was shown that TRs belong to the superfamily of nuclear hormone receptors, which consist, among others, of steroid, vitamin D, and retinoic acid receptors (RXR) (Sap *et al.* 1986; Weinberger *et al.* 1986; Beato, Herrlich, and Schutz 1995; Lazar 1993). The understanding of TR structures and isoforms was pushed forward with the extraordinary findings of Vennström and Evans in 1986, when they independently cloned cDNAs of two different TRs and showed that, surprisingly, the amino acid sequence was comparable to the viral oncogene product *v-erbA* and that they are presumably homologs. By then it was generally acknowledged that T_3 effects require prior RNA transcription and that they do so *via* high affinity nuclear receptors (Tata and Widnell 1966; Oppenheimer *et al.* 1972; Samuels and Tsai 1973). Soon after, it was found that different TR isoforms exist and that the regulation of gene transcription is possibly not their only mode of action (Vennstrom and Bishop 1982; Weinberger *et al.* 1986; Lazar 1993).

Thyroid hormone receptor structure and isoforms

Research in the following years revealed that two major TR isoforms, TRα and TRβ, with a subset of different splicing forms exist and are encoded by the *THRA* and *THRB* gene locus on chromosome 17 and 3, respectively (Izumo and Mahdavi 1988; Mitsuhashi, Tennyson, and Nikodem 1988; Nakai *et al.* 1988). The two known TRs are highly conserved in vertebrates and have been shown to result from gene duplication in *Xenopus laevis* (Lazar 1993; Nuclear Receptors Nomenclature 1999; Yaoita, Shi, and Brown 1990). TRs are composed of an N-

terminal A/B domain with a specific coactivator binding site (AF1 domain), a central DNA-binding domain (DBD) which contains two zinc fingers for recognition and binding to thyroid hormone response elements (TREs) (Figure 5), and a C-terminal ligand binding domain (LBD) (Green *et al.* 1988; Nagaya, Madison, and Jameson 1992; Yen *et al.* 1995). The LBD has been shown to be not only essential for TH binding but also for dimerisation, transactivation and basal repression of aporeceptor (Renaud *et al.* 1995; Bourguet *et al.* 1995; Wagner *et al.* 1995; Forman and Samuels 1990; Yen *et al.* 1995). Within the connecting hinge region, an amino acid sequence associated with nuclear localisation (NLS) is localised, and evidence suggests that the hinge region is also involved in transcriptional repression by binding to corepressors (Evans 1988; Horlein *et al.* 1995; Chen and Evans 1995). In addition to the NLS, a nuclear export sequence (NES) allows TRs to enter and leave the nucleus and thus regulate gene transcription further (Baumann *et al.* 2001). The ligand, T_3, binds within a hydrophobic pocket of the LBD and causes conformational changes in helix 12, which contains the activating function domain 2 (AF2) and thus regulates association with coactivators (Apriletti *et al.* 1998; Darimont *et al.* 1998; Feng *et al.* 1998; Yen 2001).

Interestingly, over time many TR isoforms with different lengths, functions and localisations have been identified. TRα gene transcription results in two initial mRNAs encoding for TRα1 and TRα2, with the latter being unable to bind to T_3 or activate gene expression due to its weak DNA-binding (Figure 5) (Koenig *et al.* 1989). Up to date, a variety of alternative splicing forms (TRα1, TRα2, TRαΔ1, TRαΔ2, TRα p30 and TRα p43) have been reported for TRα, but, while many have not yet been ascribed a function, it is assumed that those so called non-authentic TRs regulate target gene expression by competing for TRE binding (Lazar, Hodin, and Chin 1989; Chassande *et al.* 1997; Hollenberg, Monden, and Wondisford 1995). The regulation of mRNA isoforms has been shown to be cell type dependent and thereby contribute to tissue specific TH effects (Hodin *et al.* 1989; Hodin, Lazar, and Chin 1990; Jones and Chin 1991). TRα p43, for example, localises to the mitochondrial matrix where it acts as a transcription factor, whereas TRα p30 cannot be found in the nucleus or mitochondria. This shows that the truncated TRα versions serve regulatory purposes at different sites in the cell (Wrutniak-Cabello, Casas, and Cabello 2001; Kalyanaraman *et al.* 2014). In contrast to TRα, TRβ encodes two N-terminal variants through different promotor regions and thus transcription leads to two different variants of the receptor: TRβ1 and TRβ2, which are both able to bind TREs as well as TH (Hodin *et al.* 1989; Wood *et al.* 1996; Koenig *et al.* 1988; Murray *et al.* 1988). While numerous insights were

gained through *in vitro* studies, the knowledge of TR action was greatly improved *via in vivo* mouse studies of TR knockout and mutant strains. Overall, gene deletions of various receptor isoforms have shown that TRs display a certain redundancy, indicating that the loss of one variant can be overcome by activity of another TR (Forrest *et al.* 1996; Fraichard *et al.* 1997; Gauthier *et al.* 1999; Gothe *et al.* 1999; Wikstrom *et al.* 1998). Despite this redundancy of TR presence, discrete roles of the two TRs have been shown for different tissues and will be discussed in the following.

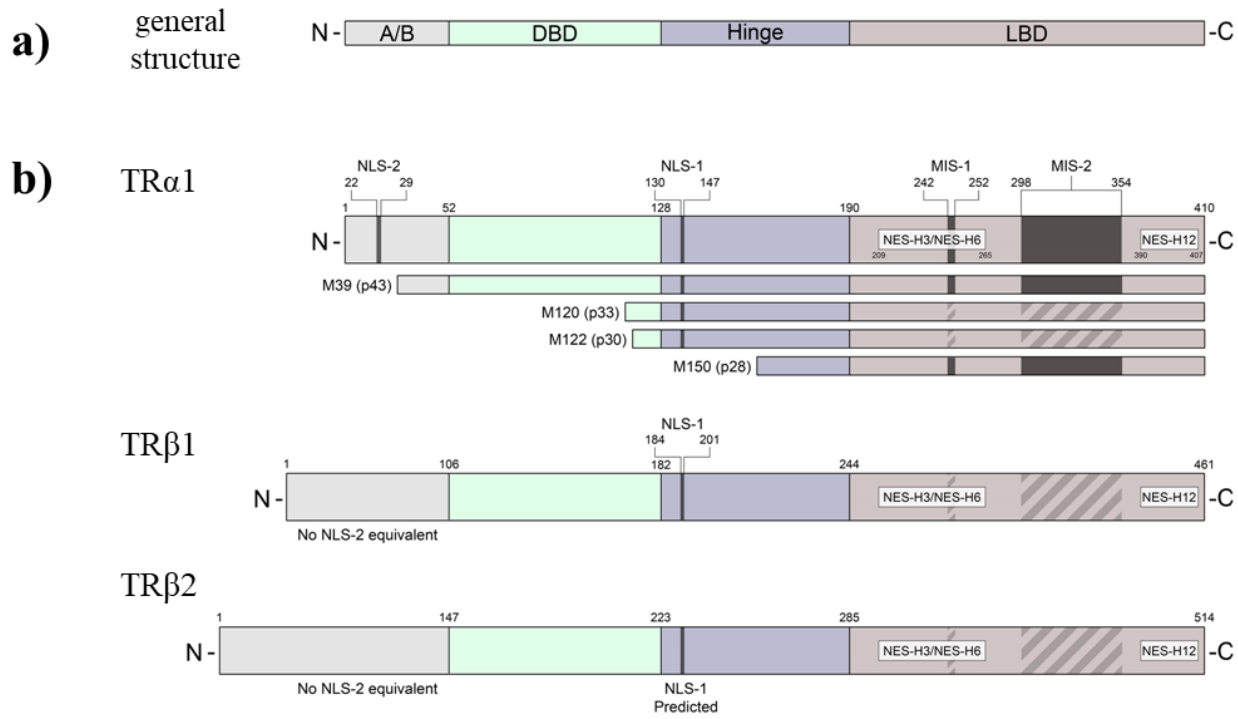

Figure 5: General and thyroid hormone receptor subtype structure. *a) General structure of TR display N-terminal A/B domain (A/B), DNA-binding domain (DBD), hinge domain and ligand-binding domain (LBD). b) TRα and TRβ isoform-specific TR structures are composed of nuclear localisation signal (NLS), nuclear export signal (NES) and mitochondrial import sequence (MIS) motifs. Solid bars indicate known, and predicted bars show domains based on sequence homology. TRα1 mRNA encodes several truncated versions (Anyetei-Anum, Roggero, and Allison 2018).*

Physiological effects of thyroid hormone receptor action

The role of TH/TR action in organ development and maintenance was studied thoroughly in patients through the investigation of abnormal TH serum levels in thyroid dysfunctions or impaired TR signalling in the syndrome of resistance to TH (RTH) (Bochukova *et al.* 2012; Sakurai *et al.* 1989). Thyroid dysfunctions are common in adults and the resulting symptoms

allow drawing conclusions on TH/TR activity. Whereas hypothyroidism generally leads to reduced metabolic and cardiovascular functions indicated for example by fatigue, cold intolerance, weight gain and bradycardia, hyperthyroidism increases bodily functions and results in weight loss, heat intolerance, nervousness, insomnia and tachycardia (Ladenson *et al.* 2000). By adding the investigation of several TR knockout and mutant mouse models, the understanding of TH/TR actions in the body was deepened further (Gauthier *et al.* 1999).

Biological activity of TH highly depends on their own availability, cell-type specific TH transporters, involvement of coactivators and corepressors, TR specific action as well as crosstalk in development and metabolism (Liu and Brent 2010; Bernal 2007; Morte and Bernal 2014). TRs are essential for a variety of diverse processes in nearly all tissues including bone, heart, fat, liver and pituitary, and the brain and their splicing forms can be found in various tissues with varying quantities (Yen 2001; Oppenheimer *et al.* 1987). For example TRα1 is expressed highest in bone, the intestine, cardiac and skeletal muscle and the CNS, whereas TRα2 and TRα3 can be found in the brain, kidney, testis, brown adipose tissue and skeletal muscle (Bassett and Williams 2016; Plateroti *et al.* 2001; Milanesi *et al.* 2016; Guissouma *et al.* 2014). Deleting the *Thra* gene locus completely ($TR\alpha^0$ mouse) caused delayed postnatal development marked by body weight, bone development and maturation as well as general growth (Macchia *et al.* 2001). TRβ1 is predominantly expressed in the liver, kidney and inner ear, and TRβ2 is the main receptor in the hypothalamus, pituitary, cochlea and retina, while TRβ4 is highly expressed in the brain and kidney (Vella and Hollenberg 2017; Flamant and Gauthier 2013; Hahm, Schroeder, and Privalsky 2014).

Keeping in mind that mRNA levels of the respective TRs does not equal the final amount of protein in the cells, one can roughly say that TRα is the predominant receptor in the postnatal development, cardiovascular system and bone growth and maintenance, while TRβ regulates metabolism and the negative feedback system of the HPT axis (Mullur, Liu, and Brent 2014; Wiersinga 2010; Shibusawa *et al.* 2003). Although most tissues express one TR isoform predominantly other TRs are not completely absent. For example, in ventricular myocytes TRα1 makes up ≈70% of total expressed TR. However, the residual 30% is TRβ1 (Refetoff, Weiss, and Usala 1993).

TRα knockout variants in mice proved its importance in cardiovascular regulation and maintenance. Mice lacking TRα variants have been reported to display a reduced heart rate

(≈20%) as well as decreased expression of the pacemaker channels potassium/sodium hyperpolarisation-activated cyclic nucleotide-gated ion channel 2 (*Hcn2*) and 4 (*Hcn4*) and increased QRS intervals in electrocardiograms, whereas TRβ$^-$ mice showed elevated heart rates which were unresponsive to TH stimulation. This finding suggests that TRα has a major role in basal heart rate regulation, whereas TRβ might mediate heart rate in response to TH stimulation (Johansson *et al.* 1999; Wikstrom *et al.* 1998). Moreover, cardio-protective TRα effects have been described by Pantos and colleagues. They reported that acute T_3 treatment protected hearts against ischemia-reperfusion injury through TRα1 and that recovery of cardiac functions after myocardial infarction in patients is mediated *via* stress-induced growth kinase activation (Pantos *et al.* 2011; Pantos and Mourouzis 2014). TRα$^-$/β$^-$ double knockout mice also have reduced heart rates and defects in temperature regulation, which suggests that TRβ contributes to these processes (Gauthier *et al.* 1999). Furthermore, the deletion of TRα1 (TRα$^-$) showed that TRα is involved in body temperature adjustments as it caused a decrease of about 0.5 °C. As *Thra* is predominantly expressed in tissues associated with body temperature regulation, i.e. the brain, vasculature, muscle and BAT, the role of TRα in this process becomes more evident (Mittag 2019). TH have been shown to be crucial for obligatory thermogenesis (resulting from cellular metabolic pathways) and facultative thermogenesis, which occurs when additional heat is required to maintain the ideal body temperature at temperatures below thermoneutrality (Johann *et al.* 2019). Facultative thermogenesis is achieved through muscle shivering or BAT activation *via* uncoupling protein 1 (UCP1) in the mitochondrial membrane (Silva 2001). Interestingly, body temperature regulation is realised by synergistical action of both TRα and TRβ. While TRα1 mediated the sympathetic responsiveness in the tissue, TRβ controls *Ucp1* expression and thus long-term temperature adjustment. Additionally, TRα is involved in regulating dissipating excess heat via tail artery dilation (Warner *et al.* 2013; Warner and Mittag 2014). Correlating with heart rate and body temperature is the TH influence on activity. Hypothyroid patients are known to suffer from fatigue and listlessness and thus be less active, whereas hyperthyroidism can be marked by restlessness and hyperactivity (Louwerens *et al.* 2012). Similar behavioural patterns have been observed in mice after comparing locomotor activity in eu-, hypo- and hyperthyroid animals (Rakov *et al.* 2017). Previous studies by Vennström and colleagues have shown that the deletion of TRα resulted in mice with locomotor deficiencies, possibly due to impaired neuronal development (Wallis *et al.* 2008). Other studies reported that TRα expression is needed in brain regions involved in behaviour. By knocking out different TRα isoforms and

inducing hypo- and hyperthyroidism in these mice, decreased activity and increased anxiety/fear in open field tests was observed (Wilcoxon *et al.* 2007). Moreover, T_3 treatment resulted in normalised locomotor activity in mice harbouring a dominant-negative mutation in TRα that reduced TR-T_3 affinity 10-fold, suggesting that TRα contributes to locomotor activity control (Venero *et al.* 2005).

Thyroid hormone receptor signalling

After ascribing TRα and TRβ to the nuclear receptor superfamily and finding that TH exert their effects *via* TR-mediated gene transcription regulation, it was long assumed that their role as transcription factors is the sole function of TRs (Mangelsdorf *et al.* 1995). However, in addition to this 'classical' action, numerous TH effects within short time frames have been observed. Since these effects appeared to be too rapid for a transcription-mediated response, it has been suggested that TH can also act by pathways independent of TR-DNA interaction called the 'nongenomic' signalling.

TRs are constitutively bound to TREs in the promoter region of TH target genes where they associate in homo- or heterodimers with RXR (Williams *et al.* 1994). TR-dependent gene regulation takes place in a ligand bound and unbound state. When T_3 is bound to TRs this so-called holoreceptor can activate gene transcription of positively regulated genes, whereas the unliganded TR is referred to as aporeceptor, which interacts with corepressors in order to suppress gene transcription (Koenig 1998). Up to date, two corepressors have been cloned and investigated: nuclear corepressor (N-Cor) and silencing mediator of retinoid and thyroid receptors (SMRT) (Chen and Evans 1995; Sande and Privalsky 1996). They bind to apo-TRs building a scaffold for the association of histone deacetylases, which facilitate an inactivated, more compact chromatin structure, keeping away key transcription factors and thereby preventing gene transcription (Nagy *et al.* 1997; Yen 2015). Upon T_3 binding the receptor undergoes conformational changes and traps T_3 in the binding pocket, resulting in the replacement of the corepressor complex by a coactivator complex (Horlein *et al.* 1995; Xu, Glass, and Rosenfeld 1999). TR coactivators include the nuclear receptor coactivator 1 (NCoA-1) also known as steroid coactivator family (SRC1) as well as p300 (McKenna and O'Malley 2002; Wu and Koenig 2000; Vella *et al.* 2014; Vella and Hollenberg 2017). The coactivators have a histone acetyltransferase activity facilitating histone hyperacetylation, a process associated with gene

activation and thus lead to a decondensed activated chromatin structure (Ogryzko *et al.* 1996; Spencer *et al.* 1997). Ultimately, gene transcription is started through the association of basal transcription factors and the RNA polymerase II (Bassett, Harvey, and Williams 2003; Watson, Fairall, and Schwabe 2012).

In contrast to this classical or canonical DNA-dependent mode, noncanonical signalling does not depend on gene expression regulation but on cytoplasmic pathway activation. It has first been observed in an experiment in 1979 where primary rat thymocytes were stimulated with T_3, and a rapid glucose uptake that could not have been mediated through a nuclear-dependent mechanism, was observed (Segal and Ingbar 1979). Moreover, by using an inhibitor for mRNA translation (cycloheximide), they confirmed that the observed TH effect was indeed independent of protein synthesis (Segal and Ingbar 1981; Segal, Buckley, and Ingbar 1985; Segal and Ingbar 1985). Noncanonical signalling has been observed at the plasma membrane, in the cytoplasm and in cellular organelles, resulting in the modulation of Na^+, K^+, Ca^{2+} and glucose transport. Moreover, it has been shown that noncanonical TR signalling results in activation of protein kinase C and A (PKC/PKA), the extracellular-signal regulated kinase (ERK) and mitogen-activated protein kinase (MAPK) pathways as well as the regulation of phospholipid metabolism through activation of phospholipase C and D (Kavok, Krasilnikova, and Babenko 2001). Upon activation of these proteins, rapid phosphorylation cascades transfer the signal (Kenessey and Ojamaa 2006; De Gregorio *et al.* 2007; Moeller, Dumitrescu, and Refetoff 2005; Moeller, Cao, *et al.* 2006). *In vitro* studies revealed that T_4 was able to induce PIP_3 (phosphatidylinositol-3,4,5-phosphate) and calcium signalling *via* PKC and PKA, but independent of gene transcription (Davis, Davis, and Lawrence 1989; Lakatos and Stern 1991; Davis and Davis 2002). *In vivo* T_3 treatment has been demonstrated to enhance cardiac output (CO) and reduce systemic vascular resistance (SVR) within 3 min and T_4 regulated thermogenesis and catecholamine activity within 30 min. Both effects occurred with a very short latency and thus were mediated *via* noncanonical TR signalling (Lynch, Andrews, and Moore 1985; Schmidt *et al.* 2002). Noncanonical effects have also been observed in the pituitary cells, where T_3 stimulation resulted in ether-a-go-go related gene potassium channel and, ultimately, PI3K and Rac GTPase activation, suggesting that noncanonical signalling might be involved in negative feedback regulation (Storey, O'Bryan, and Armstrong 2002). Noncanonical TRα effects were demonstrated by Hiroi and colleagues when they treated vascular endothelial cells with T_3 and observed increased association of TRα1 with the p85α subunit of the PI3K complex, which ultimately resulted in activation of protein kinase B

(AKT) and endothelial nitric oxide synthase (eNOS). Thus, both TRα and TRβ have been shown to mediate noncanonical TH effects *in vitro* and *in vivo*. Further evidence for noncanonical TH/TR interaction with PI3K was found when T_3-dependent production of NO in vascular smooth muscle cells (VSMC) was greatly attenuated after pre-treating cells with the selective PI3K inhibitors wortmannin or LY (Carrillo-Sepulveda *et al*. 2010). It was further demonstrated that PI3K interacts with the TR C-terminus and that a phosphorylation step within the zinc finger region, as well as Lyn kinase binding, is needed for TRβ to activate PI3K (Furuya *et al.* 2007; Martin *et al.* 2014). Cao *et al*. showed that overesxpression of TRα in neuronal cells caused T_3-induced activation of PI3K (Cao *et al.* 2009). Strikingly, Moeller *et al.* demonstrated that nongenomic activation of TH targets might ultimately lead to gene expression changes *via* TRβ and PI3K, indicating that noncanonical activation is only the initial step and that TRE-independent genes could be activated as a consequence (Moeller, Dumitrescu, and Refetoff 2005; Moeller *et al.* 2005). Taken together, a variety of canonical and noncanonical effects have been observed *in vitro*, however most have to be confirmed and studied further *in vivo* to demonstrate a clinical relevance.

With more and more signalling pathways being discovered, the distinction into canonical and noncanonical mechanisms was updated by Flamant *et al.* in 2017 (Figure 6). They extended the two categories to four with type 1 describing TR-dependent signalling that requires direct contact to the DNA, corresponding to the previously discussed canonical signalling (Flamant *et al.* 2017). Type 2 describes TR-dependent signalling without direct contact to DNA, since older findings suggest that TH/TR can exert effects *via* other transcription factors but independent of their own DNA binding (Saatcioglu *et al.* 1993; Desbois *et al.* 1991). TR dependent signalling without DNA binding (type 3) describes the previously discussed noncanonical signalling and ultimately a TR-independent pathway was proposed (type 4). Here, TH act *via* integrin $\alpha_V\beta_3$ activation at the cell membrane (Latteyer *et al.* 2019; Davis, Goglia, and Leonard 2016; Cheng, Leonard, and Davis 2010). In 2003 Shibusawa aimed to prove whether or not TRβ-DNA binding is indeed essential for all TH binding and created an *in vitro* and *in vivo* model by mutating the DBD P-box without affecting any other domains of the receptor ($TR\beta^{GS}$). *In vitro* analysis proved that this mutation completely abrogated DNA binding of TRβ, while *in vivo* examination of $TR\beta^{GS}$ mice revealed that they had disrupted regulation of the HPT axis, demonstrated by two to threefold increased total T_3 and T_4 in comparison to WT mice. Yet despite increased TH serum levels, TSH was not reduced in $TR\beta^{GS}$ mice, resulting in central TH resistance that is equal in $TR\beta^{GS}$ and

TRβ^{-} mice. By comparing retina development, hearing capacities and outer hair cell development, it was concluded that an alternative TRE-independent signalling pathway mediated TH effects (Shibusawa *et al.* 2003). Interestingly, Martin *et al.* developed a complementary mouse model by deleting the rapid signalling pathway (Martin *et al.* 2014). With the creation of this mouse model the authors created the perfect tool for distinguishing between the previously described canonical and noncanonical TR signalling pathways by deleting one of the two. Hence, the GS mutant mouse strains were created in our group not only for TRβ but also TRα. Firstly, it was shown that the GS mutation abrogated DNA binding and that consequently known TRE-dependent TR effects, such as TRα-dependent gene regulation in cardiac muscle tissue or TRβ-dependent regulation of TH target genes in the liver, were absent (Hones *et al.* 2017). Myosin Heavy Chain 6 (*Myh6*) was significantly downregulated in both TRα^{0} and TRα^{GS} mice, and *Myh7* was strongly increased in TRα^{0} hearts (≈15-fold) but less so in TRα^{GS} tissue (≈10-fold).

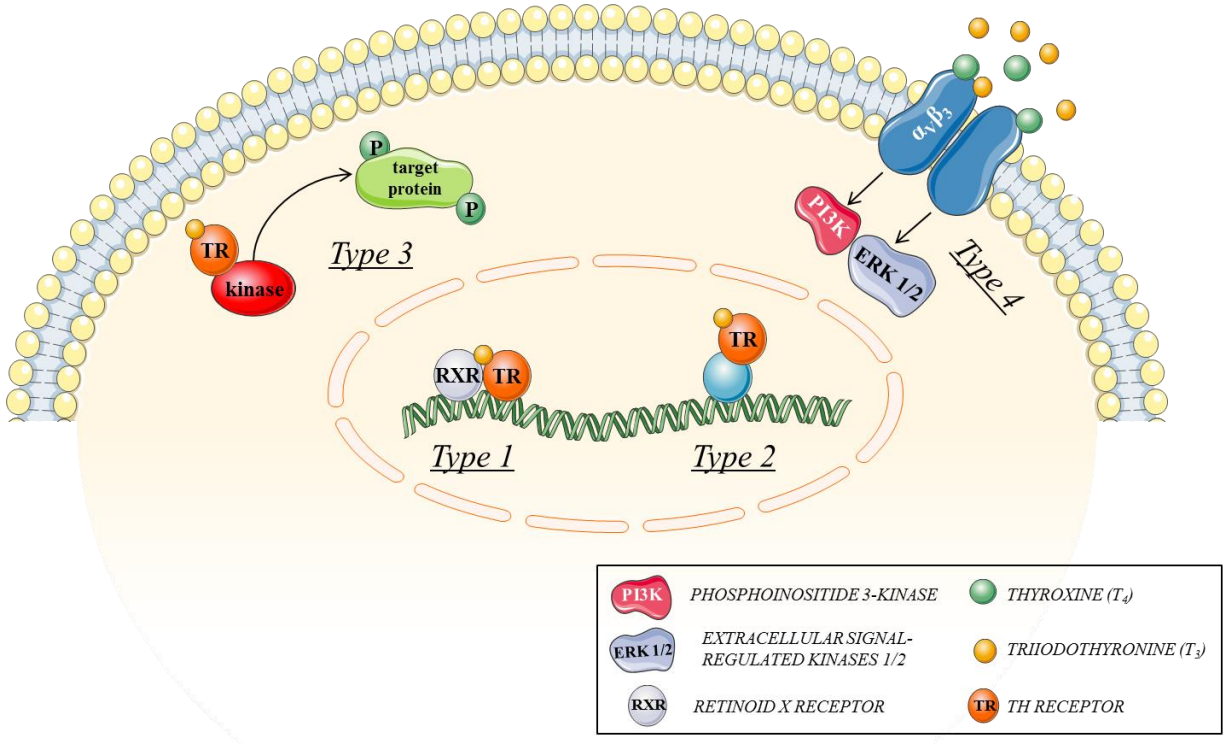

Figure 6: Thyroid hormone signalling pathways within cells. *TH can exert a variety of effects via TRs in target cells. TRs are constitutively bound to TH response elements (TREs) in homo- or heterodimers with RXRs. Upon binding of T_3, TRs are stimulated to either activate or repress target gene expression (type 1, canonical signalling). This gene expression regulation could also occur indirectly with an additional regulatory factor between TR and TRE (type 2). Both pathways ultimately lead to the synthesis of new proteins. Noncanonical (type 3) signalling is a rapid effect independent of DNA binding and synthesis of new proteins and is mediated by the activation of cytoplasmic kinases. Additionally, TH can activate membrane bound integrins and 2nd messenger signalling pathways (type 4). Whereas type 1 to type 3 signalling is activated by T_3, αvβ3 can also be activated by T_4.*

Moreover, it was shown that canonical signalling is crucial in TRα-mediated control of bone development. By measuring growth curves of WT, $TR\alpha^{GS}$ and $TR\alpha^{0}$ as well as $TR\beta^{GS}$ and $TR\beta^{-}$ mice, a delayed growth was observed in $TR\alpha^{0}$ and $TR\alpha^{GS}$ while no differences were seen between TRβ strains. Skeletal analysis revealed that this growth delay results from decreased bone lengths, vertebral heights and reduced bone mineral content of vertebrae in both $TR\alpha^{0}$ and $TR\alpha^{GS}$ mice in addition to delayed endochondral ossification of the growth plate and overall displayed a phenotype known for impaired T_3 action (Bassett and Williams 2016; Bassett *et al.* 2010). Glucose uptake in response to T_3 is a rapid effect and was found to be preserved in $TR\beta^{GS}$ mice while it was absent in $TR\beta^{-}$ mice (Segal and Ingbar 1979). Interestingly, noncanonical TRβ signalling has been observed to contribute to body temperature regulation and locomotor activity, and noncanonical TRα signalling plays a role in extrinsic regulation of basal heart rates. By comparing data from non-invasive electrocardiography, it was demonstrated that $TR\alpha^{0}$ mice had significantly lower heart rates than WT animals, which was not the case in $TR\alpha^{GS}$ mice. In isolated hearts however, the cardiac rhythm was comparable between $TR\alpha^{0}$ and $TR\alpha^{GS}$ mice, meaning that a central noncanonical TRα effect might regulate heart rates in an extrinsic matter (Hones *et al.* 2017). These are some effects that could be attributed to either canonical or noncanonical signalling, although many more have to be investigated to categorise them and understand the underlying mechanisms.

Thyroid hormone action in the cardiovascular system

The connection between the thyroid gland and cardiovascular system has long been known (Klein 1990). Hyperthyroidism has been reported to be associated with increased morbidity and mortality from cardiovascular disease. Thyroid dysfunctions lead to altered TH levels in the blood and ultimately direct and indirect effects in target organs such as the heart and vascular system. Systolic hypertension, cardiomyopathy, atrial fibrillation and enlargement, as well as heart failure, are among the cardiac complications that are caused by hyperthyroidism. In hyperthyroid patients mortality due to cardiovascular risk is increased by 20% (Brandt *et al.* 2011). Treating those patients with an anti-thyroid therapy reduces cardiovascular risk symptoms, however it has been reported that some abnormalities persist despite an effective treatment (Osman *et al.* 2007). As a consequence of thyroid dysfunctions, SVR can be severely affected. Whereas SVR is increased in hypothyroid patients, it is decreased in hyperthyroidism due to peripheral vasodilation and increased blood volume (Lekakis *et al.* 1997; Napoli *et al.* 2001; Sorisky 2016; Klein and Danzi 2007).

Heart anatomy and function

The heart is a muscular organ located in the chest, with the main function of pumping blood through the circulatory system to supply all organs and tissues with oxygen. It is divided into four distinct chambers, with ventricle and atrium on each side (Figure 7a). The large thick-walled left (LV) and right ventricle (RV) are separated by the interventricular septum (IVS). Positioned above each ventricle are the respective thin-walled left (LA) and right atrium (RA). LA and LV are separated by the mitral valve, and the tricuspid valve divides the RA and RV. In the RA and RV two important excitable nodes are located: the heart's pacemeaker, the sinoatrial (SA node) and the atrioventricular node (AV node), which forward electrical stiumulations *via* the conducting system in the heart and thereby coordinate contractions (Cabrera and Sanchez-Quintana 2013) (Figure 7b). The cardiac cycle consists of rhythmic contractions (systole) and relaxations (diastole) of both atria and ventricles. The contraction of atria occurs simultaneously, followed by the contraction of ventricles (Smolenskii and Kovalev 1966). The cardiac muscle is an involuntary striated muscle and is composed of cardiac myocytes, which are built from myofibrils and, lastly, sarcomeres (Beams, Evans, and *et al.* 1949). Those subunits are connected end-to-end by intercalated discs and organised into layers wrapped around the ventricles, which

allow them to mediate contractions when they are stimulated by the SA node, resulting in a decreased chamber size and ejection of blood (Huxley 1961; Barr, Dewey, and Berger 1965). Cardiac muscle cells (cardiomyocytes) make up the myocardium and possess a high amount of mitochondria to cover the energy demand of the heart (Porter *et al.* 2011). Neonatal hearts have been shown to be capable of substantial regeneration following injury until postnatal day 7, and few stem cells continue dividing even in adult hearts (Beltrami *et al.* 2001; Kajstura *et al.* 2010; Muralidhar and Sadek 2016). This process is largely facilitated through cardiomyocytes proliferation and the regulation of their cell cycle arrest (Pasumarthi and Field 2002). However, adult cardiomyocytes have been reported to have a residual turnover rate of ≈1% at the age of 20 and ≈0.3% at the age of 75. In total, less than 50% of adult cardiomyocytes are renewed during a human lifespan, which is strongly associated with chronic heart failure as damage cannot be repaired in adult hearts (Bergmann *et al.* 2009). Yet, in mice conflicting results have been reported where results ranged from no to considerable regeneration of cardiomyocytes after injury (Hsieh *et al.* 2007).

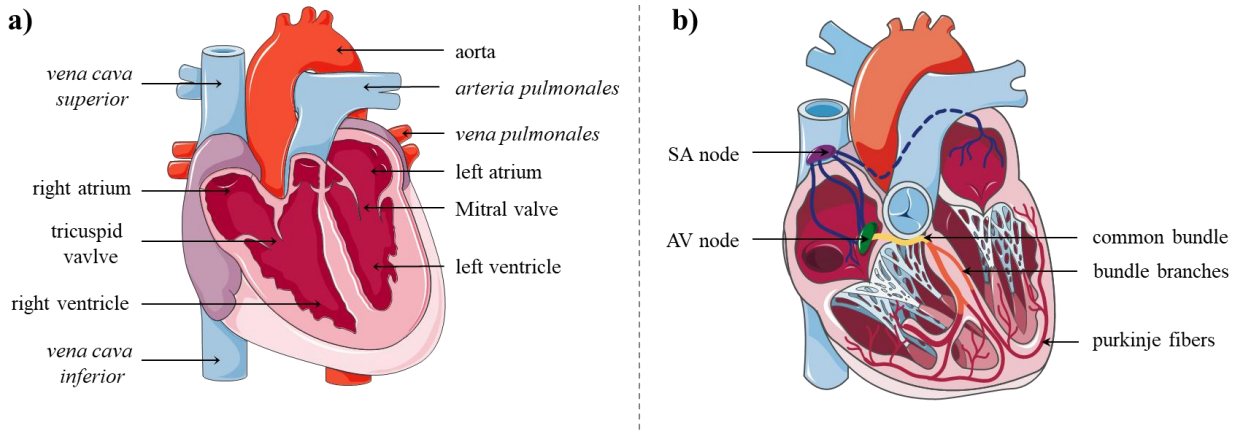

Figure 7: Anatomy of the heart. *a) The heart is divided into the left (LV, LA) and right (RV, RA) ventricle and atrium. The LA and LV are divided by the mitral valve whereas the tricuspid valve divides the RA and RV. When the heart relaxes, blood flows from both atria into the ventricles, which expand in response. This is followed by the ejection period, during which the LV pumps oxygen-rich blood into the aorta, from where it travels along the arteries, delivers oxygen and picks up carbon dioxide. Oxygen-low blood is transported back to the RA/RV via the vena cava superior and inferior. The RV pumps oxygen-low blood into the arteria pulmunales and, ultimately, into capillaries, where carbon dioxide is released, and oxygen enters the bloodstream and gets transported to the heart. b) Pumping of the heart is determined by pacemaking cells in the sinoatrial node (SA node), which creates an electrical signal that is forwarded to the atrioventricular node (AV node). Subsequently, the signal travels to the common bundle, which branches off into the left and right bundle branch and, eventually, the purkinje fibers that transmit the electric signal into the ventricular muscle.*

The reduced ability of cardiomyocytes correlates with increased polyploidy or binucleation of the cells (Walsh *et al.* 2010; Ye *et al.* 2019). Although the doubling of chromatin after binucleation would be expected to result in a doubling of the surface-to-volume-ratio, the result is only an increase of 1.6-fold, suggesting that chromatin is differently assembled within the nucleus and thus different genes being accessible and active (Tchernaenko *et al.* 2008; Comai 2005). Cardiomyocytes that cannot proliferate anymore show a transition to hypertrophy, i.e. the growth of individual cells, and thereby the main reason of cardiac growth (Ahuja, Sdek, and MacLellan 2007).

Arterial blood pressure regulation

SVR is the resistance in the peripheral vascular system that is utilised to create blood pressure. It helps to create blood flow and is therefore a parameter of cardiac function that is connected with and correlates with heart rate, CO and cardiac hypertrophy (Lekakis *et al.* 1997). SVR can be altered by intrinsic and extrinsic mechanism. Firstly, by decreasing (vasoconstriction) or increasing (vasodilation) their diameter, arteries are able to adjust SVR in response to temperature, partial pressure of oxygen, adrenaline, NO, endothelin-1, TH and other stimuli (Charkoudian 2010; Tayefeh *et al.* 1997; Halbrugge *et al.* 1991). The cardiovascular state is sensed by baroreceptors in the carotid sinus, aortic arch and right atrium, chemoreceptors in the carotid and aortic bodies as well as higher brain regions (cerebral cortex, hypothalamus and limbic system) and can thus be adjusted depending on the situation (Somers, Mark, and Abboud 1991; Sinski *et al.* 2014; Guyenet 2006). SVR can also be adjusted by the blood viscosity or blood volume, which is regulated by the renin-angiotensin-aldosterone system in the kidney or by altering CO, heart rate or stroke volume (Moon 2013; Vincent 2008).

To increase blood flow, arteries dilate by relaxation of vascular muscle cells which make up the media cell layer of vessels. Muscle cells are surrounded by the external and internal elastic lamina and the outer adventitia as well the endothelial cell layer that is directed to the blood stream (Tucker and Mahajan 2020). The process of vasodilation has been associated with endothelium-dependent NO production. eNOS produces NO which diffuses to the muscle cells, where it activates soluble guanylyl cyclase, resulting in the production of cyclic guanosine monophosphate (cGMP). This leads to the activation of protein kinase G (PKG), decreased Ca^{2+} levels within the cell and, ultimately, smooth muscle relaxation *via* the activation of myosin light chain kinase and the inhibition of myosin light chain phosphatase (Khalaf *et al.* 2019).

Despite multiple insights from basic and clinical studies, the precise mechanism of T_3-induced vascular relaxation is still pending. In patients a negative correlation between TH levels and blood pressure has been observed, suggesting that TH may contribute to blood pressure control. In healthy male volunteers T_3 injections caused a direct reduction in SVR and CO. Remarkably, TH administrations caused a significantly higher reduction of SVR and increase of CO in a time span of 3 min than placebo administration (Schmidt *et al.* 2002). In isolated rat hearts in a Langendorff machine, bolus injections of either 100 nmol T_3 or T_4 led to a rapid decrease of coronary perfusion pressure, further supporting the assumption of vasodilation by TH (Yoneda *et al.* 1998). T_3-mediated vasodilatation was not only shown in isolated hearts but also in mouse *in vivo* investigation. Here, T_3 injections led to reduced arterial pressure values in WT mice (Hiroi *et al.* 2006). In addition to eNOS, the phosphoinositide 3-kinase (PI3K) seems to contribute to vascular relaxation (Abeyrathna and Su 2015; de Castro *et al.* 2015). Early studies showed that rat skeletal muscle resistance arteries dilated in response to T_3 and T_4 with T_3 having a stronger effect than T_4 (30% and 20% respectively) (Park *et al.* 1997). Studies with rat aortic rings showed that arteries pre-treated with T_3 exhibited an increased endothelium-dependent vasodilation when stimulated with acetylcholine. In this study it was also shown that the PI3K, as well as eNOS, play significant roles in the downstream signalling of T_3-mediated vasodilation (Samuel *et al.* 2017). Makino *et al.* found that TRα is the predominant TR isoform in coronary smooth muscle cells and therefore has profound effects on the regulation of vascular tone (Makino *et al.* 2012). The role of TRα in T_3-mediated vasodilatation was investigated on isolated arteries from $TR\alpha^{WT}$ and $TR\alpha^{0}$ mice. Whereas WT arteries dilated in a dose-responsive manner, no effect was observed in $TR\alpha^{0}$ vessels, leading to the assumption that T_3-induced vascular relaxation is mediated by TRα (Liu *et al.* 2014). Considering the quick decrease of blood pressure in mice as well as human patients in response to T_3 administration, a noncanonical TH/TRα effect is most likely but has yet to be proven. TH-induced vasodilation and therefore reduced SVR caused an increase in heart rate and left ventricular end diastolic volume, which, ultimately caused increased preload and decreased afterload. The resulting increased stroke volume leads to increased CO and oftentimes cardiac hypertrophy (Kasturi and Ismail-Beigi 2008; Fadel *et al.* 2000; Shimizu *et al.* 2002).

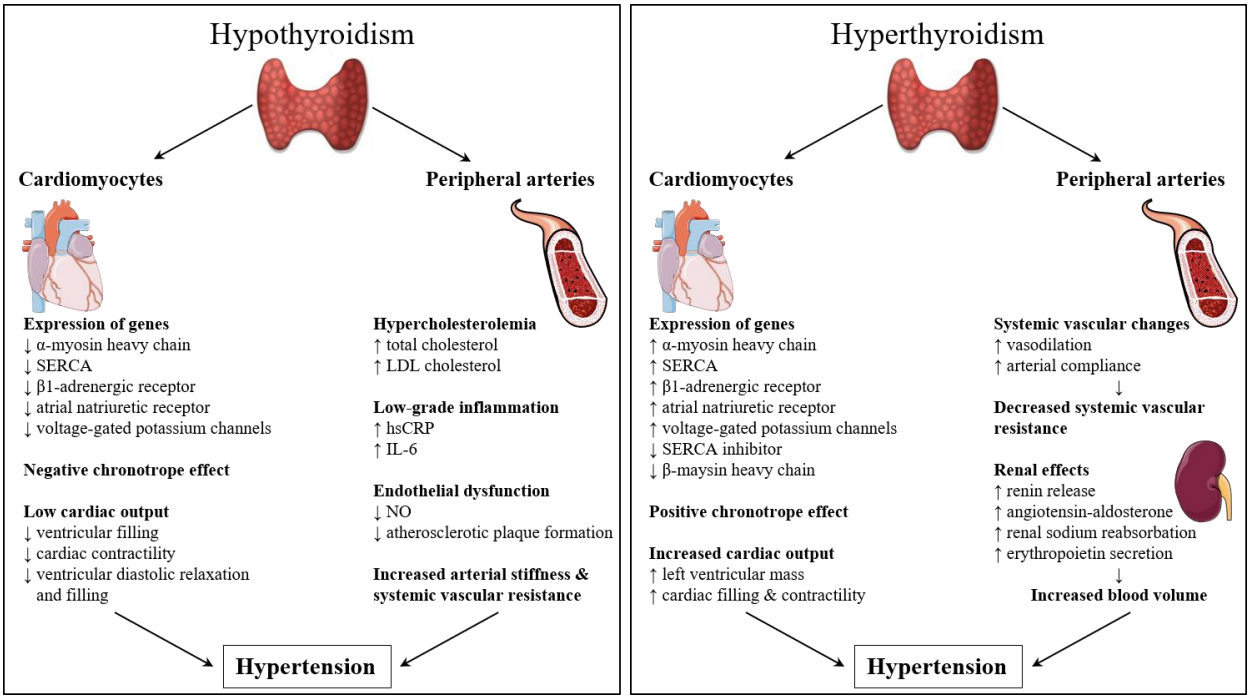

Figure 8: Consequences of long-term thyroid dysfunctions on arterial blood pressure. *Hypothyroidism leads to alteration of cardiac gene expression and therefore low CO. In addition, metabolic changes lead to hypercholesterolemia, low-grade inflammation and endothelial dysfunction and thus increased arterial stiffness and increased systemic vascular resistance, resulting in hypertension. Hyperthyroidism affects cardiac gene expression in an opposed manner and results in increased CO and vasodilation and, consequently, decreased systemic vascular resistance. Additionally, hyperthyroidism activates the renin-angiotensin-aldosterone system resulting in increased blood volume and ultimately hypertension as well. Modified from (Berta et al. 2019).*

In addition to the cellular mechanisms in vasodilation, the long-term effects of thyroid dysfunctions on the vascular system have been studied. This is a relevant condition in patients where both hypo- and hyperthyroidism have been associated with hypertension (Figure 8) (Cappola and Ladenson 2003; Prisant, Gujral, and Mulloy 2006). In an overt hyperthyroid state metabolic rate, cardiac preload and ventricular contractility increase, whereas SVR decreases, resulting in augmented CO and hypertension. In an echocardiography study pulmonary hypertension was found as a common complication in hyperthyroid patients (Muthukumar *et al.* 2016). In hypothyroid patients lipid metabolism is strongly affected, resulting in hypercholesterolemia, increased levels of triglycerides, lipoproteins and apolipoproteins due to reduced hepatic activity (Lithell e*t al.* 1981; Nikkila and Kekki 1972). In addition to hyperlipidemia hypercoagulable state, endothelial dysfunction and arterial stiffness lead to arterial hypertension in hypothyroid patients (Obuobie *et al.* 2002; Muller *et al.* 2001). Overall, arterial stiffness appears to be a common feature in hyperthyroidism and is associated with

hypertension (Inaba *et al.* 2002; Prisant, Gujral, and Mulloy 2006; Owen, Sabit, and Lazarus 2007). The association between hypothyroidism and reduced secretion of endothelium-dependent dilation factors is well known to result in endothelial dysfunction, an early step in the development of atherosclerosis (Berta *et al.* 2019). In a previous study hypothyroidism was confirmed to be associated with increased augmentation of aortic pressure and central arterial stiffness, which could be reversed after TH treatment (Obuobie *et al.* 2002).

Cardiac hypertrophy

Cardiac hypertrophy, i.e. the thickening of the ventricular heart muscle, occurs in two different forms. Normal growth in children or during pregnancy or training (athlete's heart) is referred to as physiological hypertrophy and is associated with normal cardiac function (Figure 9). Pathological hypertrophy however is connected to cardiac dysfunction and is induced by hypertension, myocardial infarction or prolonged and abnormal hemodynamic stress (Shimizu and Minamino 2016). Fibrosis, capillary rarefaction, increased production of pro-inflammatory cytokines and cellular dysfunctions can lead to cardiac remodelling, reduced systolic and diastolic function and progresses towards heart failure (Nakamura and Sadoshima 2018). While cardiomyocytes growth in physiological hypertrophy is accompanied with a corresponding expansion of the capillary network, cardiomyocyte growth in pathological hypertrophy exceeds the capacity of the capillaries, which leads to impaired nutrient and oxygen supply of the cells and, ultimately, cardiac hypoxia and fibrotic remodelling in rodents (Shimizu *et al.* 2010; Sano *et al.* 2007). Previous studies suggest that physiological and pathological hypertrophy differ in signal pathway activation, but some overlap. For example, the activation of AKT has been reported for both pathways (Shimizu and Minamino 2016). Animal studies have shown that distinct features mark physiological and pathological hypertrophy. In healthy hearts a fine collagen network surrounds cardiac myocytes. In response to pathological but not physiological stimuli, fibroblasts and extracellular matrix expand extensively and result in fibrosis. The resulting stiffness contributes to decreased CO and dysfunction (Iemitsu *et al.* 2001; Brower *et al.* 2006). By studying a broad set of transgenic and exercise mouse models, signalling pathway for both physiological and pathological hypertrophy have been identified. One of the prominent signalling pathways in physiological hypertrophy is the insulin-like growth factor 1 (IGF1) PI3K pathway. Mice in which this pathway was enhanced showed cardiac hypertrophy with a normal or enhanced cardiac function, and knocking out this pathway resulted in smaller hearts,

suggesting that IGF1–PI3-K (p110a) signalling is important for physiological growth of hearts (Reiss *et al.* 1996; McMullen *et al.* 2004; Shioi *et al.* 2000). Pathological hypertrophy has been demonstrated to be mediated *via* activation of protein kinase C and MAPK or calmodulin/calcineurin signalling G-protein-coupled receptors and thus the G_{aq} pathway regulation. Cardiac-specific overexpression of one of these components resulted in cardiac hypertrophy associated with cardiac dysfunction and premature death, whereas the deletion of the signalling pathway did not result in cardiac hypertrophy in response to pressure overload (D'Angelo *et al.* 1997; Mende *et al.* 1998; Wettschureck *et al.* 2001). Furthermore, ERK1/2, which plays a crucial role in development of hypertrophy, has been shown to undergo autophosphorylation, phosphorylate nuclear targets, and thereby cause cardiac hypertrophy (Lorenz *et al*. 2009).

TH are known to rapidly rise after birth and be involved in postnatal physiological heart growth by promoting neonatal cardiomyocyte growth through the activation of p38MAPK and PI3K/AKT/mTOR (mammalian target of rapamycin) signalling (Stubbe *et al.* 1978; Kinugawa *et al.* 2005; Kenessey and Ojamaa 2006). Cardiac muscle growth in response to hyperthyroidism results from many causes (Morgan and Baker 1991). Firstly, TH have direct effects on the myocardium and its protein synthesis (Coleman *et al.* 1989). Furthermore, the previously described increased hemodynamic load of the heart is compensated by increased CO and thus a higher workload for the heart. Moreover, increased sympathetic activity and an increased blood volume add to the previous effects (Klein 1990; Morgan and Baker 1991). In a clinical study increased IVS, left ventricular posterior wall (LVPW) and left ventricular mass (LVM) were observed. While stroke volume, CO, systolic blood pressure and heart rate were augmented, diastolic blood pressure and SVR were decreased in hyperthyroid patients. Interestingly, treatment that resulted in a euthyroid state did not reverse the cardiac remodelling and LVM did not seem to be reversible (Marcisz *et al.* 2006; Petretta *et al.* 2001). TH-induced cardiac hypertrophy has been thoroughly studied in mice, where T_4 administration resulted in a hypertrophic phenotype as early as after three to four days of treatment (Eliades and Weiss 1989; Limas and Limas 1987). Still, the precise signalling pathway that mediated this process is under investigation. Early studies claim that TRβ is the responsible receptor (Weiss *et al.* 2002; Imperio *et al.* 2015). Yet, in their study Imperio *et al.* used a dominant negative TRβ mutant which could have occupied the TREs and thus abolished a possible TRα effect in the process.

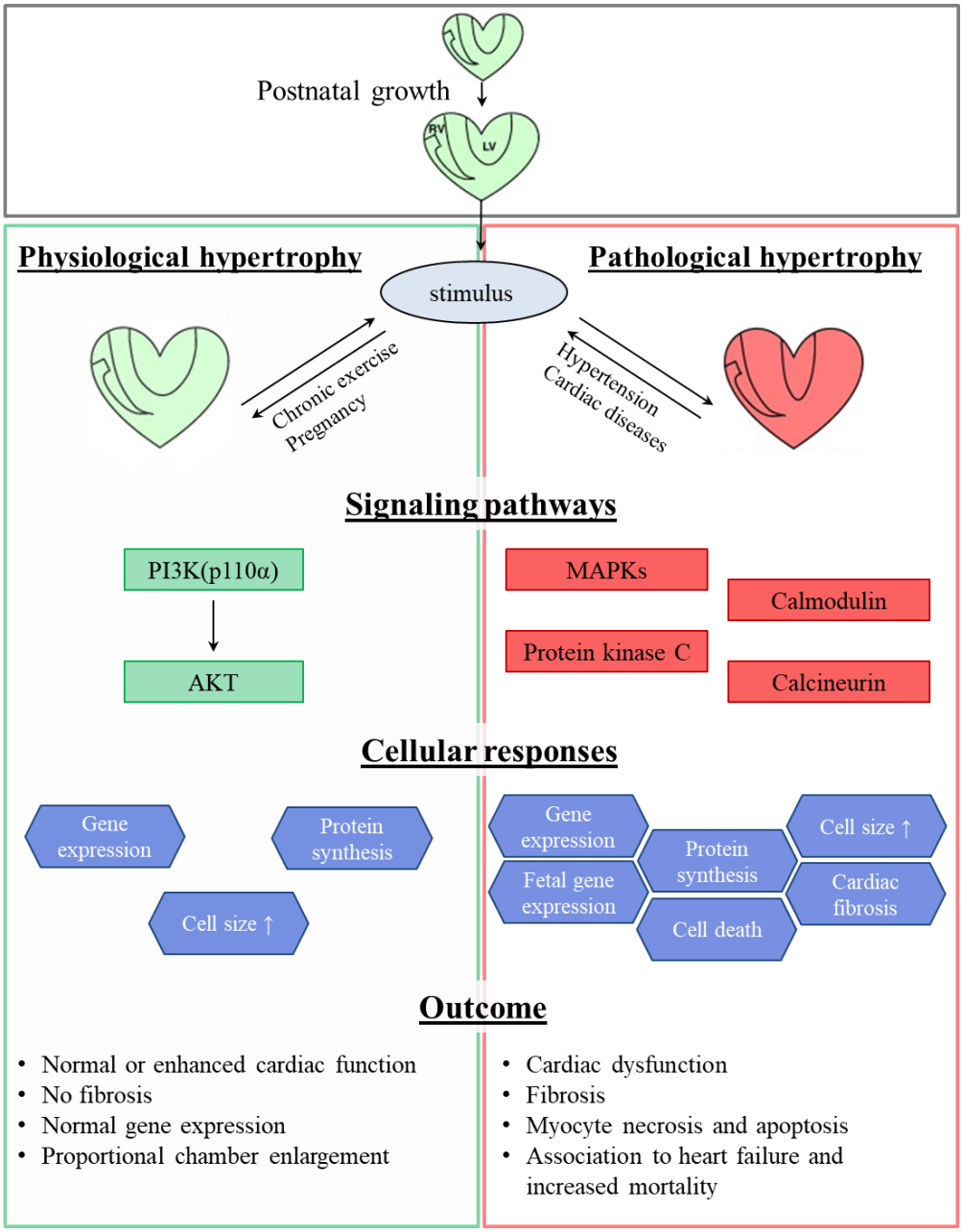

Figure 9: Physiological and pathological cardiac hypertrophy. *Neonatal cardiac tissue grows and develops until cellular arrest causes cardiac myocytes to stop proliferating. Cardiac enlargement at a later point can result in either physiological or pathological cardiac hypertrophy. In response to chronic exercise or pregnancy the heart overcomes an increased workload, resulting in a compensatory increase in size (physiological hypertrophy). Pathological hypertrophy is induced by abnormal hemodynamic stress due to hypertension and other cardiac diseases. Different pathways are activated in the two subtypes, which results in gene expression and protein synthesis and thus increased cell size in physiological hypertrophy. In addition, pathological hypertrophy is marked by fibrosis, apoptosis and ultimately cardiac dysfunctions. Modified from (Bernardo et al. 2010)*

In addition, TRα is the predominantly expressed receptor in the heart and has many effects in the regulation of cardiac homeostasis (Pantos and Mourouzis 2014; Kahaly and Dillmann 2005). TRα1 overexpression in cardiomyocytes resulted in a hypertrophic phenotype. Strikingly, this process could be further increased by T_3 but not by the TRβ-specific agonist GC-1 (Kinugawa *et al.* 2005). These inconsistent data justifiy a study to identify the responsible receptor with mice of the same background and treatment to allow comparison of the role of one or both of the receptor isoforms in the development of TH-induced cardiac hypertrophy. While this part is still unclear and has to be addressed in future studies, some indications about the TR signalling pathway have been brought up lately. Kuzman and colleagues observed that T_4 treatment activated cytoplasmic AKT/mTOR signalling which lead to increased heart weight in rats. More importantly, they were able to show that the mTOR-specific inhibitor rapamycin can prevent this effect (Kuzman *et al.* 2005; Kuzman, O'Connell, and Gerdes 2007). The involvement of cytoplasmic AKT and mTOR was also observed by Kenessey and Ojamaa who could as well show that TRα1 directly interacts with the p85α subunit of PI3K (Kenessey and Ojamaa 2006). Taken together, these results suggest that noncanonical TRα signalling mediates TH-induced cardiac hypertrophy through activation of PI3K and its downstream targets. However, cardiac hypertrophy does not only result from direct effects of TH on the cellular level but is also connected to the arterial pressure and altered heart rate in thyroid disease.

Heart rate

Heart rate needs to be adjusted in response to the body's need for oxygen and nutrients under altering conditions. The cardioregulatory centre controls antagonistic effects of the parasympathetic and sympathetic neurons of the autonomic nervous system. The sympathetic system releases norepinephrine and thus prepares the body for energy expenditure by increasing heart rate and myocardial contractility, whereas the parasympathetic system releases acetylcholine and is activated under restful conditions resulting in decreased heart rate. Overall, the heart rate results from the net balance between the opposing effects of both systems (Gordan, Gwathmey, and Xie 2015; Kishi 2012; Silvani *et al.* 2016). Additionally, the cardioregulatory centre can also activate neurons in the adrenal medulla resulting in increased excretion of epinephrine, which further increases heart rate and stroke volume (Vollmer 1996). Another mode of regulation is the SA node, which acts as a pacemaker as part of the intrinsic conduction system (Figure 7b). Heart rate is permanently sensed by baroreceptors and chemoreceptors in the internal

wall of the carotid artery and the carotid body and forwarded to the cardioregulatory centre in the medulla oblongata by sensory neurons (Haymet and McCloskey 1975).

Besides the central (autonomic nervous system) and intrinsic (SA node) factors influence on heart rate, additional determinants such as hormones can further modulate cardiac activity. Hyperthyroidism causes a hyper adrenergic state in the body, marked amongst others by increased heart rate, CO, and myocardial contractility (Levey and Klein 1990). 24 hour electrocardiogram (ECG) monitoring in patients with overt hyperthyroidism showed that their heart rate was constantly increased during the day, while a circadian rhythm was preserved (Cacciatori *et al.* 1996; Chen *et al.* 2006). Although the use of β-blockers usually results in attenuated tachycardia, heart rates remained slightly increased in comparison to euthyroid controls, indicating that TH are able to directly activate the SA node within the heart (Sun *et al.* 2001). To address how TH act on the heart, sympathetic system and vascular system and thus the heart rate, mice with different receptor deficiencies were studied. In 1998 Wikström *et al.* found out that TRα1 knockout mice had about 20% lower heart rates than control mice in both euthyroid and hyperthyroid state. They also observed that those mice had prolonged QRS- and QT_{end}-durations in ECG (Wikstrom *et al.* 1998). The reduced expression of the hyperpolarisation activated cyclic nucleotide-gated potassium channel 2 (HCN2), which is an essential player in pacemaking, appeared to be involved in the regulation (Kahaly and Dillmann 2005). In studies by Dillmann and coworkers it was seen that the deletion of TRα but not TRβ yielded in markedly decreased heart rate and contractile performance which is mainly mediated by upregulation of sarcoplasmic/endoplasmic reticulum calcium ATPase (SERCA) (Dillmann 2002). Since heart rate is not only controlled *via* intrinsic pacemaker activity of myocytes in the SA node but also by the autonomic nervous system in the brain, a sympathetic input might be involved in TH-induced tachycardia. Furthermore, a mutated version of TRα with a strongly reduced ligand affinity showed only a mild phenotype *in vivo* but severe impairment of contractility *in vitro*, i.e. separated from the CNS (Tavi *et al.* 2005; Mittag *et al.* 2010). Additionally, the involvement of PI3Kγ *via* second messenger signalling of cAMP and sarcoplasmic reticulum Ca^{2+} handling has been proposed after observing that respective knockout mice had altered heart rate and SA node activity in response to atropine and propranolol injections (Rose, Kabir, and Backx 2007). Further studies demonstrated that spontaneous beating of isolated atria from WT mice was higher than in hearts from TRα deficient animals, suggesting that TH impact on heart rate regulation is an intrinsic effect (Mittag *et al.* 2010). Taken together, previous research has demonstrated that

TRα contributes to heart rate regulation, yet it is so far unknown which signalling pathway, canonical or noncanonical, is involved in this process.

Hypothesis and Aims of the Study

Recent studies showed that TH/TR cannot only exert their effects *via* TRE-dependent transcriptional changes but also by rapid activation of cytoplasmic proteins. With the creation of the $TR\alpha^{GS}$ mouse model a tool for distinguishing TRα signalling pathways *in vivo* was established. Whereas canonical and noncanonical signalling are both present in WT and absent in $TR\alpha^{0}$ mice, only noncanonical signalling remains in $TR\alpha^{GS}$ mice. It was previously shown that noncanonical signalling is physiologically relevant *in vivo* (Hones *et al.* 2017). Thus, the aim of this study was to compare WT, $TR\alpha^{0}$ and $TR\alpha^{GS}$ mice and thereby identify canonical and noncanonical TH/TR effects in the cardiovascular system.

Aims of this study

(1) Clinical data and mouse studies show that TH have short- and long-term effects on the vascular system. Previous studies have shown that TH-induced vasodilation was mediated *via* TRα and that T_3 caused rapid decrease of arterial pressure. Taken together, this suggests that noncanonical TRα signalling could mediate T_3-induced vasodilation. Studying $TR\alpha^{WT}$, $TR\alpha^{0}$ and $TR\alpha^{GS}$ mice will allow the identification of the underlying TR pathway. Furthermore, we aim to determine which mediators and cell types are involved in, and what impact long-term thyroid dysfunctions have on T_3-induced vasodilation.

(2) Hyperthyroidism can cause cardiac hypertrophy in humans and mice. Yet, inconsistent findings have been reported in regard to which receptor, TRα or TRβ, mediates cardiac growth in hyperthyroidism. Therefore, we aim to determine which TR and which pathway, canonical or noncanonical, mediates cardiac hypertrophy. Finally, we plan to identify key mediators of cardiac growth by comparing cellular changes such as cardiomyocyte size, gene expression of TH target genes and hypertrophy-associated genes as well as activation of proteins related to cardiac hypertrophy development.

(3) Hyper- and hypothyroidism are known to result in tachycardia and bradycardia, respectively. However, the investigation of unadulterated heart rate in mice is difficult as they are usually influenced by anaesthesia or stress-inducing handling of animals. Here, a radio telemetry approach was chosen in order to measure heart rate, body temperature and locomotor activity in conscious, freely moving mice. Thereby the contribution of canonical and noncanonical TRα signalling to these parameters should be clarified.

Materials and Methods

Materials

Chemicals

Table 1 - *Chemicals used in this study*

Chemicals	Supplier
10x PCR Rxn Buffer	Invitrogen/Life Technologies, Carlsbad, California, USA
10x T-EDTA buffer, pH 9.0	Zytomed Systems, Berlin, Germany
20x wash buffer for histology	Zytomed Systems, Berlin, Germany
3- (N-morpholino) propanesulfonic acid	Sigma-Aldrich, St. Louis, USA
3,3′,5-Triiodo-L-thyronine sodium salt (T_3)	Sigma-Aldrich, St. Louis, USA
Acetic acid, 99,7%	Sigma-Aldrich, St. Louis, USA
Agarose	Sigma-Aldrich, St. Louis, USA
Beta-mercaptoethanol	Sigma-Aldrich, St. Louis, USA
BlueJuice™ Gel Loading Buffer (10X)	Thermo Fischer Scientific Inc. Waltham, USA
Bovine Serum Albumin (BSA)	Sigma-Aldrich, St. Louis, USA
Calcium chloride ($CaCl_2x_2$ H_2O)	AppliChem, Darmstadt, Germany
Carbachol	Sigma-Aldrich, St. Louis, USA
Carbogen 5% CO_2/O_2	Air Liquide, Düsseldorf, Germany
Clarity Western ECL substrate	Bio-Rad, Munich, Germany
cOmplete Ultra, EDTA-free protease inhibitor	Roche, Berlin, Germany
Deoxy nucleotide mix	Invitrogen/Life Technologies, Carlsbad, California, USA
Depilatory creme	Balea, DM, Karlsruhe, Germany
Diethyl pyrocarbonate	Sigma-Aldrich, St. Louis, USA
DMSO	Sigma-Aldrich, St. Louis, USA
Entellan	Merck, Darmstadt, Germany
Eosin Y-solution 0.2 % aqueous	Sigma-Aldrich, St. Louis, USA
Ethanol (technical)	Pharmacy, UK Essen, Essen, Germany
Ethylenediaminetetraacetic (EDTA)	AppliChem, Darmstadt, Germany

Formafix, buffered formalin	Formafix Global Technologies Ltd., Düsseldorf, Germany
Formaldehyde solution 37,5%	Sigma-Aldrich, St. Louis, USA
GelPilot 100 bp Ladder	Qiagen, Hilden, Germany
Glucose	AppliChem, Darmstadt, Germany
Glycine	Carl Roth GmbH & Co. KG, Karlsruhe, Germany
Haemalaun (Mayer)	Merck, Darmstadt, Germany
Hematoxilin	Süsse Labortechnik, Gudensberg, Germany
Heparin-sodium 25000	Ratiopharm, Ulm, Germany
Hydrochloride acid (36.5-38.0%)	Sigma-Aldrich, St. Louis, USA
Hydrogen peroxide 35%	Carl Roth GmbH & Co. KG, Karlsruhe, Germany
Immu-Mount	Thermo Fischer Scientific Inc. Waltham, USA
Isopropanol (2-propanol)	Sigma-Aldrich, St. Louis, USA
LightCycler® 480 SYBR Green I Master Mix	Roche, Berlin, Germany
Magnesium chloride	Invitrogen/Life Technologies, Carlsbad, California, USA
Magnesium sulfate ($MgSO_4x7\ H_2O$)	AppliChem, Darmstadt, Germany
Methimazole (MMI)	Sigma-Aldrich, St. Louis, USA
N(G)-Nitro-L-arginine methyl ester (L-NAME)	MP biomedicals, Ohio, USA
Neoclear	Merck, Darmstadt, Germany
Neomount	Merck, Darmstadt, Germany
Norepinephrine bitartrate	Sigma-Aldrich, St. Louis, USA
Panthenol	Ratiopharm, Ulm, Germany
PaP Pen	Sigma-Aldrich, St. Louis, USA
Phosphate-buffered saline (PBS)	Gibco, Paisley, UK
PhosStop Phosphatase Inhibitor	Roche, Berlin, Germany
Potassium chloride (KCl)	AppliChem, Darmstadt, Germany
Potassium hydrogen phosphate (KH_2PO_4)	AppliChem, Darmstadt, Germany

Protein-Marker IX	VWR International GmbH, Langenfeld, Germany
RNase-Free Water	Qiagen, Hilden, Germany
Roti®-GelStain	Carl Roth GmbH & Co. KG, Karlsruhe, Germany
ROTI®Load RNA	Carl Roth GmbH & Co. KG, Karlsruhe, Germany
Rotiphorese A	Carl Roth GmbH & Co. KG, Karlsruhe, Germany
Rotiphorese B	Carl Roth GmbH & Co. KG, Karlsruhe, Germany
Saccharine	Sigma-Aldrich, St. Louis, USA
Saline	B.Braun, Melsungen, Germany
Sodium bicarbonate ($NaHCO_3$)	AppliChem, Darmstadt, Germany
Sodium chloride (NaCl)	AppliChem, Darmstadt, Germany
Sodium dodecyl sulfate (SDS)	Sigma-Aldrich, St. Louis, USA
Sodium hydroxide (NaOH)	Carl Roth GmbH & Co. KG, Karlsruhe, Germany
Sodium nitroprusside (SNP)	Sigma-Aldrich, St. Louis, USA
Sodium orthovanadate ($NaVO_4$)	Sigma-Aldrich, St. Louis, USA
Sodium perchlorate (ClO_{4-})	Sigma-Aldrich, St. Louis, USA
Taq DNA Polymerase, recombinant	Invitrogen/Life Technologies, Carlsbad, California, USA
Terg-A-Zyme enzyme detergent	Sigma-Aldrich, St. Louis, USA
Tris/Glycine/SDS-Puffer	Bio-Rad, Munich, Germany
Tris-Base	Sigma-Aldrich, St. Louis, USA
Tris-HCl	Sigma-Aldrich, St. Louis, USA
Tween20	Sigma-Aldrich, St. Louis, USA
Wortmannin	Sigma-Aldrich, St. Louis, USA
Xylol	AppliChem, Darmstadt, Germany

Buffers

Krebs-Henseleit buffer (KHB)	119 mM NaCl 4.7 mN KCl 2.5 mM $CaCl_2$x2 H_2O 1.17 mM $MgSO_4$×7 H_2O 25 mM $NaHCO_3$ 1.18 mM KH_2PO_4 0.027 mM EDTA 5.5 mM Glucose
Mouse biopsy lysis solution (B1; pH 12)	25 mM NaOH 0.02 mM EDTA
Mouse biopsy neutralisation solution (B2; pH 5)	40 mM Tris-HCl
Electrophoresis buffer (TAE)	40 mM Tris-Base 19.97 mM Acetic acid 0.97 mM EDTA
Immunoblotting wash buffer	19.81 mM Tris Base 200 mM NaCl 4.48 mM Tween20
RIPA Buffer	150 mM NaCl 50 mM Tris-HCl 1% Tergitol-type NP-40 0.5% Sodiumdeoxycholate 0.1% SDS 2 mM EDTA 50 mM Sodium flouride
Immunoblotting transfer buffer (TG)	24.76 mM Tris Base 191.82 mM Glycine
RNA electrophoresis buffer (pH 7)	20 mM MOPS 5 mM Sodium acetate 1 mM EDTA

Anaesthesia and analgesics

For echocardiography and *in vivo* blood pressure measurements mice were anesthetised with pentobarbital (20 mg/g body weight). Surgery in preparation of radio telemetry experiments was performed with a fully antagonisable anaesthesia (see Table 2), which offers the advantage of waking up the animals straight after finishing surgery and treating them with an analgesic (carprofen 5 mg/kg body weight).

Table 2 – *Fully antagoniseable anaesthesia for radio telemetry transmitter implantation*

		Agent [mg/g body weight]
Anaesthesia	Domitor 1 mg/mL	0.0005
	Midazolam 5 mg/mL	0.005
	Fentanyl 0,05 mg/mL	0.00005
Antagonist	Antisedan 5 mg/mL	0.00214
	Flumazenil 0,5 mg/5 mL	0.00043
	Naloxan 0,4 mg/mL	0.00103

Primer and Enzymes

Table 3 - *Genotyping primer for TRα and TRβ knock-out and mutant mice*

Strain	**Primer**	**5‘-3‘ Sequence**
TRαM	*TRα_71GS Fw*	GTTTTGGCCCCATCTAAGCC
	TRα_71GS Rv	AGCCGTGCCAGGTGAATTAG
TRαKO	*TRαWT Fw*	TCCTGAAGAGTGGGACCTGAT
	TRαWT Rv	GCCTTCTTACCAGGAATTTTCGC
	TRαKO Fw	GCATCGCCTTCTATCGCCTT
	TRαKO Fw	GAGGATGATCTGGTCTTCGCAA
TRβKO	*TRβWT Fw*	CCTCTCACCTTTCTACTTTGC
	TRβWT Rv	CAGGAATTTCCGCTTCTGCTT
	TRβKO Fw	TGAACCTATTATCTCGGGTCTTTCTC
	TRβKO Rv	GCCTCTTCGCTATTACGCCA

Table 4 – *List of qRT-PCR primers for gene expression analysis*

Gene	Forward	Reverse	Accession No.
Polr2a	CTTTGAGGAAACGGTGGATGTC	TCCCTTCATCGGGTCACTCT	NM_001291068
Myh6	CAGACAGAGATTTCTCCAACCCA	GCCTCTAGGCGTTCCTTCTC	NM_010856.4
Myh7	CACGTTTGAGAATCCAAGGCTC	CTCCTTCTCAGACTTCCGCA	NM_080728.2
Hcn2	CCAGTCCCTGGATTCGTCAC	TCACAATCTCCTCACGCAGT	NM_008226.2
Adrb1	GCCCTTTCGCTACCAGAGTT	ACTTGGGGTCGTTGTAGCAG	NM_007419.2
Adrb2	ACTTCTGGTGCGAGTTCTGG	GCTCTGGTACTTGAAGGGCG	NM_007420.2
ATP2a2	AACTACCTGGAACAACCCGC	TCATGCAGAGGGCTGGTAGA	NM_001110140.
Pln	TTCATGCTCTGCACTGTGACG	GCCAAATGTGAGCTGTCTTCT TTT	NM_001141927.1
Actc1	TAG CAC GCC TAC AGA ACC CA	GGATACCTCGCTTGCTCTGG	NM_009608.4
Bcl3	CTGAACCTGCCTACTCACCC	AGTATTCGGTAGACAGCGGC	NM_033601.3
Bax	TTTTGCTACAGGGTTTCATCCAG	TTCATCTCCAATTCGCCGGA	NM_007527.3
Prkcb	GGATTCCAGTGTCAAGTCTGCT	GGTCACAGAAGG TAG CA	NM_001316672.1
Pkb	GGATTCCAGTGTCAAGTCTGC T	GGTCACAGAAGGTAGCA	NM_008855.2
18s	CGGCTACCACATCCAAGGAA	GCTGGAATTACCGCGGCT	NR_003278.3
Ppia	CTTGGGCCGCGTCTCCTTCG	GCG TGTAAAGTCACCACCCTGGC	NM_008907.7
Gapdh	CCTCGTCCCGTAGACAAAATG	TGAAGGGGTCGTTGATGG C	NM_001289726.1

Taq DNA Polymerase (Invitrogen) was used for all polymerase chain (PCR) reactions and FastDigest *Eco32I* and *Mph1103I* (Thermo Fischer) were used for restriction of the TR^{GS} PCR products, allowing the distinction of mutated and WT alleles.

Technical devices

Table 5 - *Technical devices*

Device	Manufacturer
Autoclave VX-150	Systec, Linden, Germany
Bendelin Sonoplus HD 2070	Bandelin, Berlin, Germany
Biometra Compact electrophoresis chambers	Biometra, Jena, Germany

Dataquest A.R.T. exchange matrix	Data Science International, New Brighton; USA
Dataquest acquisition Card	Data Science International, New Brighton; USA
DSI PhysioTel® Transmitter (ETA-F10)	Data Science International, New Brighton; USA
Heraeus™ Fresco 17	Thermo Fischer Scientific Inc. Waltham, USA
Heraeus™ Megafuge™ 16R	Thermo Fischer Scientific Inc. Waltham, USA
Heratherm™ General Protocol Oven	Thermo Fischer Scientific Inc. Waltham, USA
IKA™ Vortex 4 Basic Small Shaker	IKA, Staufen, Germany
Kern EMB 100-3	Kern & Sohn, Balingen, Germany
LightCycler® 480 II	Roche, Berlin, Germany
Mini-PROTEAN® Tetra Vertical Electrophoresis Cell	Bio-Rad, Munich, Germany
Molecular Imager® VersaDoc™ MP 4000 system	Bio-Rad, Munich, Germany
Multi wire myograph system 620M	Danish Myo Technology, Aarhus, Denmark
NanoDrop 2000	Thermo Fischer Scientific Inc. Waltham, USA
Olympus BX51 microscope	Olympus, Waltham, USA
P25T Standard Power Pack	Biometra, Jena, Germany
PhysioTel® Receivers (RPC1)	Data Science International, New Brighton; USA
ProfessionalTrio Thermocycler	Biometra, Jena, Germany
SevenCompact pH meter	Mettler Toledo, Columbus, USA
SI-114A scale	Denver Instruments, Bohemia, USA
T 25 digital ULTRA-TURRAX®	IKA®-Werke GmbH & CO. KG, Staufen, Germany
Ultrasonic bath Sonorex	Bandelin, Berlin, Germany

VersaMax Microplate Reader	Molecular Devices, Biberach an der Riß, Germany
Water bath SW22	Julabo, Labortechnik GMBH, Seelbach, Germany

Antibodies

Table 6 - *Antibodies*

Antigene	Host	Supplier	Catalog#
Anti-mouse IgG HRP linked	Goat	Cell Signaling	7076S
Anti-Rabbit IgG HRP linked	Goat	Cell Signaling	7074S
CD31	Rabbit	Cell signalling	77699S
GAPDH	Mouse	Acris	ACR001P
GAPDH	Rabbit	Cell signaling	2118L
mTOR	Rabbit	Cell signaling	2972S
p44/42 MAPK (Erk1/2)	Rabbit	Cell signaling	4695S
P-mTOR (Ser2448)	Rabbit	Cell signaling	5536S
P-p-42/44 MAPK (Thr202/Tyr204) P-ERK	Rabbit	Cell signaling	4370T
P-S6 Ribosomal Protein (Ser235/236)	Rabbit	Cell signaling	2211S
S6 Ribosomal Protein	Mouse	Cell signaling	2317S

Kits

Table 7 - *Commercially available kits*

Kit	Manufacturer
BCA Protein Assay Kit	Thermo Fischer Scientific Inc. Waltham, USA
DAB Substrate Kit	Zytomed Systems, Berlin, Germany
Free T_3 ELISA	DRG Diagnostics GmbH, Marburg, Germany
Free T_4 ELISA	DRG Diagnostics GmbH, Marburg, Germany

QIAshredder	Qiagen, Hilden, Germany
RNeasy Mini Kit	Qiagen, Hilden, Germany
SuperScript™ III Reverse Transcriptase	Thermo Fischer Scientific Inc. Waltham, USA
SuperScript™ III Reverse Transcriptase	Invitrogen/Life Technologies, Carlsbad, California, USA
Total T_4 ELISA	DRG Diagnostics GmbH, Marburg, Germany
Zytochem Plus HRP Polymer Bulk Kit	Zytomed Systems, Berlin, Germany

Consumables

Table 8 - *Consumables*

0.2 mL reaction tubes	Biozym Biotech Trading, Wien, Austria
0.5 mL reaction tubes	Biozym Biotech Trading, Wien, Austria
1.5 mL reaction tubes	Eppendorf, Hamburg, Germany
2 mL reaction tubes	Eppendorf, Hamburg, Germany
Adhesion microscope slides SuperFrost Plus®	R. Langenbrinck GmbH, Emmendingen, Germany
BD Eclipse™ needle 23G	Becton Dickinson, Franklin Lakes, USA
BD Eclipse™ needle 25G	Becton Dickinson, Franklin Lakes, USA
BD Micro-Fine U-100 Insulin Syringe 0.5ml	Becton Dickinson, Franklin Lakes, USA
BRAND® pipette 1 mL	Sigma-Aldrich, St. Louis, USA
BD 2 Pc 2 mL Discardit II™ Syringe	Becton Dickinson, Franklin Lakes, USA
BD 2 Pc 10 mL Discardit II™ Syringe	Becton Dickinson, Franklin Lakes, USA
Cover slips 24x60 mm	Engelbrecht GmbH, Edermünde, Germany
Embedding cassettes	Süsse Labortechnik, Gudensberg, Germany
Greiner CELLSTAR® serological pipette 5 mL	Greiner bio-one, Essen, Germany
Greiner CELLSTAR® serological pipette 10 mL	Greiner bio-one, Essen, Germany
Greiner CELLSTAR® serological pipette 25 mL	Greiner bio-one, Essen, Germany
Greiner CELLSTAR® serological pipette 50 mL	Greiner bio-one, Essen, Germany
Greiner centrifuge tubes 15 mL	Greiner bio-one, Essen, Germany
Greiner centrifuge tubes 50 mL	Greiner bio-one, Essen, Germany

Immun-Blot® PVDF Membrane	Bio-Rad, Munich, Germany
LightCycler® 480 Multiwell Plate 96, white	Roche, Berlin, Germany
LightCycler® 480 Sealing Foil	Roche, Berlin, Germany
Microvette	Sarstedt, Nümbrecht, Germany
PARAFILM® M	Sigma-Aldrich, St. Louis, USA
Pipette tips 0.1-10.0 µL	Eppendorf, Hamburg, Germany
Pipette tips 2-200 µL	Sarstedt, Nümbrecht, Germany
Pipette tips 100-1000 µL	Sarstedt, Nümbrecht, Germany
Snap lid glasses	Carl Roth GmbH & Co. KG, Karlsruhe, Germany
Stainless steel wire 25 µm	Danish Myo Technology, Aarhus, Denmark
Tungsten wire 40 µm	Danish Myo Technology, Aarhus, Denmark
Whatman paper	
Microscope slides, SuperFrost	Thermo Fischer Scientific Inc. Waltham, USA
Cover slips 24x60 mm	Engelbrecht, Edermünde, Germany

Methods

Animal studies

TR^{KO} and TR^{GS} mouse strains

$TR\alpha^{0}$ and $TR\beta^{-}$ mice were acquired from the European Mouse Mutant Archive (https://www.infrafrontier.eu). $TR\alpha^{GS}$ and $TR\beta^{GS}$ mutant mice were created with a zinc finger nuclease approach as described previously (Hones *et al.* 2017). In short, the GS point mutations were introduced into the *Thra* (NM_178060.3) and *Thrb* (NM_001113417.1) gene *loci* of C57BL/6J mice. In addition, a silent mutation was created to generate an artificial restriction site for *Eco32I* (TRα) and *Mph1103I* (TRβ), respectively, allowing the distinction of mutated and native alleles during genotyping. To ensure comparability, all mice underwent backcrossing with C57BL/6J mice for at least 5 generations.

Animal housing

All mice and Lewis rats were housed in individually ventilated cages (IVC) at 21±1 °C in an alternating 12:12 hour light-dark cycle. Mice were bred and housed in the central animal facility at the University Hospital Essen, with standard chow (Sniff, Soest, Germany) and tap water provided *ad libitum*, unless chronic hypo- or hyperthyroidism was induced (see mouse *in vivo* studies; p 56). Mouse studies for radio telemetry measurements were performed in rooms with an inverse 12:12 hour light-dark cycle of the behavioural unit in the animal facility (Zentrales Tierlaboratorium, University Hospital-Essen) to ensure minimal disturbances during the measurement periods.

Genotyping of TR^{KO} and TR^{GS} mice

In order to investigate the role of canonical and noncanonical TR signalling, different mouse models were bred in heterozygous couples due to strong effects of TR deficient parent animals on their offspring (Srichomkwun *et al.* 2017; Alonso *et al.* 2007). Because of this, the genotype of all offspring had to be determined via PCR after birth. To do so 3-4 week old mice were marked with ear punches. Genomic DNA was extracted from the resulting skin piece by lysing cells in 75 µL of lysis buffer (B1, see 6.1.2.) for 45 min at 95 °C. Following the PCR reaction, the

solution was neutralised with the same amount of neutralisation buffer and thoroughly mixed (B2, see 6.1.2.).

Primers (5 pmol) for knockout or mutated TR gene loci were added to the PCR reaction mix together with 2 µL of the previously obtained genomic DNA (see table 8 and 9). After mixing and spinning down the content in the reaction tubes, PCR programs were run specifically for either TR^{KO} or TR^{GS} genotyping (see Table 10).

Table 9 - *TR^{KO} genotyping PCR recipe*

Ingredients	Amount
Nuclease free H_2O	11.7 µL
10 PCR Rxn Buffer	2.0 µL
$MgCl_2$ 50 mM	1.5 µL
dNTP 100 mM	0.4 µL
Primer WT Fw	0.5 µL
Primer WT Rev	0.5 µL
Primer KO Fw	0.5 µL
Primer KO Rev	0.5 µL
Taq	0.2 µL
Genomic DNA	2.0 µL
	20.0 µL

Table 10 - *TR^{GS} genotyping PCR recipe*

Ingredients	Amount
Nuclease free H_2O	12.7 µL
10 PCR Rxn Buffer	2.0 µL
$MgCl_2$ 50 mM	1.5 µL
dNTP 100 mM	0.4 µL
Primer GS Fw	0.5 µL
Primer GS Rev	0.5 µL
Taq	0.2 µL
Genomic DNA	2.0 µL
	20.0 µL

Table 11 - *TR^{KO} and TR^{GS} PCR program*

		TR^{KO}	TR^{GS}	
1	Initial denaturation	95 °C; 3 min	94 °C; 3 min	
2	Denaturation	95 °C; 15 sec	94 °C; 15 sec	*40 cycles*
3	Annealing	60 °C; 15 sec	62 °C; 10 sec	
4	Elongation	72 °C; 20 sec	72 °C; 20 sec	
5	Final elongation	72 °C; 2 min	72 °C; 2 min	
6		4 °C; ∞	4 °C; ∞	

Subsequently, 10 µL of the TR^{GS} PCR product underwent enzymatic restriction with 0.5 µL of *Eco32I* or *Mph1103I*. Ultimately, all resulting products were mixed with 2 µL of Blue Juice loading buffer (Thermo Fischer) and separated on a 2% agarose gel (w/v in TAE buffer). For identification of resulting bands on the gel, 3.5 µL of 100 bp DNA ladder was used. The gel was run at 110 V for 40 min. Results were visualised in a Molecular Imager® VersaDoc™ MP 4000 system (Bio-Rad).

Isometric tension measurement in a wire myograph system

Prior to isolation of arteries, Krebs-Henseleit-Buffer (KHB) was prepared as described above (see buffers) and pre-warmed to 37° C in a waterbath, where it was constantly fumigated with carbon dioxide gas. Mice were sacrificed by cervical dislocation, and the intestine was rapidly removed and placed in KHB. Perivascular tissue and veins were carefully removed, and arteries were cut into segments of 2 mm length. These segments were mounted on a 25 µm stainless steel wire and subsequently fastened between the jaws of a wire myograph chamber (Danish Myo Technology). Upon inserting a second wire, all ends were connected to the force transducer and micrometre, respectively. Femoral arteries were carefully prepared from both legs and placed in KHB where they were mounted on 40 µm tungsten wires and primed for vasomotor assays as described for mesenteric arteries. To obtain endothelium-free mesenteric arteries, Lewis rats were sacrificed under anaesthesia with enflurane, and their intestine was placed in KHB. Endothelial cells were removed with a cat whisker. Arteries were kept in carbonated KHB at all times in order to imitate a physiological milieu.

All arteries underwent normalisation according to the manufacturer's protocol to adjust the vessels to the same force (Kleinbongard, Schleiger, and Heusch 2013). Briefly, the tension was increased stepwise and adjusted to an inner lumen diameter the artery would have had *in vivo* at a transmural pressure of 100 mm Hg. Afterwards, arteries were equilibrated for 30 min while performing repeated buffer changes. During the normalisation process, inner and outer diameters of the arteries were determined by the software (LabChart Data, ADInstruments).

Viability and integrity of endothelial and muscle cell layers of isolated arteries

After equilibration at resting pressure, all arteries were analysed for the viability and integrity of the endothelial and muscle cell layer. First, maximal vasoconstriction (measured as active wall

tension in mN) was induced by repeated depolarisation with potassium chloride. Mouse mesenteric and femoral arteries were stimulated with 0.6×10^{-1} mol/L twice and 1.2×10^{-1} mol/L once for 2 min, respectively. Rat mesenteric arteries were stimulated with 1.2×10^{-1} mol/L KCl thrice. Between depolarisation steps, arteries were washed with multiple buffer changes until baseline force was reached again.

To test endothelial cell integrity, arteries were pre-constricted with noradrenaline (1×10^{-4} mol/L) until a stable plateau was reached for 2 min. Vasodilation was induced for 2 min with carbachol (1×10^{-4} mol/L), an endothelial-dependent vasodilator. Muscle cell integrity was induced *via* sodium nitroprusside dependent ($1x10^{-4}$ mol/L) vasodilation. The resulting vasodilation (Δ force [mN]) was normalised to maximum contraction with noradrenalin and expressed as percent. Specific quality criteria for further inclusion into the T_3 experiments are listed in Table 12.

Table 12 - *Inclusion criteria for isolated mouse and rat mesenteric arteries*

Criteria	Mouse	Rat	
		+ Endothelium	- Endothelium
Diameter [µm]	150 – 250	300 – 450 µm	300 – 450 µm
KCl Constriction [mN]	≥ 2	≥ 6 mN	≥ 6 mN
Endothelium-dependent (carbachol) relaxation of maximum constriction [%]	≥ 35%	≥ 80%	≤ 10%
Endothelium-independent (SNP) relaxation of maximum constriction [%]	≥ 60%	≥ 90%	≤ 80%

Thyroid hormone- stimulated vasodilation

T_3-induced vasodilation was measured in WT and TRα^0 arteries after pre-constriction with noradrenaline and adding increasing doses of T_3 (1×10^{-15} mol/L to 1×10^{-5} mol/L) in 2 min intervals for cumulative concentration response curves (CRC). The maximum extent of T_3-mediated vasodilation in WT, TRα^0 and TRα^{GS} mesenteric arteries was determined by stimulating vasodilation with 1×10^{-5} mol/L T_3 for 2 min.

CRCs in mouse femoral and rat mesenteric arteries ± endothelial cells ranged from 1×10^{-8} to 1×10^{-5} mol/L T_3. The potential role of the PI3K was investigated by pre-incubating mouse

mesenteric arteries with wortmannin ($1x10^{-7}$ mol/L) for 30 min and inducing vasodilation with T_3. Wortmannin and T_3 are not soluble in water, so the respective solvents were used as controls DMSO (0.005%) and NaOH (400 µM). The effect of eNOS in T_3-mediated vasodilation was examined by pre-incubating rat and mouse mesenteric arteries (30 min) with the eNOS-inhibitor L-NG-nitroarginine methyl ester (L-NAME, 10^{-4} mol/L). Here, CRCs were performed with T_3 doses between 1×10^{-8} to 1×10^{-5} mol/L.

Mouse in vivo studies

Study approval and declaration

All animal experiments were approved by the Landesamt für Natur, Umwelt und Verbraucherschutz Nordrhein-Westfalen (LANUV-NRW) and performed in accordance with the German regulations for Laboratory Animal Science (GVSOLAS) and the European Health Law of the Federation of Laboratory Animal Science Associations (FELASA) (reference number 84-02.04.2017.A157).

Induction of chronic hypo- and hyperthyroidism

To mimic thyroid dysfunctions, chronic hypo- and hyperthyroidism was induced in mice. Hyperthyroidism for wire myograph experiments was induced by adding 1 µg/mL T_4 to the drinking water for 3 weeks. To induce chronic hyperthyroidism for echocardiography studies, 400 ng/mL T_3 (Sigma-Aldrich, USA) was added to the drinking water for 7 weeks. This dosage was chosen to induce not a thyrotoxicosis but a mild hyperthyroidism comparable to patients (Chen *et al.* 2018). A hypothyroid state was reached by feeding mice a low-iodine diet (LID; TD.95007, Harlan Laboratories) and supplementing the drinking water with 0.02% methimazole, 0.5% sodium perchlorate (ClO_4^-) and 0.3% saccharine as sweetener for 3 weeks. A control diet was fed to control and hyperthyroid animals (TD.95007 with added potassium iodide (0.0012 g/kg); TD.97350). Radio telemetry studies were performed over a time span of 7 weeks, including 10-14 days of recovery after surgery. Subsequently, hypothyroidism was induced as described above, and hyperthyroidism was induced by adding 600 ng/mL T_3 to the drinking water.

In vivo arterial pressure measurement

For *in vivo* analysis of T_3-mediated vasodilation, a short surgery in anesthetised mice was performed. Mice were sedated with pentobarbital (80 mg/kg i.p.), which was confirmed by absent toe reflexes. During the whole procedure, heart rate and electrocardiography were recorded *via* subcutaneously placed ECG needles, and anaesthesia was maintained with additional doses when needed. Mice were intubated and ventilated with a respirator (Hugo Sachs Elektronik) and supplied with oxygen while they were kept at 37° C to reduce heat loss and hypoxia. Once the surgical stage of anaesthesia was reached, a small opening in the neck-abdomen area was made to gain access to the carotid artery and jugular vein. Then a small incision was made into the carotid artery, and a catheter with a saline-heparin solution (0.9% NaCl; 0.01% heparin) was carefully inserted. Upon connecting the catheter to a transducer, and thereby an interface, *in vivo* blood pressure could be recorded. Followed by the isolation of the jugular vein, the blood pressure was recorded for 4 min. Finally, a single dose of either T_3 (500 ng) or the corresponding amount of PBS (solvent control) was injected into the jugular vein, and blood pressure recording was continued for 4 min in the LabChart software (ADInstruments).

Implantation of radio telemetry transmitters

For *in vivo* measurements of heart rate, activity and temperature a radio telemetry system was used (Data Science International). Prior to the first implantation, transmitter electrodes of implantable transmitters (DSI PhysioTel® Transmitter (ETA-F10)) were cut to fit the mouse's measurements, and the ends were formed into loops (Figure 10a).

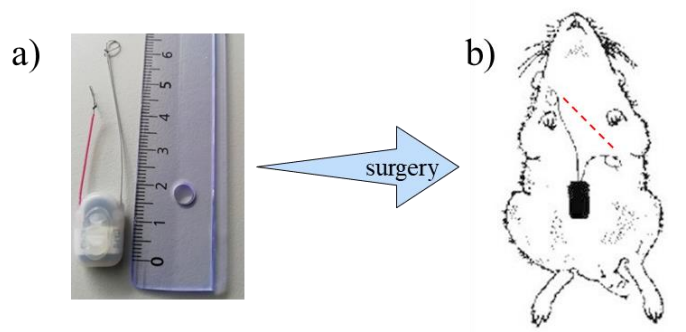

Figure 10: Scheme of radio telemetry transmitter implantation *via* surgery (Cesarovic *et al.* 2011) *a) Radio telemetry transmitter ETA-F10 has a length of approximately 1.5 cm and a weight of 1.5 g. The red (cathode) and white (anode) wire ends are formed into a loop for fixation during surgery. b) Sketch of implanted transmitter and position of electrode attachment.*

For surgery, all instruments were sterilised at 180 °C for 30 min. On the day of implantation, transmitters were thoroughly cleaned with ethanol and sterile PBS and then stored in sterile PBS. 4-5 month old mice with a minimal body weight of 25 g were anesthetised with fully

antagonisable anaesthesia (i.p., see Table 2) followed by a subcutaneous injection of carprofen (5 mg/kg BW). After hair was removed from the neck and abdominal region, mice were placed on a 37 °C warm heating plate to avoid hypothermia, and their eyes were covered with eye cream to prevent them from drying out during surgery. Once stable anaesthesia was confirmed by absence of reflexes, the surgery area was cleaned with a disinfectant. The abdomen was opened with a 2 cm incision and the neck with a 0.5 cm incision. One transmitter was taken from the sterile PBS and immediately placed into the abdominal cavity. The anode was tunnelled subcutaneously to the neck incision, where the loop was attached to a muscle with surgical thread. The cathode was attached to a muscle below the heart so that both electrodes formed a diagonal line over/near the heart for heart rate measurements (Figure 10b). Abdominal wall and skin were both closed with surgical stiches. Following surgery, mice were supplied with 15% glucose solution as drinking water and steeped food pellets of a control diet at the bottom of the cage. Mice were allowed to recover for 10-14 days and were treated with analgesic for 4 days. Body weight was recorded to monitor health of all animals.

Heart rate, body temperature and activity measurement via radio telemetry

Following surgery, mice were housed individually to reduce post-surgery complications (Figure 11). During the recovery period, hardware and software (Dataquest ART, DSI) were set up. The system consists of transmitters (DSI PhysioTel® Transmitter (ETA-F10)), an acquisition card (Dataquest acquisition Card), exchange matrix (Dataquest A.R.T. exchange matrix) and receiver plates (PhysioTel® Receivers (RPC1)). After connecting the computer carrying the acquisition card with the data exchange matrix (DEM 1/2) and thereby the receiver plates, each transmitter was configured with its transmitter type, individual serial number and the exact factory calibration values for ECG/EEG and temperature.

After a 14-day recovery period, the 3 day long euthyroid measurement started. Transmitters were activated by touching each mouse with a magnet and placing a telemetry receiver plate under each cage. Heart rate, body temperature and activity were constantly recorded, and, simultaneously, mean values of 30 second periods were saved. The measurement was stopped by touching the mice with the magnet again and the collected data were prepared for further examination in the Dataquest analysis program. After treating mice with hypothyroidism-inducing food and drinking water for 3 weeks, the recording was done as described above. Directly after measuring the mice in their hypothyroid state, the drinking water was changed to

induce hyperthyroidism without stopping the measurement. The hyperthyroid measuring period lasted for 6 days to investigate the transition from hypo- to early (day 1-3) as well as late hyperthyroidism (day 4-6). Ultimately, mice were sacrificed, and serum and tissues were collected. Transmitters were cleaned with 1% Terg-A-Zyme (Sigma) for 5-6 hours in a first step and then put in fresh solution overnight. Afterwards, they were thoroughly cleaned in PBS, dried and stored until further use.

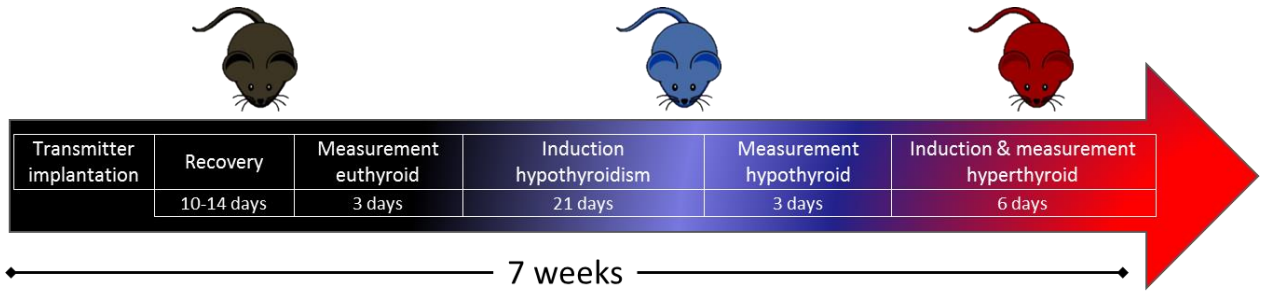

Figure 11: Experimental setup for radio telemetry experiments. *This study was performed over a time span of 7 weeks. After surgery, mice were treated with analgesic for four days and allowed to further recover for a total of 10-14 days. Afterwards, mice were measured in all three thyroid states: euthyroidism (3 days), hypothyroidism (3 days) and hyperthyroidism (6 days, divided into early and late hyperthyroidism). Thyroid dysfunction was induced via drinking water and food. Induction of hypothyroidism lasted for 21 days.*

Electrocardiography and echocardiography

Electrocardiography (ECG) and echocardiography analysis were performed with 15 week old mice in the framework of a broad scale phenotyping study at the German Mouse Clinic (GMC) in Munich. All mice were bred at the same time to ensure comparable age, and subsequently genotyped at the age of 3-4 weeks. 15 male and female $TR\alpha^{0}$, $TR\alpha^{GS}$ and their respective WT littermates ($\sum$ 120 animals), as well as 10 male and female WT, $TR\beta^{-}$ and $TR\beta^{GS}$ mice ($\sum$ 80 animals), were sent to the GMC at the age of 8 weeks *via* overnight shipping. Upon arrival, they were housed for 2 weeks before they entered the phenotyping pipeline. During this phenotyping pipeline, cardiovascular analysis in the form of electrocardiograms and echocardiography was performed.

This study was performed with euthyroid mice only. Whereas mice were anesthetised for echocardiography, they were conscious during ECG measurements. Here, electrocardiograms – voltage plotted versus time – were recorded to monitor the heart activity. By detecting small electrical changes, which represent the muscle de- and repolarisation of each cardiac cycle, the

heartbeat can be calculated (Farraj, Hazari, and Cascio 2011). All ECG parameters and their explanations are listed in Figure 12.

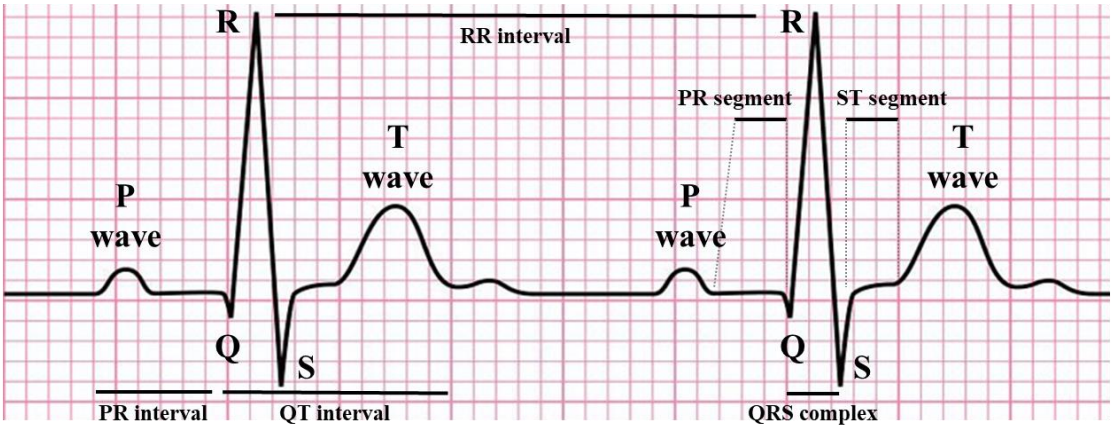

P wave	Depolarization of atria	**PR segment**	Time between onset of atrial and ventricular depolarization
QRS complex	Depolarization of the ventricles	**QT interval**	Duration of ventricle contraction
T wave	Repolarization of ventricles	**ST segment**	Isoelectric period of ventricles between depolarization and repolarization
RR interval	Time between two R waves (reciprocal to heart rate)		

Figure 12: Schematic representation of electrocardiograms (ECG) and the readout parameters. *During ECG the repeated de- and repolarisation is measured to assess heart functions. The cycle starts with the depolarisation of atria (P wave), followed by depolarisation (QRS complex) and repolarisation (T wave) of ventricles. The duration between the onset of atrial and ventricular depolarisation is described by the PR segment and the length of ventricle contraction by the QT interval. The isoelectric period between de- and repolarisation of ventricles is the ST segment. The time between two QRS complexes is referred to as RR interval, and its reciprocal is used to calculate heart rate.*

In our build-up study, euthyroid and hyperthyroid TRα and TRβ mice were analysed *via* echocardiography measurements over 7 weeks (Figure 13). Approximately 8-week-old male mice were divided into control and hyperthyroid groups. Echocardiography measurements were performed at day 1, after 3.5 weeks and after 7 weeks. In the first study cohort, TRα and TRβ deficient mice were treated with T_3 and investigated in order to determine which receptor mediates TH-induced cardiac hypertrophy. In the next step, the TRα or TRβ GS strain was included to determine whether this process is mediated by canonical or noncanonical signalling. Lastly, untreated mice of all previous groups were included to generate basal reference parameters. Prior to echocardiography, mice were anesthetised with pentobarbital (20 mg/g body weight), and hair was removed from the thorax region. Afterwards, mice were fixed on a movable and heatable investigation surface of the echocardiography device (Vevo2100,

VisualSonics) and examined with a 30 MHz ultrasound head for small animals (RMV-707B). Since the animals were anesthetised during the echocardiography investigation, the resulting heart rate values served as an inclusion criterion and internal control in this study. The so-called *M-mode* (M=motion) allows the two-dimensional depiction of motion sequences, as it shows the vertical amplitude of the ultrasound signal in relation to the time depicted horizontally. In addition, the following parameters can be extracted from the *M-mode* measurements: end diastolic and end systolic IVS, LVPW and left ventricular inner dimension (LVID). Furthermore, those parameters allow the calculation of fractional shortening, which describes the shortening of the left ventricular diameter between end-diastole and end-systole and ejection fraction, which refers to the amount of blood that is pumped out of the ventricle with each contraction. Echocardiography was performed by Prof. Dr. Kristina Lorenz (Leibniz-Institute for Analytical Sciences, Dortmund & Institute of Pharmacology and Toxicology, University of Wuerzburg).

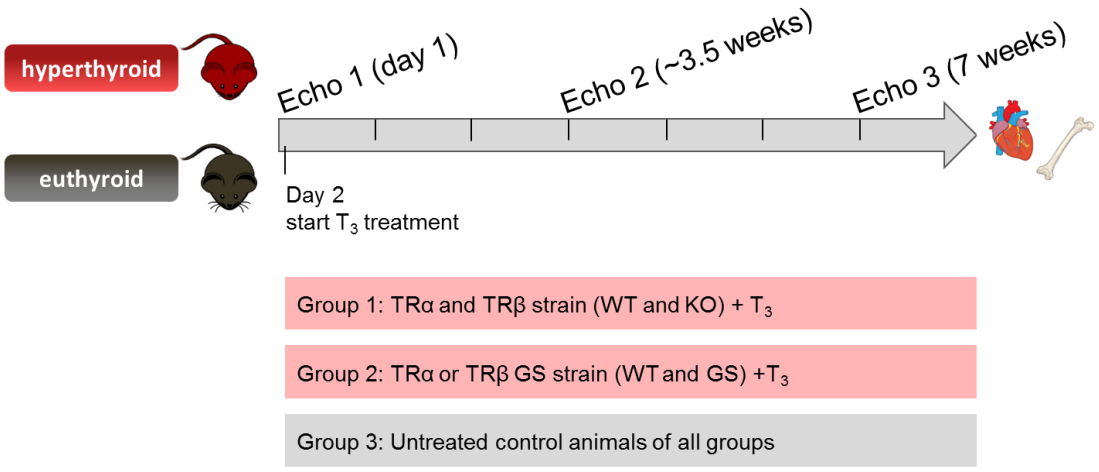

Figure 13: Echocardiography study design. 8-week-old *male mice were examined via echocardiography at experimental day 1 (Echo 1). From day 2 until the end of the experiment, they were treated with T_3 in the drinking water (400 ng/mL) or received tap water (control). Additional echo measurements followed after 3.5 (Echo 2) and 7 weeks (Echo 3) in the hyperthyroid group. The euthyroid control group was examined on day 1 (Echo 1) and after 7 weeks (Echo 3). Afterwards, mice were sacrificed, and organs were collected for further analysis and hypertrophy calculation.*

Post mortem tissue sampling

After concluding telemetry and echocardiography experiments, mice were sacrificed by cervical dislocation. First, body weight of all mice was noted for normalisations. Next, blood was quickly collected *via* heart puncture from the right ventricle and mice were perfused with 8-10 mL of PBS containing 5 U/mL heparin, followed by a second perfusion with PBS. For this study hearts

were removed, and to measure heart weights, both atria were removed, and ventricles were dried on a tissue before weighing them. Afterwards, hearts were divided, the upper part was stored in paraformaldehyde, and the lower part was cut in small pieces, frozen in liquid nitrogen and stored at -80 °C.

Lastly, tibia length was measured and later used for normalising heart weights, and then used to determine the state of cardiac hypertrophy. All samples were either fixed in paraformaldehyde and embedded in paraffin wax or stored at -80 C° until protein or mRNA isolation for biochemical analysis. In order to obtain serum for determination of T_3 and T_4 concentrations, blood was collected in Microvette® tubes for capillary blood collection (Sarstedt, Germany) and stored on ice for 30 min to induce coagulation. After centrifugation at 4 °C with 17.000×g for 25 min, serum was aliquoted and stored at -80 °C until TH level analysis.

Isolation of adult primary cardiomyocytes

Adult mouse cardiomyocytes were isolated as described before (Schmid *et al.* 2015). Briefly, cardiomyocytes were isolated by retrograde perfusion of mouse hearts and enzymatic dissociation of cells before they were stained and fixed on microscopy slides for further analysis. Cardiomyocyte isolation was performed in the group of Prof. Dr. Kristina Lorenz.

Histological analysis

Haematoxylin and Eosin staining

For cardiomyocyte evaluation, haematoxylin and Eosin (H&E) staining was conducted. For this, paraffin sections of 5 µm thickness were cut and dried at 37 °C overnight. Sections were treated with neoclear, a decreasing ethanol series and distilled water, before they were stained with haematoxylin and eosin. Followed by ethanol and neoclear incubation, sections were covered with neomount and cover slips. Nuclei appear violet/blue, whereas the cytoplasm is stained red/pink.

Immunohistochemistry

For immunohistochemistry analysis, samples were prepared as described in the previous section. Samples were deparaffinised in xylene, rehydrated in a series of decreasing ethanol concentrations and rinsed with water. Slides were placed in wash buffer (T-EDTA, pH 9.0) and

incubated at 95 °C for 45 min, washed and blocked with 3% H_2O_2 before the diluted antibody was added for incubation overnight. After washing and incubating samples with Poly HRP (Zytomed Systems, Berlin) for antigen staining, nuclei were stained with ZytoDAB and cellular structures were stained with haematoxylin. For dehydration, samples were treated with increasing concentrations of ethanol and xylene. Finally, Entellan (Merck, Darmstadt) was applied, and samples were concealed with a cover slip and examined with an Olympus BX51 microscope (Olympus, Waltham).

Nucleus staining of primary cardiomyocytes

After perfusion and enzymatic dissociation, cardiomyocyte nuclei were stained with Hoechst. In preparation, microscopy slides were coated with poly-L-lysine for better adhesion. Cells were fixed with 4% formaldehyde at room temperature for 15 min, washed with PBS once, incubated with Hoechst for 15 min and carefully rinsed with PBS, before a cover slip was added and the slides were dried at 4 °C overnight.

Biochemical analysis

Gene expression analysis via qRT-PCR

For gene expression analysis, total RNA was isolated from approximately 20-30 mg heart tissue with a commercially available kit (*QIAshredder* and *RNeasy Mini Kit*, Sigma). Upon homogenisation in 300 µL lysis buffer (*RLT buffer* containing beta-mercaptoethanol) using round bottom tubes and the ultra-turrax homogenizer, the protocol from the manufacturer was followed. The lysate was digested with 600 µL *proteinase K* (10 µL in 590 µL water) at 37 °C for 30 min, subsequently loaded onto *QIAshredder*™ columns and then centrifuged for 2 min at full speed for further cell lysis. One volume of 70% technical grade ethanol was added to each sample, and RNA was bound to the matrix of *RNeasy* columns by centrifugation (15 sec at full speed). After washing columns with 350 µL *RW1-buffer* (centrifuge for 15 sec at full speed), matrices were incubated with RNase free DNase solution (10 µL) in *RDD-buffer* (70 µL) for 15 min at RT. After an additional wash step with 350 µL *RW1-buffer* (15 sec at full speed), two wash steps with 500 µL *RPE-buffer* followed (first 15 sec and second 2 min at full speed). Next, columns were centrifuged for 1 min at full speed to remove residual buffer. For elution of total RNA, 20 µL RNase-free water were added on the matrices, incubated for 5 min and centrifuged for 1 min at

full speed. To enhance RNA yield, the eluate was loaded onto the column and the elution step was repeated.

Determination of RNA concentration and integrity

Total RNA was measured at a *NanoDrop2000* before an integrity analysis *via* electrophoresis. For this, a 1.2% agarose gel was prepared with RNA-free water (0.1-% diethyl pyrocarbonate and RNA electrophoresis buffer containing paraformaldehyde). 1 µg of total RNA in a volume of 2.5 µL was added to 7.5 µL RNA sample loading buffer (ROTI®Load RNA, Roth). Samples were incubated at 65 °C for 10 min before being loaded on the agarose gel which was run at 110 V for 40 min and visualised at a Molecular Imager® VersaDoc™.

Reverse transcription of RNA to cDNA

1 µg of total RNA from each sample was transcribed into cDNA by using a SuperScript™ III Reverse Transcriptase kit (Invitrogen) and random hexamer primers. In a total volume of 10 µL nuclease free water, 2 µL random hexamers, 1 µL dNTPs and the required amount of RNA were incubated at 65 °C for 5 min and afterwards cooled down to 4 °C. 10 µL of cDNA synthesis master mix consisting of 2 µL 10× RT Buffer, 4 µL 25 mM $MgCl_2$, 0,1 M DTT, 1 µL RNAseOut™ and 1 µL SuperScript® were added to the reaction tube and incubated at 25 °C for 10 min. Followed by 50 min of incubation at 50 °C, the reaction was terminated at 85 °C for 5 min. Finally, 1 µL of RNase H was added to the reaction and incubated at 37 °C for 20 min to digest all residual RNA in the mix.

The resulting cDNA was then used for qRT-PCR. To test primer efficiency, a pooled RNA sample from all groups was created and transcribed with all other samples and included on all qRT-PCR plates. For qRT-PCRs, Roche SYBR Green I Master mix was used. 2.5 µL of cDNA (1 ng/µL) 5 µL of SYBR Green I Master Mix, 2.4 µL nuclease free water, and 0.05 µL of respective forward and reverse primers (100 pM) were mixed and pipetted into a 96-well plate, before running the PCR program in a light cycler LC480® (Roche) (see Table 13).

Table 13 - *qRT PCR program*

Step	Temperature	Duration	
Melting	95 °C	5 min	*40 cycles*
Melting	95 °C	15 sec	

Annealing	60 °C	10 sec
Extension	72 °C	20 sec

First, the homogeneity of euthyroid control and T_3-treated hyperthyroid WT samples was tested with one reference gene (*Polr2a*) and two TH target genes (*Myh6* and *Myh7*). This was done to create pooled WT groups to use on all further gene analysis plates, allowing the comparison of all groups, which would not be possible if they were done on different qRTC plates. In all further gene analysis three reference genes were used (*18S*, *Gapdh* and *Pol2a*2). For analysis and calculation of gene expression fold change, only Ct values below 35 cycles were evaluated using the efficiency corrected method (Pfaffl 2001). All primer sequences are listed in Table 4.

Immunoblot analysis

Protein isolation

20-30 µg of heart tissue were placed in RIPA buffer with phospho-stop and EDTA and shredded, resulting in a homogenous solution. All samples were centrifuged and transferred to a reaction tube and treated with an ultrasonic probe. Samples were placed on ice to shake for 10 min and centrifuged to separate the cell lysate into protein solution and cell debris. The supernatant was transferred to a fresh reaction tube, snap frozen in liquid nitrogen and stored at -80 °C.

SDS-PAGE and immunoblot assays

Prior to immunoblots the amount of protein was determined with a commercial BCA Protein Assay Kit (Thermo, Waltham), and the corresponding amount of 20 µg of protein was separated on an SDS PAGE gel. Proteins were transferred to a polyvinyl difluoride membrane (Roti-Fluoro® PVDF, Roth) for 16-18 hours at 15V in a tank blotter (BioRad). After blocking with either 5% non-fat milk in TBS-T (Tris-buffered saline with 150 mM NaCl, 0.5% Tween20 and pH 7.4) or 5% bovine serum albumin (BSA) in TBS-T, membranes were incubated with antibodies against the phosphorylated and total proteins listed in Table 6. Membranes were incubated with primary antibodies for 18 hours, washed in TBS-T and incubated with respective horseradish peroxidase-labelled secondary antibodies for 90 min. Membranes were coated with ECL Western Blotting Substrate and bands were visualised with a VersaDocMP4000 (BioRad),

and densities of proteins of interest were normalised to GAPDH density using Image Lab software (BioRad). Upon normalisation phosphorylated/total protein amount was calculated.

Thyroid hormone serum concentration tests (ELISA)

TH serum levels were measured with commercial fT_3, fT_4 and TT_4 ELISA kits according to the manufacturer's instructions (DRG Instruments GmbH, Marburg). As standards, serum samples with known TH concentrations were used. According to the manufacturer, minimum detectable levels of TH are 0.5 µg/dL for TT_4, 0.05 ng/dL for fT_4 and 0.05 pg/mL for fT_3. Lastly, samples were measured with a VersaMax Microplate Reader (Molecular Devices, Biberach) and TH levels were calculated.

Statistics and software

Acquisition of wire myograph results was done with Labchart 6 (ADinstruments, Dunedin, New Zealand). For telemetry measurements, Dataquest A.R.T. 4.2 (Advanced Research Technology) from DSI (Data Science International, New Brighton; USA) was used. Figures were designed using infographics from https://smart.servier.com/.

Data analysis was done with GraphPad Prism 6 (GraphPad, San Diego, USA). Presentation of data is mean ± standard error of mean (SEM). All data sets were tested for normality and subsequently analysed for significance *via* one-way ANOVA with Tukey‘s multiple comparison test for comparison of all groups, Sidak’s multiple comparison test for comparison of selected groups and Dunnett’s multiple comparison test for comparing all groups to one reference group. Alternatively, two-way ANOVA with Bonferroni‘s *post hoc* correction was used for dose response curves. Differences were considered significant with $p<0.05$. Data sets without normal distribution were analysed *via* Mann-Whitney unpaired t-test.

Results

Effects of thyroid hormones on arterial pressure regulation

TH are crucial for development and regular function of the cardiovascular system, and exert multiple effects on heart rate, heart muscle development and maintenance of arterial pressure (Cappola *et al.* 2019; Berta *et al.* 2019). Acute and chronic TH effects on the vasculature have been demonstrated in the past. However, the underlying mechanism, especially the type of TR signalling, is not yet fully understood (Liu *et al.* 2014; Gachkar *et al.* 2019). In order to investigate TH influence on arterial pressure, *in vitro* vasodilation of mouse mesenteric arteries and *in vivo* blood pressure responses to T_3 were examined. The underlying mechanism of T_3-induced vasodilation was investigated by analysing $TR\alpha^{WT}$, $TR\alpha^{0}$ and $TR\alpha^{GS}$ mesenteric arteries, comparing mesenteric and femoral arteries, identifying the role of eNOS and PI3K with specific inhibitors and determining the role of endothelial and muscle cells in T_3-mediated vasodilation (Kleinbongard, Schleiger, and Heusch 2013; Cai *et al.* 2015; Toral *et al.* 2018). Chronic effects of thyroid dysfunctions on arteries were identified by comparing vasodilation in mesenteric arteries from hypo- and hyperthyroid mice, which was confirmed by TH serum level analysis (Engels *et al.* 2016). T_3 effects on blood pressure regulation were investigated *in vivo* through blood pressure measurements in $TR\alpha^{WT}$, $TR\alpha^{0}$ and $TR\alpha^{GS}$ mice. To determine the mode of action that caused blood pressure reduction, a catheter was inserted into the carotid artery and blood pressure was recorded prior and in response to T_3/solvent injections (Hiroi *et al.* 2006).

T_3-induced vasodilation is mediated by noncanonical TRα action in vitro

Vascular responses to T_3 were investigated in mesenteric arteries from $TR\alpha^{WT}$ and $TR\alpha^{0}$ mice by stimulating them with T_3 in a wire myograph system. Mesenteric arteries were pre-constricted with noradrenalin and stimulated with increasing doses of T_3, and vasodilation of intact arteries was calculated as % after constriction. Interestingly, T_3 caused increasing vasodilation in $TR\alpha^{WT}$, but not in $TR\alpha^{0}$ arteries (Figure 14a). To identify if this process is caused by canonical or noncanonical TRα signalling, T_3-mediated vasodilation in arteries from $TR\alpha^{WT}$, $TR\alpha^{0}$ and $TR\alpha^{GS}$ mice was compared. Here, only the highest T_3 dose (10^{-5} mol/L) was added for 2 min. In solvent treated control arteries, only a slight decrease of tension was observed (≈5%), but already within

2 min after T_3 treatment $TR\alpha^{WT}$ arteries showed a relaxation. As previously demonstrated in the dose response curve, no T_3-induced vasodilation occurred in $TR\alpha^0$ arteries (Figure 14b). In arteries from $TR\alpha^{GS}$ mice, however, the effect was almost fully preserved and was comparable to $TR\alpha^{WT}$ arteries. In all wire myograph experiments, only arteries with a responsive endothelium and muscle cell layer, proven by carbachol and SNP dependent vasodilation, were used (see Table 12).

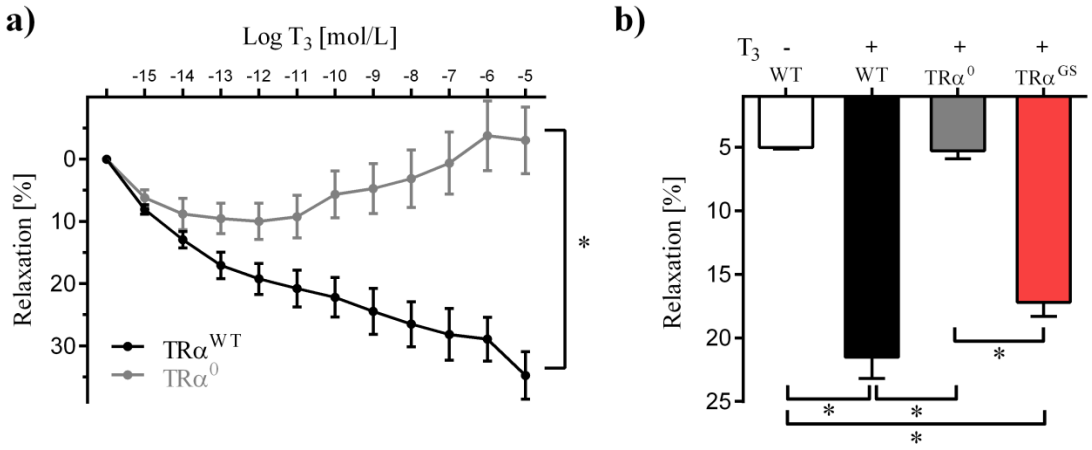

Figure 14: T_3-mediated vasodilation in mesenteric arteries is a noncanonical TRα effect *in vitro*. *a) Concentration response curve with increasing T_3 doses (1×10^{-15} to 1×10^{-5} mol/L) in $TR\alpha^{WT}$ (black, n=9) and $TR\alpha^0$ (grey, n=6) mouse mesenteric arteries (two-way repeated ANOVA with Bonferroni's multiple comparison test). b) Relaxation 2 min after stimulation with either solvent control (NaOH $4*10^{-6}$ mol/L; n=6) or 10^{-5} mol/L T_3 in mesenteric arteries from WT (black, n=15), $TR\alpha^0$ (grey, n=6) and $TR\alpha^{GS}$ (red, n=18) mice (one-way ANOVA with Tukey's multiple comparison test). Values are mean ± SEM; * $p < 0.05$.*

T_3 causes rapid decrease of arterial pressure via noncanonical TRα action in vivo

In addition to this *ex vivo* measurement, we investigated T_3 effects on the vascular tone *in vivo* in order to understand if these TH/TR-mediated effects have physiological relevance. Arterial blood pressure was measured in response to T_3 or solvent with a catheter in the carotid artery in $TR\alpha^{WT}$, $TR\alpha^0$ and $TR\alpha^{GS}$ mice. Already within one minute after T_3 injection into the jugular vein, blood pressure of WT mice decreased significantly (Figure 15a). This T_3-mediated decrease of arterial pressure was absent in $TR\alpha^0$ mice, (Figure 15d), confirming the previous *in vitro* experiments. Notably, the decrease of arterial pressure was fully preserved in $TR\alpha^{GS}$ mice, (Figure 15g), which demonstrates *in vivo* that this T_3/TRα effect is independent from DNA-binding of TRα.

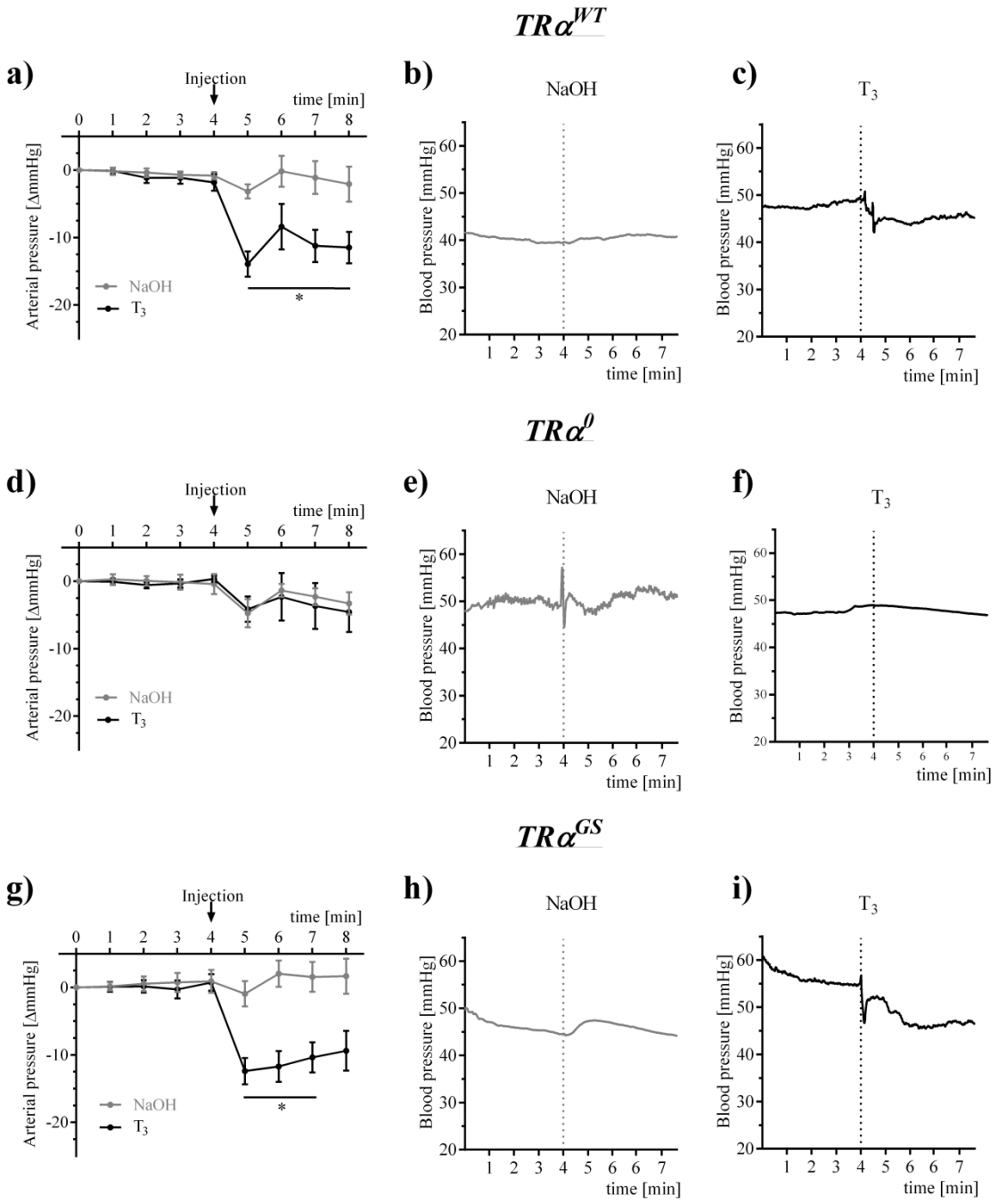

Figure 15: T_3-mediated reduction of arterial pressure is a noncanonical TRα effect *in vivo*. *Arterial pressure measurement was conducted through a catheter in the carotid artery and either 500 ng T_3 (black) or solvent control (PBS, grey) doses were injected into the jugular vein after recording a stable plateau of 4 min. After the respective injections, measurement was continued for 4 min. Mean reductions of arterial pressure in response to solvent and T_3 injections are shown in the left panel, and exemplary original recordings are shown in the middle and right panel. a-c) $TR\alpha^{WT}$ mice, d-f) $TR\alpha^{0}$ mice and g-i) $TR\alpha^{GS}$ mice. (n=3-5) (Mann-Whitney unpaired t-test for data sets with no normal distribution. Values are mean ± SEM; * $p < 0.05$).*

Exemplary original recordings of one mouse per treatment and genotype illustrate the rapidity of the T_3 effect in comparison to the solvent control injection as well as the absence of blood pressure reduction in $TR\alpha^0$ mice. Reactions to injections were individual for each mouse and caused rapid peaks in some animals, whereas in others injection altered the curve progression only slightly. Importantly, the PBS injection effect which can for example be observed in $TR\alpha^{GS}$ mice is only temporary, whereas T_3 injections had lasting effects in $TR\alpha^{WT}$ and $TR\alpha^{GS}$ mice (Figure 15 middle and right panel).

Influence of thyroid state on T_3-mediated vasodilation

To examine how long-term thyroid dysfunctions influence the reactivity of mesenteric arteries to T_3, mice were rendered hypothyroid with low-iodine diet and MMI/ClO_4- in the drinking water, and hyperthyroidism was induced with T_4 in the drinking water for 3-4 weeks.

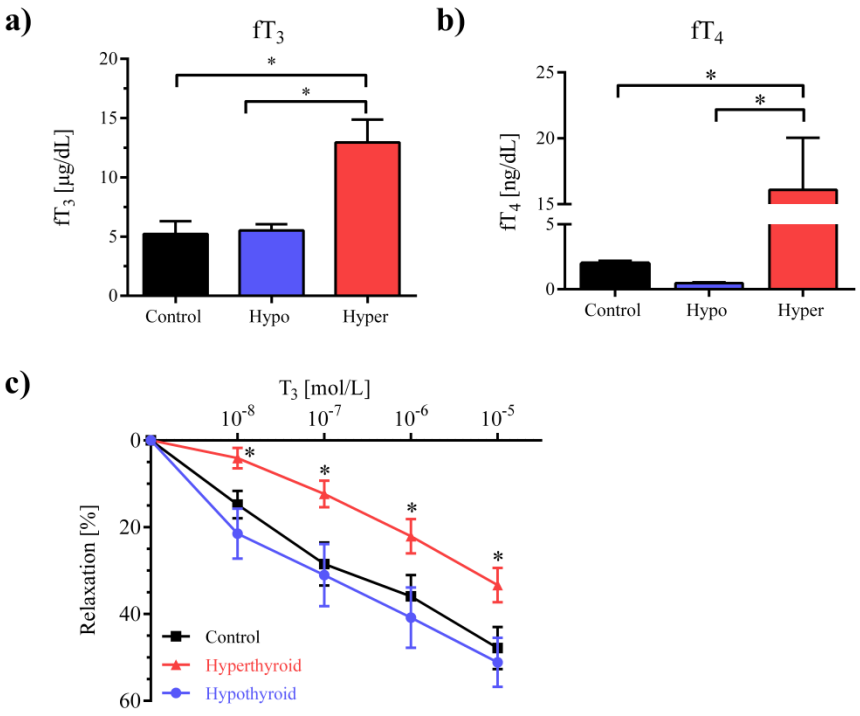

Figure 16: Thyroid dysfunctions affect T_3-mediated vasodilation in mesenteric arteries. *a + b) fT_3 and fT_4 values from untreated as well as hypo- and hyperthyroid mice (one-way ANOVA with Tukey's multiple comparison test).* c) *Concentration response curve with increasing T_3 doses (1×10^{-8} to 1×10^{-5} mol/L) in WT mouse mesenteric arteries from euthyroid control (black, n=8) mice in comparison to hypo- (hypo, blue, n=8) and hyperthyroid (hyper, red, n=13) mice after three weeks of treatment (two-way repeated ANOVA with Bonferroni's multiple comparison test). Values are mean ± SEM; * $p < 0.05$.*

Subsequently, mesenteric arteries were isolated and investigated. The successful induction of chronic hypo- and hyperthyroidism was proven by serum TH level analysis via ELISAs. Here, free T_3 levels were unaltered in hypo- but 2.5-fold higher in hyperthyroidism (Figure 16a). Free T_4 levels were strongly reduced in hypothyroid mice, whereas they were significantly increased in hyperthyroid mice, showing that the induction of hypo- and hyperthyroidism was successful (Figure 16b). Interestingly, mesenteric arteries from euthyroid and hypothyroid mice were well responsive to T_3. Pre-constricted arteries dilated 15% and 20% 2 minutes after treatment with 10^{-8} M T_3 (Figure 16a). A maximum dilation of approximately 50% was observed with 10^{-5} M T_3. In contrast, arteries from hyperthyroid mice dilated only 5% at the lowest T_3 dose with a maximal response of 33%. These results demonstrate that the vasodilatory effects are preserved in long-term hypothyroidism.

T_3-mediated vasodilation is similar in different artery entities and suggests a general mechanism

To determine whether T_3-mediated vasodilation is an effect found only in mesenteric arteries or applies to other arteries as well, we studied femoral arteries which differ from mesenteric arteries in size and morphology (Figure 17a,b). Mesenteric and femoral arteries have different diameters, and femoral arteries are marked by a thicker muscle cell layer, whereas the endothelial cell layer is similar in both entities, causing different vasomotor reactivity. Nonetheless the vasodilatory response to T_3 was similar in both entities (Figure 17c). Thus, the T_3 effect on vasodilation is not restricted to mesenteric arteries, suggesting a general mechanism.

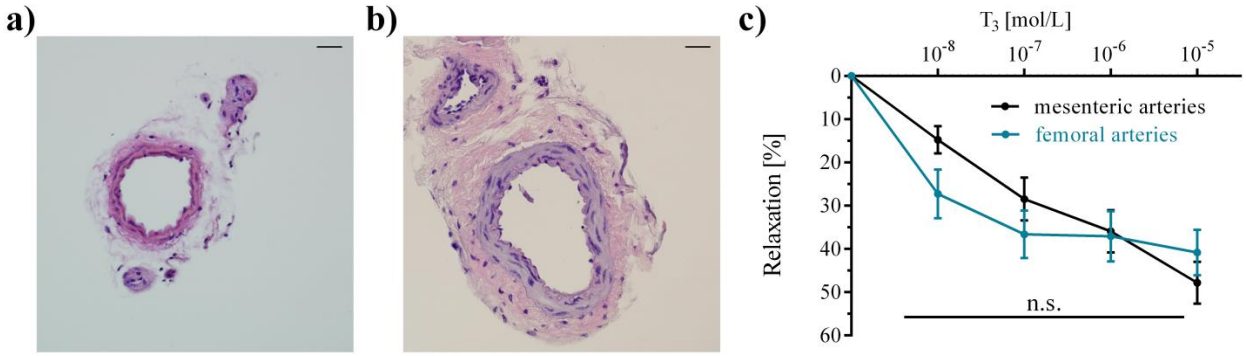

Figure 17: T_3-mediated vasodilation is similar in mesenteric and femoral arteries. *Haematoxylin and eosin staining of a) mouse mesenteric artery, b) mouse femoral artery (40x magnification; scale bar represents 50 µm) and* c) *Concentration response curve with increasing T_3 doses (1×10^{-8} to 1×10^{-5} mol/L) in WT mouse mesenteric (black, n=10) and femoral arteries (turquoise, n=8) (two-way repeated ANOVA with Bonferroni's multiple comparison test). Values are mean ± SEM; n.s.=not significant.*

PI3-kinase and eNOS in endothelial cells contribute to T_3-induced vasodilation

Next, the role of different cell types in T_3-induced vasodilation was examined. To find out whether the main effect occurs in the endothelium or in the muscular layer or are evenly distributed, rat arteries with an intact endothelium were compared with endothelium denuded arteries. In concentration response curves of pre-constricted rat mesenteric arteries, a remarkable difference between whole and denuded arteries was observed. Whereas T_3 caused strong vasodilation in whole arteries (black curve), this effect was abolished in arteries without endothelium (blue curve), proving its crucial role in vasodilation (Figure 18a).

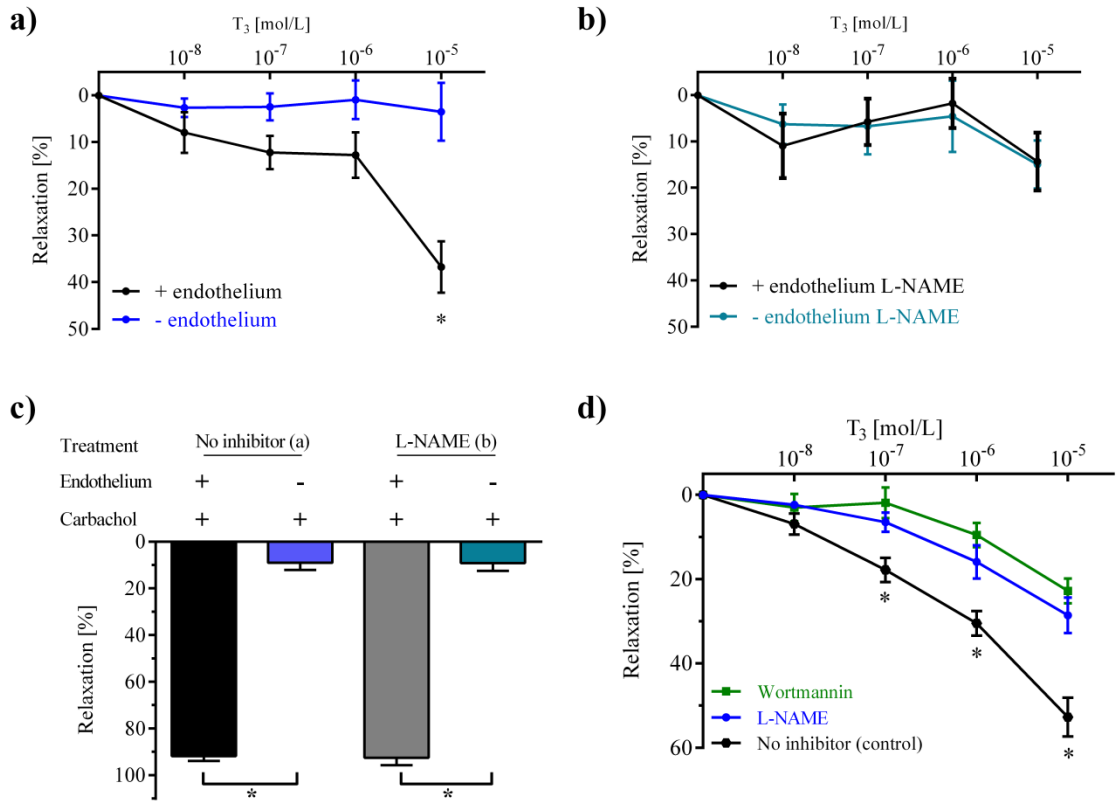

Figure 18: T_3-mediated vasodilation depends on eNOS and PI3K activation in the endothelium. *a) T_3 dose response curve in rat mesenteric arteries with endothelium (black; n=9) and without endothelium (blue, n=7). b) T_3 dose response curve in whole (black, n=6) and endothelium-free (turquoise, n=6) rat mesenteric arteries after eNOS inhibition (100µM L-NAME) (two-way repeated ANOVA with Bonferroni's multiple comparison test). Values are mean ± SEM; * p < 0.05. c) Endothelium-dependent vasodilation stimulated with carbachol in whole (black/grey) and endothelium-free (blue/turquoise) rat mesenteric arteries used in (a) and (b) demonstrates the successful removal of endothelial cells (one-way ANOVA with Sidak's multiple comparison test; endothelium vs. no endothelium). Values are mean ± SEM; *<0.05. d) T_3 concentration response curve (1×10^{-8} to 1×10^{-5} mol/L) in WT control (black, n=9) and L-NAME (10^{-4} mol/L, blue, n=6) or wortmannin (10^{-7} mol/L, green, n=7) pre-treated mouse mesenteric arteries (two-way repeated ANOVA with Bonferroni's multiple comparison test). Values are mean ± SEM; * p < 0.05.*

Additionally, the role of eNOS was examined in rat mesenteric arteries. Here, eNOS inhibition (turquoise curve) abolished the difference between whole and denuded arteries, indicating that eNOS is a key mediator of T_3-induced vasodilation in rat mesenteric arteries (Figure 18b). The successful removal of endothelial cells was confirmed *via* the endothelium-dependent dilator carbachol. Whereas intact pre-constricted arteries dilated up 85% in response to carbachol, endothelium denuded arteries only reached less than 10% (Figure 18c). These results demonstrate that T_3-induced vasodilation requires the intact endothelial cells layer and the NO-producing enzyme eNOS.

Subsequently, the role of eNOS was confirmed in mouse mesenteric arteries and expanded by the investigation PI3-kinase by blocking their respective actions with specific inhibitors. Here, untreated pre-constricted mouse mesenteric arteries (black curve) responded to T_3 in a dose dependent manner up to 53%, whereas eNOS inhibition by L-NAME (blue curve) reduced this effect to 29%, and PI3K inhibition with wortmannin (green curve) caused a slightly stronger reduction to 23%. This finding suggests that both eNOS and PI3K play a role in T_3-mediated vasodilation in mice (Figure 18d). Taken together, this proves that eNOS and PI3K in the endothelium are crucial for T_3-induced vasodilation, and furthermore, comparable mechanisms are present in mice and rats.

Thyroid hormone impact on cardiac hypertrophy development

Heart development and function are strongly affected by TH levels, and both chronic hypo- and hyperthyroidism affect the cardiovascular system negatively if left untreated (Danzi and Klein 2020; Razvi *et al.* 2018). Whereas hypothyroidism can lead to atherosclerosis and thus reduced functionality of the vasculature, hyperthyroidism can result in cardiac hypertrophy and consequently impaired heart function (Billon *et al.* 2014; Capettini *et al.* 2011; Dillmann 2010). TH-induced cardiac hypertrophy has been studied in different TR mutant mouse models. While some studies suggested that TH-induced cardiac hypertrophy is mediated by TRβ, others put forward that TRα is the receptor responsible for cardiac functions (Weiss *et al.* 2002; Imperio *et al.* 2015; Kinugawa *et al.* 2005). At the same time, it is still unclear whether canonical or noncanonical TR signalling causes hypertrophy. Nonetheless, in previous studies hypertrophy pathway activation (AKT, mTOR, ERK) and the time needed for these activations were investigated, and it was implied that noncanonical signalling might be the underlying mechanism (Kuzman *et al.* 2005; Kuzman, O'Connell, and Gerdes 2007; Kenessey and Ojamaa 2006). Nevertheless, this has never been studied with a suitable mouse model. Here we compared euthyroid and hyperthyroid $TR\alpha^{WT}$, $TR\alpha^{0}$, $TR\beta^{WT}$ and $TR\beta^{-}$ as well as TR^{GS} mice in an echocardiography study to determine a) the responsible TR isoform and b) the underlying mechanism of TH-induced cardiac hypertrophy. The required induction of mild hyperthyroidism state was confirmed by TH serum level analysis. Echocardiography, as well as *ex vivo* heart weight analysis, yielded significant results.

Analysis of basal heart functions in euthyroid male and female mice by electrocardiography

At the age of 15 weeks, cardiac parameters of euthyroid male and female TRα and TRβ mice were examined *via* echocardiography in the GMC. However, no significant differences were observed between WT and TRα or TRβ knockout or mutant mice (Table 14). Although some variations can be observed in heart rates, these differences are not significant and should be interpreted carefully as the animals were anesthetised. None of the examined functional parameters such as ejection fraction, fractional shortening or stroke volume yielded any differences in the compared groups. These findings demonstrate that in euthyroid unconscious mice, heart function does not differ between the genotypes in either male or female mice.

Table 14 - Echocardiography analysis of heart function and morphology in euthyroid TRα and TRβ mice. *Euthyroid male and female mice (n=10-15) were anesthetised, examined via echocardiography and compared within the respective genotype sex groups (e.g. male $TR\alpha^{WT}$ vs. $TR\alpha^{0}$, $TR\alpha^{WT}$ vs. $TR\alpha^{GS}$). Heart rate, body weight, ejection fraction, fractional shortening, corrected left ventricular mass (LV mass corr.) as well as end-diastolic interventricular septum wall thickness (IVS;d), left ventricular posterior wall thickness (LVPW;d) and left ventricular inner diameter (LVID;d) and stroke volume were recorded. (one-way ANOVA with Sidak's multiple comparison test). Values are mean ± SEM; * p < 0.05.*

	Male							Female						
	$TR\alpha^{WT}$	$TR\alpha^{0}$	$TR\alpha^{WT}$	$TR\alpha^{GS}$	$TR\beta^{WT}$	$TR\beta^{-}$	$TR\beta^{WT}$	$TR\beta^{GS}$	$TR\alpha^{WT}$	$TR\alpha^{0}$	$TR\alpha^{WT}$	$TR\alpha^{GS}$	$TR\beta^{WT}$	$TR\beta^{GS}$
Heart Rate [bpm]	515±36	512±38	439±46	537±38	502±55	364±40	309±29	311±47	471±48	545±38	561±41	561±38	309±40	311±19	476±61	443 ±55
Body weight [g]	27.6±0.58*	23.4±0.58*	27.4±0.30	25.9±0.43	29.0±0.57	26.4±0.68	27.1±0.60	25.1±0.95	22.4±0.40	22.2±0.34	23.1±0.55	21.9±0.40	21.3±0.16	21.5±0.70	20.1±0.28	20.1±0.64
Ejection fraction [%]	75.3±3.6	74.6±3.7	70.2±2.6	72.0±3.0	77.0±3.7	74.0±3.5	74.7±3.3	80.1±3.8	81.8±1.7	73.8±3.4	82.8±2.4	78.9±2.0	75.5±2.3	77.2±3.1	83.4±3.5	86.1±2.1
Fractional shortening [%]	44.6±3.1	43.2±3.3	39.0±2.0	40.6±2.4	45.4±3.4	42.6±3.3	43.1±2.9	49.1±3.6	49.3±1.8	42.0±2.7	51.0±2.7	46.5±2.2	43.4±2.0	46.0±3.5	52.4±3.9	54.7±2.6
LV mass corr. [mg]	36.6±2.9	30.2±2.6	35.3±2.4	31.4±2.5	30.6±3.0	33.9±3.5	35.7±2.9	32.9±4.6	28.4±1.9	27.6±2.3	26.3±2.3	25.5±1.5	36.9±2.6	41.0±3.9	27.3±3.1	25.5±2.7
IVS;d [mm]	0.55±0.01	0.55±0.01	0.55±0.01	0.55±0.01	0.55±0.01	0.55±0.01	0.54±0.01	0.54±0.01	0.55±0.01	0.55±0.01	0.54±0.01	0.53±0.01	0.57±0.01	0.56±0.01	0.55±0.01	0.55±0.01
LVPW;d [mm]	0.54±0.01	0.54±0.01	0.54±0.01	0.54±0.01	0.54±0.01	0.55±0.01	0.54±0.01	0.54±0.01	0.53±0.01	0.54±0.01	0.54±0.01	0.54±0.01	0.54±0.01	0.55±0.01	0.55±0.01	0.54±0.01
LVID;d [mm]	3.1±0.15	2.7±0.15	3.0±0.12	2.8±0.12	2.8±0.15	2.9±0.18	3.0±0.15	2.8±0.20	2.6±0.12	2.6±0.12	2.5±0.14	2.5±0.08	3.1±0.15	3.2±0.13	2.4±0.16	2.4±0.16
Stroke volume [µL]	26.5±1.8	20.4±2.0	24.7±2.1	20.6±2.0	20.8±2.1	22.5±2.8	25.4±2.3	23.6±3.8	20.9±1.9	17.2±1.2	19.7±2.0	17.9±1.3	27.8±2.9	29.8±2.9	16.8±2.5	17.7±2.4

Heart rates were about 500 bpm in most groups but slightly lower in some TRβ genotypes, such as male and female $TR\beta^{-}$ and male $TR\beta^{GS}$ mice. Ejection fraction ranged from approx. 75% to 85 %, and fractional shortening was between 40% and 50 %, with no significant differences or variations in the groups of both sexes. The same was observed in the morphological parameters, i.e. the end-diastolic IVS (IVS;d) and LVPW (LVPW;d) and the LVID (LVID;d). LVM was about 30 mg to 36 mg in males and between 25 mg to 35 mg in female mice. Both IVS;d and LVPW;d showed a narrow range of 0.53-0.57 mm, demonstrating that hearts in all groups had similar a wall thickness. LVID;d did not differ significantly between WT and mutant mice. However, a tendency of a slightly smaller diameter was observed in male $TR\alpha^{0}$, $TR\alpha^{GS}$ and $TR\beta^{GS}$ mice in comparison to their WT siblings. This difference was not observed in female mice, though. In summary, the phenotyping of euthyroid mice demonstrated that all TRα and TRβ mice of both sexes had similar cardiac functions and morphologies, and suggested the investigation of hyperthyroid mice in a follow-up study in order to examine how long-term hyperthyroidism influences and changes these parameters.

Long-term hyperthyroidism leads to cardiac hypertrophy via noncanonical TRα signalling

After the basal cardiovascular phenotyping performed at the GMC, we aimed to gain more insight into TR impact on mouse heart function and morphology. To investigate which TR, TRα or TRβ, and which signalling pathway, canonical or noncanonical, leads to TH-induced cardiac hypertrophy, mice were treated with 400 ng/mL T_3 in the drinking water and examined in serial echocardiography measurements. Serum was collected and analysed for TH levels of all mice to determine the extent of hyperthyroidism. 7 weeks of T_3 treatment resulted in a significant increase of fT_3 levels in all genotypes when compared to their control groups. In this study, we aimed for the induction of a mild hyperthyroidism, which was achieved with a 1.5-2 fold increase of fT_3 levels (Figure 19a). Due to T_3 treatment, fT_4 levels were strongly reduced (below detection limit), and TT_4 was significantly reduced as well (Figure 19 b,c). Overall, these results confirm the successful induction of a mild hyperthyroidism. Mice underwent echocardiography measurements, with the first measurement at the age of 8-10 weeks, and the last examination at the age of 16-18 weeks. Ventricular weight analysis of T_3 treated and control mice revealed that hyperthyroidism causes significantly larger hearts except in $TR\alpha^{0}$ and $TR\beta^{-}$ mice (Figure 20a).

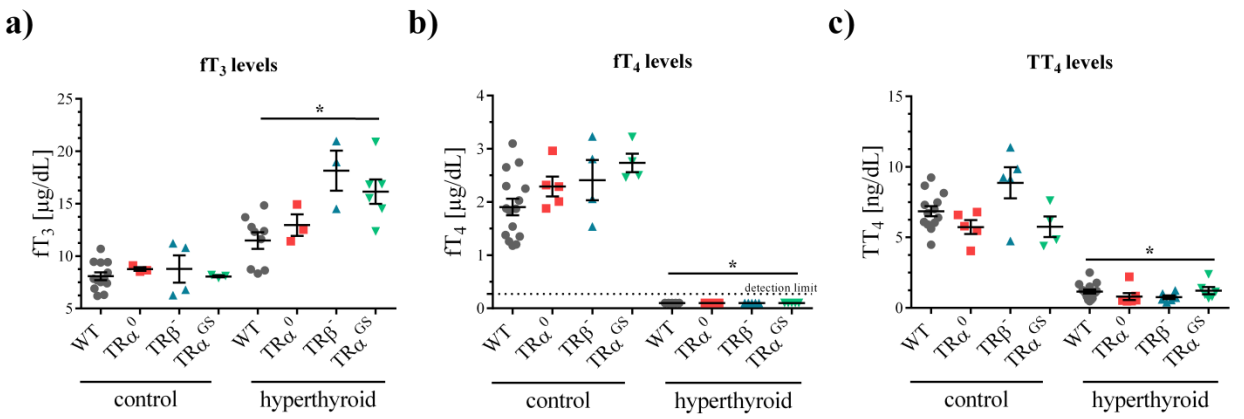

Figure 19: Thyroid hormone serum concentration of control and hyperthyroid WT, TRα^{0}, TRβ^{-} and TRα^{GS} mice. *Thyroid hormone serum concentrations of a) Free T_3 (fT_3), b) free T_4 (fT_4) and c) total T_4 (TT_4) from control and hyperthyroid WT (grey, n=9-15), TRα^{0} (red, n=3-5), TRβ^{-} (blue, n=3-5) and TRα^{GS} (green, n=3-6) mice were measured with commercially available ELISA assays. (one-way ANOVA with Sidak's multiple comparison test; control vs. hyperthyroid). Values are mean ± SEM; * p < 0.05.*

Since organ weights are generally related to body weight, mice were weighed, and no significant differences were observed for body weight in any group (Figure 20b), which allows for the body weight to be used as a normalisation parameter. When normalised to body weight, the ventricular weight is significantly higher in all T_3 treated groups in comparison to their untreated control groups except for TRα^{0} mice, suggesting that TH-induced cardiac hypertrophy is mediated by TRα (Figure 20c). In addition, we normalised the ventricular weight to tibia length, which is a well-accepted parameter of cardiac hypertrophy analysis and even more precise than body weight. This confirmed the previous observation and strengthened the conjecture that cardiac hypertrophy in response to hyperthyroidism is caused by TRα (Figure 20 d,e). Hypertrophy development was observed in both TRβ^{WT} and TRβ^{-} mice (blue panel), suggesting that this effect is not majorly mediated by TRβ. While no hypertrophy development could be observed in TRα^{0} mice (red), the effect was preserved in TRα^{GS} mice (green), indicating that cardiac hypertrophy is facilitated by noncanonical TRα signalling independent of gene expression.

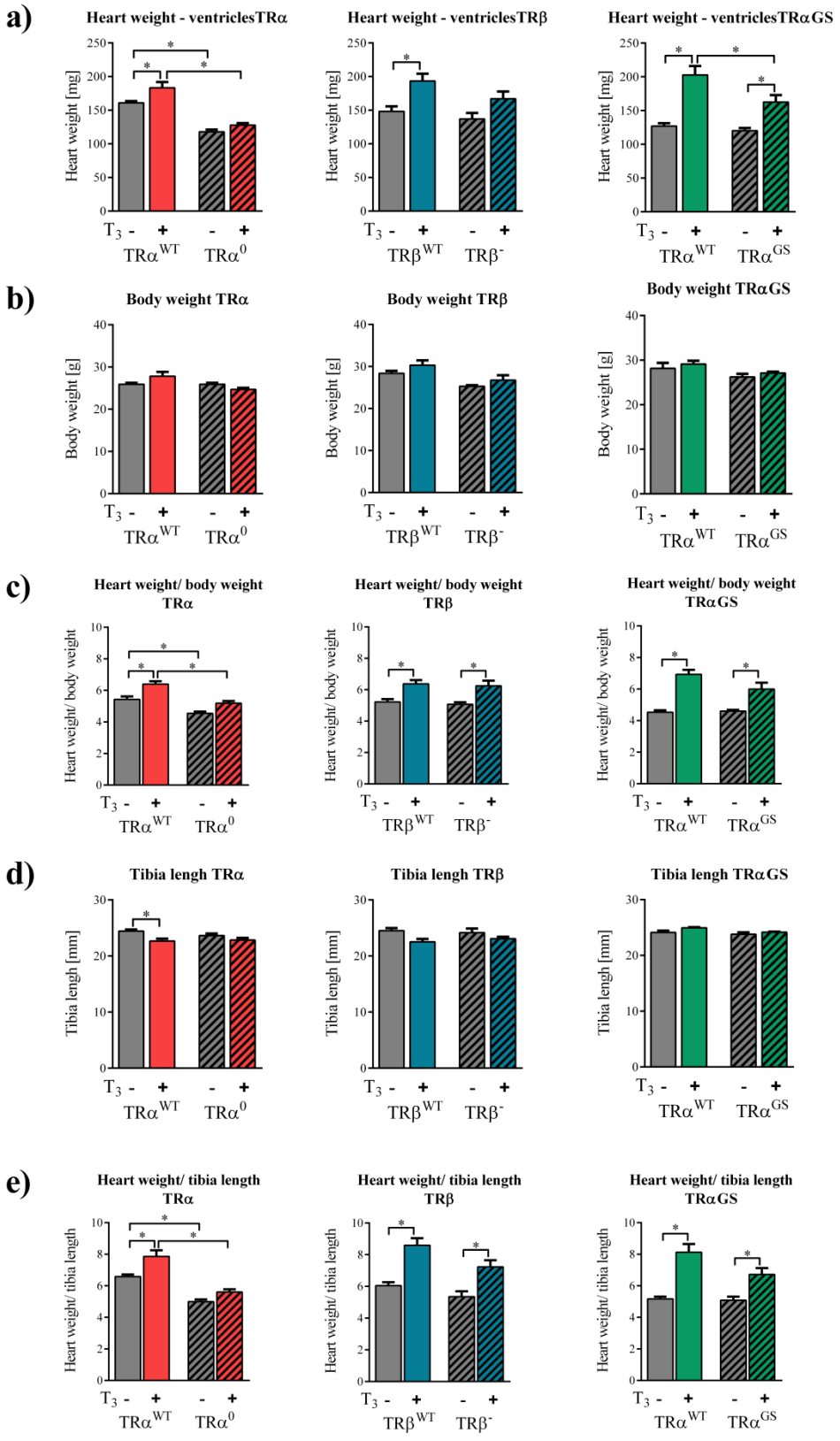
a)
Heart weight - ventriclesTRα
Heart weight - ventriclesTRβ
Heart weight - ventriclesTRαGS
Heart weight [mg]
b)
Body weight TRα
Body weight TRβ
Body weight TRαGS
Body weight [g]
c)
Heart weight/ body weight TRα
Heart weight/ body weight TRβ
Heart weight/ body weight TRαGS
Heart weight/ body weight
d)
Tibia lengh TRα
Tibia lengh TRβ
Tibia lengh TRαGS
Tibia lengh [mm]
e)
Heart weight/ tibia length TRα
Heart weight/ tibia length TRβ
Heart weight/ tibia length TRαGS
Heart weight/ tibia length
T3 - + - +
TRαWT TRα0
TRβWT TRβ-
TRαWT TRαGS

Figure 20: *Ex vivo* heart weight analysis in control and hyperthyroid TRα and TRβ mice shows that TH-induced cardiac hypertrophy is a noncanonical TRα effect. *Untreated and hyperthyroid TRα^{WT} (grey, n=8), TRα^{0} (red, n=6), TRβ^{WT} (grey, n=5), TRβ^{-} (blue, n=6), TRα^{WT} (grey, n=5) and TRα^{GS} (green, n=7) mice were sacrificed after echo 3. a) Ventricular heart weight, b) body weight and d) tibia length were recorded, and heart weight was normalised to either body weight (c) or tibia length (e) to calculate the extent of ventricular growth. (one-way ANOVA with Tukey's multiple comparison test). Values are mean ± SEM; *<0.05.*

Noncanonical TRa signalling leads to morphological changes in mouse hearts after long-term T_3 treatment

In this study, serial echocardiography measurements were performed during the induction of hyperthyroidism to monitor the development of functional and morphological heart parameters. Echocardiography measurements yielded changes in morphological parameters, which were monitored over time. Here, we examined IVS;d, LVPW;d and LVID;d. This analysis revealed differences in the euthyroid control group. For example, untreated TRα^{0} mice already had a smaller IVS;d and LVPW;d than their WT littermates at echo 1, which did not increase significantly between the first and last measurement. In the corresponding WT mice however IVS;d and LVPW;d increased over time (Figure 21, left panel). This difference was absent in the TRβ and TRα^{GS} strains, where both genotypes grew at a similar rate. After 7 weeks of hyperthyroidism, wall thickness in TRα^{0} mice was not significantly increased and significantly smaller than in their WT littermates. LVPW;d, for example, was significantly higher at echo 3 than it was at echo 1 in TRα^{WT} mice. This further strengthened the assumption that cardiac hypertrophy in hyperthyroidism is mediated by TRα. Wall thickness increased significantly over time in both TRβ^{WT} and TRβ^{-} mice, which further supports the hypothesis that TRβ is not the responsible receptor for T_3-mediated cardiac hypertrophy. In both TRα^{WT} and TRα^{GS} mice, IVS;d and LVPW;d were strongly increased over time. This analysis of TRα^{GS} mice gave further evidence for the surmise that noncanonical TR signalling caused the observed hypertrophy (Figure 21a,b). In addition, LVID;d increased only in hyperthyroid TRα^{0} mice over time, possibly due to the lack of increased wall thickness that occurred in all other groups, further strengthening the role of TRα in hypertrophy development (Figure 21c). In the hyperthyroid group T_3 treatment started after echo 1, followed by the second measurement after 3.5 weeks (echo 2) and the third measurement after 7 weeks (echo 3). In the euthyroid control group, hearts were only investigated at echo 1 and 3. Here, we compared a) WT mice with their respective knockout or mutant mice and b) the different time points of measurements within the genotype groups.

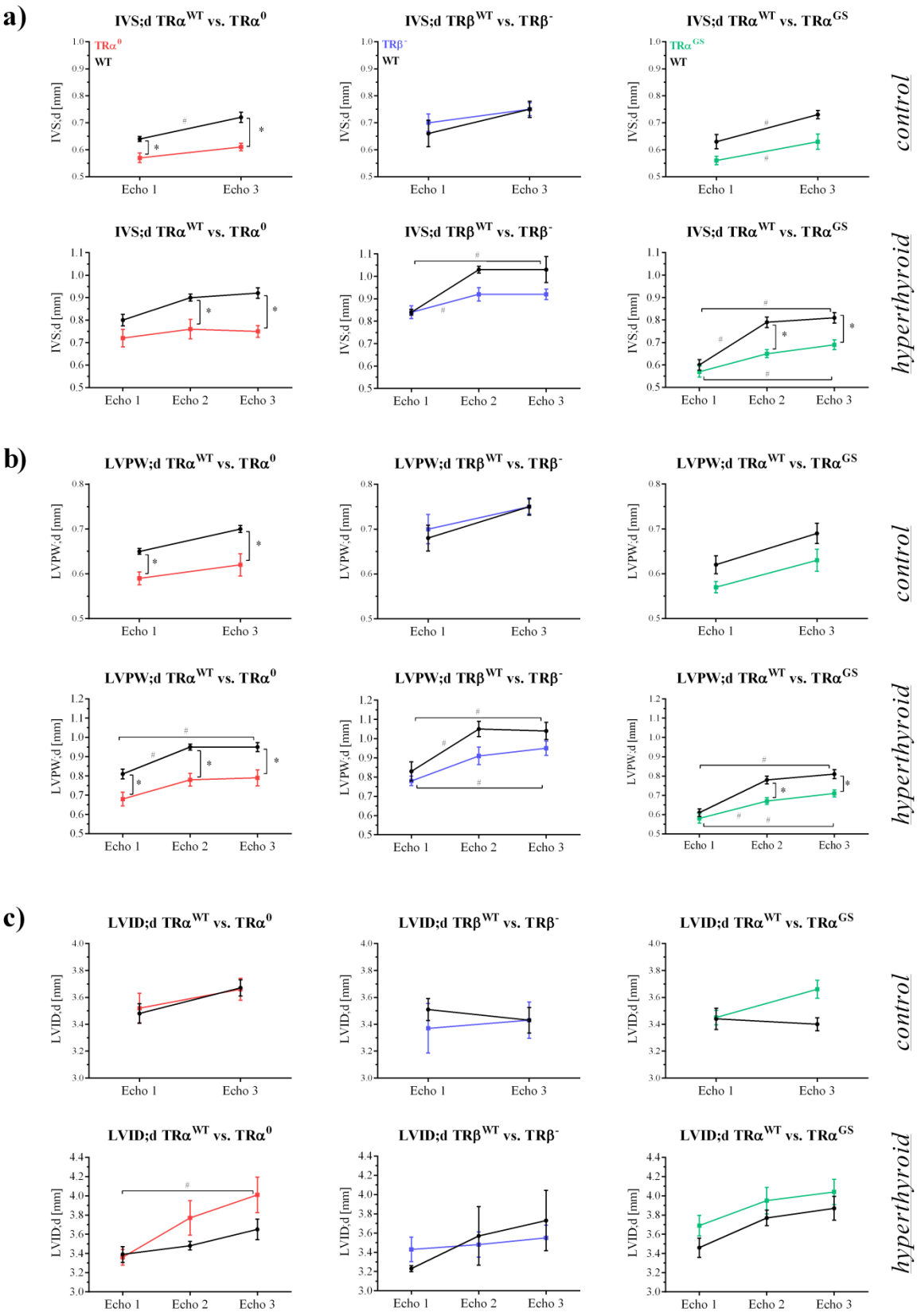
a)
IVS;d TRα^WT vs. TRα^0
IVS;d TRβ^WT vs. TRβ^-
IVS;d TRα^WT vs. TRα^GS
TRα^0
TRβ^-
TRα^GS
WT
IVS,d [mm]
Echo 1
Echo 2
Echo 3
control
hyperthyroid
b)
LVPW;d TRα^WT vs. TRα^0
LVPW;d TRβ^WT vs. TRβ^-
LVPW;d TRα^WT vs. TRα^GS
LVPW,d [mm]
c)
LVID;d TRα^WT vs. TRα^0
LVID;d TRβ^WT vs. TRβ^-
LVID;d TRα^WT vs. TRα^GS
LVID,d [mm]

Figure 21: Noncanonical TRα signalling causes morphology changes in hyperthyroid mouse hearts. *Echocardiography measurements were conducted on experimental day 1, after 3.5 weeks and after 7 weeks in hyperthyroid WT (black, n=6-10), TRα^0 (red, n=7-9), TRβ$^-$ (blue, n=7-9) and TRα^{GS} (green, n=8) mice. Control WT (black, n=6-10), TRα^0 (red, n=8), TRβ$^-$ (blue, n=7) and TRα^{GS} (green, n=8-10) mice were examined on day 1 and after 7 weeks. a) Interventricular septum thickness (IVS;d), b) Left ventricular posterior wall thickness (LVPW;d) and c) Left ventricular inner dimensions (LVID;d) were determined. (two-way repeated ANOVA with Bonferroni's multiple comparison test). Values are mean ± SEM; *<0.05 WT vs. KO/mutant and #<0.05 echo 1 vs. echo 2 vs. echo 3.*

Long-term hyperthyroidism does not affect functional heart parameters

The analysis of functional echocardiography parameters did not yield significant differences in any group. Mice were under anaesthesia during the whole procedure, which is why the observed heart rates served as an internal control and inclusion criterion rather than a read-out parameter. For example, only mice with a heart rate higher than 400 and lower than 700 bpm were included in the evaluation to ensure comparability of other echocardiography parameters (Figure 22a). Neither ejection fraction nor fractional shortening were significantly altered in either control or T_3 treated mice after 7 weeks (Figure 22 b,c). Nevertheless, in euthyroid mice both parameters showed an upwards tendency from echo 1 to echo 3, suggesting a higher ejection fraction, i.e. more blood being pumped with each stroke, and fractional shortening, which describes the shortening of the heart during constriction. In the hyperthyroid group, on the other hand, both parameters either stayed at a similar level or showed a downward tendency, suggesting that the observed hypertrophy worsened the heart function to a certain degree. However, based on this analysis neither the responsible TR isoform nor signalling pathway that caused T_3-mediated cardiac hypertrophy, could be identified. Overall, the observed morphological changes did not translate into impaired or reduced cardiac function.

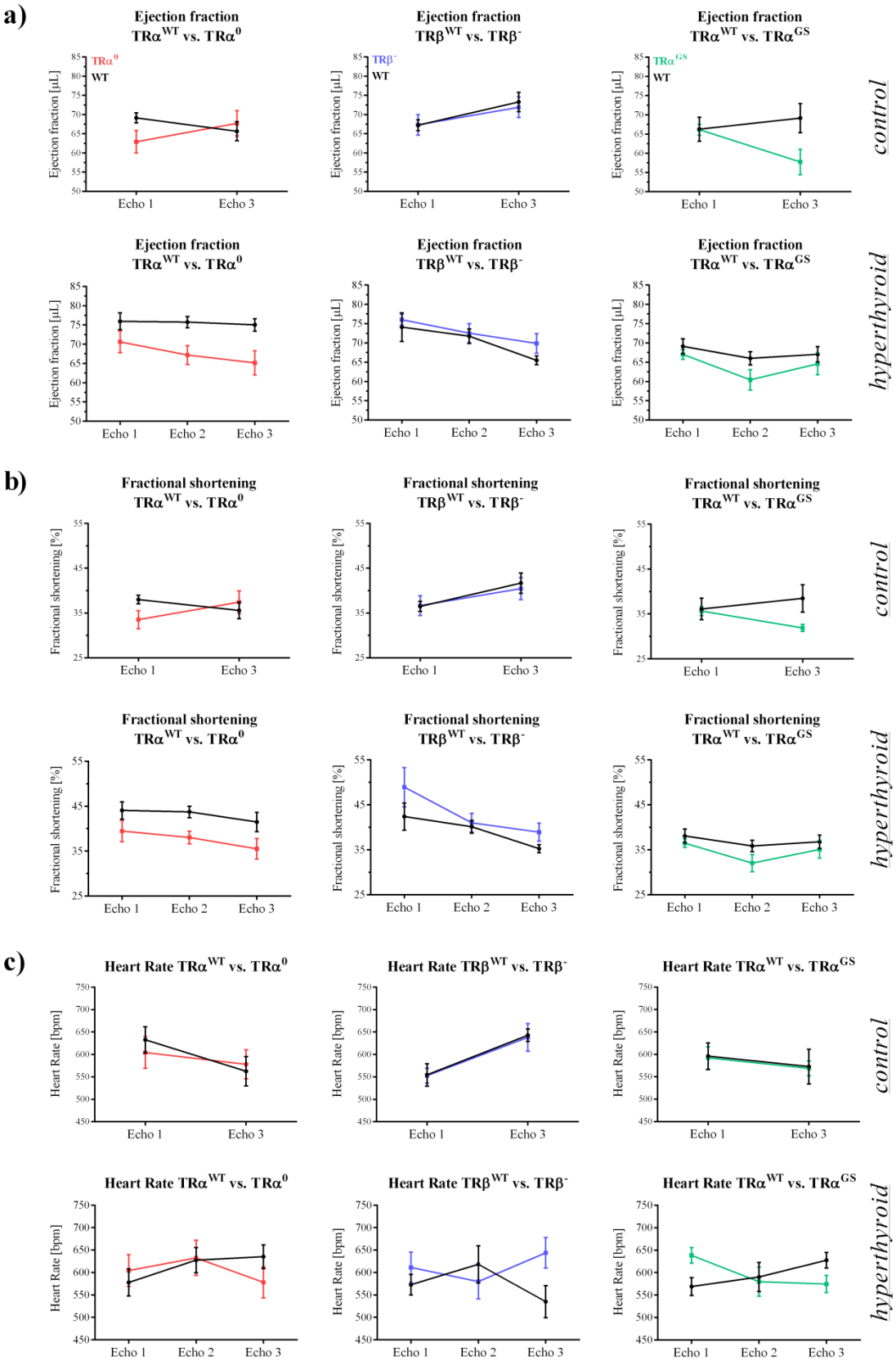
a)
Ejection fraction
TRα^WT vs. TRα^0
TRα^0
WT
Ejection fraction [µL]
Echo 1
Echo 3
Ejection fraction
TRβ^WT vs. TRβ^-
TRβ^-
WT
Ejection fraction
TRα^WT vs. TRα^GS
TRα^GS
WT
control
Echo 2
hyperthyroid
b)
Fractional shortening
TRα^WT vs. TRα^0
Fractional shortening [%]
Fractional shortening
TRβ^WT vs. TRβ^-
Fractional shortening
TRα^WT vs. TRα^GS
c)
Heart Rate
TRα^WT vs. TRα^0
Heart Rate [bpm]
Heart Rate
TRβ^WT vs. TRβ^-
Heart Rate
TRα^WT vs. TRα^GS

Figure 22: Hyperthyroidism has minor effects on functional parameters in mouse hearts. *Echocardiography measurements were conducted on experimental day 1, after 3.5 weeks and after 7 weeks in hyperthyroid WT (black, n=6-10), TRα^0 (red, n=7-9), TRβ$^-$ (blue, n=7-9) and TRα^{GS} (green, n=8) mice. Control WT (black, n=6-10), TRα^0 (red, n=8), TRβ$^-$ (blue, n=7) and TRα^{GS} (green, n=8-10) mice were examined on day 1 and after 7 weeks. a+b) Ejection fraction and fractional shortening were determined during echocardiography measurements. c) Heart rate was recorded as an internal control. (two-way repeated ANOVA with Bonferroni's multiple comparison test). Values are mean ± SEM; *<0.05.*

Cardiac growth in hyperthyroidism is a result of cardiomyocyte hypertrophy

In theory, cardiac hypertrophy can result from two different causes: myocyte hypertrophy (increase in size without a change of total myocyte number) or hyperplasia (myocyte proliferation) (Grajek *et al.* 1992). By performing H&E staining on heart sections and determining myocyte size, we aimed to define whether the observed cardiac hypertrophy is caused by myocyte hypertrophy or hyperplasia. For the determination of cardiomyocytes size, only cells with nuclei clearly visible (same section and focus) in the middle of the cell, as indicated in Figure 23a, were evaluated. The comparison of microscopy images from control (black) and T_3-reated (red) animals revealed a significant increase of cell size in response to hyperthyroidism (Figure 23b). This effect occurred in all groups except TRα^0 mice and was preserved in TRα^{GS} mice, suggesting that TH-induced cardiac hypertrophy is a consequence of TRα-mediated myocyte hypertrophy, and again suggests that noncanonical TRα action mediates hypertrophy.

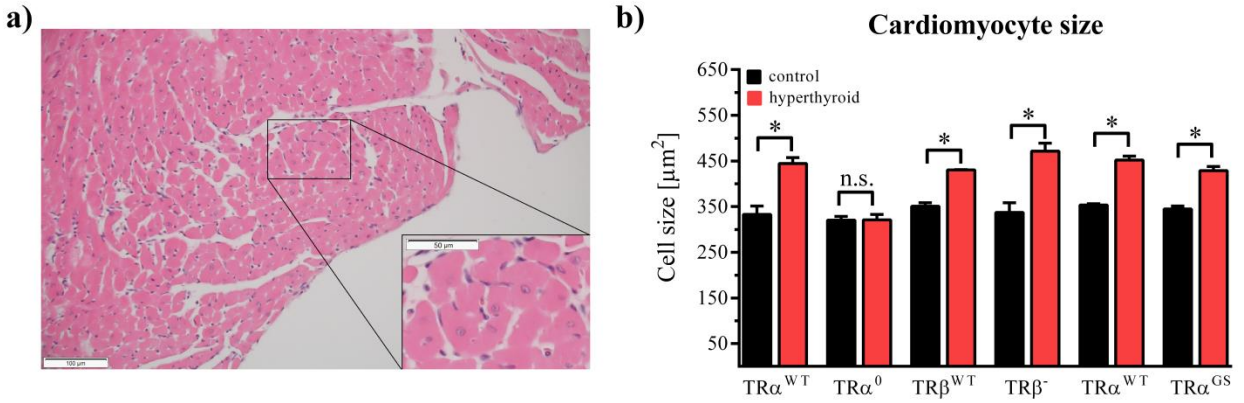

Figure 23: Hyperthyroidism results in myocyte hypertrophy *via* noncanonical TRα signalling. *Heart sections of control and hyperthyroid mice were stained with haematoxylin and eosin and examined via light microscopy. a) H&E stained heart section from a control WT mouse. A minimum of 500 cells was evaluated per group. Myocytes with comparable morphology (nucleus in focus in the middle of the cell) as shown in the amplified section were assessed. Scale bars represent 100 and 50 µm respectively. b) Cardiomyocyte size of control (black) and T_3-treated (red) WT (n=3-4), TRα^0 (n=3-4), TRβ$^-$ (n= 4-6) and TRα^{GS} (n= 4) sections were measured and calculated with ImageJ. (one-way ANOVA with Sidak's*

*multiple comparison test; control vs. hyperthyroid within one genotype group). Values are mean ± SEM; *<0.05; n.s.= not significant.*

Noncanonical TRα signalling appears to impact cardiomyocyte cell cycle arrest

Nuclei in primary cardiomyocytes from adult euthyroid male WT, $TR\alpha^0$ and $TR\alpha^{GS}$ mice were stained with Hoechst, examined with a fluorescence microscope, and nuclei per cell were counted. In $TR\alpha^0$ cardiomyocytes the amount of mononucleated myocytes was significantly higher than in WT mice, indicating that the loss of TRα results in more mononucleated cells. This was not the case in $TR\alpha^{GS}$ mice, which suggests that noncanonical signalling might be involved in the process of binucleation. No differences were found in the relative amount of binucleated cells (Figure 24 a,b). In addition, a difference between the two WT groups was observed for trinucleated cells, but no significant differences occurred for tetranucleated cardiomyocytes (Figure 24 c,d). The lack of binucleation in $TR\alpha^0$ mice leads to the conclusion that TRα exerts an effect on cell cycle arrest *via* noncanonical signalling and might therefore promote hypertrophy development.

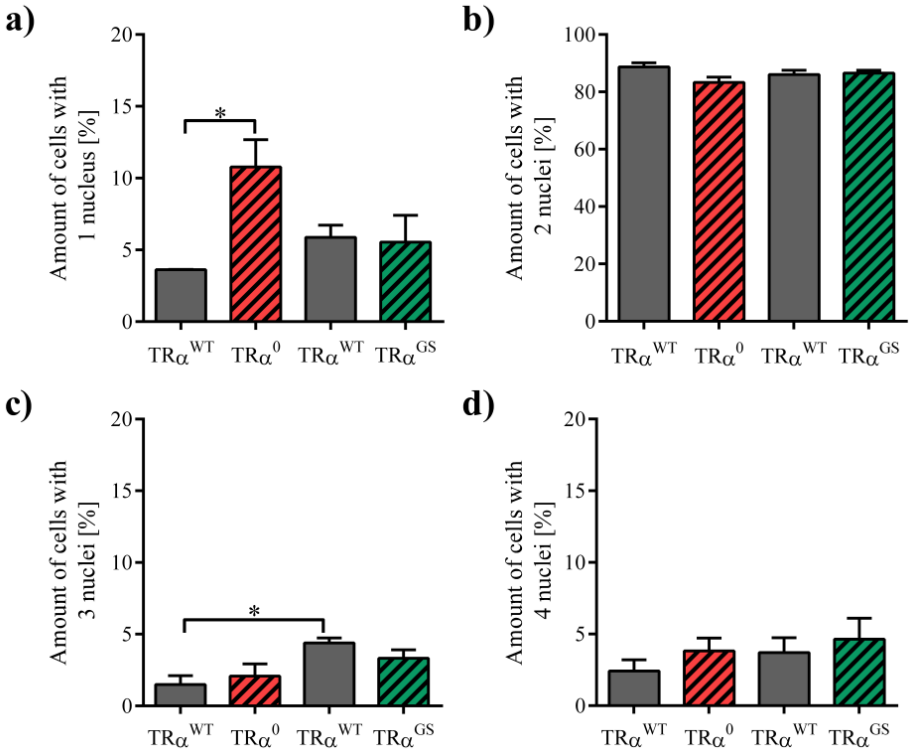

Figure 24: Noncanonical TRα action contributes to binucleation in euthyroid mouse cardiomyocytes. *Adult primary cardiomyocytes were isolated via enzymatic digestion, DNA (nuclei) was stained with Hoechst, and nuclei per cell were counted after fluorescence microscopy. 300-500 cells per mouse were examined (n=3 mice per group). (one-way ANOVA with Tukey's multiple comparison test). Values are mean ± SEM; *<0.05.*

T_3-induced cardiac hypertrophy is likely independent of canonical TR action

In the previous experiments, we identified noncanonical TRα signalling as the underlying mechanism of TH-induced cardiac hypertrophy. This appeared to be a consequence of myocyte hypertrophy and might correlate with the multinucleated status in cardiomyocytes of all but $TR\alpha^0$ mice. Yet, the molecular mechanisms that caused this phenotype are unknown and were therefore the aim of the following investigations by means of of gene expression and protein activation analysis. In a pre-test, gene expression of TH target and reference genes in control and hyperthyroid WT hearts were compared. Here, two TH target (*Myh6* & *Myh7*) and one reference gene (*Polr2a*) were analysed in all WT samples to see if there were any strain background differences between the three used mouse strains ($TR\alpha^{KO}$, $TR\beta^{KO}$ & $TR\alpha^{GS}$). However, no differences could be observed in expression of *Pol2ra*, *Myh6* or *Myh7*, for neither the control nor the hyperthyroid group (Figure 25). Interestingly, *Myh6*, which has previously been shown to be a TH responsive gene, was not upregulated in the investigated hearts (Lin *et al*. 2013).

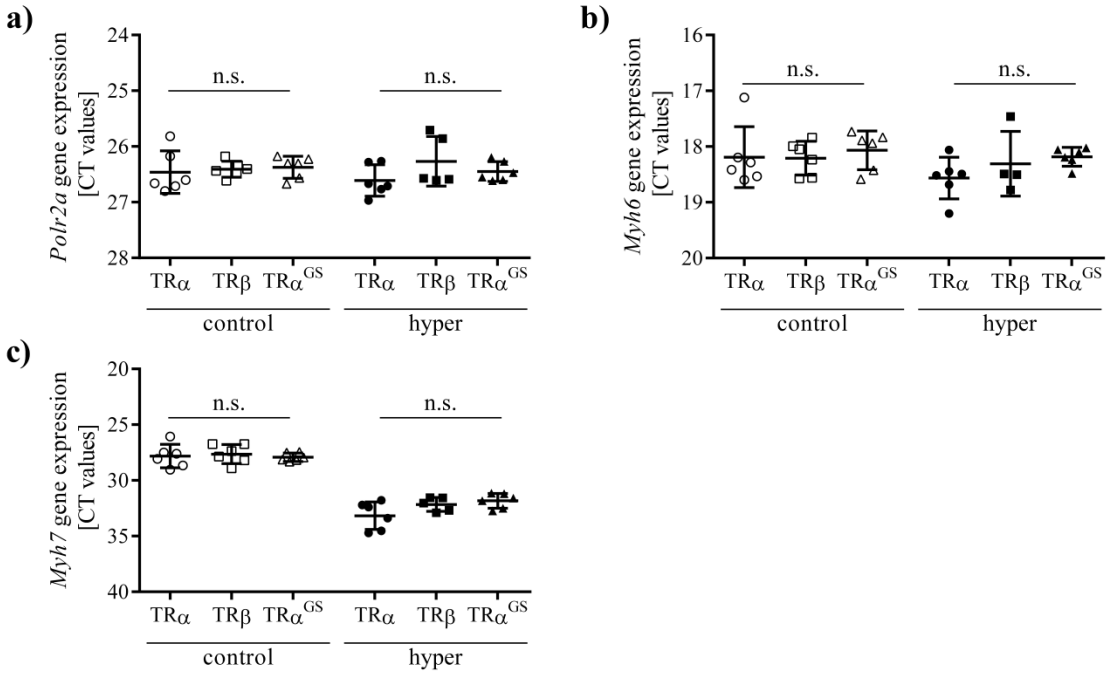

Figure 25: Gene expression analysis of reference and TH-responsive genes in euthyroid and hyperthyroid WT mouse hearts. *Gene expression (CT values) of a) Polymerase (RNA) II Subunit A (Polr2a), b) myosin heavy chain 6 (Myh6) and c) myosin heavy chain (Myh7) in euthyroid and hyperthyroid WT mice of $TR\alpha^{KO}$, $TR\beta^{KO}$ & $TR\alpha^{GS}$ (n=5-6 each) strains. (one-way ANOVA with Sidak's multiple comparison test; comparison within control and hyperthyroid). Values are mean ± SEM; n.s.= not significant.*

Myh7, on the other hand, was significantly downregulated (Figure 25 b,c), whereas the reference gene *Polr2a* was not regulated in any manner. In summary, this pre-test demonstrated that there are no background differences in the studied mouse strains and allowed creating pooled WT groups for further gene analysis.

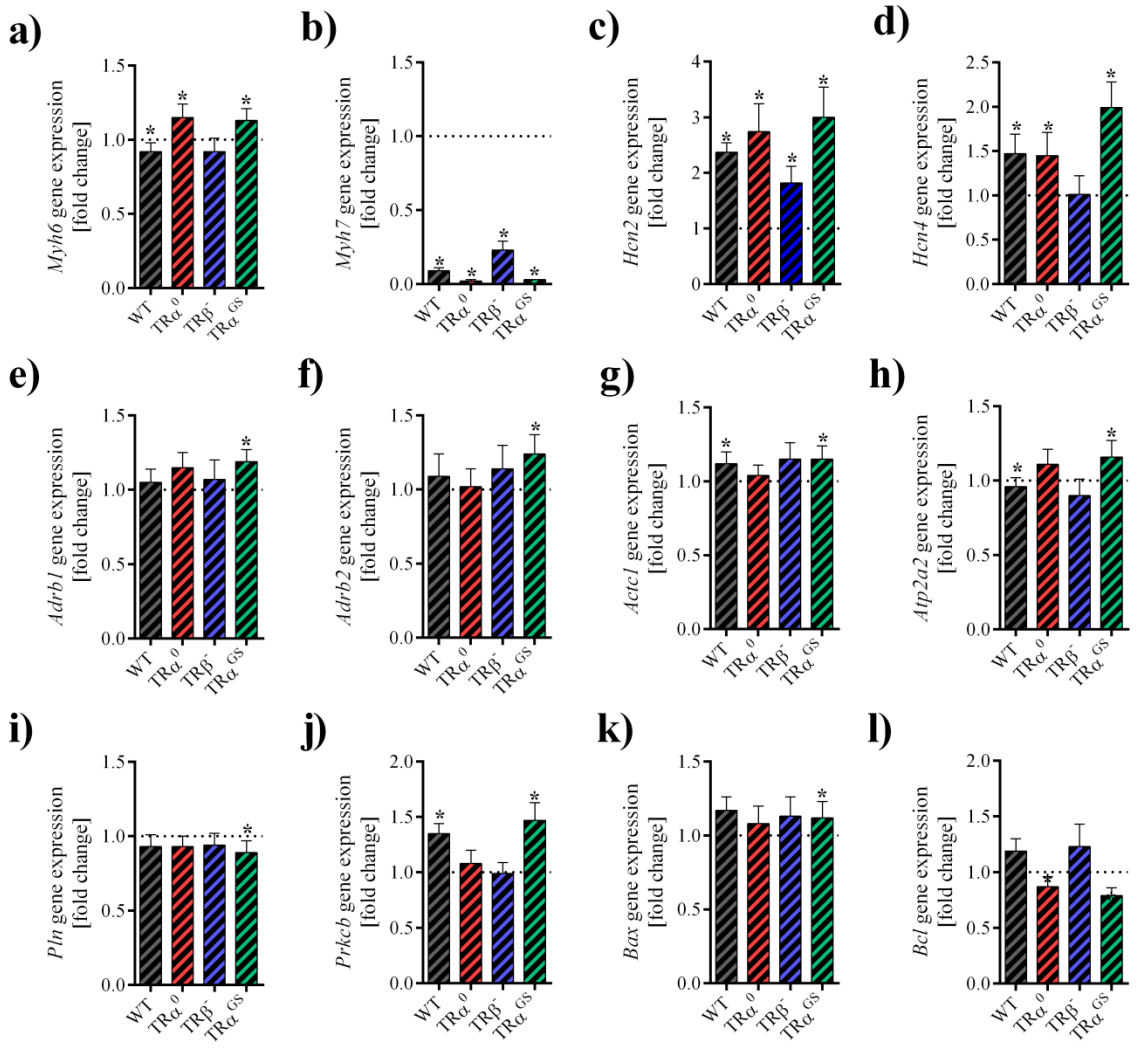

Figure 26: Impact of long-term hyperthyroidism on cardiac hypertrophy associated gene expression. *Gene expression fold changes of hyperthyroid hearts in comparison to respective control hearts (n=5-6 each) of WT (grey), TRα^0 (red), TRβ$^-$ (blue) and TRα^{GS} (green) mice. a) myosin heavy chain 6 (Myh6), b) Myh7, c) activated cyclic nucleotide gated potassium channel 2 (Hcn2), d) Hcn4, e) adrenergic receptor 1 (Adrb1), f) Adrb2, g) actin alpha cardiac muscle 1 (Actc1), h) sarco(endo)plasmic reticulum calcium-ATPase 2 (Serca2) (Atp2a2), i) phospholamban (Pln), j) protein kinase C beta (Prkcb), k) Bcl2 associated X protein (Bax) and l) B-cell lymphoma (Bcl). (Unpaired t-test control vs. hyperthyroid for each group) Values are mean ± SEM; *<0.05.*

With a collective WT group, as well as the knockout and mutant samples, a variety of known hypertrophy and TH target genes were investigated. Whereas *Myh6* was slightly increased in $TR\alpha^{0}$ and $TR\alpha^{GS}$ hearts, gene transcript of *Myh7* was strongly reduced in all groups. In addition, expression of *Hcn2* was two to three fold higher in hyperthyroid hearts when compared to their respective controls (Figure 26 a-c). Although significant, the upregulation of *Hcn2* was much lower in $TR\beta^{-}$ hearts than in all other groups. *Hcn4* was significantly upregulated in all groups except $TR\beta^{-}$ mice (Figure 26d), suggesting a possible role of TRβ in ion channel regulation. Interestingly, both adrenergic receptors (*Adrb1* and *Adrb2*) as well as the muscle specific SERCA inhibitor phospholamban (*Pln*) and the apoptosis regulator BAX (*Bax*) were only upregulated in $TR\alpha^{GS}$ mice (Figure 26 e,f,I,k). Expression of actin alpha cardiac muscle 1 (*Actc1*), SERCA (*Atp2a2*) and protein kinase C beta (*Prkcb*) was significantly increased in WT and $TR\alpha^{GS}$ but not $TR\alpha^{0}$ and $TR\beta^{-}$ hearts (Figure 26 g,h,j). *Adrb2* and *Actc1* expressions showed a tendency towards this pattern, although expression was not significantly altered. Overall the up- or downregulation of most genes was rather mild.

Activation of cytoplasmic cardiac hypertrophy pathways remains unaltered after long-term induction of hyperthyroidism

Since gene expression analysis did not yield an explanation for increased heart size after hyperthyroidism, the involvement of classical hypertrophy associated pathways was investigated in TRα mouse hearts. Namely, protein phosphorylation of $ERK1/2_{thr200/tyr204}$, $mTOR_{ser2448}$ and ribosomal protein S6 kinase ($S6\text{-}kinase_{ser235/236}$) were compared between control abd hyperthyroid hearts (Figure 27). Protein phosphorylation of ERK (Figure 27a), mTOR (Figure 27b) and S6-kinase (Figure 27c) did not differ significantly between hyperthyroid and control hearts. A slight decrease of ERK1/2 phosphorylation could be found in hyperthyroid hearts of both $TR\alpha^{WT}$ and $TR\alpha^{0}$ mice. However, this difference was not significant and, as it occurred in both genotypes, did not explain cardiac hypertrophy development in $TR\alpha^{WT}$ and lack thereof in $TR\alpha^{0}$ hearts. Overall, the investigation of these proteins did not reveal key mediators and requires further studies.

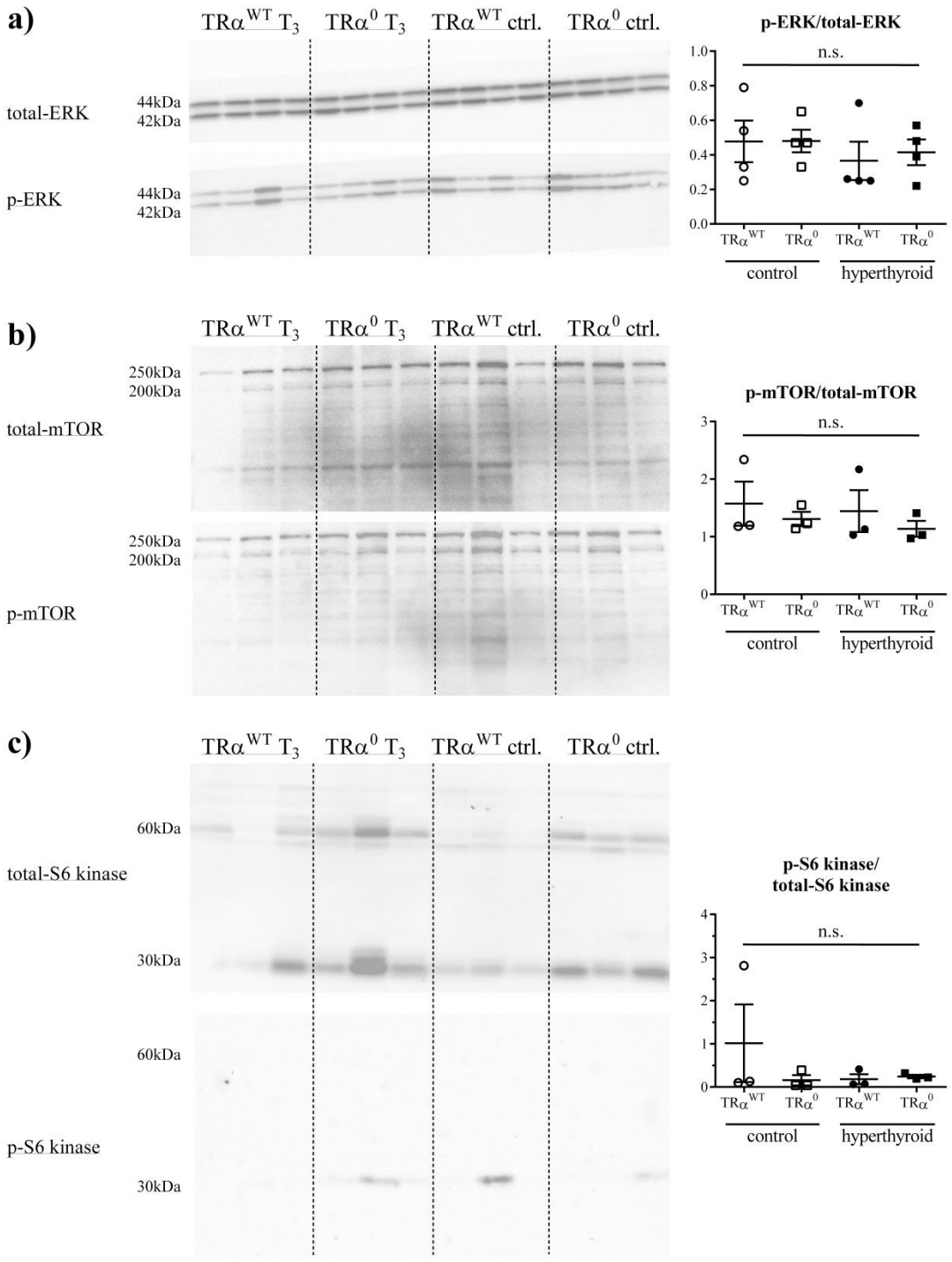

Figure 27: Phosphorylation of ERK, mTOR and ribosomal protein S6 kinase in TRα mouse hearts. *a) total-ERK and phospho-ERK (extracellular-signal regulated kinases; 42 and 44 kDA), b) total-mTOR and phospho-mTOR (mammalian target of rapamycin; 289 kDa) and c) total-S6 kinase and phospho-S6 kinase (ribosomal protein S6 kinase; 32 kDa). Proteins were isolated from hyperthyroid and control $TR\alpha^{WT}$ and $TR\alpha^{0}$ mouse hearts. Phosphorylation of proteins from the respective control and knockout samples was normalised to total protein amount. (one-way ANOVA with Sidak's multiple comparison test; $TR\alpha^{WT}$ vs. $TR\alpha^{0}$ and control vs. hyperthyroid). Values are mean ± SEM; n.s.= not significant.*

Long-term hyperthyroidism does not affect the amount of vascularisation in cardiac hypertrophy development

CD31, a marker for endothelial cells and thereby vascularisation and angiogenesis, was stained on sections from paraffin embedded hearts and analysed *via* light microscopy. Here, euthyroid control and hyperthyroid hearts were compared in order to test for increased vascularisation. All appearing arteries were counted on the basis of stained segments, be it cross or front, and normalised to heart weights. However, no differences could be observed between TR^{WT}, $TR\alpha^0$ or $TR\beta^-$ mice and the untreated control (Figure 28). This result suggests, that the the duration and dose of T_3 treatment did not result in a significant increase of vascularisation.

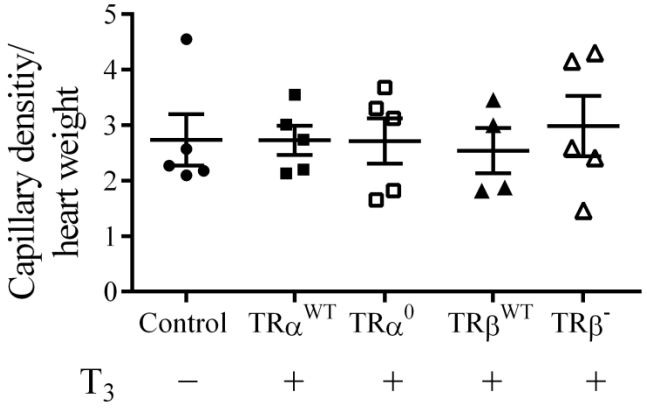

Figure 28: Vascularisation of control and hyperthyroid hearts. C*apillary density was determined in hearts of untreated control and hyperthyroid* TR^{WT}, $TR\alpha^0$ *and* $TR\beta^-$ *mice and normalised to heart weights. (one-way ANOVA with Dunnett's multiple comparison test, control vs. hyperthyroid each). Values are mean ± SEM.*

Thyroid hormone influence on heart rate, body temperature and activity

Cardiovascular, metabolic and behavioural functions are strongly affected by thyroid dysfunctions. By using TR knockout and mutant mouse models, we aimed to gain insight into the development, progression and regulation of those processes. However, producing unadulterated data for heart rate, body temperature and activity is difficult whenever mice have to be handled or anesthetised for the experiment. For example, electrocardiography offers the advantage of measurements in conscious mice without anaesthesia, but the handling and restraining activates the adrenergic system and causes great stress for the animals and thus influences the results and *vice versa* (Ho *et al.* 2011). With a radio telemetry approach in contrast, conscious, freely moving mice can be investigated completely undisturbed, which yields purer results (Cesarovic *et al.* 2011). In cooperation with the GMC, heart rates of untreated TRα and TRβ mice resulting from an electrocardiography study within a broad-scale phenotyping were analysed. Based on these results, as well as the previous echocardiography study, heart rate, core body temperate and locomotor activity were examined through radio telemetry measurements. Here, we investigated all three thyroid states, eu-, hypo- and hyperthyroidism, consecutively in $TR\alpha^{WT}$, $TR\alpha^{0}$ and $TR\alpha^{GS}$ mice. In addition to the evaluation of thyroid state and the role of TRα, this study also allowed the comparison of biorhythm (active and inactive phase), a parameter that is often overlooked in mouse studies but is undoubtedly an important factor (Tankersley *et al.* 2002).

TRα influences basal heart rate in electrocardiography measurements

15-week-old male and female TRα and TRβ mice were examined *via* electrocardiography to gain insight into heart rate regulation. In the TRα study cohort, increased RR-intervals and consequently lower heart rates could be observed in male and female $TR\alpha^{0}$ mice as well as male $TR\alpha^{GS}$ mice in comparison to their respective WT littermates (Figure 29). This data suggests that the lower heart rate results from the increased time of a singular de- and repolarisation of atria and ventricles. However, no differences in P interval and only slight tendencies in QRS interval duration could be observed for those mice. Electrocardiograms from male and female TRβ mice did not show any differences in heart rate associated parameters (Figure 30). Neither heart rate nor the individual interval durations were affected by the absence or mutation of TRβ.

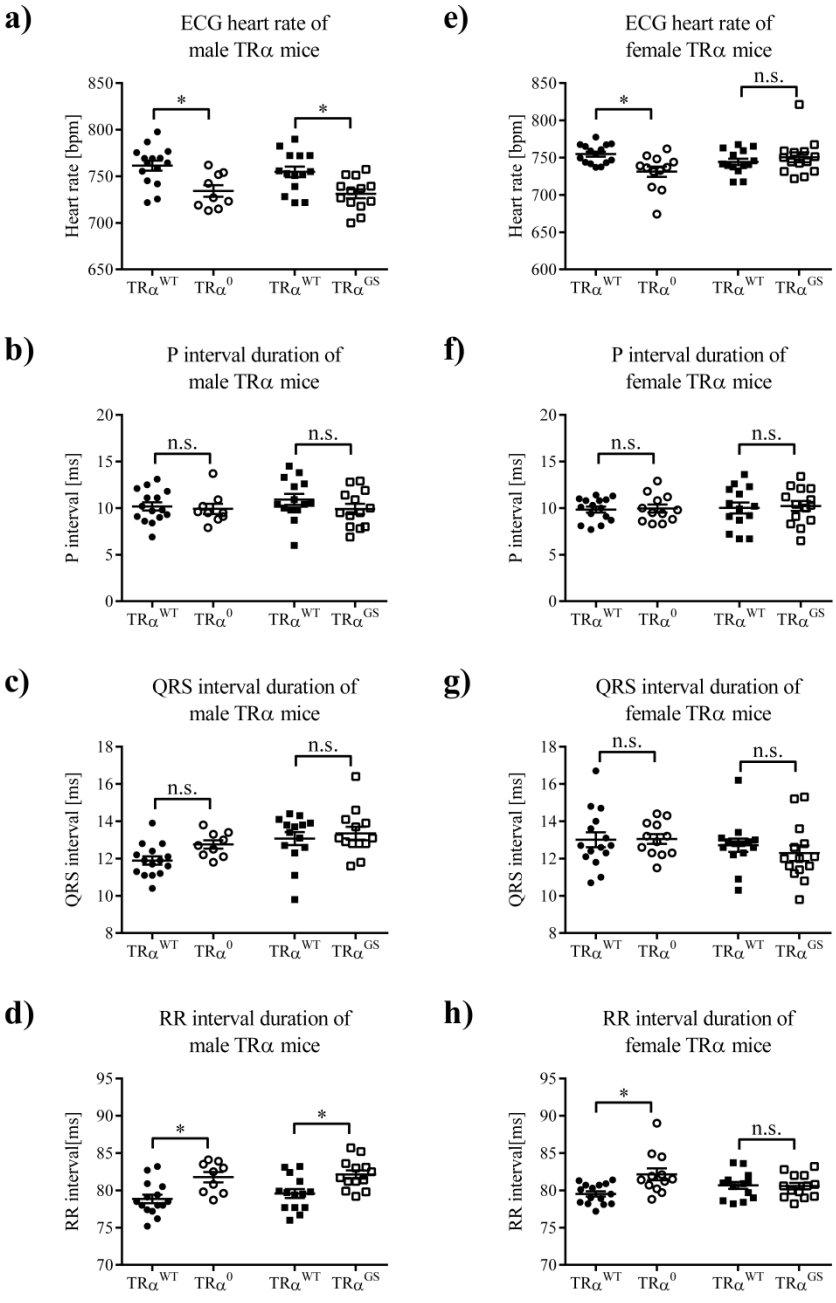

Figure 29: Electrocardiography reveals that the lack of TRα results in reduced heart rates *in vivo*. *Heart rate, P interval duration, QRS duration and RR interval duration were analysed in conscious euthyroid male (a-d; n=9-15) and female (e-h; n=12-15) WT, $TR\alpha^0$ and $TR\alpha^{GS}$ mice via electrocardiography at the age of 15 weeks (GMC). (one-way ANOVA with Sidak's multiple comparison test, $TR\alpha^{WT}$ vs. $TR\alpha^0$ and $TR\alpha^{GS}$ respectively). Values are mean ± SEM; *<0.05; n.s.= not significant.*

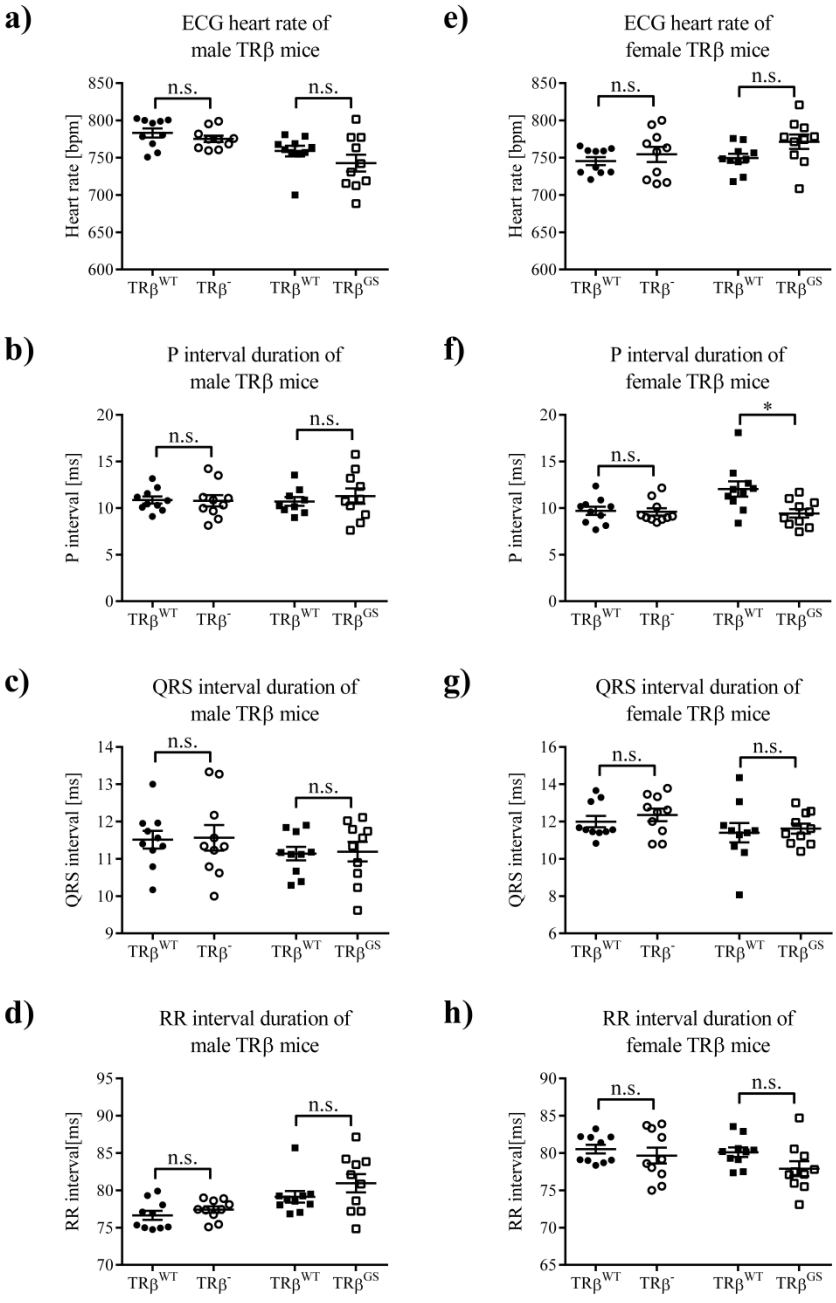

Figure 30: Electrocardiography reveals that TRβ does not regulate heart *in vivo*. *Heart rate, P interval duration, QRS duration and RR interval duration were analysed in conscious euthyroid male (a-d; n=10) and female (e-h; n=10) WT, TRβ^{-} and TRβ^{GS} mice via electrocardiography at the age of 15 weeks (GMC). (one-way ANOVA with Sidak's multiple comparison test, TRβ^{WT} vs. TRβ^{0} and TRβ^{GS} respectively). Values are mean ± SEM; *<0.05; n.s.= not significant.*

Interestingly, heart rate was not affected in TRβ^{-} mice, which have an intact TRα receptor and increased TH levels due to the impaired HPT axis (Figure 30). In electrocardiography as well as echocardiography studies, heart rates were influenced by stress and handling of the animals or anaesthesia. To gain data from conscious, freely moving animals, and thus answer how TRs are able to mediate heart rate, radio telemetry studies with TRα mice were performed. Here, heart rate, body temperature and activity were recorded not only in euthyroid but also in the hypo- and hyperthyroid state of conscious mice, without adding stress and thereby gaining adulterated data. Upon concluding the experiment, mice were in the hyperthyroid state, and serum TH levels were compared to euthyroid WT samples from the cardiac hypertrophy study. Free T_3 levels doubled after 9-10 days of hyperthyroid treatment, whereas free T_4 levels were below the assay detection limit and total T_4 was significantly reduced as well (Figure 31).

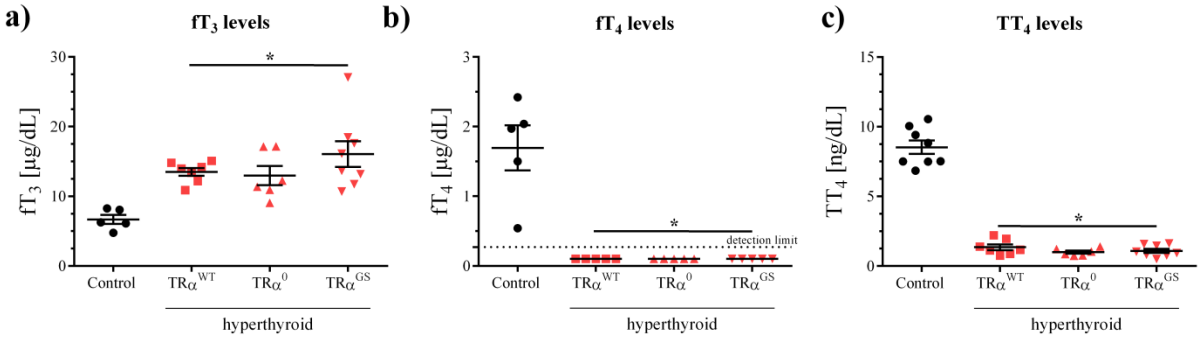

Figure 31: Thyroid hormone serum concentration of control WT and hyperthyroid WT, TRα^{0} and TRα^{GS} mice. a) *Free T_3 (fT_3), b) free T_4 (fT_4) and c) total T_4 (TT_4) of WT, TRα^{0} and TRα^{GS} mice were measured with commercially available ELISA assays. (one-way ANOVA with Dunnett's multiple comparison test, control vs. hyperthyroid each). Values are mean ± SEM; * p < 0.05 vs. control*

Heart rate regulation in thyroid dysfunctions is controlled by canonical TRα signalling

Three days of heart rate recordings were divided into an active and inactive phase and averaged, and the relative frequencies of heart rates between 200 and 800 bpm were blotted as %. In euthyroid active WT mice, heart rates ranged from 300 to 800 bpm with the highest frequencies around 400 bpm as well as 600 bpm (Figure 32a, left panel). When mice were rendered hypothyroid, heart rates were lowered and covered the area between 300 and 650 bpm, which was clearly visible by a shift to the left. Two strong peaks (ticked lines) with a frequency of 400 and 550 bpm were observed in this state of WT mice. In late hyperthyroidism, on the other hand, a slope between 300 and 800 bpm with only one peak (ticked line) at 750 bpm was observed, indicating that heart rates have shifted to higher values.

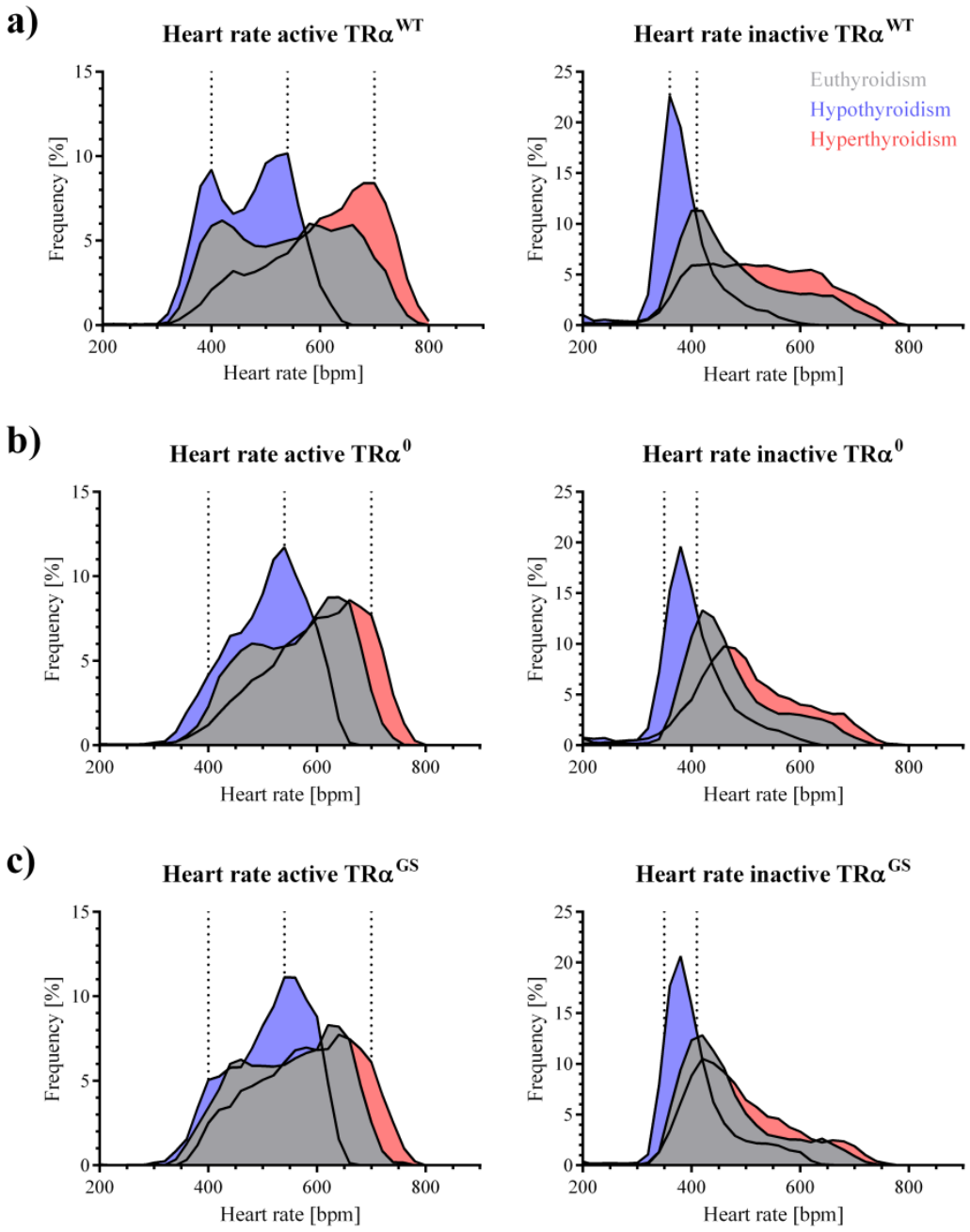

Figure 32: Heart rate regulation in hypo- and hyperthyroidism is controlled by canonical TRα signalling. *Heart rate was recorded for three days in eu- (grey), hypo- (blue) and early and late hyperthyroid (red) state of male TRα^{WT}, TRα^{0} and TRα^{GS} mice. Mean values were saved every 30 sec, divided into active and inactive phase and averaged for each genotype (n=6-8). Relative frequency for heart rate values was calculated in 20 bpm steps and expressed as %.*

In the inactive phase, mice had only one peak in the euthyroid (425 bpm) and hypothyroid (350 bpm) state each (Figure 32a, right panel). The decrease of heart rate became obvious not only in the reduced peak value from 425 to 375 bmp but also in the doubling of occurrence of

this lower frequency. Hyperthyroidism resulted in a flat course of the curve between 350 to 800 bpm with no peak at all, and all heart rates occurred. Taken together, heart rate was downregulated in hypothyroidism and upregulated in hyperthyroidism in the active and inactive phase.

Interestingly, $TR\alpha^{0}$ and $TR\alpha^{GS}$ mice showed an altered pattern with heart rate frequencies ranging from 350 to 750 bpm and an overall narrower curve than in $TR\alpha^{WT}$ mice, visible already in the active euthyroid state (Figure 32b,c left panel). $TR\alpha^{0}$ mice showed only one peak at 625 bpm but did so with a higher frequency. A similar pattern, although less pronounced, could be seen for $TR\alpha^{GS}$ mice. In both groups, hypothyroidism yielded in curves with only one peak ($TR\alpha^{WT}$ ticked lines as comparison) at 550 bpm as seen in $TR\alpha^{WT}$ mice but did so with a slightly higher frequency. Only the induction of hyperthyroidism did not yield in major differences of curve progression between $TR\alpha^{WT}$ and mutant mice (Figure 32 b,c left panel). In the euthyroid inactive phase, heart rate of $TR\alpha^{0}$ and $TR\alpha^{GS}$ mice peaked at 425 instead of 400 bpm with a higher frequency as well. A similar shift to higher heart rates was observed in the hypothyroid peak in both TRα mutant groups (380 bpm), although here the frequency of these events were slightly reduced. Remarkably, the most prominent effect in the inactive phase could be observed after the induction of hyperthyroidism. Whereas $TR\alpha^{WT}$ mice displayed a flat course of curve progression, $TR\alpha^{0}$ and $TR\alpha^{GS}$ mice showed peaks at 475 and 425 bpm, respectively. However, higher heart rates occurred with lower frequencies in these groups than in $TR\alpha^{WT}$ mice (Figure 32 b,c right panel). In conclusion, the induction of hypothyroidism causes a shift to lower heart rates and hyperthyroidism results in higher heart rates. This regulation is impaired in $TR\alpha^{0}$ and $TR\alpha^{GS}$ mice indicating that canonical TRα signalling regulates heart rate alteration in thyroid dysfunctions.

In addition to the relative heart rate frequencies, the heart rate development over time was investigated in all three thyroid states and compared between $TR\alpha^{WT}$ and $TR\alpha^{0}$ (group A) as well as $TR\alpha^{WT}$ and $TR\alpha^{GS}$ (group B) mice. Here, it became obvious that, in both groups, the majority of differences were observed in hypothyroidism (Figure 33a). Comparisons within group A showed that $TR\alpha^{0}$ mice (red curve) had, at some points, higher heart rates than WT controls (black curve), mainly at the end of each active phase. The induction of hypothyroidism a) increased the amount of significantly different heart rate events, b) strengthened the differences between $TR\alpha^{WT}$ and $TR\alpha^{0}$ at the different time points and c) lead to differences not only in the

active but also inactive phase, demonstrating that hypothyroidism leads to decreased heart rates in TRα^{WT} but not TRα^{0} mice.

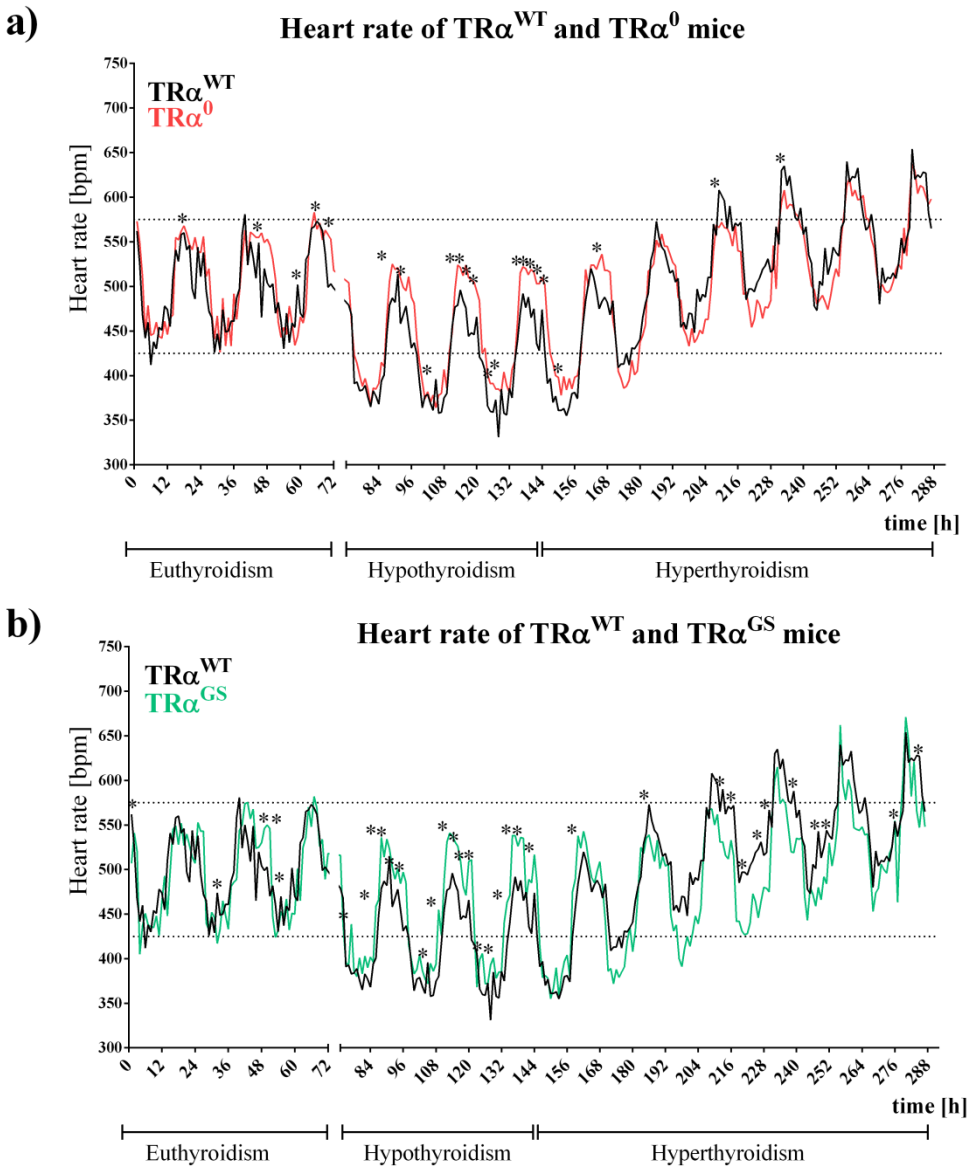

Figure 33: Development of heart rate changes over time in hypo- and hyperthyroidism is a canonical TRα effect. *Heart rate was recorded for three days in eu-, hypo- and early and late hyperthyroid state of male TRα^{WT}, TRα^{0} and TRα^{GS} mice. a) Comparison of TRα^{WT} (black curve) and TRα^{0} (red curve) and b) Comparison of TRα^{WT} (black curve) and TRα^{GS} (green curve) mice. Values blotted are hourly mean values averaged for each genotype (n=6-8). Multiple t-test calculated for hourly values TRα^{WT} vs. TRα^{0} and TRα^{GS} respectively. * p < 0.05.*

Interestingly, during hyperthyroidism, the differences became less pronounced and occurred less often, but $TR\alpha^{WT}$ mice were able to overtake $TR\alpha^{0}$ mice and displayed higher heart rates in the end. The lack of TRα is characterised by less reduction in hypothyroidism and less increase in hyperthyroidism, suggesting $TR\alpha^{0}$ has a strong impact on heart rate regulation in hypo- and hyperthyroidism (Figure 33b). Comparisons in group B lead to a similar result: euthyroid $TR\alpha^{GS}$ mice (green curve) showed higher heart rates than $TR\alpha^{WT}$ mice (black curve) at the end of each active phase, hypothyroidism lead to strong heart rate downregulation in $TR\alpha^{WT}$ but not in $TR\alpha^{GS}$ mice, and in hyperthyroidism heart rates were strongly upregulated in $TR\alpha^{WT}$ mice only. Here, the differences were even more pronounced than within group A with the main differences at the end of active and inactive phases of hyperthyroidism (Figure 33c). Overall, these results demonstrated that heart rate regulation in hypo- and hyperthyroidism was impaired in $TR\alpha^{0}$ as well as $TR\alpha^{GS}$ mice, indicating that canonical TRα signalling controls short- and long-term adjustment of heart rate.

Heart rate development already revealed that major differences occur at the end of the active and inactive phases and was mostly found in the hypothyroid state. Therefore, the active and inactive phases were divided into two sections, resembling the first and second half of the day and night, respectively. Hence, the active phase consisted of section I and II and the inactive phase was defined as section III and IV. Here, a circadian rhythm over the course of section I-IV became clear in all groups (Figure 34a). No noteworthy differences could be found in the active euthyroid state where all groups displayed heart rates of about 550 bpm, while the early inactive phase showed a small tendency of higher heart rates in $TR\alpha^{0}$ and $TR\alpha^{GS}$ mice, suggesting that the regulation of heart rate might be impaired in both groups. This effect was even more pronounced in the active hypothyroid state where $TR\alpha^{WT}$ mice had strongly reduced heart rates of less than 450 bpm. $TR\alpha^{0}$ and $TR\alpha^{GS}$ mice conversely seem to be unable to respond to hypothyroidism with reduced heart rates in the active state. During phase III the differences between controls and $TR\alpha^{0}$ and $TR\alpha^{GS}$ mice, respectively, was not significant and almost absent in phase IV (Figure 34b). During the hyperthyroid phase I heart rates were increased from 425 bpm to 490 bpm in $TR\alpha^{WT}$ mice (Δ65 bpm), which was less pronounced in $TR\alpha^{0}$ and $TR\alpha^{GS}$ mice (Δ30-35 bpm) (Figure 34c). A similar pattern of heart rate changes was also found in the phase II as well as throughout the inactive phase.

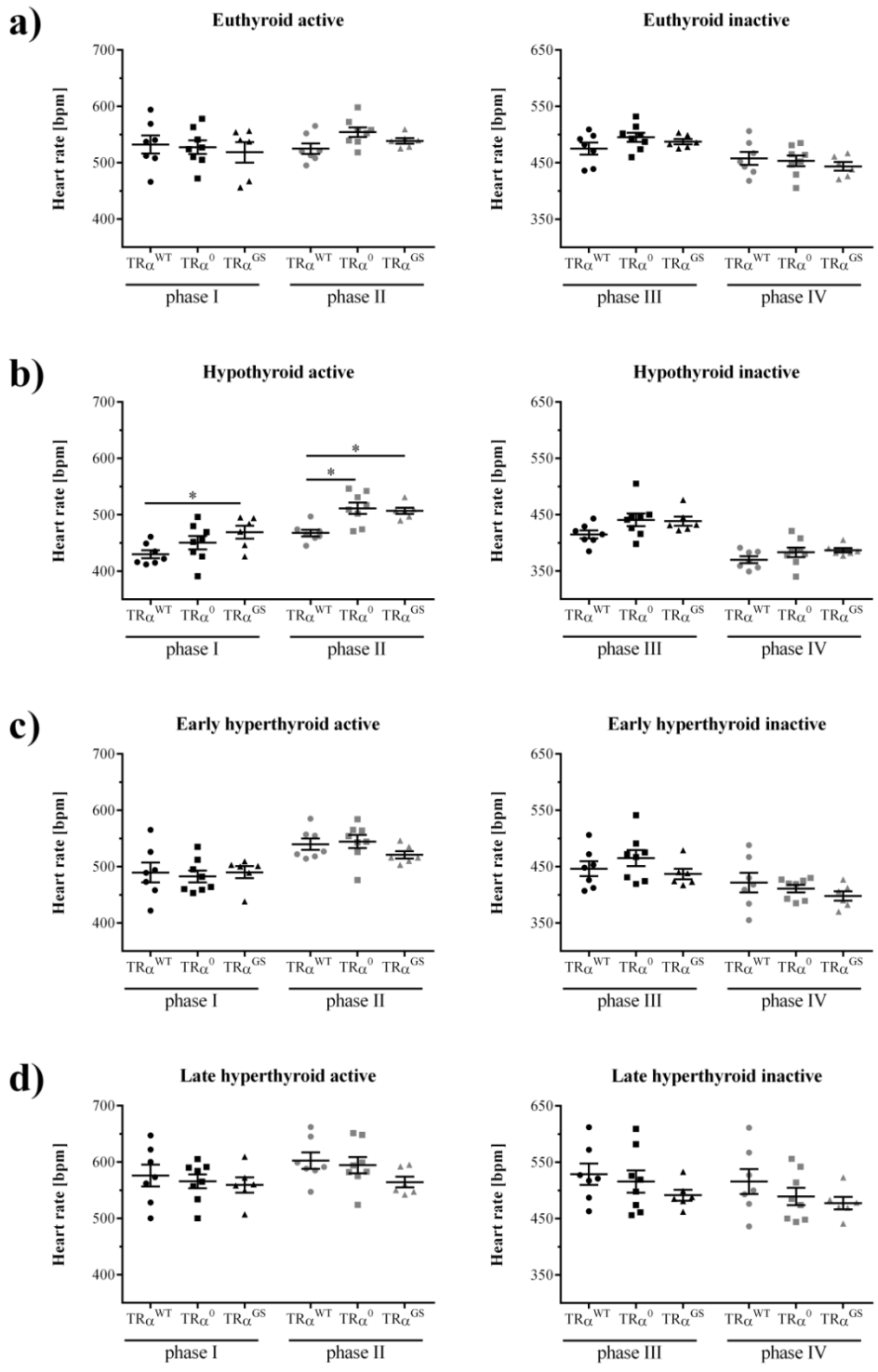

Figure 34: Average heart rate changes during the circadian rhythm depend on canonical TRα signalling. *Average heart rate from eu-, hypo- and hyperthyroid male $TR\alpha^{WT}$, $TR\alpha^{0}$ and $TR\alpha^{GS}$ mice (n=6-8) was calculated for 6 hour intervals resulting in phase I-IV representing the early and late active (black) and inactive (grey) phase respectively. (one-way ANOVA with Sidak's multiple comparison test; comparison of genotypes within each phase). Values are mean ± SEM; * $p < 0.05$.*

In late hyperthyroidism, no significant differences between genotypes could be found, although the overall heart rate values continued to increase in response to T_3 treatment (Figure 34d). In summary, circadian rhythm regulation of heart rates was impaired in TRα^0 and TRα^{GS} mice. Differences were most pronounced during hypothyroidism but tendencies could be observed in eu- and hyperthyroidism. Overall, this data confirms the previous examinations of heart rate frequencies and development and demonstrates that heart rate regulation is a canonical TRα effect.

Body temperature adjustment in thyroid dysfunctions is regulated via canonical TRα signalling

Core body temperature from TRα^{WT}, TRα^0 and TRα^{GS} mice during all three thyroid states was measured and averaged, and relative frequencies were compared. Body temperature ranged from 35 °C to 39 °C in the active and 34 °C to 38 °C in the inactive phase of TRα^{WT} mice. In euthyroid active mice, the body temperature peak was observed at 37.5 °C, which shifted to 37.25 °C in hypothyroidism and 38 °C in hyperthyroidism. Overall, curves from all three thyroid states displayed a similar trend in which the hypothyroid curve was shifted to lower and the hyperthyroid curve was shifted to higher temperature frequencies. During the inactive phase, body temperature was decreased in hypothyroidism and increased in hyperthyroidism, demonstrated by the shifted peaks from 35.5 °C to 35.0 °C and 36 °C, respectively (Figure 35a). This effect, however, was strongly diminished in TRα^0 mice, where almost no regulation from the euthyroid to the hypothyroid state and only minor shifts in hyperthyroidism were observed in the active phase. Here, the curves appeared much narrower than in control mice, suggesting that TRα plays an important role in body temperature adjustment during thyroid dysfunctions and its absence prohibits the temperature increase in hyper- and decrease in hypothyroidism. In inactive TRα^0 mice, minor body temperature changes in both directions could be found, although the changes, especially in hypothyroidism, were much less pronounced than in TRα^{WT} mice. Relative frequencies of body temperatures in hyperthyroidism, however, were comparable to those of control mice (Figure 35b). In active TRα^{GS} mice, body temperature regulation was comparable to that of TRα^0 mice, with only the frequencies of peak values being different between the two groups. Specifically, TRα^{GS} mice displayed higher peak temperatures during euthyroidism but lower temperatures for hypo- and hyperthyroidism, resulting in a slightly less pronounced phenotype than TRα^0 mice.

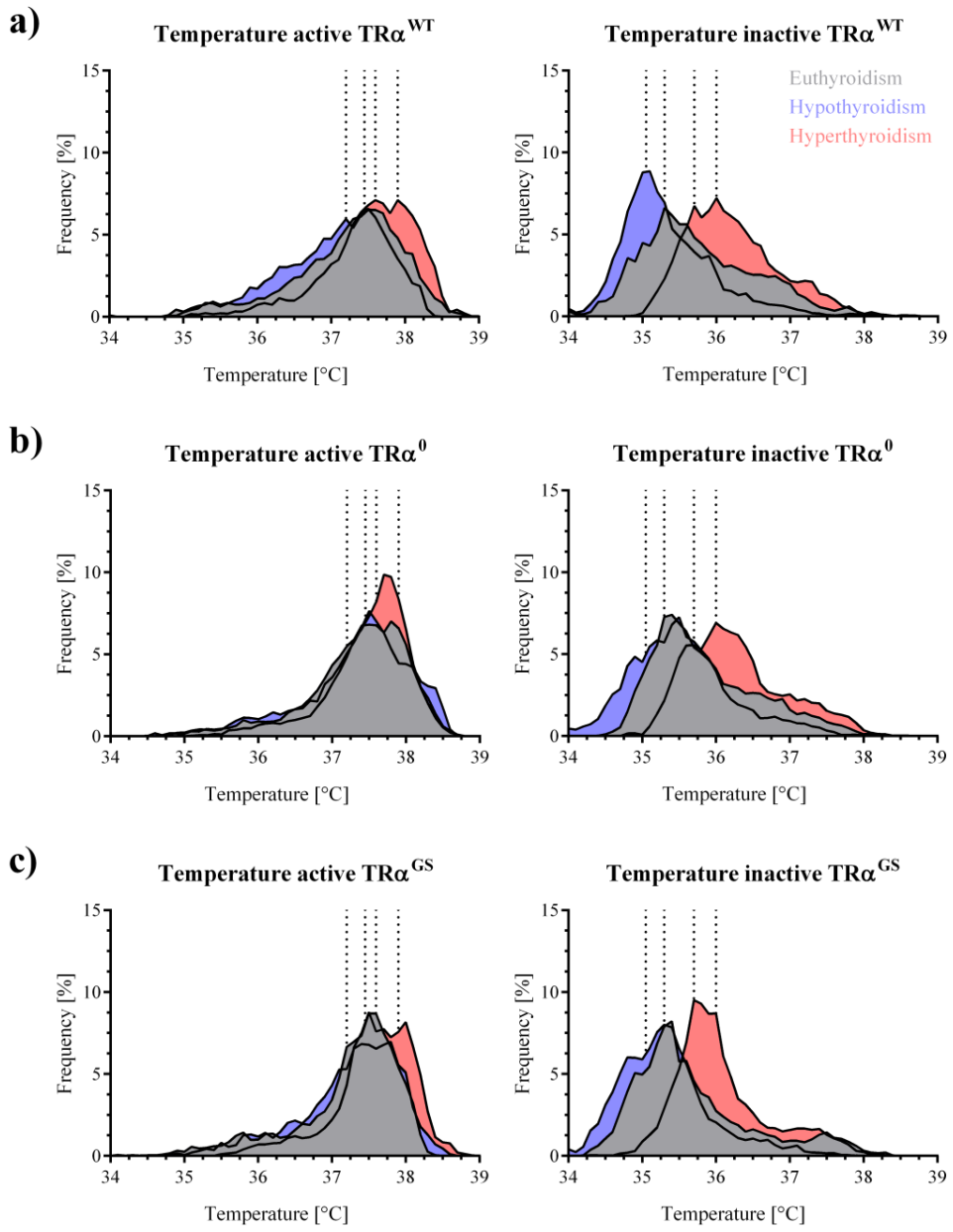

Figure 35: Body temperature regulation in thyroid dysfunctions is controlled by TRα. *Body temperature was recorded for three days in the eu- (grey), hypo-(blue) and early and late hyperthyroid (red) state of male TRα^{WT}, TRα^{0} and TRα^{GS} mice. Mean values were saved every 30 sec, divided into active and inactive phase and averaged for each genotype (n=6-8). Relative frequency for body temperature values was calculated in 0.1 °C steps and expressed as %.*

This tendency was also observed in the inactive phase where TRα^{GS} mice displayed a unique shift of relative body temperature frequencies in hyperthyroidism (Figure 35c). In summary, these results did not allow a clear distinction into canonical or noncanonical signalling in body temperature regulation.

To bring further insight into body temperature regulation, the progression in all three thyroid states over time was analysed. Here, we found that euthyroid TRα^{0} mice have higher temperatures at the end of each active phase in comparison to control mice (Figure 36**).** This effect became even more distinct with the induction of hyperthyroidism due to the lowering of body temperature in control mice and the lack thereof in TRα^{0} mice. Only minor differences were observed in hyperthyroidism in which TRα^{WT} mice started out with lower body temperature values than TRα^{0} mice but overtook those in late hyperthyroidism (Figure 36b). Euthyroid and hypothyroid TRα^{GS} mice had higher body temperatures at the end of each active phase, but the curves equalled during hyperthyroidism with only slight differences in the active and inactive phases (Figure 36c). Overall, the main differences in body temperature regulation were observed in the active phases and were comparable in TRα^{0} and TRα^{GS} mice, suggesting that canonical signalling could mediate temperature adjustment in response to thyroid dysfunctions.

Since both, the relative frequency and body temperature development during thyroid dysfunctions, did not allow a definite assignment to either canonical or noncanonical TRα action, mean body temperature was calculated for 6-hour intervals, resulting in 4 phases (Figure 37). This analysis revealed that core body temperature in TRα^{WT} mice decreased slightly after the induction of hypothyroidism and increased significantly in response to hyperthyroidism. This pattern could be observed in the active and inactive state to a similar extent and illustrates a circadian rhythm with increasing temperatures during the day and decreasing values during the night (Figure 37a). A similar pattern was observed in phase I and III of TRα^{0} mice, but no significant regulation was found in phase II and IV, where the latter might be due to the high variations. Nonetheless, the differences between thyroid states during phase II are absent in these mice (Figure 37b). Interestingly, TRα^{GS} mice were comparable to TRα^{0} mice in most phases. Here, body temperature of TRα^{GS} mice was lowered in response to hypothyroidism and increased in hyperthyroidism of phase I and III, whereas no significant differences were observed for phase II. However, in contrast to TRα^{0} mice, TRα^{GS} animals in phase IV had higher body temperatures in hyperthyroidism, presumably due to the less pronounced variations in this group (Figure 37c). The lack of differences in phase II of TRα^{0} and TRα^{GS} might explain the differences between

them and respective controls that were observed at the end of active phase in Figure 36. Overall, the calculation of average body temperature during the circadian rhythm suggests that body temperature adjustment is regulated *via* canonical TRα signalling.

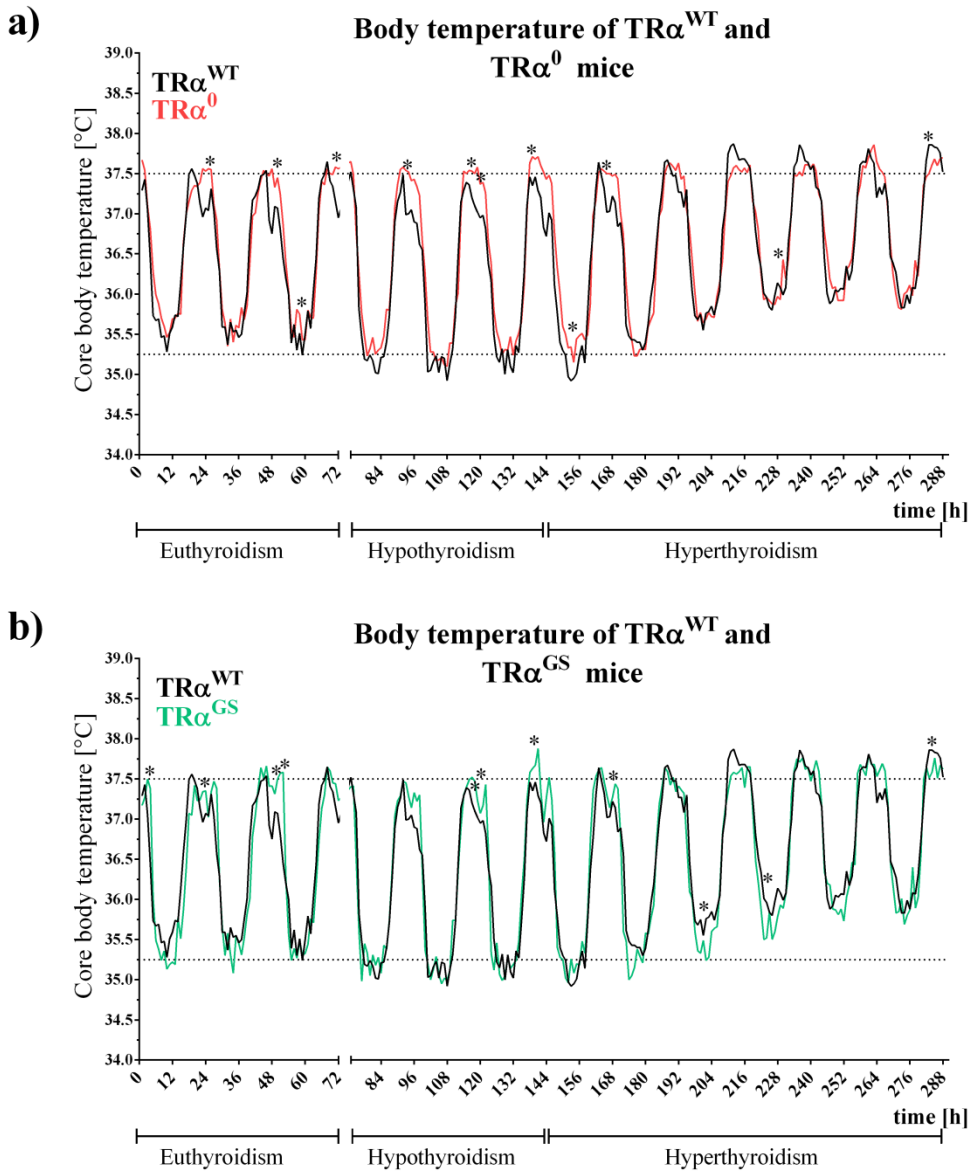

Figure 36: Development of core body temperature changes over time in hypo- and hyperthyroidism is a consequence of TRα signalling. *Body temperature was recorded for three days in eu-, hypo- and early and late hyperthyroid state of male TRα^{WT}, TRα^{0} and TRα^{GS} mice. a) Comparison of TRα^{WT} (black curve) and TRα^{0} (red curve) mice and b) Comparison of TRα^{WT} (black curve) and TRα^{GS} (green curve) mice. Values blotted are hourly mean values averaged for each genotype (n=6-8). Multiple t-test calculated for hourly values for b&c respectively (one-way ANOVA with Tukey's multiple comparison test). Values are mean ± SEM; * p < 0.05.*

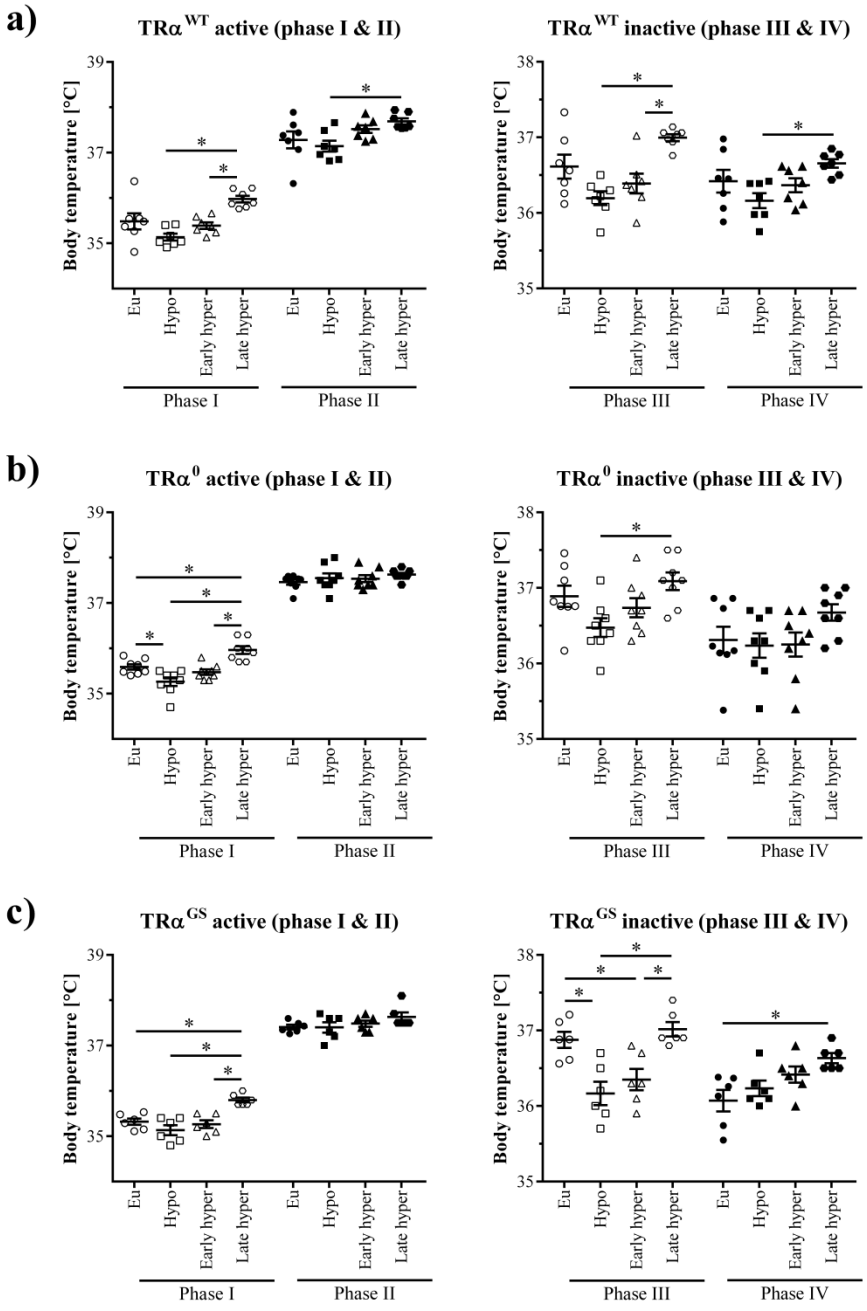

Figure 37: TRα contributes to body temperature adjustment during the circadian rhythm in thyroid dysfunctions. *Body temperature of eu-, hypo- and hyperthyroid male TRα^{WT}, TRα^{0} and TRα^{GS} mice (n=6-8) was calculated for 6-hour intervals, resulting in an early (empty symbols) and late (filled symbols) half for the active and inactive phase, respectively. (one-way ANOVA with Sidak's multiple comparison test; comparison of thyroid state within each phase). Values are mean ± SEM; * p < 0.05.*

This study revealed that the adjustment of core body temperature during thyroid dysfunctions is partially regulated by TRα with a residual regulatory in both $TR\alpha^{0}$ and $TR\alpha^{GS}$ mice suggesting that other TR isoforms or pathways are involved. Whereas the evaluation of body temperature frequencies did not allow a classification into canonical or noncanonical TRα signalling, the analysis of temperature progression and average temperature during circadian phases suggest that canonical TRα signalling contributes to circadian control of body temperature.

Locomotor activity in thyroid dysfunctions is affected by canonical TRα signalling

Changes of locomotor activity were compared between $TR\alpha^{WT}$ and $TR\alpha^{0}$ (group A) as well as $TR\alpha^{WT}$ and $TR\alpha^{GS}$ mice (group B). This revealed that $TR\alpha^{0}$ and $TR\alpha^{GS}$ were more active at the end of active phases than control animals. Moreover, the majority of differences could be found in the hypothyroid state in both groups (Figure 38). Comparisons within group A revealed that euthyroid $TR\alpha^{WT}$ mice (black curve) were more active in the first half of the active phase, whereas $TR\alpha^{0}$ mice (red curve) failed to reduce their activity at the end of the active phase (Figure 38b). Interestingly, the number of activity counts per hour was not decreased in hypothyroidism in either $TR\alpha^{WT}$ or $TR\alpha^{0}$ mice, while the induction of hyperthyroidism lead to increased activity in both genotypes. A similar pattern could be observed within group B. Euthyroid $TR\alpha^{GS}$ mice (green curve) showed higher activity at the end of active phases in comparison to $TR\alpha^{WT}$ animals, which were more active in the beginning. Hypothyroidism caused increased activity in $TR\alpha^{GS}$ mice, and hyperthyroidism resulted in increased locomotor activity in both genotypes (Figure 38c). These results suggest that canonical TRα signalling contributes to locomotor activity control in thyroid dysfunctions, as the presence of noncanonical signalling is not sufficient to restore TRα control in this process.

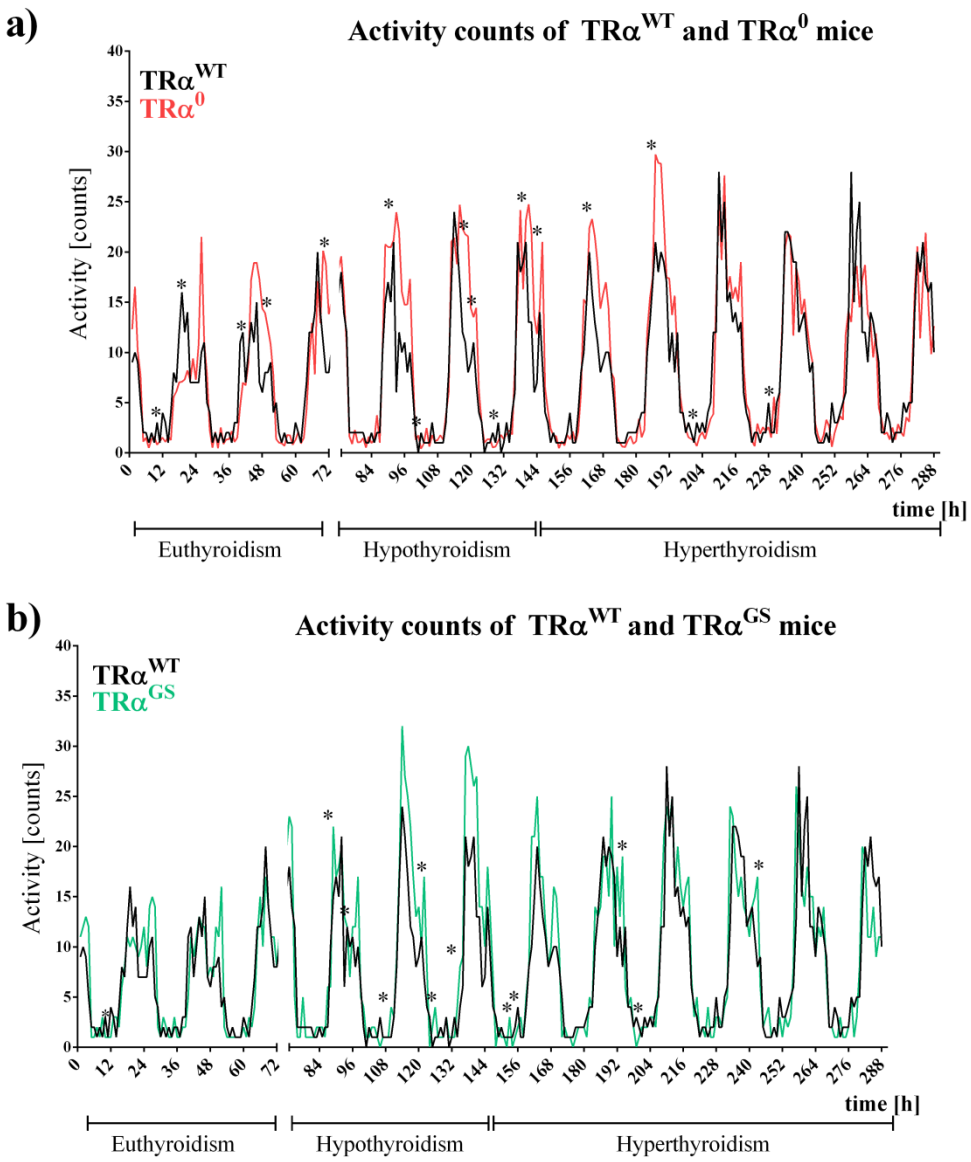

Figure 38: Development of locomotor activity in hypo- and hyperthyroidism is a canonical TRα effect. *Activity counts were recorded for three days in eu-, hypo- and early and late hyperthyroid state of male TRα^{WT}, TRα^{0} and TRα^{GS} mice. a) Comparison of TRα^{WT} (black curve) and TRα^{0} (red curve) and b) Comparison of TRα^{WT} (black curve) and TRα^{GS} (green curve) mice. Values blotted are hourly mean values averaged for each genotype (n=6-8). Multiple t-test calculated for hourly values for b&c respectively. * p < 0.05.*

Due to the oscillation of activity counts during the day and night, the active and inactive phases were divided into two sections, respectively, resulting in 6-hour intervals to be analysed. Here, no significant differences between control mice and neither TRα^{0} nor TRα^{GS} mice could be found. Yet, some tendencies give clues as to how TRα affects locomotor activity (Figure 39). In the

euthyroid phase II, where $TR\alpha^{WT}$ animals appear to have reduced their activity from approximately 15 to 10 counts/hour, $TR\alpha^{0}$ and $TR\alpha^{GS}$ mice were still as active as in the first half of the active phase and even had higher rates than the control group. This effect, however, was absent in the inactive phases where only minor differences between the groups were observed (Figure 39a). Interestingly, none of the three genotypes reacted to the induction of hypothyroidism with reduced but with increased activity in the active phase, which was even more pronounced with approximately 20 counts/hour in both $TR\alpha^{0}$ and $TR\alpha^{GS}$ mice than in controls (Figure 39b). Again, the inactive phase was mostly unaffected in all genotypes, and values were comparable to those in the euthyroid state, suggesting that the active phase might be more affected than the inactive phase. The induction of hyperthyroidism slowly increased activity over time, so that $TR\alpha^{WT}$ mice ultimately had higher activity counts in phase I than $TR\alpha^{0}$ and $TR\alpha^{GS}$ mice (Figure 39b, c). Furthermore, the long-term induction of hyperthyroidism affected the locomotor activity in the inactive state as well, indicated especially by phase IV (Figure 39d). Taken together with the previous analysis, this examination further supports a contribution of canonical TRα signalling in locomotor activity control during thyroid dysfunctions. However, the observed effects are only tendencies and should be interpreted carefully, and other contributing factors have to be taken into consideration.

Lastly, we analysed how often mice were completely inactive by comparing the relative frequency of the zero-count event in all groups. Here, the inactive phase was more affected than the active phase, during which no significant differences could be observed (Figure 40a-c).

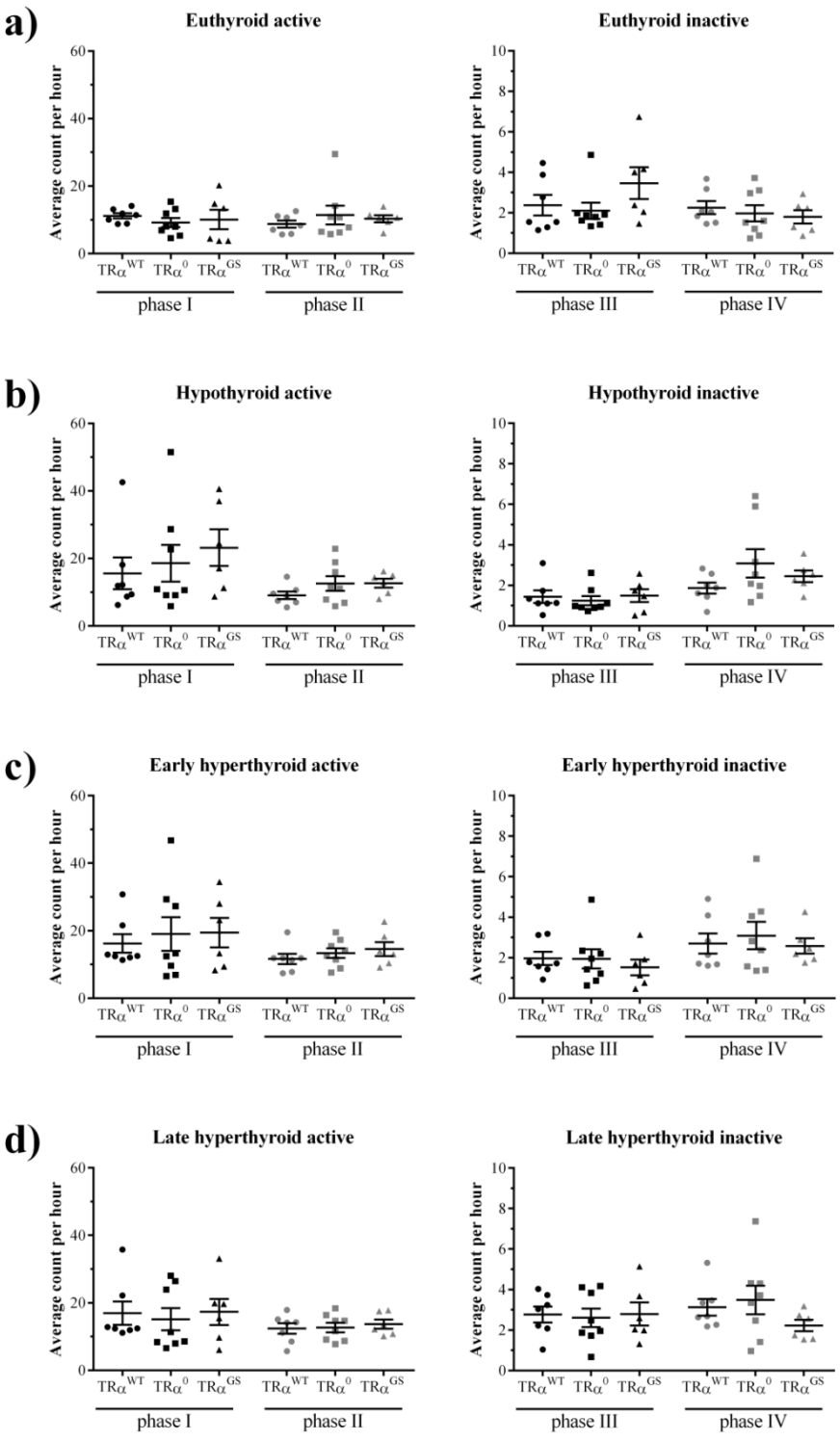

Figure 39: Average locomotor activity in thyroid dysfunctions is affected by canonical TRα signalling. *Locomotor activity counts from eu-, hypo- and hyperthyroid male TRα^{WT}, TRα^{0} and TRα^{GS} mice (n=6-8) was calculated for 6-hour intervals resulting in phase I-IV representing the early and late active (black) and inactive (grey) phase, respectively. (one-way ANOVA with Sidak's multiple comparison test, phase I vs. phase II and phase III vs. phase IV). Values are mean ± SEM; * p < 0.05.*

In inactive TRα mice, the induction of hypothyroidism caused an increased number of events where mice did not move from one spot to another. This was significantly reduced in hyperthyroidism (Figure 40d). In $TR\alpha^0$ mice, only the development from hypo- to hyperthyroidism was comparable to control animals, and no significant differences were found in $TR\alpha^{GS}$ animals (Figure 40e, f). This adds to the assumption that canonical TRα signalling is part of a network that alters locomotor activity in response to a lack or abundance of thyroid hormones.

In conclusion, the analysis of locomotor activity through different approaches gave evidence for the involvement of canonoical TRα signalling. However, the observed differences were minor and need to be interpretated carefully and further explored by additional studies.

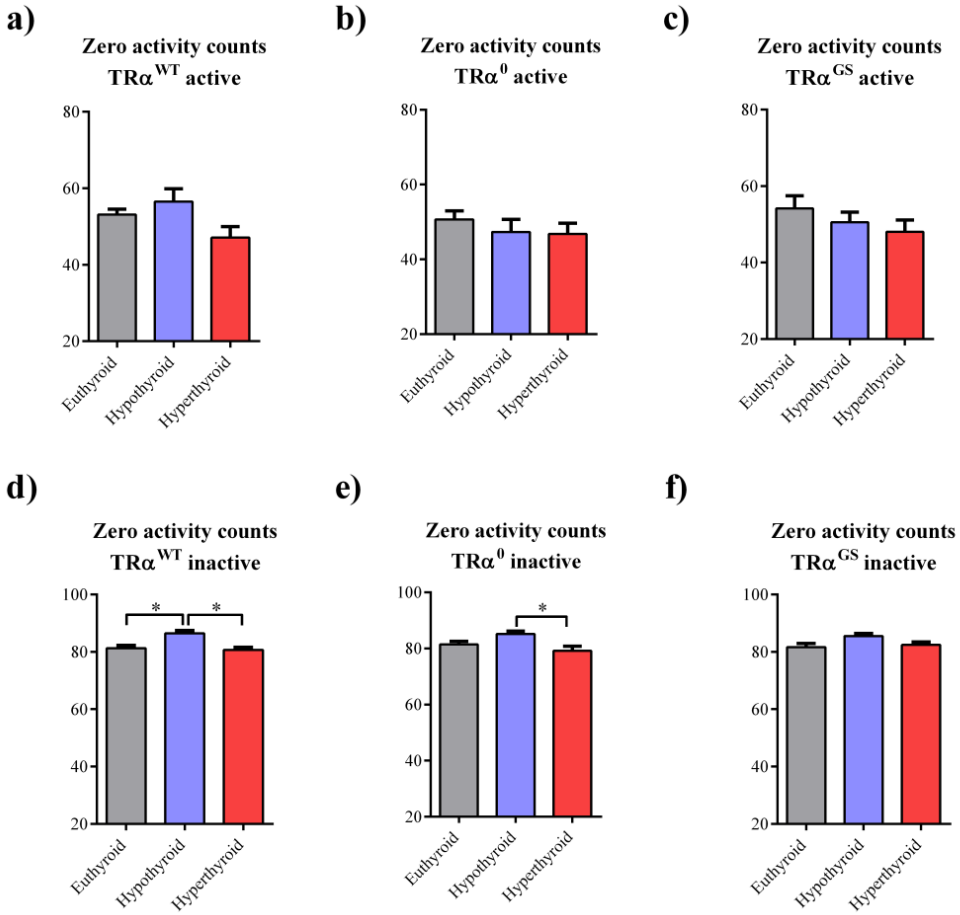

Figure 40: Activity alteration in thyroid dysfunctions is a canonical TRα effect. *Activity was recorded for three days in eu- (grey), hypo- (blue) and early and late hyperthyroid (red) state of male $TR\alpha^{WT}$, $TR\alpha^0$ and $TR\alpha^{GS}$ mice. Amount of zero activity counts was calculated for all thyroid states and genotypes to determine how often mice did not change their position. (one-way ANOVA with Tukey's multiple comparison test). Values are mean ± SEM; * $p < 0.05$.*

Discussion

TH control and maintain numerous processes in development, metabolism and the CVS, where blood pressure, heart rate and cardiac growth are among the targets. Because of this, thyroid dysfunctions can cause profound malfunctions in the CVS. Consequently, in order to exploit beneficial effects for suitable medical approaches, it is relevant to investigate the underlying mechanisms and relations. Until recently, the paradigm of TH/TR action consisted mainly of TRE-dependent change of target gene transcription. However, this could not explain rapid TH effects such as glucose uptake or arterial vasodilation, which occurred within seconds to minutes (Segal and Ingbar 1979; Hiroi *et al.* 2006). Many years of research revealed that a DNA-independent TR signalling pathway exists in addition to the canonical action (Cao *et al*. 2005; Simoncini *et al*. 2000; Storey *et al*. 2006; Moeller, Ulanowski, *et al*. 2006; Carrillo-Sepulveda *et al*. 2010; Martin *et al*. 2014). Yet, with the finding of noncanonical signalling, the following question came up: Which known TH effects in the CVS are mediated by canonical action and which are regulated *via* noncanonical signalling? In order to clarify if this pathway has a physiological relevance and, if so, categorise known TH effects into canonical and noncanonical signalling, a suitable mouse model was created. Since both pathways are present in WT and absent in $TR\alpha^{0}$ mice, the DNA binding of TRs was disrupted, allowing only the cytoplasmic action of TRs ($TR\alpha^{GS}$). The relevance of noncanonical signalling *in vivo* was demonstrated in a recent study where several cardio-metabolic effects were categorised and described. However, many more effects, especially in the CVS, where TRα mediates most effects, have yet to be studied (Hones *et al.* 2017). In order to clarify how TH and TRα impact blood pressure, cardiac hypertrophy development as well as heart rate and body temperature $TR\alpha^{WT}$, $TR\alpha^{0}$ and $TR\alpha^{GS}$ mice were studied, and TH effects in the CVS could be attributed to canonical and noncanonical TR action.

Noncanonical TRα action induces vasodilation and thereby influence vascular tone

Patients with thyroid dysfunctions suffer from altered arterial pressure due to direct effects on the vascular system and secondary effects resulting from metabolic alterations. Yet, the vasodilatory properties of the vascular system in this state have not been studied detail. Here, vasomotor

activity of arteries from hypo- and hyperthyroid mice was examined. Additionally, the role of TRα in this process was investigated since previous studies demonstrated that arteries from $TR\alpha^0$ mice were not able to dilate in response to T_3 (Liu *et al.* 2014). However, up to date, it was unknown, which signalling pathway mediates T_3-induced vasodilation. Furthermore, our study included the identification of key mediators as well as different artery entities and the identification of the endothelium as the crucial cell type.

T_3-induced vasodilation is mediated by noncanonical TRα signalling

The aim of this study was to answer how TH mediate vasodilation. Consistent with recent research and clinical studies, TRα could be shown to be the responsible receptor for T_3-mediated vasodilatation (Liu *et al.* 2014; Goumidi *et al.* 2011). The use of a knock-in mouse model in which canonical signalling was absent, demonstrated that this relaxation of arteries in response to TH administration was a consequence of noncanonical signalling *in vivo* and *in vitro* (Figure 14 & Figure 15). This finding was further supported by the short time period between hormone administration and observed dilatory effect. This observation is concordant with a clinical study in which blood pressure was significantly reduced within three minutes after TH administration (Schmidt *et al.* 2002). Interestingly, T_3-induced vasodilation did not differ between mesenteric and femoral arteries, suggesting that this is a general effect in the vascular system and, accordingly, TH play an important role in blood pressure regulation (Figure 17). Still, the vasomotor assay was performed with isolated arteries, and additional *in vivo* studies were performed to conclude a physiological relevance. In these *in vivo* blood pressure measurements, the reduction of arterial pressure in response to T_3 injections was observed within seconds and lasted throughout the measurement period. Strikingly, this effect was absent in $TR\alpha^0$ yet preserved in $TR\alpha^{GS}$ mice. Taken together, these observations could not be explained with the canonical pathway, since the alteration of target gene transcription and subsequent production of proteins would require several hours, leaving the activation of cytoplasmic kinases *via* noncanonical TRα signalling as the most plausible option.

T_3-mediated vasodilation depends on eNOS and PI3K activation in the endothelium

To further clarify the steps following TRα activation, PI3K and eNOS action was blocked with specific inhibitors, resulting in significantly reduced responses to T_3. Consequently, both proteins

were identified as key proteins in T_3-mediated vasodilatation (Figure 18). However, the inhibition of PI3K had a greater effect than eNOS inhibition, which could be due to the upstream position of PI3K in the regulatory chain (Hien *et al*. 2012). Hence, an amplification of the signal from up- to downstream could explain the difference between PI3K and eNOS inhibition (≈10%). Upon identifying key mediators in T_3-induced vasodilation, the role of endothelial cells and VSMCs was studied. Since previous studies have reported that both cell types are targets for TH actions, the next aim was to identify the responsible cell type in TH-mediated artery dilatation (Cai *et al.* 2014; Ojamaa, Klemperer, and Klein 1996). Therefore, rat mesenteric arteries without endothelium and whole arteries were compared. This experiment revealed that endothelial cells are crucial for T_3-mediated vasodilatation (Figure 18). This however, does not exclude possible T_3 effects in VSMCs. Overall, the importance of eNOS and AKT phosphorylation, and thus the production of NO as a vasodilatory signalling molecule in the endothelium, were proven as a crucial step in this study.

Thyroid dysfunctions affect T_3-mediated vasodilation

Clinical and experimental studies have shown that patients with hypo- or hypothyroidism are prone to develop cardiovascular diseases and have been associated with a highly increased risk for vascular morbidity and mortality, indicating that thyroid dysfunctions have a great impact on vascular health (Hak *et al.* 2000; Walsh *et al.* 2005; Cappola *et al.* 2006). More than 10% of women aged >55 years suffer from subclinical hypothyroidism, and 1-2% have subclinical hyperthyroidism, and even minor changes in circulating hormone concentration can be sufficient for causing detrimental effects on the cardiovascular system (Canaris *et al.* 2000; Laurberg *et al.* 1998; Vadiveloo *et al.* 2011). Hence, to find an explanation for abnormal arterial pressure in chronic hypo- and hyperthyroidism, both states were artificially induced in mice. Interestingly, arteries from hypothyroid mice were as responsive as control vessels, suggesting that arterial blood pressure regulation in formerly hypothyroid patients might be restored through TH treatment. On the contrary, reduced responsiveness to T_3 was found in arteries from hyperthyroid mice (Figure 16). This might occur due to an oversaturation of hormone within the cells, causing only minor responses to T_3 in the vasomotor assay. Different vasodilatory and vasoconstricting substances have been tested on hypo- and hyperthyroid rat arteries with results ranging from reduced, unchanged to enhanced responsiveness, indicating that those responses are tissue- and time specific and depend on the preparation of arteries (Vargas *et al*. 2006). The connection of

NO production and TH availability appears to be a relevant influence on arterial pressure and can be seen in both states of thyroid dysfunction (Klein 1990; Danzi and Klein 2003; Vargas *et al.* 1995). Previous studies demonstrated that this is linked to altered NOS expression and occurs, firstly, due to noncanonical TRα-mediated PI3K and thus NOS activation and, secondly, due to increased circulation in the case of hyperthyroidism (Ray *et al.* 2013; Quesada *et al.* 2002). These epidemiological findings fit with the preserved vasodilatory activity of hypothyroid mesenteric arteries. Another explanation for the reduced responsiveness of hyperthyroid arteries might be found in the cellular level. For example, muscle cells could be affected, since hyperthyroidism has been shown to have impact on *Myh6* and *Myh7* composition in cardiomyocytes. Hence, similar effects on the vascular myocytes would be plausible (Janssen, Muller, and Simonides 2017). Furthermore, a down regulation of TH transporters on endothelial cell surfaces might contribute to the observed phenotype as this has been previously reported to be a consequence in livers of hyperthyroid mice (Engels *et al.* 2015). Thus, by limiting the amount of intracellular TH, the organism is able to reduce severe consequences of hyperthyroidism.

Despite unveiling many central steps of the process, there are still numerous aspects to consider. First, TH are not the only substances able to regulate arterial pressure. Features ranging from salt intake, obesity and insulin resistance, the renin-angiotensin system and sympatric nervous system have been studied as well as genetic backgrounds, endothelial dysfunction, nutrition and neurovascular anomalies. Regular blood pressure is the result of a balance between CO and peripheral vascular resistance, and multiple factors contribute to that balance (Beevers, Lip, and O'Brien 2001). By administering vasodilatory or constricting substances, this balance shifts in either direction, and counteracting reactions can follow. For instance NO, one of the most important dilatory molecules, has a very short half-life time in the blood where it disappears within milliseconds to seconds (Kelm and Schrader 1990). Downstream effects of NO are deactivated in a similarly quick way. For example soluble guanylyl cyclase, the first target of NO, is deactivated within milliseconds of NO removal (Bellamy and Garthwaite 2001). This mechanism of reversible agonist binding with a conformational change of the enzyme makes a rapid regulation possible. The phosphorylation of eNOS and AKT, on the other hand, is more stable with p-AKT staying in its active form for approximately 20 minutes (Baker *et al.* 2005). The interaction of both aspects might explain the curve progression of our *in vivo* studies where T_3 injections lead to rapid reduction of arterial pressure, but opposing effects appeared to result in

an increased blood pressure soon after injections (Figure 15) and might be connected to long-term effects as seen in Figure 16.

In this study, T_3-mediated vasodilatation was identified to be mediated through noncanonical TRα signalling by *ex vivo* and *in vivo* experiments. For the functionality of this mechanism, intact endothelium was crucial. This could expain why endothelial dysfunctions is often observed in hypothyroid patients. Moreover, reduced responsiveness to T_3 was observed in arteries from hyperthyroid mice, while hypothyroid arteries were comparable to controls. This observation adds to the understanding of long-term consequences on arterial pressure regulation in hypo- and hyperthyroid patients and might contribute to optimised treatments.

T_3-induced cardiac hypertrophy is mainly mediated by noncanonical TRα signalling

Cardiac hypertrophy has long been recognised to be a consequence of untreated hyperthyroidism (Bedotto *et al.* 1989; Morgan and Baker 1991; Razvi *et al.* 2018). In numerous clinical studies and laboratory experiments, the underlying mechanisms were investigated. Still, it has not been clarified which receptor, TRα or TRβ, is crucial for the development of cardiac hypertrophy in response to TH excess, and conflicting results in this regard have been published in the past. Hence, the aim of this study was to compare $TR\alpha^{WT}$, $TR\alpha^{0}$ and $TR\beta^{-}$ mice and thereby determine in which group TH-induced hypertrophy was absent. Furthermore, the respective TR^{GS} mouse of this receptor was studied to attribute TH-induced cardiac hypertrophy to canonical or noncanonical TR action.

Noncanonical TRα signalling mediates T_3-induced cardiac hypertrophy according to echocardiography and heart weight analysis

First, echocardiography studies with untreated 15-week-old male and female TR^{WT}, TR^{KO} and TR^{GS} mice yielded no significant differences between TR^{WT} and their respective knockout or mutant mice (Table 14). None of the functional parameters, i.e. heart rate, ejection fraction and fractional shortening, nor the morphological features of the heart (wall thickness, left ventricular weight) differed significantly in these cohorts. This is why we planned a build-up study in which echocardiography examinations of untreated and hyperthyroid mice were performed serially to monitor hypertrophy development. For this study, a mild induction of hyperthyroidism was

chosen in order to create a phenotype as it can be found in patients (Chen *et al.* 2018). According to TH serum level analysis, the chosen T_3 dose resulted in a 1.5-2-fold increase of fT_3 and a strong down-regulation of both, fT_4 and TT_4 in mice, which resembles the required mild hyperthyroidism (Figure 19). As all animals in this study were investigated during anaesthesia, this parameter was used as a control and inclusion criterion (Figure 21). Due to comparable heart rates, we were able to compare the other echo parameters and exclude heart rate-mediated changes. In this study, the induction of hyperthyroidism did not cause detrimental changes in ejection fraction or fractional shortening. However, it is noteworthy that in the control group mostly upward tendencies of these functional parameters could be observed during growth while the opposite was true in hyperthyroid mice. Consequently, T_3 treatment affected the heart function slightly. In previous studies, overt hyperthyroidism has been associated with reduced contractility and ejection fraction (Klein and Ojamaa 2001; Bengel *et al.* 2000; Kahaly *et al.* 1995). Yet, the minor changes in this study probably result from the mild T_3 treatment or the duration of the study and could potentially be increased with higher T_3 doses.

Insight into the role of TRs in hypertrophy development was gained from the heart morphology, which was clearly affected by hyperthyroidism. The comparison of control and hyperthyroid mice revealed that T_3 caused increased wall thickness over time in TR^{WT} and $TR\beta^{-}$ but not $TR\alpha^{0}$ mice. Generally, heart weight is better normalised to tibia length than body weight as the latter can change drastically in animals, especially when group size varies, which makes it a less suitable parameter for normalisation (Kamakura *et al.* 2016). Moreover, body weight might differ in various genotypes. Nonetheless, as TRα is known to impact bone development, both normalisations were calculated here, showing that TH-induced cardiac hypertrophy was mediated *via* TRα (Figure 20) (Duncan Bassett and Williams 2003; Bassett *et al*. 2006). This result was supported by the echocardiography measurements, which revealed that $TR\alpha^{0}$ was the only group in which T_3 did not increase wall thicknesses (LVPW;d & IVS;d). Interestingly, those were also the only animals which had higher LVID;d. Taken together, the morphological changes caused by hyperthyroidism did not translate into impaired cardiac function in this study and thus suggests the physiological subtype of cardiac hypertrophy to be the result (Dillmann 2010). Yet, this result was in opposition to some previous studies where hypertrophy was absent in mice with a non-functional TRβ (Imperio *et al.* 2015). However, mice in this previous study carried a TRβ mutation that resulted in a dominant negative receptor, which presumably inhibits not only TRβ but also TRα. In another study by Weiss *et al.*, $TR\alpha^{0}$ and $TR\beta^{-}$ mice were compared in an

echocardiography study. Interestingly, they found that heart rate regulation was strongly impaired in $TR\alpha^0$ but not $TR\beta^-$ mice, while T_4-induced cardiac hypertrophy appeared to be a consequence of TRβ (Weiss *et al.* 2002). However, in this study absolute heart weight values, as well as heart weight normalised to body weight and not tibia length, were evaluated.

After we identified TRα as the main mediator of TH-induced hypertrophy development through echocardiography and *ex vivo* analysis, the next aim was to identify the underlying signalling pathway. Therefore, control and hyperthyroid $TR\alpha^{WT}$ and $TR\alpha^{GS}$ mice were added to the study. Remarkably, cardiac hypertrophy development in response to prolonged TH excess appeared to be a consequence of noncanonical signalling, which is in accordance with previous studies where cytoplasmic AKT/mTOR activation appeared to be relevant in cardiac growth and could be abolished by rapamycin inhibition (Kuzman *et al.* 2005; Kuzman, O'Connell, and Gerdes 2007; Kenessey and Ojamaa 2006). In $TR\alpha^{WT}$ and $TR\alpha^{GS}$ mice, lower wall thickness and heart weights in comparison to the TRα and TRβ strain were observed in the initial measurements. In this study, the initial measurement was done with mice aged 8 to 10 weeks. Age analysis revealed that the average age was lowest in the $TR\alpha^{GS}$ strain, which might explain those differences (Figure 20).

Possible underlying mechanisms for the development of cardiac hypertrophy

In order to find explanations for the observed phenotype, an experimental setup of microscopy, qRT-PCR and immunoblot assays was chosen. Firstly, cardiomyocyte size analysis revealed that hyperthyroidism resulted in cell size increase of ≈25% in all but $TR\alpha^0$ hearts (Figure 23). Cardiac growth can result from myocyte hypertrophy or proliferation, yet cell growth was the more plausible solution since adult cardiomyocytes enter cellular arrest and are therefore unable to divide (Walsh *et al.* 2010; Ye *et al. 2*019; Grajek *et al.* 1992). This cellular arrest is strongly associated with binucleation of myocytes, while mononucleated myocytes have not yet entered this arrest and are still able to proliferate and repair cardiac damage (Pasumarthi and Field 2002; Kajstura *et al.* 2010; Muralidhar and Sadek 2016). Hypothyroidism and the lack of TRα reduce binucleation of myocytes, and it was therefore concluded that TRα and TH availability are relevant for this process (Chattergoon *et al.* 2012; Hirose *et al.* 2019). Consequently, we compared nucleation of $TR\alpha^{WT}$, $TR\alpha^0$ and $TR\alpha^{GS}$ cardiomyocytes. Here we observed that the amount of myocytes with one nucleus was increased in $TR\alpha^0$ hearts. The amount of nuclei in $TR\alpha^{GS}$, however, was comparable to WT mice, suggesting that TRα contributed to binucleation

through noncanonical action. Due to the lack of binucleation and thus cellular arrest, $TR\alpha^0$ myocytes are able to proliferate in contrast to WT and $TR\alpha^{GS}$ myocytes, where stimulation results in myocytes hypertrophy. This might connect binucleation, myocytes hypertrophy and ultimately cardiac hypertrophy development (Figure 24).

In addition, vascularisation in all control and hyperthyroid hearts has been examined, since cardiac growth has been reported to be accompanied by a corresponding expansion of the capillary network in physiological hypertrophy (Shimizu *et al*. 2010; Sano *et al*. 2007). Moreover, TRβ has been found to be associated with coronary angiogenesis in pathological cardiac hypertrophy (Makino *et al*. 2009). In our study, no significant differences between untreated control hearts and hearts of hyperthyroid TR^{WT}, $TR\alpha^0$ and $TR\beta^-$ hearts could be observed (Figure 28). Since the TRβ-dependend angiogenesis was observed during pathological hypertrophy and our treatment caused a rather mild physiological hypertrophy resembling result, this result seems plausible. Additionally, other studies showed that myocardial vasculature is remodelled in hyperthyroidism, resulting in a muscularisation rather than neo-angiogenesis (Savinova *et al*. 2011).

After determining that the cause for cardiac growth is myocyte hypertrophy and not proliferation, we aimed to find key mediators on the cellular level. For that reason, gene expression levels in control and hyperthyroid hearts were determined *via* qRT-PCR. Since noncanonical TRα signalling was found to mediate TH-induced cardiac hypertrophy, gene expression analysis might seem contradictory at first. However, it has been demonstrated that noncanonical activation of cytoplasmic targets can ultimately lead to transcriptional changes *via* TRβ and PI3K, and that noncanonical signalling can result in TRE-independent gene expression of e.g. HIF-1α or ZAKI-4α (Moeller, Dumitrescu, and Refetoff 2005). Furthermore, increased phosphorylation of AKT/PKB was found in mice with increased PI3K stimulation showing that myocyte hypertrophy is linked to PI3K activity and that it might therefore be associated with noncanonical TR action (Crackower *et al*. 2002). In accordance with the long-term treatment of mice in this study, the aim was to identify gene expression differences in cardiac hypertrophy markers and TH responsive genes. The previously demonstrated switch from slow myosin heavy chain to fast myosin heavy chain in hyperthyroid cardiac tissue was only partially observed in this study. *Myh6* was not significantly up regulated in this study whereas expression of *Myh7*, a negatively regulated gene, was reduced. Aside from the myosin composition, the expression of *Hcn2* was increased in all groups, and *Hcn4* was increased in all groups except $TR\beta^-$ in respsonse to

hyperthyroidism. Here, *Hcn2* expression was increased in hyperthyroid hearts and thereby caused changes in heart rate, which is associated with increased CO and, ultimately, enhances cardiac hypertrophy (Lorell and Carabello 2000; Larsson 2010). Interestingly, this up regulation is weakest in TRβ^{-} hearts, suggesting that it could be mediated by TRβ, and that this TR thereby contributes to hypertrophy development after all. In addition, it is noteworthy that the negative feedback system in the HPT-axis is disrupted in TRβ^{-} and that control animals in this group have higher serum TH levels *per se*. Therefore, it is plausible that the extent of upregulation from control to hyperthyroid state is smaller than in the other groups (Hashimoto *et al.* 2013). Adrenergic receptors *Adrb1* and *Adrb2* remained largely unaltered in this study, suggesting that adrenergic stimulation did not play a significant role in hypertrophy development. In addition, cardiac alpha actin was marginally affected by TH treatment as indicated by *Actc1* expresion. The slight increase in TRα^{WT}, TRα^{GS} and TRβ^{-} gives reason to speculate that actin alpha cardiac muscle 1 protein might be involved in myocyte hypertrophy. *Atp2a2* encodes the ATPase SERCA and has previously been shown to be a negatively regulated target gene after six weeks of T_4 injections (Engels *et al.* 2016). However, T_3 treatment in this study only caused a minor decrease of SERCA in TR^{WT} and TRβ^{-} hearts, suggesting that the regulation of intracellular Ca^{2+} content, and thereby muscle contraction and relaxation, is not majorly altered in hyperthyroid hearts in this study. Heart weight analysis showed that T_3 treatment resulted in a milder type of cardiac hypertrophy in this study. This is in accordance with the expression of the pro-apoptotic gene *Bax*, which is only slightly increased in all hyperthyroid hearts, while it is known to be strongly increased in severe hyperthyroidism, thereby causing apoptosis in the myocardium (Elnakish *et al.* 2015). Yet, the lack of this expression pattern suggests that the dose and duration of T_3 treatment did not result in myocardial apoptosis (Fernandes *et al.* 2011). Taken together, this analysis provides evidence that TH target and cardiac hypertrophy relevant genes can be activated *via* TRα and TRβ canonical and noncanonical signalling and that the cytoplasmic activation can ultimately lead to transcriptional changes. However, many expression changes were marginal, and statistically significant results do not mirror biological relevance and *vice versa*. Here, it is conceivable that counteracting mechanisms were activated during the treatment and counteracted the hypertrophy inducing signals. For example, the tumour suppressor protein TIP30 has recently been identified to counteract cardiac hypertrophy by inhibiting translational elongation (Grund *et al.* 2019). In other studies, molecules such as ATP, the helicase CHAMP and retinoic acid have been identified as negative regulators of cardiac hypertrophy (Liao *et al.*

2003; Liu and Olson 2002; Zhou *et al.* 1995). This is especially interesting since retinoic acid can activate retinoid acid receptors (RAR) and RXRs, which in turn have been shown to interact with TRs (Allenby *et al.* 1993; Wu, Yang, and Koenig 1998). Thus, it is plausible that cardiac hypertrophy inducing pathways might have been activated and caused cardiac growth, while at a certain point counteracting pathways were activated to protect the heart from damage.

Similar results were found in immunoblot analysis where the amount of total as well as phosphorylated ERK, mTOR and S6-kinase in $TR\alpha^{WT}$ and $TR\alpha^{0}$ hearts was not affected by hyperthyroidism (Figure 27). The MAPK-ERK pathway is a key mediator of cardiac hypertrophy and in context with TH has been reported to facilitate pathological hypertrophy (Dillmann 2010). In this study, no ERK, mTOR and S6-kinase activation could be observed in hyperthyroid hearts. This could be due to the fact that the observed mild hypertrophy is presumably a physiological hypertrophy, and therefore those proteins were not activated. Alternatively, the previously mentioned counteracting mechanisms might have shut down the activation of the protein before hearts were examined (Dillmann 2010).

Influence of thyroid dysfunctions and TRα on heart rate, body temperature and activity

The regulation of heart rate can be greatly affected in thyroid dysfunctions and has been associated with the lack of TR function. Yet, it is still unclear how canonical and noncanonical signalling influence those processes. In this study, we examined basal heart rates in TRα and TRβ KO and GS mutant mice and observed lower heart rates in TRα-deficient mice. Hence, in order to identify the underlying mechanisms in response to thyroid dysfunctions, heart rate modulation of those mice was studied *via* radio telemetry. In addition to heart rate, the core body temperature and locomotor activity were recorded and analysed in $TR\alpha^{WT}$, $TR\alpha^{0}$ and $TR\alpha^{GS}$ mice. The aim of this study was the comparison of those three parameters in our mouse models, the modulation in thyroid dysfunctions and the development of circadian rhythm in those thyroid states.

Basal heart rate is controlled by canonical TRα signalling in vivo

In this study, ECG analysis revealed that male and female $TR\alpha^{0}$ mice have lower heart rates than controls. Additionally, the same was true for male $TR\alpha^{GS}$ mice, suggesting that heart rate was

controlled by canonical TRα signalling *in vivo* because the absence of TRα and the absence of any DNA binding in $TR\alpha^{GS}$ mice show the same phenotype.

This is in accordance with a previous study where the observed differences resulted from prolonged QRS- and QTend-durations (Wikstrom *et al.* 1998). Here, heart rate differences presumably resulted from increased PR interval durations and slightly increased QRS intervals as a consequence of reduced expression of the pacemakers *Hcn2* and *Hcn4* (Figure 29) (Pachucki, Burmeister, and Larsen 1999). Interestingly, the variations in $TR\alpha^{GS}$ mice could only be observed in male but not female mice, which could result from differential regulations on the cellular level since TH are known to exert sex-specific effects (Rakov *et al*. 2014). Yet, the values in male $TR\alpha^{GS}$ mice showed a high variance and should thus be considered carefully and would then fit to previous studies from our group where noncanonical TRα signalling has been shown to contribute to extrinsic heart rate regulation (Hones *et al*. 2017).

No differences in basal heart rates were observed between $TR\beta^{WT}$, $TR\beta^{-}$ and $TR\beta^{GS}$ for either sex. The lack of TRβ causes malfunctions in the negative feedback regulation of the HPT axis, leaving those animals with increased TH serum levels (Gothe *et al*. 1999; Shibusawa, Hollenberg, and Wondisford 2003). Remarkably, in this study the mild hyperthyroidism did not cause higher heart rates in $TR\beta^{-}$ mice which possess a functional TRα (Figure 30). In previous studies, it was shown that untreated $TR\beta^{-}$ mice had 11% higher heart rates than controls (Weiss *et al*. 1998). In their study, Weiss *et al*. showed that total T_4 in $TR\beta^{-}$ mice was two fold higher than in WT mice. However, this difference was less pronounced in our study, where $TR\beta^{-}$ mice had about 25% higher TT_4 levels than WT mice which might explain the lack of increased heart rates in $TR\beta^{-}$ mice in ECG measurements. Yet, when $TR\beta^{-}$ mice were rendered euthyroid, they had normal heart rates and contractile performance showing that, overall, TRα was more relevant in TH-dependent heart rate regulation (Dillmann 2002). Additionally, the role of TRα in heart rate regulation was demonstrated when overexpression of TRα1 in neonatal cardiomyocytes induced increased spontaneous beating, which could be enhanced by T_3 administration. Meanwhile TRβ1 overexpression caused significantly lower pacing activity and could not be enhanced by T_3. Both patterns have been linked to *Hcn2/Hcn4* expression and indicate that intrinsic heart rate control is mediated through TRα. Nonetheless, the reduced beating capacity in TRβ1-overexpression myocytes promotes a regulatory role of this aporeceptor isoform and could influence pacemaker function by interacting with TRα (Gassanov *et al*. 2009). Moreover, the influence of stress during awake ECG investigation could contribute to heart rate differences in different strains. Overall,

this demonstrates that both receptors play a role in control of basal heart rate but does not explain the lack of increased heart rate in TRβ^{-} mice, and the role of both receptors needed further investigation.

Heart rate modulation during thyroid dysfunctions is mediated via canonical TRα signalling

Subsequently, heart rate modulation was further studied *via* radio telemetry to identify the underlying mechanisams in response to thyroid dysfunctions. Here, the induction of hypothyroidism resulted in bradycardia in TRα^{WT} mice, whereas hyperthyroidism caused tachycardia (Figure 32). This adjustment during thyroid dysfunctions was strongly impaired in both TRα^{0} and TRα^{GS} mice, demonstrating that this modulation was mediated *via* canonical TRα signalling. However, a residual regulatory effect in response to hypo- and hyperthyroidism remained indicating that TRβ also contributes to heart rate regulation. Moreover, the analysis of heart rate progression showed that TRα^{0} and TRα^{GS} mice had higher heart rates than TRα^{WT} mice at the end of euthyroid active phases (Figure 33). This observation was in discordance to previous radio telemetry studies from Wikström *et al.* where knockout mice had lower heart rates (Wikstrom *et al*. 1998). This difference can be explained by their use of TRα1 knockout mice where the regulatory isoform TRα2 was still present and possibly binds to TREs and thus exerts a dominant negative effect and blocks other regulatory TRs. The absence of TRα2 in our strain might explain the observed differences between TRα^{-} and TRα^{0} mice. Nonetheless, the observation that canonical TRα signalling regulates heart rate intrinsically is in accordance with investigations of isolated mouse hearts *via* Langendorff where cardiac rhythm was comparable between TRα^{0} and TRα^{GS} mice (Hones *et al*. 2017).

In TRα^{WT} mice, hypothyroidism caused bradycardia, an effect that was reduced but not completely absent in both TRα^{0} and TRα^{GS} mice. Hypothyroidism-induced bradycardia has been observed in patients as well as in animal studies before (Klein 1990; Udovcic *et al*. 2017). We could now attribute this effect to canonical TRα signalling. During the induction of hyperthyroidism, heart rate in TRα^{WT} mice increased progressively. At the end of this progression, WT mice had higher heart rates than TRα^{0} and TRα^{GS} mice, although they had to overcome the downregulation from the hypothyroid state. This delayed increase of heart rate in response to TH administration has also been observed in a study with TRα1 knockout mice where the authors found that different time courses increased heart rate in TRα1 knockout and WT mice

after 4 days of TH treatment. The conclusion was that different mechanisms might mediate TH-induced tachycardia and that differences in heart rate regulation appeared to be a heart-intrinsic effect (Johansson, Vennstrom, and Thoren 1998). Further studies could confirm heart intrinsic TH/TRα influences on heart rate regulation, yet long-term secondary effects might influence CO as well (Tavi *et al.* 2005; Mittag *et al.* 2010). For example, in hypothyroidism metabolic alterations lead to endothelial dysfunctions, arterial stiffness and, ultimately, hypertension (Obuobie *et al.* 2002). Yet, this is not a heart intrinsic effect, and it is mediated by both TRβ and TRα. However, it eventually affects heart rate too, showing how complex the endocrine system is and how *in vivo* investigations such as the present one help in understanding it (Delitala *et al.* 2017; Zhu and Cheng 2010).

Canonical TRα signalling contributes to core body temperature modulation

TRα and TRβ contribute to body temperature regulation (Gauthier *et al*. 1999; Warner *et al*. 2013; Warner and Mittag 2014). Therefore, we aimed to identify how conscious and freely moving $TR\alpha^{WT}$, $TR\alpha^{0}$ and $TR\alpha^{GS}$ mice control their body temperature during induced thyroid dysfunctions. Core body temperature was 0.5 °C lower in TRα1 deficient ($TR\alpha^{-}$) mice in comparison to WT controls (Wikstrom *et al*. 1998). This was different to our findings and might again be a consequence of the different TRα knockout mouse models used ($TR\alpha^{-}$ vs. $TR\alpha^{0}$). Here, body temperature of control mice declined during the progression of the active phase. This circadian development, however, was impaired in $TR\alpha^{0}$ and $TR\alpha^{GS}$ mice, not only in euthyroidism but also during hypo- and hyperthyroidism, suggesting that circadian body temperature adjustment was mediated by canonical TRα signalling in all three thyroid states (Figure 36). Circadian core body temperature rhythms were already observed in humans in 1842 when a 0.9° C difference was measured between early evening and morning (Krauchi 2002). The main heat generation results from muscular activity and overall circadian body temperature results from a combination of heat generation and loss (Hardy 1961).

The analysis of temperature progression showed a slight reduction in hypothyroidism but a remarkable increase of body temperature during hyperthyroidism. Since this was observed in all genotypes this data suggests that long-term adjustment of body temperature might be mediated by TRβ and not TRα. This finding is in accordance with previous studies, which reported that TRα1 mediated the sympathetic responsiveness in tissues, and TRβ controled *Ucp1* expression and thus long-term temperature (Figure 36) (Ribeiro *et al*. 2001; Marrif *et al*. 2005; Ribeiro *et al*.

2010). The comparison of treatment with T_3 and GC-1, a TRβ-specific TH analogue, in a previous study showed that heat generation was TRα-specific and could not be mediated by TRβ (Ribeiro *et al*. 2001). Strangely, the effect of hypothyroidism was more pronounced in the inactive than active state. Moreover, temperature was reduced in $TR\alpha^0$ and $TR\alpha^{GS}$ mice as well. It is plausible that hypothyroid mice counteracted the effect of TH deprivation through thermogenesis during the active state, but were unable to do so while asleep, when they suffer from increased heat loss (Figure 35). In the resting phase in humans, the majority of heat generation (ca. 70%) results from metabolic activity of the liver, intestines, kidneys, heart and brain (Aschoff 1958). Heart rate and body temperature are equally affected by the circadian rhythm, and it is therefore plausible that both processes would be regulated by the same TR pathway, i.e. canonical TRα signalling (Krauchi and Wirz-Justice 1994). Interestingly, the analysis of activity counts revealed that all mice were more active in hypo- than euthyroid active phases, possibly in an attempt to generate more heat by muscle movement (Figure 39). Thus, it is conceivable that the heat generation in the active hypothyroid control mice results from the stimulation of the norepinephrine signalling pathway. This is a TRα1 mediated effect, which explains the lack of heat generation in $TR\alpha^0$ mice (Silva 2001). The fact that it is also absent in $TR\alpha^{GS}$ mice shows that it is mediated by canonical signalling. Overall, the temperature adjustment during phases I to IV showed that circadian regulation could be regulated through canonical signalling. Yet, the residual observed regulatory effects in $TR\alpha^0$ and $TR\alpha^{GS}$ mice suggest that other TR isoforms or pathways contribzte to body temperature control as well.

Hypothyroidism leads to lower body temperature in patients, and this study, together with previous investigations, suggests that this effect is attributable to TRα-dependent reduced beta-adrenergic responsiveness (Fregly *et al*. 1975). In addition to the local action of rapid vasodilation, central effects have been shown to induce tail vasodilation and thereby reduce body temperature (Gachkar *et al*. 2019).

In response to hyperthyroidism, average body temperature in all 4 phases increased progressively in WT animals. Significant differences were mainly observed between hypo- and late hyperthyroidism (Figure 37). A shift to higher body temperature frequencies occurred in hyperthyroid active control mice, whereas only minor effects were observed in $TR\alpha^0$ mice. Interestingly, the shift in $TR\alpha^{GS}$ mice appeared to be between the control and $TR\alpha^0$ group, which raises the question if different TH/TR-related body temperature control might be regulated by

different TR isoforms *and* signalling pathways (Figure 35). Hyperthyroidism caused an increase of 0.5° C in resting patients when compared to control subjects. This has been associated with metabolic changes and heat intolerance. One influencing factor appeared to be the loss of thermodynamic control in mitochondria in response to hypo- and hyperthyroidism (Nazar *et al*. 1978). In summary, this study showed that different TRα influences circadian control of body temperature through canonical signalling. The fact that $TR\alpha^{0}$ and $TR\alpha^{GS}$ mice showed residual regulatory effects in long-term adjustment suggests an involvement of TRβ. In conclusion, this study demonstrates that control of body temperarure is a complex process, which is, amongst other parameters, influenced by different TR isoforms and actions.

TRα signalling affects locomotor activity during thyroid dysfunctions

Hypothyroid patients suffer from listlessness and fatigue and are less active than euthyroid control subjects, while hyperthyroidism causes restlessness and hyperactivity (Louwerens *et al*. 2012). Surprisingly, the analysis of locomotor activity in this study did not completely mirror this observation from patients. Here, the induction of hypothyroidism actually increased locomotor activity in all groups (Figure 38). This finding was surprising at first but might be explained by body temperature regulation. As previously discussed, we hypothesise that increased locomotor activity might be an attempt to generate heat and thereby maintain core body temperature. Open field tests in previous studies showed that hypothyroid mice were less active than control mice and thus were comparable to patients (Rakov *et al*. 2017). Testing of mice in this study only lasted for 5 minutes at a time, and events of rearing, freezing, grooming and jumping were recorded. In contrats, activity events, i.e. every time a mouse moved from one position to another, were counted in our study over the time span of 72 hours per thyroid state.

Here, activity counts in control mice were highest in the early active phase, reduced in the late active phase and almost zero in the resting state. Again, this reduction was impaired in $TR\alpha^{0}$ mice and to a lesser extent in $TR\alpha^{GS}$ mice. The calculation of average activity counts per hour or the amount of zero count did not yield significant differences and thus a definite classification of locomotor activity to canonical or noncanonical action. Yet, it can be concluded that it was affected by TRα and showed tendencies towards the canonical signalling (Figure 39, Figure 40). Whereas the circadian rhythm of locomotor activity was affected, the long-term adjustment to hypo- as well as hyperthyroidism remained intact in both $TR\alpha^{0}$ and $TR\alpha^{GS}$ mice, suggesting that

this receptor isoform might not majorly influence activity. TRα is involved in brain development, and its absence might affect the behavioural aspects such as activity (Billon *et al*. 2002; Bernal 2002). Interestingly, mice with resistance to TRβ showed elevated locomotor activity in an open field in comparison to controls, suggesting that TRβ might also influence locomotor activity (McDonald *et al*. 1998). In addition, behavioural and metabolic analysis of our group has previously been reported to be contributing to locomotor activity *via* noncanonical TRβ action (Hones *et al*. 2017). Generally, a variety of aspects influences behaviour and behavioural tests are usually very prone to mistakes. Thus, in order to draw conclusions on TH influence on locomotor activity, further testing is required.

Conclusion and Future Perspective

The results of this present study indicate that both canonical and noncanonical TRα signalling are physiologically relevant in the regulation of cardiovascular functions. Firstly, noncanonical TRα action contributes to the regulation of arterial pressure *via* eNOS and PI3K activation in endothelial cells (Figure 14 - Figure 18). TR signalling pathway, cell type and mechanism allowed making connections to hypertension, arterial stiffness and endothelial dysfunction in patients suffering from thyroid diseases. For future studies, it would be interesting to investigate how TH enter the endothelial cells, to compare effects of TH and TH analoga and to determine their vasodilatory effects in comparison to T_3. Furthermore, wire myograph investigation of arteries and *in vivo* blood pressure measurement should be repeated with muscle cell and endothelium-specific $TR\alpha^0$ and $TR\alpha^{GS}$ mice in order to confirm this cell type specific action.

Hyperthyroidism causes cardiac hypertrophy. However, it is still unclear by which TR and pathway this this is mediated. Therefore, mice were exposed to long-term hyperthyroidism and examined in echocardiography and *ex vivo* analysis. Overall, regular echocardiography measurements and final heart weight analysis showed that TH-induced cardiac hypertrophy was mainly mediated *via* noncanonical TRα signalling (Figure 20 & Figure 22).

By analysing cardiomyocyte size, heart growth in response to T_3 could be attributed to myocyte hypertrophy. Interestingly, cardiomyocyte growth can be stimulated through PI3K activation. As PI3K is associated with cytoplasmic noncanonical TR action this might provide a link between the observed myocyte proliferation and proposed mechanism of TH-induced cardiac hypertrophy. Yet, the determination of the exact underlying mechanisms could not be achieved in this study. Immunoblot analysis of typical hypertrophy mediating proteins did not reveal activations in TRα mouse hearts and could not serve as an explanation for the observed heart growth (Figure 27). Gene expression patterns were altered in a manner that suggests a role of TRα as well as TRβ in the regulation of cardiac hypertrophy relevant and TH target genes (Figure 26). However, those changes were marginal for many genes and it is conceivable that activations and gene expression changes have been reversed due to counter regulatory processes during the study. Additionally, it is conceivable that the duration of treatment has a physiological consequence although the changed in gene expression or protein phosphorylation were not detectable in our experiments. Therefore, a kinetic of heart analysis could help clarify the cellular mechanisms. T_3

administration and heart removal after short periods such as 15, 30 and 60 minutes as well as intermediate durations of several days would be crucial for examination of gene expression changes and protein activation, thereby identifying how noncanonical TRα signalling causes cardiomyocyte growth. Furthermore, adding more cardiac hypertrophy related genes to the previously examined TH target genes might bring further insight into the cellular mechanism at different time points.

In this study, heart rate was measured *in vivo* and has been observed to be controlled by canonical TRα signalling (Figure 32). Yet, residual regulation in $TR\alpha^{0}$ mice during hypo- and hyperthyroidism suggests a role of TRβ in heart rate regulation during thyroid dysfunctions. Accordingly, the investigation could be completed by respective telemetry studies of TRβ deficient mice. Furthermore, it would be interesting to induce hyperthyroidism in TRα mice directly after the euthyroid state and determine the extent of heart rate regulation in response to TH. Since the induction of hypothyroidism was more pronounced in $TR\alpha^{WT}$ than $TR\alpha^{0}$ and $TR\alpha^{GS}$ mice, this would ensure better comparability of hyperthyroidism effects. Moreover, by investigating cardiomyocyte-specific $TR\alpha^{0}$ and $TR\alpha^{GS}$ mice, the contribution of heart intrinsic and central TH action to regulation of heart rate could be determined.

In this study, canonical TRα action mediated circadian adaptation of body temperature (Figure 37) and was impaired in hypo- and hyperthyroidism (Figure 35). However, long-term adjustment of core body temperature was preserved in $TR\alpha^{0}$ and $TR\alpha^{GS}$ mice, indicating that this is a consequence of TRβ rather than TRα and suggesting that this study should be performed with $TR\beta^{-}$ and $TR\beta^{GS}$ mice in the future. Furthermore, the identification of regulatory processes would be improved by repeating the measurements in thermoneutrality. Mice have a thermoneutral zone of ≈ 30°C but are usually housed at 20°C which means they constantly have to produce more heat. This disruptive factor could be removed at thermoneutrality.

Lastly, locomotor activity was compared between TRα mice in eu, hypo- and hyperthyroidism. Here, a tendency towards noncanonical TRα action could be observed. However, this appears to be a minor effect, and it is possible that TRα does not play a relevant role. Consequently, it would be of interest to investigate respective TRβ mice and determine the involvement of TRβ action. Additionally, behavioural tests are prone to mistakes and difficult to interpret. Therefore, different approaches in further behavioural studies need to be included in this evaluation to determine TR action in locomotor activity.

In conclusion, the use of TR mutant mice allowed the distinction of canonical and noncanonical TR action and suggests a promising approach for the development of TR isoform and pathway as well as cell type specific drug development. One example for the application of the knowledge gained in this study could be the treatment of heart failure. By applying a drug which specifically activates noncanonical TRα action in the heart and associated vasculature one could induce vasodilation and thus decrease work load for the heart stimulate myocyte growth and thereby a mild physiological cardiac hypertrophy which temporarily improves cardiac function. By targeting only one of the two isoforms and pathways in target cells, it would also be able to strongly reduce side effects when treating TH/TR-related diseases and it should therefore be further explored in basic research and clinical studies. By using global TRα knockout and mutant mice, we were able to attribute TH effects to canonical and noncanonical TRα action *in vivo*. This data paves the way to study canonical and noncanonical action in a cell-specific manner to further deepen the understanding of TH/TR action in the cardiovascular system.

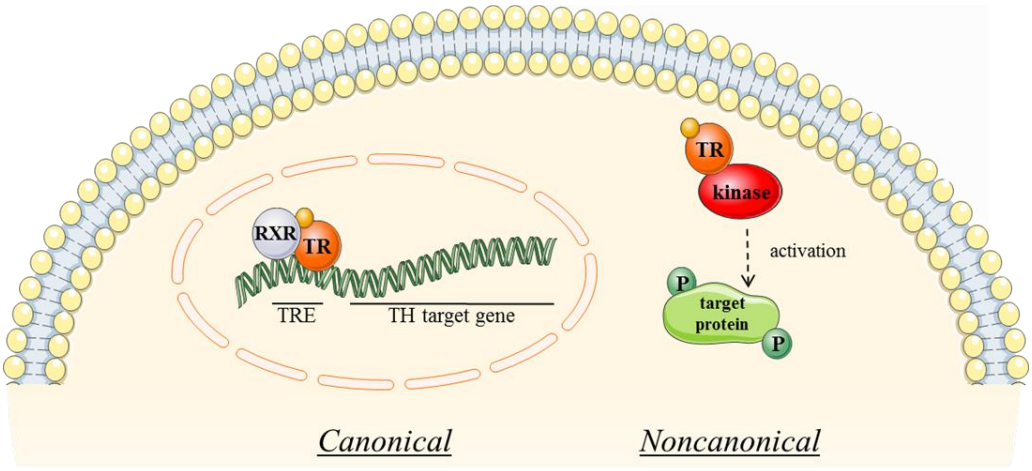

Canonical TRα effects:

- Maintenance of basal heart rate in euthyroidism
- Circadian and long-term heart rate regulation in hypo- and hyperthyroidism
- Circadian regulation of body temperature
- Influence on locomotor activity

Noncanonical TRα effects:

- T_3-induced vasodilation *in vitro* and *in vivo*
- T_3-mediated cardiac hypertrophy
- T_3-induced cardiomyocyte growth
- Binucleation of cardiomyocytes

Figure 41: Canonical and noncanonical TRα actions in the cardiovascular system.

References

Abeyrathna, P., and Y. Su. 2015. 'The critical role of Akt in cardiovascular function', *Vascul Pharmacol*, 74: 38-48.

Ahuja, P., P. Sdek, and W. R. MacLellan. 2007. 'Cardiac myocyte cell cycle control in development, disease, and regeneration', *Physiol Rev*, 87: 521-44.

Allenby, G., M. T. Bocquel, M. Saunders, S. Kazmer, J. Speck, M. Rosenberger, A. Lovey, P. Kastner, J. F. Grippo, P. Chambon, and et al. 1993. 'Retinoic acid receptors and retinoid X receptors: interactions with endogenous retinoic acids', *Proc Natl Acad Sci U S A*, 90: 30-4.

Alonso, M., C. Goodwin, X. Liao, D. Page, S. Refetoff, and R. E. Weiss. 2007. 'Effects of maternal levels of thyroid hormone (TH) on the hypothalamus-pituitary-thyroid set point: studies in TH receptor beta knockout mice', *Endocrinology*, 148: 5305-12.

Alquier, C., J. Ruf, A. M. Athouel-Haon, and P. Carayon. 1989. 'Immunocytochemical study of localization and traffic of thyroid peroxidase/microsomal antigen', *Autoimmunity*, 3: 113-23.

Andros, G., and S. H. Wollman. 1967. 'Autoradiographic localization of radioiodide in the thyroid gland of the mouse', *Am J Physiol*, 213: 198-208.

Anyetei-Anum, Cyril S, Vincent R Roggero, and Lizabeth A Allison. 2018. 'Thyroid hormone receptor localization in target tissues', *Journal of Endocrinology*, 237: R19-R34.

Apriletti, J. W., R. C. Ribeiro, R. L. Wagner, W. Feng, P. Webb, P. J. Kushner, B. L. West, S. Nilsson, T. S. Scanlan, R. J. Fletterick, and J. D. Baxter. 1998. 'Molecular and structural biology of thyroid hormone receptors', *Clin Exp Pharmacol Physiol Suppl*, 25: S2-11.

Aschoff, J.; Wever, J. 1958. 'Kern und Schale im Wiirmehaushalt des Menschen', *Die Naturwissenschaften*, 20: 478-85.

Baker, A. F., T. Dragovich, N. T. Ihle, R. Williams, C. Fenoglio-Preiser, and G. Powis. 2005. 'Stability of phosphoprotein as a biological marker of tumor signaling', *Clinical cancer research : an official journal of the American Association for Cancer Research*, 11: 4338-40.

Barr, L., M. M. Dewey, and W. Berger. 1965. 'Propagation of Action Potentials and the Structure of the Nexus in Cardiac Muscle', *J Gen Physiol*, 48: 797-823.

Bassett, J. H., A. Boyde, P. G. Howell, R. H. Bassett, T. M. Galliford, M. Archanco, H. Evans, M. A. Lawson, P. Croucher, D. L. St Germain, V. A. Galton, and G. R. Williams. 2010. 'Optimal bone strength and mineralization requires the type 2 iodothyronine deiodinase in osteoblasts', *Proc Natl Acad Sci U S A*, 107: 7604-9.

Bassett, J. H., C. B. Harvey, and G. R. Williams. 2003. 'Mechanisms of thyroid hormone receptor-specific nuclear and extra nuclear actions', *Mol Cell Endocrinol*, 213: 1-11.

Bassett, J. H., P. J. O'Shea, O. Chassande, J. Samarut, S. Y. Cheng, B. Vennstrom, P. G. Howell, A. Boyde, and G. R. Williams. 2006. 'Analysis of skeletal phenotypes in thyroid hormone receptor mutant mice', *Scanning*, 28: 91-93.

Bassett, J. H., and G. R. Williams. 2016. 'Role of Thyroid Hormones in Skeletal Development and Bone Maintenance', *Endocrine Reviews*, 37: 135-87.

Baumann, C. T., P. Maruvada, G. L. Hager, and P. M. Yen. 2001. 'Nuclear cytoplasmic shuttling by thyroid hormone receptors. multiple protein interactions are required for nuclear retention', *The Journal of biological chemistry*, 276: 11237-45.

Beams, H. W., T. C. Evans, and et al. 1949. 'Electron microscope studies on the structure of cardiac muscle', *Anat Rec*, 105: 59-81, incl 3 pl.

Beato, M., P. Herrlich, and G. Schutz. 1995. 'Steroid hormone receptors: many actors in search of a plot', *Cell*, 83: 851-7.

Bedotto, J. B., R. G. Gay, S. D. Graham, E. Morkin, and S. Goldman. 1989. 'Cardiac hypertrophy induced by thyroid hormone is independent of loading conditions and beta adrenoceptor blockade', *J Pharmacol Exp Ther*, 248: 632-6.

Beevers, G., G. Y. Lip, and E. O'Brien. 2001. 'ABC of hypertension: The pathophysiology of hypertension', *BMJ*, 322: 912-6.

Bellamy, T. C., and J. Garthwaite. 2001. 'Sub-second kinetics of the nitric oxide receptor, soluble guanylyl cyclase, in intact cerebellar cells', *The Journal of biological chemistry*, 276: 4287-92.

Beltrami, A. P., K. Urbanek, J. Kajstura, S. M. Yan, N. Finato, R. Bussani, B. Nadal-Ginard, F. Silvestri, A. Leri, C. A. Beltrami, and P. Anversa. 2001. 'Evidence that human cardiac myocytes divide after myocardial infarction', *The New England journal of medicine*, 344: 1750-7.

Bengel, F. M., S. G. Nekolla, T. Ibrahim, C. Weniger, S. I. Ziegler, and M. Schwaiger. 2000. 'Effect of thyroid hormones on cardiac function, geometry, and oxidative metabolism assessed noninvasively by positron emission tomography and magnetic resonance imaging', *J Clin Endocrinol Metab*, 85: 1822-7.

Bergmann, O., R. D. Bhardwaj, S. Bernard, S. Zdunek, F. Barnabe-Heider, S. Walsh, J. Zupicich, K. Alkass, B. A. Buchholz, H. Druid, S. Jovinge, and J. Frisen. 2009. 'Evidence for cardiomyocyte renewal in humans', *Science*, 324: 98-102.

Bernal, J. 2002. 'Action of thyroid hormone in brain', *J Endocrinol Invest*, 25: 268-88.

———. 2007. 'Thyroid hormone receptors in brain development and function', *Nat Clin Pract Endocrinol Metab*, 3: 249-59.

Bernal, J., A. Guadano-Ferraz, and B. Morte. 2015. 'Thyroid hormone transporters-functions and clinical implications', *Nat Rev Endocrinol*, 11: 690.

Bernardo, B. C., K. L. Weeks, L. Pretorius, and J. R. McMullen. 2010. 'Molecular distinction between physiological and pathological cardiac hypertrophy: experimental findings and therapeutic strategies', *Pharmacol Ther*, 128: 191-227.

Berta, E., I. Lengyel, S. Halmi, M. Zrinyi, A. Erdei, M. Harangi, D. Pall, E. V. Nagy, and M. Bodor. 2019. 'Hypertension in Thyroid Disorders', *Front Endocrinol (Lausanne)*, 10: 482.

Bianco, A. C., and B. W. Kim. 2006. 'Deiodinases: implications of the local control of thyroid hormone action', *The Journal of clinical investigation*, 116: 2571-9.

Bianco, A. C., D. Salvatore, B. Gereben, M. J. Berry, and P. R. Larsen. 2002. 'Biochemistry, cellular and molecular biology, and physiological roles of the iodothyronine selenodeiodinases', *Endocrine Reviews*, 23: 38-89.

Billon, C., L. Canaple, S. Fleury, A. Deloire, M. Beylot, D. Dombrowicz, P. Del Carmine, J. Samarut, and K. Gauthier. 2014. 'TRalpha Protects Against Atherosclerosis in Male Mice: Identification of a Novel Anti-Inflammatory Property for TRalpha in Mice', *Endocrinology*, 155: 2735-45.

Billon, N., C. Jolicoeur, Y. Tokumoto, B. Vennstrom, and M. Raff. 2002. 'Normal timing of oligodendrocyte development depends on thyroid hormone receptor alpha 1 (TRalpha1)', *EMBO J*, 21: 6452-60.

Bochukova, E., N. Schoenmakers, M. Agostini, E. Schoenmakers, O. Rajanayagam, J. M. Keogh, E. Henning, J. Reinemund, E. Gevers, M. Sarri, K. Downes, A. Offiah, A. Albanese, D. Halsall, J. W. Schwabe, M. Bain, K. Lindley, F. Muntoni, F. Vargha-Khadem, M. Dattani, I. S. Farooqi, M. Gurnell, and K. Chatterjee. 2012. 'A mutation in the thyroid hormone receptor alpha gene', *The New England journal of medicine*, 366: 243-9.

Bourguet, W., M. Ruff, P. Chambon, H. Gronemeyer, and D. Moras. 1995. 'Crystal structure of the ligand-binding domain of the human nuclear receptor RXR-alpha', *Nature*, 375: 377-82.

Brandt, F., A. Green, L. Hegedus, and T. H. Brix. 2011. 'A critical review and meta-analysis of the association between overt hyperthyroidism and mortality', *Eur J Endocrinol*, 165: 491-7.

Brix, K., D. Fuhrer, and H. Biebermann. 2011. 'Molecules important for thyroid hormone synthesis and action - known facts and future perspectives', *Thyroid Res*, 4 Suppl 1: S9.

Brower, G. L., J. D. Gardner, M. F. Forman, D. B. Murray, T. Voloshenyuk, S. P. Levick, and J. S. Janicki. 2006. 'The relationship between myocardial extracellular matrix remodeling and ventricular function', *Eur J Cardiothorac Surg*, 30: 604-10.

Cabrera, J. A., and D. Sanchez-Quintana. 2013. 'Cardiac anatomy: what the electrophysiologist needs to know', *Heart*, 99: 417-31.

Cacciatori, V., F. Bellavere, A. Pezzarossa, A. Dellera, M. L. Gemma, K. Thomaseth, R. Castello, P. Moghetti, and M. Muggeo. 1996. 'Power spectral analysis of heart rate in hyperthyroidism', *J Clin Endocrinol Metab*, 81: 2828-35.

Cai, Y., M. M. Manio, G. P. Leung, A. Xu, E. H. Tang, and P. M. Vanhoutte. 2014. 'Thyroid hormone affects both endothelial and vascular smooth muscle cells in rat arteries', *Eur J Pharmacol*.

———. 2015. 'Thyroid hormone affects both endothelial and vascular smooth muscle cells in rat arteries', *Eur J Pharmacol*, 747: 18-28.

Canaris, G. J., N. R. Manowitz, G. Mayor, and E. C. Ridgway. 2000. 'The Colorado thyroid disease prevalence study', *Arch Intern Med*, 160: 526-34.

Cao, X., F. Kambe, L. C. Moeller, S. Refetoff, and H. Seo. 2005. 'Thyroid hormone induces rapid activation of Akt/protein kinase B-mammalian target of rapamycin-p70S6K cascade through phosphatidylinositol 3-kinase in human fibroblasts', *Mol Endocrinol*, 19: 102-12.

Cao, X., F. Kambe, M. Yamauchi, and H. Seo. 2009. 'Thyroid-hormone-dependent activation of the phosphoinositide 3-kinase/Akt cascade requires Src and enhances neuronal survival', *Biochem J*, 424: 201-9.

Capettini, L. S., S. F. Cortes, J. F. Silva, J. I. Alvarez-Leite, and V. S. Lemos. 2011. 'Decreased production of neuronal NOS-derived hydrogen peroxide contributes to endothelial dysfunction in atherosclerosis', *Br J Pharmacol*, 164: 1738-48.

Cappola, A. R., A. S. Desai, M. Medici, L. S. Cooper, D. Egan, G. Sopko, G. I. Fishman, S. Goldman, D. S. Cooper, S. Mora, P. J. Kudenchuk, A. N. Hollenberg, C. L. McDonald, and P. W. Ladenson. 2019. 'Thyroid and Cardiovascular Disease Research Agenda for Enhancing Knowledge, Prevention, and Treatment', *Circulation*, 139: 2892-909.

Cappola, A. R., L. P. Fried, A. M. Arnold, M. D. Danese, L. H. Kuller, G. L. Burke, R. P. Tracy, and P. W. Ladenson. 2006. 'Thyroid status, cardiovascular risk, and mortality in older adults', *JAMA : the journal of the American Medical Association*, 295: 1033-41.

Cappola, A. R., and P. W. Ladenson. 2003. 'Hypothyroidism and atherosclerosis', *J Clin Endocrinol Metab*, 88: 2438-44.

Carrillo-Sepulveda, M. A., G. S. Ceravolo, Z. B. Fortes, M. H. Carvalho, R. C. Tostes, F. R. Laurindo, R. C. Webb, and M. L. Barreto-Chaves. 2010. 'Thyroid hormone stimulates NO production via activation of the PI3K/Akt pathway in vascular myocytes', *Cardiovasc Res*, 85: 560-70.

Carvalho, D. P., and C. Dupuy. 2013. 'Role of the NADPH Oxidases DUOX and NOX4 in Thyroid Oxidative Stress', *Eur Thyroid J*, 2: 160-7.

Cesarovic, N., P. Jirkof, A. Rettich, and M. Arras. 2011. 'Implantation of radiotelemetry transmitters yielding data on ECG, heart rate, core body temperature and activity in free-moving laboratory mice', *J Vis Exp*.

Charkoudian, N. 2010. 'Mechanisms and modifiers of reflex induced cutaneous vasodilation and vasoconstriction in humans', *J Appl Physiol (1985)*, 109: 1221-8.

Chassande, O., A. Fraichard, K. Gauthier, F. Flamant, C. Legrand, P. Savatier, V. Laudet, and J. Samarut. 1997. 'Identification of transcripts initiated from an internal promoter in the c-erbA alpha locus that encode inhibitors of retinoic acid receptor-alpha and triiodothyronine receptor activities', *Mol Endocrinol*, 11: 1278-90.

Chattergoon, N. N., G. D. Giraud, S. Louey, P. Stork, A. L. Fowden, and K. L. Thornburg. 2012. 'Thyroid hormone drives fetal cardiomyocyte maturation', *FASEB J*, 26: 397-408.

Chen, J. D., and R. M. Evans. 1995. 'A transcriptional co-repressor that interacts with nuclear hormone receptors', *Nature*, 377: 454-7.

Chen, J. L., H. W. Chiu, Y. J. Tseng, and W. C. Chu. 2006. 'Hyperthyroidism is characterized by both increased sympathetic and decreased vagal modulation of heart rate: evidence from spectral analysis of heart rate variability', *Clin Endocrinol (Oxf)*, 64: 611-6.

Chen, X., Y. Zhou, M. Zhou, Q. Yin, and S. Wang. 2018. 'Diagnostic Values of Free Triiodothyronine and Free Thyroxine and the Ratio of Free Triiodothyronine to Free Thyroxine in Thyrotoxicosis', *Int J Endocrinol*, 2018: 4836736.

Cheng, S. Y., J. L. Leonard, and P. J. Davis. 2010. 'Molecular aspects of thyroid hormone actions', *Endocrine Reviews*, 31: 139-70.

Chiamolera, M. I., and F. E. Wondisford. 2009. 'Minireview: Thyrotropin-releasing hormone and the thyroid hormone feedback mechanism', *Endocrinology*, 150: 1091-6.

Coleman, P. S., M. S. Parmacek, M. Lesch, and A. M. Samarel. 1989. 'Protein synthesis and degradation during regression of thyroxine-induced cardiac hypertrophy', *J Mol Cell Cardiol*, 21: 911-25.

Comai, L. 2005. 'The advantages and disadvantages of being polyploid', *Nat Rev Genet*, 6: 836-46.

Crackower, M. A., G. Y. Oudit, I. Kozieradzki, R. Sarao, H. Sun, T. Sasaki, E. Hirsch, A. Suzuki, T. Shioi, J. Irie-Sasaki, R. Sah, H. Y. Cheng, V. O. Rybin, G. Lembo, L. Fratta, A. J. Oliveira-dos-Santos, J. L. Benovic, C. R. Kahn, S. Izumo, S. F. Steinberg, M. P. Wymann, P. H. Backx, and J. M. Penninger. 2002. 'Regulation of myocardial contractility and cell size by distinct PI3K-PTEN signaling pathways', *Cell*, 110: 737-49.

D'Angelo, D. D., Y. Sakata, J. N. Lorenz, G. P. Boivin, R. A. Walsh, S. B. Liggett, and G. W. Dorn, 2nd. 1997. 'Transgenic Galphaq overexpression induces cardiac contractile failure in mice', *Proc Natl Acad Sci U S A*, 94: 8121-6.

Danzi, S., and I. Klein. 2003. 'Thyroid hormone and blood pressure regulation', *Curr Hypertens Rep*, 5: 513-20.

———. 2020. 'Thyroid Abnormalities in Heart Failure', *Heart Fail Clin*, 16: 1-9.

Darimont, B. D., R. L. Wagner, J. W. Apriletti, M. R. Stallcup, P. J. Kushner, J. D. Baxter, R. J. Fletterick, and K. R. Yamamoto. 1998. 'Structure and specificity of nuclear receptor-coactivator interactions', *Genes Dev*, 12: 3343-56.

Davis, P. J., and F. B. Davis. 2002. 'Nongenomic actions of thyroid hormone on the heart', *Thyroid*, 12: 459-66.

Davis, P. J., F. B. Davis, and W. D. Lawrence. 1989. 'Thyroid hormone regulation of membrane Ca2(+)-ATPase activity', *Endocr Res*, 15: 651-82.

Davis, Paul J., Fernando Goglia, and Jack L. Leonard. 2016. 'Nongenomic actions of thyroid hormone', *Nat Rev Endocrinol*, 12: 111-21.

de Castro, A. L., A. V. Tavares, R. O. Fernandes, C. Campos, A. Conzatti, R. Siqueira, T. R. Fernandes, P. C. Schenkel, C. L. Sartorio, S. Llesuy, A. Bello-Klein, and A. S. da Rosa Araujo. 2015. 'T3 and T4 decrease ROS levels and increase endothelial nitric oxide synthase expression in the myocardium of infarcted rats', *Mol Cell Biochem*, 408: 235-43.

De Gregorio, G., A. Coppa, C. Cosentino, S. Ucci, S. Messina, A. Nicolussi, S. D'Inzeo, A. Di Pardo, E. V. Avvedimento, and A. Porcellini. 2007. 'The p85 regulatory subunit of PI3K mediates TSH-cAMP-PKA growth and survival signals', *Oncogene*, 26: 2039-47.

Delitala, A. P., G. Fanciulli, M. Maioli, and G. Delitala. 2017. 'Subclinical hypothyroidism, lipid metabolism and cardiovascular disease', *Eur J Intern Med*, 38: 17-24.

Desbois, C., D. Aubert, C. Legrand, B. Pain, and J. Samarut. 1991. 'A novel mechanism of action for v-ErbA: abrogation of the inactivation of transcription factor AP-1 by retinoic acid and thyroid hormone receptors', *Cell*, 67: 731-40.

Dillmann, W. 2010. 'Cardiac hypertrophy and thyroid hormone signaling', *Heart Fail Rev*, 15: 125-32.

Dillmann, W. H. 2002. 'Cellular action of thyroid hormone on the heart', *Thyroid*, 12: 447-52.

Duncan Bassett, J. H., and Graham R. Williams. 2003. 'The molecular actions of thyroid hormone in bone', *Trends in Endocrinology & Metabolism*, 14: 356-64.

Dunn, A. D., H. E. Crutchfield, and J. T. Dunn. 1991. 'Thyroglobulin processing by thyroidal proteases. Major sites of cleavage by cathepsins B, D, and L', *The Journal of biological chemistry*, 266: 20198-204.

Dunn, A. D., H. E. Myers, and J. T. Dunn. 1996. 'The combined action of two thyroidal proteases releases T4 from the dominant hormone-forming site of thyroglobulin', *Endocrinology*, 137: 3279-85.

Dupuy, C., R. Ohayon, A. Valent, M. S. Noel-Hudson, D. Deme, and A. Virion. 1999. 'Purification of a novel flavoprotein involved in the thyroid NADPH oxidase. Cloning of the porcine and human cdnas', *The Journal of biological chemistry*, 274: 37265-9.

Eliades, D., and H. R. Weiss. 1989. 'Role of beta adrenoceptors in the hypertrophic response to thyroxine', *J Cardiovasc Pharmacol*, 14: 58-65.

Elnakish, M. T., A. A. Ahmed, P. J. Mohler, and P. M. Janssen. 2015. 'Role of Oxidative Stress in Thyroid Hormone-Induced Cardiomyocyte Hypertrophy and Associated Cardiac Dysfunction: An Undisclosed Story', *Oxid Med Cell Longev*, 2015: 854265.

Engels, K., H. Rakov, D. Zwanziger, G. S. Hones, M. Rehders, K. Brix, J. Kohrle, L. C. Moller, and D. Fuhrer. 2016. 'Efficacy of protocols for induction of chronic hyperthyroidism in male and female mice', *Endocrine*, 54: 47-54.

Engels, K., H. Rakov, D. Zwanziger, L. C. Moeller, G. Homuth, J. Kohrle, K. Brix, and D. Fuhrer. 2015. 'Differences in Mouse Hepatic Thyroid Hormone Transporter Expression with Age and Hyperthyroidism', *Eur Thyroid J*, 4: 81-6.

Evans, R. M. 1988. 'The steroid and thyroid hormone receptor superfamily', *Science*, 240: 889-95.

Fadel, B. M., S. Ellahham, M. D. Ringel, J. Lindsay, Jr., L. Wartofsky, and K. D. Burman. 2000. 'Hyperthyroid heart disease', *Clin Cardiol*, 23: 402-8.

Farraj, A. K., M. S. Hazari, and W. E. Cascio. 2011. 'The utility of the small rodent electrocardiogram in toxicology', *Toxicol Sci*, 121: 11-30.

Fekete, C., and R. M. Lechan. 2014. 'Central regulation of hypothalamic-pituitary-thyroid axis under physiological and pathophysiological conditions', *Endocrine Reviews*, 35: 159-94.

Feng, W., R. C. Ribeiro, R. L. Wagner, H. Nguyen, J. W. Apriletti, R. J. Fletterick, J. D. Baxter, P. J. Kushner, and B. L. West. 1998. 'Hormone-dependent coactivator binding to a hydrophobic cleft on nuclear receptors', *Science*, 280: 1747-9.

Fernandes, R. O., G. J. Dreher, P. C. Schenkel, T. R. Fernandes, M. F. Ribeiro, A. S. Araujo, and A. Bello-Klein. 2011. 'Redox status and pro-survival/pro-apoptotic protein expression in the early cardiac hypertrophy induced by experimental hyperthyroidism', *Cell Biochem Funct*, 29: 617-23.

Flamant, F., S. Y. Cheng, A. N. Hollenberg, L. C. Moeller, J. Samarut, F. E. Wondisford, P. M. Yen, and S. Refetoff. 2017. 'Thyroid hormone signaling pathways. Time for a more precise nomenclature', *Endocrinology*, 158: 2052-57.

Flamant, F., and K. Gauthier. 2013. 'Thyroid hormone receptors: The challenge of elucidating isotype-specific functions and cell-specific response', *Biochim Biophys Acta*, 1830: 3900-7.

Forman, B. M., and H. H. Samuels. 1990. 'Interactions among a subfamily of nuclear hormone receptors: the regulatory zipper model', *Mol Endocrinol*, 4: 1293-301.

Forrest, D., E. Hanebuth, R. J. Smeyne, N. Everds, C. L. Stewart, J. M. Wehner, and T. Curran. 1996. 'Recessive resistance to thyroid hormone in mice lacking thyroid hormone receptor beta: evidence for tissue-specific modulation of receptor function', *EMBO J*, 15: 3006-15.

Fraichard, A., O. Chassande, M. Plateroti, J. P. Roux, J. Trouillas, C. Dehay, C. Legrand, K. Gauthier, M. Kedinger, L. Malaval, B. Rousset, and J. Samarut. 1997. 'The T3R alpha gene encoding a thyroid hormone receptor is essential for post-natal development and thyroid hormone production', *EMBO J*, 16: 4412-20.

Fregly, M. J., E. L. Nelson, Jr., G. E. Resch, F. P. Field, and L. O. Lutherer. 1975. 'Reduced beta-adrenergic responsiveness in hypothyroid rats', *Am J Physiol*, 229: 916-24.

Furuya, F., C. Lu, M. C. Willingham, and S. Y. Cheng. 2007. 'Inhibition of phosphatidylinositol 3-kinase delays tumor progression and blocks metastatic spread in a mouse model of thyroid cancer', *Carcinogenesis*, 28: 2451-8.

Gachkar, Sogol, Sebastian Nock, Cathleen Geissler, Rebecca Oelkrug, Kornelia Johann, Julia Resch, Awahan Rahman, Anders Arner, Henriette Kirchner, and Jens Mittag. 2019. 'Aortic effects of thyroid hormone in male mice', *Journal of Molecular Endocrinology*: 91-99.

Galton, V. A. 2017. 'The ups and downs of the thyroxine pro-hormone hypothesis', *Mol Cell Endocrinol*, 458: 105-11.

Galton, V. A., M. J. Schneider, A. S. Clark, and D. L. St Germain. 2009. 'Life without thyroxine to 3,5,3'-triiodothyronine conversion: studies in mice devoid of the 5'-deiodinases', *Endocrinology*, 150: 2957-63.

Gassanov, N., F. Er, J. Endres-Becker, M. Wolny, C. Schramm, and U. C. Hoppe. 2009. 'Distinct regulation of cardiac I(f) current via thyroid receptors alpha1 and beta1', *Pflugers Arch*, 458: 1061-8.

Gauthier, K., O. Chassande, M. Plateroti, J. P. Roux, C. Legrand, B. Pain, B. Rousset, R. Weiss, J. Trouillas, and J. Samarut. 1999. 'Different functions for the thyroid hormone receptors TRalpha and TRbeta in the control of thyroid hormone production and post-natal development', *EMBO J*, 18: 623-31.

Gereben, B., A. M. Zavacki, S. Ribich, B. W. Kim, S. A. Huang, W. S. Simonides, A. Zeold, and A. C. Bianco. 2008. 'Cellular and molecular basis of deiodinase-regulated thyroid hormone signaling', *Endocrine Reviews*, 29: 898-938.

Gordan, R., J. K. Gwathmey, and L. H. Xie. 2015. 'Autonomic and endocrine control of cardiovascular function', *World J Cardiol*, 7: 204-14.

Gothe, S., Z. Wang, L. Ng, J. M. Kindblom, A. C. Barros, C. Ohlsson, B. Vennstrom, and D. Forrest. 1999. 'Mice devoid of all known thyroid hormone receptors are viable but exhibit disorders of the pituitary-thyroid axis, growth, and bone maturation', *Genes Dev*, 13: 1329-41.

Goumidi, L., K. Gauthier, V. Legry, T. H. Mayi, A. Houzet, D. Cottel, M. Montaye, C. Proust, F. Kee, J. Ferrieres, D. Arveiler, P. Ducimetiere, B. Staels, J. Dallongeville, G. Chinetti, F. Flamant, P. Amouyel, and A. Meirhaeghe. 2011. 'Association Between a Thyroid Hormone Receptor-alpha Gene Polymorphism and Blood Pressure but Not With Coronary Heart Disease Risk', *American Journal of Hypertension*, 24: 1027-34.

Grajek, S., S. Paradowski, M. Zajac, and E. Kaczmarek. 1992. '[Hypertrophy or hyperplasia of myocytes in heart hypertrophy?]', *Przegl Lek*, 49: 395-8.

Green, S., V. Kumar, I. Theulaz, W. Wahli, and P. Chambon. 1988. 'The N-terminal DNA-binding 'zinc finger' of the oestrogen and glucocorticoid receptors determines target gene specificity', *EMBO J*, 7: 3037-44.

Grund, A., M. Szaroszyk, M. Korf-Klingebiel, M. Malek Mohammadi, F. A. Trogisch, U. Schrameck, A. Gigina, C. Tiedje, M. Gaestel, T. Kraft, J. Hegermann, S. Batkai, T. Thum, A. Perrot, C. D. Remedios, E. Riechert, M. Volkers, S. Doroudgar, A. Jungmann, R. Bauer, X. Yin, M. Mayr, K. C. Wollert, A. Pich, H. Xiao, H. A. Katus, J. Bauersachs, O. J. Muller, and J. Heineke. 2019. 'TIP30 counteracts cardiac hypertrophy and failure by inhibiting translational elongation', *EMBO Mol Med*, 11: e10018.

Guissouma, H., R. Ghaddab-Zroud, I. Seugnet, S. Decherf, B. Demeneix, and M. S. Clerget-Froidevaux. 2014. 'TR alpha 2 exerts dominant negative effects on hypothalamic Trh transcription in vivo', *PLoS One*, 9: e95064.

Guyenet, P. G. 2006. 'The sympathetic control of blood pressure', *Nat Rev Neurosci*, 7: 335-46.

Hahm, J. B., A. C. Schroeder, and M. L. Privalsky. 2014. 'The two major isoforms of thyroid hormone receptor, TRalpha1 and TRbeta1, preferentially partner with distinct panels of auxiliary proteins', *Mol Cell Endocrinol*, 383: 80-95.

Hak, A. E., H. A. Pols, T. J. Visser, H. A. Drexhage, A. Hofman, and J. C. Witteman. 2000. 'Subclinical hypothyroidism is an independent risk factor for atherosclerosis and myocardial infarction in elderly women: the Rotterdam Study', *Ann Intern Med*, 132: 270-8.

Halbrugge, T., K. Lutsch, A. Thyen, and K. H. Graefe. 1991. 'Vasodilatation by endothelium-derived nitric oxide as a major determinant of noradrenaline release', *J Neural Transm Suppl*, 34: 113-9.

Hardy, J. D. 1961. 'Physiology of temperature regulation', *Physiol Rev*, 41: 521-606.

Hashimoto, K., E. Ishida, A. Miura, A. Ozawa, N. Shibusawa, T. Satoh, S. Okada, M. Yamada, and M. Mori. 2013. 'Human stearoyl-CoA desaturase 1 (SCD-1) gene expression is negatively regulated by thyroid hormone without direct binding of thyroid hormone receptor to the gene promoter', *Endocrinology*, 154: 537-49.

Haymet, B. T., and D. I. McCloskey. 1975. 'Baroreceptor and chemoreceptor influences on heart rate during the respiratory cycle in the dog', *J Physiol*, 245: 699-712.

Hien, T. T., W. K. Oh, B. T. Quyen, T. T. Dao, J. H. Yoon, S. Y. Yun, and K. W. Kang. 2012. 'Potent vasodilation effect of amurensin G is mediated through the phosphorylation of endothelial nitric oxide synthase', *Biochemical pharmacology*, 84: 1437-50.

Hiroi, Y., H. H. Kim, H. Ying, F. Furuya, Z. Huang, T. Simoncini, K. Noma, K. Ueki, N. H. Nguyen, T. S. Scanlan, M. A. Moskowitz, S. Y. Cheng, and J. K. Liao. 2006. 'Rapid nongenomic actions of thyroid hormone', *Proc Natl Acad Sci U S A*, 103: 14104-9.

Hirose, K., A. Y. Payumo, S. Cutie, A. Hoang, H. Zhang, R. Guyot, D. Lunn, R. B. Bigley, H. Yu, J. Wang, M. Smith, E. Gillett, S. E. Muroy, T. Schmid, E. Wilson, K. A. Field, D. M. Reeder, M. Maden, M. M. Yartsev, M. J. Wolfgang, F. Grutzner, T. S. Scanlan, L. I. Szweda, R. Buffenstein, G. Hu, F. Flamant, J. E. Olgin, and G. N. Huang. 2019. 'Evidence for hormonal control of heart regenerative capacity during endothermy acquisition', *Science*.

Ho, D., X. Zhao, S. Gao, C. Hong, D. E. Vatner, and S. F. Vatner. 2011. 'Heart Rate and Electrocardiography Monitoring in Mice', *Curr Protoc Mouse Biol*, 1: 123-39.

Hodin, R. A., M. A. Lazar, and W. W. Chin. 1990. 'Differential and tissue-specific regulation of the multiple rat c-erbA messenger RNA species by thyroid hormone', *The Journal of clinical investigation*, 85: 101-5.

Hodin, R. A., M. A. Lazar, B. I. Wintman, D. S. Darling, R. J. Koenig, P. R. Larsen, D. D. Moore, and W. W. Chin. 1989. 'Identification of a thyroid hormone receptor that is pituitary-specific', *Science*, 244: 76-9.

Hollenberg, A. N., T. Monden, and F. E. Wondisford. 1995. 'Ligand-independent and -dependent functions of thyroid hormone receptor isoforms depend upon their distinct amino termini', *The Journal of biological chemistry*, 270: 14274-80.

Hones, G. S., H. Rakov, J. Logan, X. H. Liao, E. Werbenko, A. S. Pollard, S. M. Praestholm, M. S. Siersbaek, E. Rijntjes, J. Gassen, S. Latteyer, K. Engels, K. H. Strucksberg, P. Kleinbongard, D. Zwanziger, J. Rozman, V. Gailus-Durner, H. Fuchs, M. Hrabe de Angelis, L. Klein-Hitpass, J. Kohrle, D. L. Armstrong, L. Grontved, J. H. D. Bassett, G. R. Williams, S. Refetoff, D. Fuhrer, and L. C. Moeller. 2017. 'Noncanonical thyroid hormone signaling mediates cardiometabolic effects in vivo', *Proc Natl Acad Sci U S A*, 114: E11323-E32.

Horlein, A. J., A. M. Naar, T. Heinzel, J. Torchia, B. Gloss, R. Kurokawa, A. Ryan, Y. Kamei, M. Soderstrom, C. K. Glass, and et al. 1995. 'Ligand-independent repression by the thyroid hormone receptor mediated by a nuclear receptor co-repressor', *Nature*, 377: 397-404.

Hsieh, P. C., V. F. Segers, M. E. Davis, C. MacGillivray, J. Gannon, J. D. Molkentin, J. Robbins, and R. T. Lee. 2007. 'Evidence from a genetic fate-mapping study that stem cells refresh adult mammalian cardiomyocytes after injury', *Nat Med*, 13: 970-4.

Huang, S. A., H. M. Tu, J. W. Harney, M. Venihaki, A. J. Butte, H. P. Kozakewich, S. J. Fishman, and P. R. Larsen. 2000. 'Severe hypothyroidism caused by type 3 iodothyronine deiodinase in infantile hemangiomas', *The New England journal of medicine*, 343: 185-9.

Huxley, H. E. 1961. 'The contractile structure of cardiac and skeletal muscle', *Circulation*, 24: 328-35.

Iemitsu, M., T. Miyauchi, S. Maeda, S. Sakai, T. Kobayashi, N. Fujii, H. Miyazaki, M. Matsuda, and I. Yamaguchi. 2001. 'Physiological and pathological cardiac hypertrophy induce different molecular phenotypes in the rat', *Am J Physiol Regul Integr Comp Physiol*, 281: R2029-36.

Imperio, G. E., I. P. Ramos, L. A. Santiago, G. F. Pereira, N. A. Dos Santos Almeida, C. S. Fuziwara, C. C. Pazos-Moura, E. T. Kimura, E. L. Olivares, and T. M. Ortiga-Carvalho. 2015. 'The Impact of a Non-Functional Thyroid Receptor Beta upon Triiodotironine-Induced Cardiac Hypertrophy in Mice', *Cell Physiol Biochem*, 37: 477-90.

Inaba, M., Y. Henmi, Y. Kumeda, M. Ueda, M. Nagata, M. Emoto, T. Ishikawa, E. Ishimura, and Y. Nishizawa. 2002. 'Increased stiffness in common carotid artery in hyperthyroid Graves' disease patients', *Biomed Pharmacother*, 56: 241-6.

Izumo, S., and V. Mahdavi. 1988. 'Thyroid hormone receptor alpha isoforms generated by alternative splicing differentially activate myosin HC gene transcription', *Nature*, 334: 539-42.

Janssen, R., A. Muller, and W. S. Simonides. 2017. 'Cardiac Thyroid Hormone Metabolism and Heart Failure', *Eur Thyroid J*, 6: 130-37.

Johann, K., A. L. Cremer, A. W. Fischer, M. Heine, E. R. Pensado, J. Resch, S. Nock, S. Virtue, L. Harder, R. Oelkrug, M. Astiz, G. Brabant, A. Warner, A. Vidal-Puig, H. Oster, A. Boelen, M. Lopez, J. Heeren, J. W. Dalley, H. Backes, and J. Mittag. 2019. 'Thyroid-Hormone-Induced Browning of White Adipose Tissue Does Not Contribute to Thermogenesis and Glucose Consumption', *Cell Rep*, 27: 3385-400.e3.

Johansson, C., S. Gothe, D. Forrest, B. Vennstrom, and P. Thoren. 1999. 'Cardiovascular phenotype and temperature control in mice lacking thyroid hormone receptor-beta or both alpha1 and beta', *Am J Physiol*, 276: H2006-12.

Johansson, C., B. Vennstrom, and P. Thoren. 1998. 'Evidence that decreased heart rate in thyroid hormone receptor-alpha1-deficient mice is an intrinsic defect', *Am J Physiol*, 275: R640-6.

Jones, K. E., and W. W. Chin. 1991. 'Differential regulation of thyroid hormone receptor messenger ribonucleic acid levels by thyrotropin-releasing hormone', *Endocrinology*, 128: 1763-8.

Jordans, S., S. Jenko-Kokalj, N. M. Kuhl, S. Tedelind, W. Sendt, D. Bromme, D. Turk, and K. Brix. 2009. 'Monitoring compartment-specific substrate cleavage by cathepsins B, K, L, and S at physiological pH and redox conditions', *BMC Biochem*, 10: 23.

Kahaly, G. J., and W. H. Dillmann. 2005. 'Thyroid hormone action in the heart', *Endocrine Reviews*, 26: 704-28.

Kahaly, G., S. Mohr-Kahaly, J. Beyer, and J. Meyer. 1995. 'Left ventricular function analyzed by Doppler and echocardiographic methods in short-term hypothyroidism', *Am J Cardiol*, 75: 645-8.

Kajstura, J., K. Urbanek, S. Perl, T. Hosoda, H. Zheng, B. Ogorek, J. Ferreira-Martins, P. Goichberg, C. Rondon-Clavo, F. Sanada, D. D'Amario, M. Rota, F. Del Monte, D. Orlic, J. Tisdale, A. Leri, and P. Anversa. 2010. 'Cardiomyogenesis in the adult human heart', *Circ Res*, 107: 305-15.

Kalyanaraman, H., R. Schwappacher, J. Joshua, S. Zhuang, B. T. Scott, M. Klos, D. E. Casteel, J. A. Frangos, W. Dillmann, G. R. Boss, and R. B. Pilz. 2014. 'Nongenomic thyroid hormone signaling occurs through a plasma membrane-localized receptor', *Sci Signal*, 7: ra48.

Kamakura, R., M. Kovalainen, J. Leppaluoto, K. H. Herzig, and K. A. Makela. 2016. 'The effects of group and single housing and automated animal monitoring on urinary corticosterone levels in male C57BL/6 mice', *Physiol Rep*, 4.

Kasturi, S., and F. Ismail-Beigi. 2008. 'Effect of thyroid hormone on the distribution and activity of Na, K-ATPase in ventricular myocardium', *Arch Biochem Biophys*, 475: 121-7.

Kavok, N. S., O. A. Krasilnikova, and N. A. Babenko. 2001. 'Thyroxine signal transduction in liver cells involves phospholipase C and phospholipase D activation. Genomic independent action of thyroid hormone', *BMC Cell Biol*, 2: 5.

Kelm, M., and J. Schrader. 1990. 'Control of coronary vascular tone by nitric oxide', *Circ Res*, 66: 1561-75.

Kenessey, A., and K. Ojamaa. 2006. 'Thyroid hormone stimulates protein synthesis in the cardiomyocyte by activating the Akt-mTOR and p70S6K pathways', *The Journal of biological chemistry*, 281: 20666-72.

Khalaf, D., M. Kruger, M. Wehland, M. Infanger, and D. Grimm. 2019. 'The Effects of Oral l-Arginine and l-Citrulline Supplementation on Blood Pressure', *Nutrients*, 11.

Kinne, A., M. Wittner, E. K. Wirth, K. M. Hinz, R. Schulein, J. Kohrle, and G. Krause. 2015. 'Involvement of the L-Type Amino Acid Transporter Lat2 in the Transport of 3,3'-Diiodothyronine across the Plasma Membrane', *Eur Thyroid J*, 4: 42-50.

Kinugawa, K., M. Y. Jeong, M. R. Bristow, and C. S. Long. 2005. 'Thyroid hormone induces cardiac myocyte hypertrophy in a thyroid hormone receptor alpha1-specific manner that requires TAK1 and p38 mitogen-activated protein kinase', *Mol Endocrinol*, 19: 1618-28.

Kishi, T. 2012. 'Heart failure as an autonomic nervous system dysfunction', *J Cardiol*, 59: 117-22.

Klein, I. 1990. 'Thyroid hormone and the cardiovascular system', *Am J Med*, 88: 631-7.

Klein, I., and S. Danzi. 2007. 'Thyroid Disease and the Heart', *Circulation*, 116: 1725-35.

Klein, I., and K. Ojamaa. 2001. 'Thyroid hormone and the cardiovascular system', *The New England journal of medicine*, 344: 501-9.

Kleinbongard, P., A. Schleiger, and G. Heusch. 2013. 'Characterization of vasomotor responses in different vascular territories of C57BL/6J mice', *Exp Biol Med (Maywood)*, 238: 1180-91.

Koenig, R. J. 1998. 'Thyroid hormone receptor coactivators and corepressors', *Thyroid*, 8: 703-13.

Koenig, R. J., M. A. Lazar, R. A. Hodin, G. A. Brent, P. R. Larsen, W. W. Chin, and D. D. Moore. 1989. 'Inhibition of thyroid hormone action by a non-hormone binding c-erbA protein generated by alternative mRNA splicing', *Nature*, 337: 659-61.

Koenig, R. J., R. L. Warne, G. A. Brent, J. W. Harney, P. R. Larsen, and D. D. Moore. 1988. 'Isolation of a cDNA clone encoding a biologically active thyroid hormone receptor', *Proc Natl Acad Sci U S A*, 85: 5031-5.

Krauchi, K. 2002. 'How is the circadian rhythm of core body temperature regulated?', *Clin Auton Res*, 12: 147-9.

Krauchi, K., and A. Wirz-Justice. 1994. 'Circadian rhythm of heat production, heart rate, and skin and core temperature under unmasking conditions in men', *Am J Physiol*, 267: R819-29.

Kuzman, J. A., T. D. O'Connell, and A. M. Gerdes. 2007. 'Rapamycin prevents thyroid hormone-induced cardiac hypertrophy', *Endocrinology*, 148: 3477-84.

Kuzman, J. A., K. A. Vogelsang, T. A. Thomas, and A. M. Gerdes. 2005. 'L-Thyroxine activates Akt signaling in the heart', *J Mol Cell Cardiol*, 39: 251-8.

Ladenson, P. W., P. A. Singer, K. B. Ain, N. Bagchi, S. T. Bigos, E. G. Levy, S. A. Smith, G. H. Daniels, and H. D. Cohen. 2000. 'American Thyroid Association guidelines for detection of thyroid dysfunction', *Arch Intern Med*, 160: 1573-5.

Lakatos, P., and P. H. Stern. 1991. 'Evidence for direct non-genomic effects of triiodothyronine on bone rudiments in rats: stimulation of the inositol phosphate second messenger system', *Acta Endocrinol (Copenh)*, 125: 603-8.

Larsson, H. P. 2010. 'How is the heart rate regulated in the sinoatrial node? Another piece to the puzzle', *J Gen Physiol*, 136: 237-41.

Latteyer, S., S. Christoph, S. Theurer, G. S. Hones, K. W. Schmid, D. Fuehrer, and L. C. Moeller. 2019. 'Thyroxine promotes lung cancer growth in an orthotopic mouse model', *Endocr Relat Cancer*.

Laurberg, P., K. M. Pedersen, A. Hreidarsson, N. Sigfusson, E. Iversen, and P. R. Knudsen. 1998. 'Iodine intake and the pattern of thyroid disorders: a comparative epidemiological study of thyroid abnormalities in the elderly in Iceland and in Jutland, Denmark', *J Clin Endocrinol Metab*, 83: 765-9.

Lazar, M. A. 1993. 'Thyroid hormone receptors: multiple forms, multiple possibilities', *Endocrine Reviews*, 14: 184-93.

Lazar, M. A., R. A. Hodin, and W. W. Chin. 1989. 'Human carboxyl-terminal variant of alpha-type c-erbA inhibits trans-activation by thyroid hormone receptors without binding thyroid hormone', *Proc Natl Acad Sci U S A*, 86: 7771-4.

Lekakis, J., C. Papamichael, M. Alevizaki, G. Piperingos, P. Marafelia, J. Mantzos, S. Stamatelopoulos, and D. A. Koutras. 1997. 'Flow-mediated, endothelium-dependent vasodilation is impaired in subjects with hypothyroidism, borderline hypothyroidism, and high-normal serum thyrotropin (TSH) values', *Thyroid*, 7: 411-4.

Levey, G. S., and I. Klein. 1990. 'Catecholamine-thyroid hormone interactions and the cardiovascular manifestations of hyperthyroidism', *Am J Med*, 88: 642-6.

Liao, Y., S. Takashima, Y. Asano, M. Asakura, A. Ogai, Y. Shintani, T. Minamino, H. Asanuma, S. Sanada, J. Kim, H. Ogita, H. Tomoike, M. Hori, and M. Kitakaze. 2003. 'Activation of adenosine A1 receptor attenuates cardiac hypertrophy and prevents heart failure in murine left ventricular pressure-overload model', *Circ Res*, 93: 759-66.

Limas, C., and C. J. Limas. 1987. 'Influence of thyroid status on intracellular distribution of cardiac adrenoceptors', *Circ Res*, 61: 824-8.

Lin, J. Z., D. H. Sieglaff, C. Yuan, J. Su, A. S. Arumanayagam, S. Firouzbakht, J. J. Cantu Pompa, F. D. Reynolds, X. Zhou, A. Cvoro, and P. Webb. 2013. 'Gene specific actions of thyroid hormone receptor subtypes', *PLoS One*, 8: e52407.

Lithell, H., J. Boberg, K. Hellsing, S. Ljunghall, G. Lundqvist, B. Vessby, and L. Wide. 1981. 'Serum lipoprotein and apolipoprotein concentrations and tissue lipoprotein-lipase activity in overt and subclinical hypothyroidism: the effect of substitution therapy', *Eur J Clin Invest*, 11: 3-10.

Liu, K. L., M. Lo, L. Canaple, K. Gauthier, P. Del Carmine, and M. Beylot. 2014. 'Vascular function of the mesenteric artery isolated from thyroid hormone receptor-alpha knockout mice', *J Vasc Res*, 51: 350-9.

Liu, Y. Y., and G. A. Brent. 2010. 'Thyroid hormone crosstalk with nuclear receptor signaling in metabolic regulation', *Trends Endocrinol Metab*, 21: 166-73.

Liu, Z. P., and E. N. Olson. 2002. 'Suppression of proliferation and cardiomyocyte hypertrophy by CHAMP, a cardiac-specific RNA helicase', *Proc Natl Acad Sci U S A*, 99: 2043-8.

Lorell, B. H., and B. A. Carabello. 2000. 'Left ventricular hypertrophy: pathogenesis, detection, and prognosis', *Circulation*, 102: 470-9.

Lorenz, K., J. P. Schmitt, E. M. Schmitteckert, and M. J. Lohse. 2009. 'A new type of ERK1/2 autophosphorylation causes cardiac hypertrophy', *Nat Med*, 15: 75-83.

Louwerens, M., B. C. Appelhof, H. Verloop, M. Medici, R. P. Peeters, T. J. Visser, A. Boelen, E. Fliers, J. W. Smit, and O. M. Dekkers. 2012. 'Fatigue and fatigue-related symptoms in patients treated for different causes of hypothyroidism', *Eur J Endocrinol*, 167: 809-15.

Lynch, M. A., J. F. Andrews, and R. E. Moore. 1985. 'Low doses of T3 induce a rapid metabolic response in young lambs', *Hormone and metabolic research = Hormon- und Stoffwechselforschung = Hormones et metabolisme*, 17: 63-6.

Macchia, P. E., Y. Takeuchi, T. Kawai, K. Cua, K. Gauthier, O. Chassande, H. Seo, Y. Hayashi, J. Samarut, Y. Murata, R. E. Weiss, and S. Refetoff. 2001. 'Increased sensitivity to thyroid hormone in mice with complete deficiency of thyroid hormone receptor alpha', *Proc Natl Acad Sci U S A*, 98: 349-54.

Makino, A., J. Suarez, H. Wang, D. D. Belke, B. T. Scott, and W. H. Dillmann. 2009. 'Thyroid hormone receptor-beta is associated with coronary angiogenesis during pathological cardiac hypertrophy', *Endocrinology*, 150: 2008-15.

Makino, A., H. Wang, B. T. Scott, J. X. Yuan, and W. H. Dillmann. 2012. 'Thyroid hormone receptor-alpha and vascular function', *American journal of physiology. Cell physiology*, 302: C1346-52.

Mangelsdorf, D. J., C. Thummel, M. Beato, P. Herrlich, G. Schutz, K. Umesono, B. Blumberg, P. Kastner, M. Mark, P. Chambon, and R. M. Evans. 1995. 'The nuclear receptor superfamily: the second decade', *Cell*, 83: 835-9.

Marcisz, C., G. Jonderko, T. Wroblewski, G. Kurzawska, and F. Mazur. 2006. 'Left ventricular mass in patients with hyperthyroidism', *Med Sci Monit*, 12: CR481-6.

Marrif, H., A. Schifman, Z. Stepanyan, M. A. Gillis, A. Calderone, R. E. Weiss, J. Samarut, and J. E. Silva. 2005. 'Temperature homeostasis in transgenic mice lacking thyroid hormone receptor-alpha gene products', *Endocrinology*, 146: 2872-84.

Martin, N. P., E. Marron Fernandez de Velasco, F. Mizuno, E. L. Scappini, B. Gloss, C. Erxleben, J. G. Williams, H. M. Stapleton, S. Gentile, and D. L. Armstrong. 2014. 'A rapid cytoplasmic mechanism for PI3 kinase regulation by the nuclear thyroid hormone receptor, TRbeta, and genetic evidence for its role in the maturation of mouse hippocampal synapses in vivo', *Endocrinology*, 155: 3713-24.

McDonald, M. P., R. Wong, G. Goldstein, B. Weintraub, S. Y. Cheng, and J. N. Crawley. 1998. 'Hyperactivity and learning deficits in transgenic mice bearing a human mutant thyroid hormone beta1 receptor gene', *Learn Mem*, 5: 289-301.

McKenna, N. J., and B. W. O'Malley. 2002. 'Combinatorial control of gene expression by nuclear receptors and coregulators', *Cell*, 108: 465-74.

McMullen, J. R., T. Shioi, W. Y. Huang, L. Zhang, O. Tarnavski, E. Bisping, M. Schinke, S. Kong, M. C. Sherwood, J. Brown, L. Riggi, P. M. Kang, and S. Izumo. 2004. 'The insulin-like growth factor 1 receptor induces physiological heart growth via the phosphoinositide 3-kinase(p110alpha) pathway', *The Journal of biological chemistry*, 279: 4782-93.

Mende, U., A. Kagen, A. Cohen, J. Aramburu, F. J. Schoen, and E. J. Neer. 1998. 'Transient cardiac expression of constitutively active Galphaq leads to hypertrophy and dilated cardiomyopathy by calcineurin-dependent and independent pathways', *Proc Natl Acad Sci U S A*, 95: 13893-8.

Milanesi, A., J. W. Lee, N. H. Kim, Y. Y. Liu, A. Yang, S. Sedrakyan, A. Kahng, V. Cervantes, N. Tripuraneni, S. Y. Cheng, L. Perin, and G. A. Brent. 2016. 'Thyroid Hormone Receptor alpha Plays an Essential Role in Male Skeletal Muscle Myoblast Proliferation, Differentiation, and Response to Injury', *Endocrinology*, 157: 4-15.

Miot, F., C. Dupuy, J. Dumont, and B. Rousset. 2000. 'Chapter 2 Thyroid Hormone Synthesis And Secretion.' in L. J. De Groot, G. Chrousos, K. Dungan, K. R. Feingold, A. Grossman, J. M. Hershman, C. Koch, M. Korbonits, R. McLachlan, M. New, J. Purnell, R. Rebar, F. Singer and A. Vinik (eds.), *Endotext* (MDText.com, Inc.: South Dartmouth (MA)).

Mitsuhashi, T., G. E. Tennyson, and V. M. Nikodem. 1988. 'Alternative splicing generates messages encoding rat c-erbA proteins that do not bind thyroid hormone', *Proc Natl Acad Sci U S A*, 85: 5804-8.

Mittag, J. 2019. 'More Than Fever - Novel Concepts in the Regulation of Body Temperature by Thyroid Hormones', *Exp Clin Endocrinol Diabetes*.

Mittag, J., B. Davis, M. Vujovic, A. Arner, and B. Vennstrom. 2010. 'Adaptations of the autonomous nervous system controlling heart rate are impaired by a mutant thyroid hormone receptor-alpha1', *Endocrinology*, 151: 2388-95.

Moeller, L. C., X. Cao, A. M. Dumitrescu, H. Seo, and S. Refetoff. 2006. 'Thyroid hormone mediated changes in gene expression can be initiated by cytosolic action of the thyroid hormone receptor beta through the phosphatidylinositol 3-kinase pathway', *Nucl Recept Signal*, 4: e020.

Moeller, L. C., A. M. Dumitrescu, and S. Refetoff. 2005. 'Cytosolic action of thyroid hormone leads to induction of hypoxia-inducible factor-1alpha and glycolytic genes', *Mol Endocrinol*, 19: 2955-63.

Moeller, L. C., A. M. Dumitrescu, R. L. Walker, P. S. Meltzer, and S. Refetoff. 2005. 'Thyroid hormone responsive genes in cultured human fibroblasts', *J Clin Endocrinol Metab*, 90: 936-43.

Moeller, L. C., N. E. Ulanowski, A. M. Dumitrescu, S. Refetoff, K. Mann, and O. E. Janssen. 2006. 'The non-genomic effect of the thyroid gland hormone receptor beta in cytosol leads to the induction of stanniocalcin 1', *Medizinische Klinik*, 101: 863-64.

Moon, J. Y. 2013. 'Recent Update of Renin-angiotensin-aldosterone System in the Pathogenesis of Hypertension', *Electrolyte Blood Press*, 11: 41-5.

Morgan, H. E., and K. M. Baker. 1991. 'Cardiac hypertrophy. Mechanical, neural, and endocrine dependence', *Circulation*, 83: 13-25.

Morte, B., and J. Bernal. 2014. 'Thyroid hormone action: astrocyte-neuron communication', *Front Endocrinol (Lausanne)*, 5: 82.

Muller, B., D. A. Tsakiris, C. B. Roth, M. Guglielmetti, J. J. Staub, and G. A. Marbet. 2001. 'Haemostatic profile in hypothyroidism as potential risk factor for vascular or thrombotic disease', *Eur J Clin Invest*, 31: 131-7.

Mullur, R., Y. Y. Liu, and G. A. Brent. 2014. 'Thyroid hormone regulation of metabolism', *Physiol Rev*, 94: 355-82.

Muralidhar, S. A., and H. A. Sadek. 2016. 'Meis1 Regulates Postnatal Cardiomyocyte Cell Cycle Arrest.' in T. Nakanishi, R. R. Markwald, H. S. Baldwin, B. B. Keller, D. Srivastava and H. Yamagishi (eds.), *Etiology and Morphogenesis of Congenital Heart Disease: From Gene Function and Cellular Interaction to Morphology* (Tokyo).

Murray, M. B., N. D. Zilz, N. L. McCreary, M. J. MacDonald, and H. C. Towle. 1988. 'Isolation and characterization of rat cDNA clones for two distinct thyroid hormone receptors', *The Journal of biological chemistry*, 263: 12770-7.

Muthukumar, S., D. Sadacharan, K. Ravikumar, G. Mohanapriya, Z. Hussain, and R. V. Suresh. 2016. 'A Prospective Study on Cardiovascular Dysfunction in Patients with Hyperthyroidism and Its Reversal After Surgical Cure', *World J Surg*, 40: 622-8.

Nagaya, T., L. D. Madison, and J. L. Jameson. 1992. 'Thyroid hormone receptor mutants that cause resistance to thyroid hormone. Evidence for receptor competition for DNA sequences in target genes', *The Journal of biological chemistry*, 267: 13014-9.

Nagy, L., H. Y. Kao, D. Chakravarti, R. J. Lin, C. A. Hassig, D. E. Ayer, S. L. Schreiber, and R. M. Evans. 1997. 'Nuclear receptor repression mediated by a complex containing SMRT, mSin3A, and histone deacetylase', *Cell*, 89: 373-80.

Nakai, A., S. Seino, A. Sakurai, I. Szilak, G. I. Bell, and L. J. DeGroot. 1988. 'Characterization of a thyroid hormone receptor expressed in human kidney and other tissues', *Proc Natl Acad Sci U S A*, 85: 2781-5.

Nakamura, M., and J. Sadoshima. 2018. 'Mechanisms of physiological and pathological cardiac hypertrophy', *Nat Rev Cardiol*.

Napoli, R., B. Biondi, V. Guardasole, M. Matarazzo, F. Pardo, V. Angelini, S. Fazio, and L. Sacca. 2001. 'Impact of hyperthyroidism and its correction on vascular reactivity in humans', *Circulation*, 104: 3076-80.

Nazar, K., J. Chwalbinska-Moneta, J. Machalla, and H. Kaciuba-Uscilko. 1978. 'Metabolic and body temperature changes during exercise in hyperthyroid patients', *Clin Sci Mol Med*, 54: 323-7.

Nikkila, E. A., and M. Kekki. 1972. 'Plasma triglyceride metabolism in thyroid disease', *The Journal of clinical investigation*, 51: 2103-14.

Nuclear Receptors Nomenclature, Committee. 1999. 'A unified nomenclature system for the nuclear receptor superfamily', *Cell*, 97: 161-3.

O'Mara, B. A., W. Dittrich, T. J. Lauterio, and D. L. St Germain. 1993. 'Pretranslational regulation of type I 5'-deiodinase by thyroid hormones and in fasted and diabetic rats', *Endocrinology*, 133: 1715-23.

Obuobie, K., J. Smith, L. M. Evans, R. John, J. S. Davies, and J. H. Lazarus. 2002. 'Increased central arterial stiffness in hypothyroidism', *J Clin Endocrinol Metab*, 87: 4662-6.

Ogryzko, V. V., R. L. Schiltz, V. Russanova, B. H. Howard, and Y. Nakatani. 1996. 'The transcriptional coactivators p300 and CBP are histone acetyltransferases', *Cell*, 87: 953-9.

Ohtaki, S., H. Nakagawa, M. Nakamura, and I. Yamazaki. 1982. 'One- and two-electron oxidations of tyrosine, monoiodotyrosine, and diiodotyrosine catalyzed by hog thyroid peroxidase', *The Journal of biological chemistry*, 257: 13398-403.

Ojamaa, K., J. D. Klemperer, and I. Klein. 1996. 'Acute effects of thyroid hormone on vascular smooth muscle', *Thyroid*, 6: 505-12.

Oppenheimer, J. H., D. Koerner, H. L. Schwartz, and M. I. Surks. 1972. 'Specific nuclear triiodothyronine binding sites in rat liver and kidney', *J Clin Endocrinol Metab*, 35: 330-3.

Oppenheimer, J. H., H. L. Schwartz, C. N. Mariash, W. B. Kinlaw, N. C. Wong, and H. C. Freake. 1987. 'Advances in our understanding of thyroid hormone action at the cellular level', *Endocrine Reviews*, 8: 288-308.

Ortiga-Carvalho, T. M., M. I. Chiamolera, C. C. Pazos-Moura, and F. E. Wondisford. 2016. 'Hypothalamus-Pituitary-Thyroid Axis', *Compr Physiol*, 6: 1387-428.

Osman, F., J. A. Franklyn, R. L. Holder, M. C. Sheppard, and M. D. Gammage. 2007. 'Cardiovascular manifestations of hyperthyroidism before and after antithyroid therapy: a matched case-control study', *J Am Coll Cardiol*, 49: 71-81.

Owen, P. J., R. Sabit, and J. H. Lazarus. 2007. 'Thyroid disease and vascular function', *Thyroid*, 17: 519-24.

Pachucki, J., L. A. Burmeister, and P. R. Larsen. 1999. 'Thyroid hormone regulates hyperpolarization-activated cyclic nucleotide-gated channel (HCN2) mRNA in the rat heart', *Circ Res*, 85: 498-503.

Pantos, C., and I. Mourouzis. 2014. 'The Emerging Role of TR1 in Cardiac Repair: Potential Therapeutic Implications', *Oxid Med Cell Longev*, 2014: 481482.

Pantos, C., I. Mourouzis, T. Saranteas, V. Brozou, G. Galanopoulos, G. Kostopanagiotou, and D. V. Cokkinos. 2011. 'Acute T3 treatment protects the heart against ischemia-reperfusion injury via TRalpha1 receptor', *Mol Cell Biochem*, 353: 235-41.

Park, K. W., H. B. Dai, K. Ojamaa, E. Lowenstein, I. Klein, and F. W. Sellke. 1997. 'The direct vasomotor effect of thyroid hormones on rat skeletal muscle resistance arteries', *Anesth Analg*, 85: 734-8.

Pasumarthi, K. B., and L. J. Field. 2002. 'Cardiomyocyte cell cycle regulation', *Circ Res*, 90: 1044-54.

Peeters, R. P., and T. J. Visser. 2000. 'Metabolism of Thyroid Hormone.' in K. R. Feingold, B. Anawalt, A. Boyce, G. Chrousos, K. Dungan, A. Grossman, J. M. Hershman, G. Kaltsas, C. Koch, P. Kopp, M. Korbonits, R. McLachlan, J. E. Morley, M. New, L. Perreault, J. Purnell, R. Rebar, F. Singer, D. L. Trence, A. Vinik and D. P. Wilson (eds.), *Endotext* (South Dartmouth (MA)).

Petretta, M., D. Bonaduce, L. Spinelli, M. L. Vicario, V. Nuzzo, F. Marciano, P. Camuso, V. De Sanctis, and G. Lupoli. 2001. 'Cardiovascular haemodynamics and cardiac autonomic control in patients with subclinical and overt hyperthyroidism', *Eur J Endocrinol*, 145: 691-6.

Pfaffl, M. W. 2001. 'A new mathematical model for relative quantification in real-time RT-PCR', *Nucleic Acids Res*, 29: e45.

Pilo, A., G. Iervasi, F. Vitek, M. Ferdeghini, F. Cazzuola, and R. Bianchi. 1990. 'Thyroidal and peripheral production of 3,5,3'-triiodothyronine in humans by multicompartmental analysis', *Am J Physiol*, 258: E715-26.

Pitt-Rivers, R., and W. R. Trotter. 1953. 'The site of accumulation of iodide in the thyroid of rats treated with thiouracil', *Lancet*, 265: 918-9.

Pizzagalli, F., B. Hagenbuch, B. Stieger, U. Klenk, G. Folkers, and P. J. Meier. 2002. 'Identification of a novel human organic anion transporting polypeptide as a high affinity thyroxine transporter', *Mol Endocrinol*, 16: 2283-96.

Plateroti, M., K. Gauthier, C. Domon-Dell, J. N. Freund, J. Samarut, and O. Chassande. 2001. 'Functional interference between thyroid hormone receptor alpha (TRalpha) and natural truncated TRDeltaalpha isoforms in the control of intestine development', *Molecular and cellular biology*, 21: 4761-72.

Porter, G. A., Jr., J. Hom, D. Hoffman, R. Quintanilla, K. de Mesy Bentley, and S. S. Sheu. 2011. 'Bioenergetics, mitochondria, and cardiac myocyte differentiation', *Prog Pediatr Cardiol*, 31: 75-81.

Prisant, L. M., J. S. Gujral, and A. L. Mulloy. 2006. 'Hyperthyroidism: a secondary cause of isolated systolic hypertension', *J Clin Hypertens (Greenwich)*, 8: 596-9.

Quesada, A., J. Sainz, R. Wangensteen, I. Rodriguez-Gomez, F. Vargas, and A. Osuna. 2002. 'Nitric oxide synthase activity in hyperthyroid and hypothyroid rats', *Eur J Endocrinol*, 147: 117-22.

Rakov, H., K. Engels, G. S. Hones, K. Brix, J. Kohrle, L. C. Moeller, D. Zwanziger, and D. Fuhrer. 2017. 'Sex-specific phenotypes of hyperthyroidism and hypothyroidism in aged mice', *Biol Sex Differ*, 8: 38.

Rakov, H., K. Engels, D. Zwanziger, M. Renders, K. Brix, S. Hoenes, L. C. Moeller, and D. Fuehrer. 2014. 'Molecular mechanisms of sex-dependent thyroid hormone action on target tissues', *Experimental and Clinical Endocrinology & Diabetes*, 122.

Ray, C. A., C. L. Sauder, D. M. Ray, and Y. Nishida. 2013. 'Effect of acute hyperthyroidism on blood flow, muscle oxygenation, and sympathetic nerve activity during dynamic handgrip', *Physiol Rep*, 1: e00011.

Razvi, Salman, Avais Jabbar, Alessandro Pingitore, Sara Danzi, Bernadette Biondi, Irwin Klein, Robin Peeters, Azfar Zaman, and Giorgio Iervasi. 2018. 'Thyroid Hormones and Cardiovascular Function and Diseases', *J Am Coll Cardiol*, 71: 1781-96.

Refetoff, S., R. E. Weiss, and S. J. Usala. 1993. 'The syndromes of resistance to thyroid hormone', *Endocrine Reviews*, 14: 348-99.

Reichlin, S. 1989. 'TRH: historical aspects', *Annals of the New York Academy of Sciences*, 553: 1-6.

Reiss, K., W. Cheng, A. Ferber, J. Kajstura, P. Li, B. Li, G. Olivetti, C. J. Homcy, R. Baserga, and P. Anversa. 1996. 'Overexpression of insulin-like growth factor-1 in the heart is coupled with myocyte proliferation in transgenic mice', *Proc Natl Acad Sci U S A*, 93: 8630-5.

Renaud, J. P., N. Rochel, M. Ruff, V. Vivat, P. Chambon, H. Gronemeyer, and D. Moras. 1995. 'Crystal structure of the RAR-gamma ligand-binding domain bound to all-trans retinoic acid', *Nature*, 378: 681-9.

Ribeiro, M. O., S. D. Bianco, M. Kaneshige, J. J. Schultz, S. Y. Cheng, A. C. Bianco, and G. A. Brent. 2010. 'Expression of uncoupling protein 1 in mouse brown adipose tissue is thyroid hormone receptor-beta isoform specific and required for adaptive thermogenesis', *Endocrinology*, 151: 432-40.

Ribeiro, M. O., S. D. Carvalho, J. J. Schultz, G. Chiellini, T. S. Scanlan, A. C. Bianco, and G. A. Brent. 2001. 'Thyroid hormone--sympathetic interaction and adaptive thermogenesis are thyroid hormone receptor isoform--specific', *The Journal of clinical investigation*, 108: 97-105.

Roman, M., P. Jitaru, and C. Barbante. 2014. 'Selenium biochemistry and its role for human health', *Metallomics*, 6: 25-54.

Rose, R. A., M. G. Kabir, and P. H. Backx. 2007. 'Altered heart rate and sinoatrial node function in mice lacking the cAMP regulator phosphoinositide 3-kinase-gamma', *Circ Res*, 101: 1274-82.

Royaux, I. E., K. Suzuki, A. Mori, R. Katoh, L. A. Everett, L. D. Kohn, and E. D. Green. 2000. 'Pendrin, the protein encoded by the Pendred syndrome gene (PDS), is an apical porter of iodide in the thyroid and is regulated by thyroglobulin in FRTL-5 cells', *Endocrinology*, 141: 839-45.

Saatcioglu, F., P. Bartunek, T. Deng, M. Zenke, and M. Karin. 1993. 'A conserved C-terminal sequence that is deleted in v-ErbA is essential for the biological activities of c-ErbA (the thyroid hormone receptor)', *Molecular and cellular biology*, 13: 3675-85.

Sakurai, A., K. Takeda, K. Ain, P. Ceccarelli, A. Nakai, S. Seino, G. I. Bell, S. Refetoff, and L. J. DeGroot. 1989. 'Generalized resistance to thyroid hormone associated with a mutation in the ligand-binding domain of the human thyroid hormone receptor beta', *Proc Natl Acad Sci U S A*, 86: 8977-81.

Samuel, S., K. Zhang, Y. D. Tang, A. M. Gerdes, and M. A. Carrillo-Sepulveda. 2017. 'Triiodothyronine Potentiates Vasorelaxation via PKG/VASP Signaling in Vascular Smooth Muscle Cells', *Cell Physiol Biochem*, 41: 1894-904.

Samuels, H. H., and J. S. Tsai. 1973. 'Thyroid hormone action in cell culture: domonstration of nuclear receptors in intact cells and isolated nuclei', *Proc Natl Acad Sci U S A*, 70: 3488-92.

Sande, S., and M. L. Privalsky. 1996. 'Identification of TRACs (T3 receptor-associating cofactors), a family of cofactors that associate with, and modulate the activity of, nuclear hormone receptors', *Mol Endocrinol*, 10: 813-25.

Sano, M., T. Minamino, H. Toko, H. Miyauchi, M. Orimo, Y. Qin, H. Akazawa, K. Tateno, Y. Kayama, M. Harada, I. Shimizu, T. Asahara, H. Hamada, S. Tomita, J. D. Molkentin, Y. Zou, and I. Komuro. 2007. 'p53-induced inhibition of Hif-1 causes cardiac dysfunction during pressure overload', *Nature*, 446: 444-8.

Sap, J., A. Munoz, K. Damm, Y. Goldberg, J. Ghysdael, A. Leutz, H. Beug, and B. Vennstrom. 1986. 'The c-erb-A protein is a high-affinity receptor for thyroid hormone', *Nature*, 324: 635-40.

Savinova, O. V., Y. Liu, G. A. Aasen, K. Mao, N. Y. Weltman, B. L. Nedich, Q. Liang, and A. M. Gerdes. 2011. 'Thyroid hormone promotes remodeling of coronary resistance vessels', *PLoS One*, 6: e25054.

Schimmel, M., and R. D. Utiger. 1977. 'Thyroidal and peripheral production of thyroid hormones. Review of recent findings and their clinical implications', *Ann Intern Med*, 87: 760-8.

Schmid, E., S. Neef, C. Berlin, A. Tomasovic, K. Kahlert, P. Nordbeck, K. Deiss, S. Denzinger, S. Herrmann, E. Wettwer, M. Weidendorfer, D. Becker, F. Schafer, N. Wagner, S. Ergun, J. P. Schmitt, H. A. Katus, F. Weidemann, U. Ravens, C. Maack, L. Hein, G. Ertl, O. J. Muller, L. S. Maier, M. J. Lohse, and K. Lorenz. 2015. 'Cardiac RKIP induces a beneficial beta-adrenoceptor-dependent positive inotropy', *Nat Med*, 21: 1298-306.

Schmidt, B. M., N. Martin, A. C. Georgens, H. C. Tillmann, M. Feuring, M. Christ, and M. Wehling. 2002. 'Nongenomic cardiovascular effects of triiodothyronine in euthyroid male volunteers', *J Clin Endocrinol Metab*, 87: 1681-6.

Schneider, M. J., S. N. Fiering, S. E. Pallud, A. F. Parlow, D. L. St Germain, and V. A. Galton. 2001. 'Targeted disruption of the type 2 selenodeiodinase gene (DIO2) results in a phenotype of pituitary resistance to T4', *Mol Endocrinol*, 15: 2137-48.

Schussler, G. C. 2000. 'The thyroxine-binding proteins', *Thyroid*, 10: 141-9.

Segal, J., C. Buckley, and S. H. Ingbar. 1985. 'Stimulation of adenylate cyclase activity in rat thymocytes in vitro by 3,5,3'-triiodothyronine', *Endocrinology*, 116: 2036-43.

Segal, J., and S. H. Ingbar. 1979. 'Stimulation by triiodothyronine of the in vitro uptake of sugars by rat thymocytes', *The Journal of clinical investigation*, 63: 507-15.

———. 1981. 'Studies of the mechanism by which 3,5,3'- triiodothyronine stimulates 2-deoxyglucose uptake in rat thymocytes in vitro. Role of calcium and adenosine 3':5'-monophosphate', *The Journal of clinical investigation*, 68: 103-10.

———. 1985. 'In vivo stimulation of sugar uptake in rat thymocytes. An extranuclear action of 3,5,3'-triiodothyronine', *The Journal of clinical investigation*, 76: 1575-80.

Shibusawa, N., K. Hashimoto, A.A. Nikrodhanond, C.M. Liberman, M.L. Applebury, X.H. Liao, J.T. Robbins, S. Refetoff, R.N. Cohen, and F. E. Wondisford. 2003. 'Thyroid hormone action in the absence of thyroid hormone receptor DNA-binding in vivo', *Journal of Clinical Investigation*, 112: 588-97.

Shibusawa, N., A. N. Hollenberg, and F. E. Wondisford. 2003. 'Thyroid hormone receptor DNA binding is required for both positive and negative gene regulation', *The Journal of biological chemistry*, 278: 732-8.

Shimizu, I., and T. Minamino. 2016. 'Physiological and pathological cardiac hypertrophy', *J Mol Cell Cardiol*, 97: 245-62.

Shimizu, I., T. Minamino, H. Toko, S. Okada, H. Ikeda, N. Yasuda, K. Tateno, J. Moriya, M. Yokoyama, A. Nojima, G. Y. Koh, H. Akazawa, I. Shiojima, C. R. Kahn, E. D. Abel, and I. Komuro. 2010. 'Excessive cardiac insulin signaling exacerbates systolic dysfunction induced by pressure overload in rodents', *The Journal of clinical investigation*, 120: 1506-14.

Shimizu, T., S. Koide, J. Y. Noh, K. Sugino, K. Ito, and H. Nakazawa. 2002. 'Hyperthyroidism and the management of atrial fibrillation', *Thyroid*, 12: 489-93.

Shioi, T., P. M. Kang, P. S. Douglas, J. Hampe, C. M. Yballe, J. Lawitts, L. C. Cantley, and S. Izumo. 2000. 'The conserved phosphoinositide 3-kinase pathway determines heart size in mice', *EMBO J*, 19: 2537-48.

Silva, J. E. 2001. 'The multiple contributions of thyroid hormone to heat production', *The Journal of clinical investigation*, 108: 35-7.

Silvani, A., G. Calandra-Buonaura, R. A. Dampney, and P. Cortelli. 2016. 'Brain-heart interactions: physiology and clinical implications', *Philos Trans A Math Phys Eng Sci*, 374.

Simoncini, T., A. Hafezi-Moghadam, D. P. Brazil, K. Ley, W. W. Chin, and J. K. Liao. 2000. 'Interaction of oestrogen receptor with the regulatory subunit of phosphatidylinositol-3-OH kinase', *Nature*, 407: 538-41.

Sinski, M., J. Lewandowski, J. Przybylski, P. Zalewski, B. Symonides, P. Abramczyk, and Z. Gaciong. 2014. 'Deactivation of carotid body chemoreceptors by hyperoxia decreases blood pressure in hypertensive patients', *Hypertens Res*, 37: 858-62.

Smolenskii, G. A., and A. S. Kovalev. 1966. '[Duration and structure of the cardiac contraction cycle]', *Fiziol Zh SSSR Im I M Sechenova*, 52: 1471-5.

Somers, V. K., A. L. Mark, and F. M. Abboud. 1991. 'Interaction of baroreceptor and chemoreceptor reflex control of sympathetic nerve activity in normal humans', *The Journal of clinical investigation*, 87: 1953-7.

Sorisky, A. 2016. 'Subclinical Hypothyroidism - What is Responsible for its Association with Cardiovascular Disease?', *Eur Endocrinol*, 12: 96-98.

Spencer, T. E., G. Jenster, M. M. Burcin, C. D. Allis, J. Zhou, C. A. Mizzen, N. J. McKenna, S. A. Onate, S. Y. Tsai, M. J. Tsai, and B. W. O'Malley. 1997. 'Steroid receptor coactivator-1 is a histone acetyltransferase', *Nature*, 389: 194-8.

Srichomkwun, P., J. Anselmo, X. H. Liao, G. S. Hones, L. C. Moeller, M. Alonso-Sampedro, R. E. Weiss, A. M. Dumitrescu, and S. Refetoff. 2017. 'Fetal Exposure to High Maternal Thyroid Hormone Levels Causes Central Resistance to Thyroid Hormone in Adult Humans and Mice', *J Clin Endocrinol Metab*, 102: 3234-40.

Storey, N. M., S. Gentile, H. Ullah, A. Russo, M. Muessel, C. Erxleben, and D. L. Armstrong. 2006. 'Rapid signaling at the plasma membrane by a nuclear receptor for thyroid hormone', *Proc Natl Acad Sci U S A*, 103: 5197-201.

Storey, N. M., J. P. O'Bryan, and D. L. Armstrong. 2002. 'Rac and Rho mediate opposing hormonal regulation of the ether-a-go-go-related potassium channel', *Curr Biol*, 12: 27-33.

Stubbe, P., J. Gatz, P. Heidemann, A. Muhlen, and R. Hesch. 1978. 'Thyroxine-binding globulin, triiodothyronine, thyroxine and thyrotropin in newborn infants and children', *Horm Metab Res*, 10: 58-61.

Sun, Z. Q., K. Ojamaa, T. Y. Nakamura, M. Artman, I. Klein, and W. A. Coetzee. 2001. 'Thyroid hormone increases pacemaker activity in rat neonatal atrial myocytes', *J Mol Cell Cardiol*, 33: 811-24.

Tankersley, C. G., R. Irizarry, S. Flanders, and R. Rabold. 2002. 'Circadian rhythm variation in activity, body temperature, and heart rate between C3H/HeJ and C57BL/6J inbred strains', *J Appl Physiol (1985)*, 92: 870-7.

Tata, J. R. 1960. 'Interaction between thyroid hormones and extra and intra-cellular proteins', *Bull Soc Chim Biol (Paris)*, 42: 1171-85.

Tata, J. R., L. Ernster, O. Lindberg, E. Arrhenius, S. Pedersen, and R. Hedman. 1963. 'The action of thyroid hormones at the cell level', *Biochem J*, 86: 408-28.

Tata, J. R., and C. C. Widnell. 1966. 'Ribonucleic acid synthesis during the early action of thyroid hormones', *Biochem J*, 98: 604-20.

Tavi, P., M. Sjogren, P. K. Lunde, S. J. Zhang, F. Abbate, B. Vennstrom, and H. Westerblad. 2005. 'Impaired Ca2+ handling and contraction in cardiomyocytes from mice with a dominant negative thyroid hormone receptor alpha1', *J Mol Cell Cardiol*, 38: 655-63.

Tayefeh, F., A. Kurz, D. I. Sessler, C. A. Lawson, T. Ikeda, and D. Marder. 1997. 'Thermoregulatory vasodilation increases the venous partial pressure of oxygen', *Anesth Analg*, 85: 657-62.

Tchernaenko, V., M. Radlinska, L. Lubkowska, H. R. Halvorson, M. Kashlev, and L. C. Lutter. 2008. 'DNA bending in transcription initiation', *Biochemistry*, 47: 1885-95.

Toral, M., R. Jimenez, S. Montoro-Molina, M. Romero, R. Wangensteen, J. Duarte, and F. Vargas. 2018. 'Thyroid hormones stimulate L-arginine transport in human endothelial cells', *Journal of Endocrinology*, 239: 49-62.

Tu, H. M., G. Legradi, T. Bartha, D. Salvatore, R. M. Lechan, and P. R. Larsen. 1999. 'Regional expression of the type 3 iodothyronine deiodinase messenger ribonucleic acid in the rat central nervous system and its regulation by thyroid hormone', *Endocrinology*, 140: 784-90.

Tucker, W. D., and K. Mahajan. 2020. 'Anatomy, Blood Vessels.' in, *StatPearls* (Treasure Island (FL)).

Twyffels, L., A. Strickaert, M. Virreira, C. Massart, J. Van Sande, C. Wauquier, R. Beauwens, J. E. Dumont, L. J. Galietta, A. Boom, and V. Kruys. 2014. 'Anoctamin-1/TMEM16A is the major apical iodide channel of the thyrocyte', *American journal of physiology. Cell physiology*, 307: C1102-12.

Udovcic, M., R. H. Pena, B. Patham, L. Tabatabai, and A. Kansara. 2017. 'Hypothyroidism and the Heart', *Methodist Debakey Cardiovasc J*, 13: 55-59.

Vadiveloo, T., P. T. Donnan, L. Cochrane, and G. P. Leese. 2011. 'The Thyroid Epidemiology, Audit, and Research Study (TEARS): the natural history of endogenous subclinical hyperthyroidism', *J Clin Endocrinol Metab*, 96: E1-8.

Vargas, F., A. Fernandez-Rivas, J. Garcia Estan, and C. Garcia del Rio. 1995. 'Endothelium-dependent and endothelium-independent vasodilation in hyperthyroid and hypothyroid rats', *Pharmacology*, 51: 308-14.

Vargas, F., J. M. Moreno, I. Rodriguez-Gomez, R. Wangensteen, A. Osuna, M. Alvarez-Guerra, and J. Garcia-Estan. 2006. 'Vascular and renal function in experimental thyroid disorders', *Eur J Endocrinol*, 154: 197-212.

Vella, K. R., and A. N. Hollenberg. 2017. 'The actions of thyroid hormone signaling in the nucleus', *Mol Cell Endocrinol*, 458: 127-35.

Vella, K. R., P. Ramadoss, E. Sousa R. H. Costa, I. Astapova, F. D. Ye, K. A. Holtz, J. C. Harris, and A. N. Hollenberg. 2014. 'Thyroid hormone signaling in vivo requires a balance between coactivators and corepressors', *Molecular and cellular biology*, 34: 1564-75.

Venero, C., A. Guadano-Ferraz, A. I. Herrero, K. Nordstrom, J. Manzano, G. M. de Escobar, J. Bernal, and B. Vennstrom. 2005. 'Anxiety, memory impairment, and locomotor dysfunction caused by a mutant thyroid hormone receptor alpha1 can be ameliorated by T3 treatment', *Genes Dev*, 19: 2152-63.

Vennstrom, B., and J. M. Bishop. 1982. 'Isolation and characterization of chicken DNA homologous to the two putative oncogenes of avian erythroblastosis virus', *Cell*, 28: 135-43.

Vincent, J. L. 2008. 'Understanding cardiac output', *Crit Care*, 12: 174.

Vollmer, R. R. 1996. 'Selective neural regulation of epinephrine and norepinephrine cells in the adrenal medulla -- cardiovascular implications', *Clin Exp Hypertens*, 18: 731-51.

Wagner, R. L., J. W. Apriletti, M. E. McGrath, B. L. West, J. D. Baxter, and R. J. Fletterick. 1995. 'A structural role for hormone in the thyroid hormone receptor', *Nature*, 378: 690-7.

Wallis, K., M. Sjogren, M. van Hogerlinden, G. Silberberg, A. Fisahn, K. Nordstrom, L. Larsson, H. Westerblad, G. Morreale de Escobar, O. Shupliakov, and B. Vennstrom. 2008. 'Locomotor deficiencies and aberrant development of subtype-specific GABAergic interneurons caused by an unliganded thyroid hormone receptor alpha1', *J Neurosci*, 28: 1904-15.

Walsh, J. P., A. P. Bremner, M. K. Bulsara, P. O'Leary, P. J. Leedman, P. Feddema, and V. Michelangeli. 2005. 'Subclinical thyroid dysfunction as a risk factor for cardiovascular disease', *Arch Intern Med*, 165: 2467-72.

Walsh, S., A. Ponten, B. K. Fleischmann, and S. Jovinge. 2010. 'Cardiomyocyte cell cycle control and growth estimation in vivo--an analysis based on cardiomyocyte nuclei', *Cardiovasc Res*, 86: 365-73.

Warner, A., and J. Mittag. 2014. 'Brown fat and vascular heat dissipation: The new cautionary tail', *Adipocyte*, 3: 221-3.

Warner, A., A. Rahman, P. Solsjo, K. Gottschling, B. Davis, B. Vennstrom, A. Arner, and J. Mittag. 2013. 'Inappropriate heat dissipation ignites brown fat thermogenesis in mice with a mutant thyroid hormone receptor alpha1', *Proc Natl Acad Sci U S A*, 110: 16241-46.

Watson, P. J., L. Fairall, and J. W. Schwabe. 2012. 'Nuclear hormone receptor co-repressors: structure and function', *Mol Cell Endocrinol*, 348: 440-9.

Weinberger, C., C. C. Thompson, E. S. Ong, R. Lebo, D. J. Gruol, and R. M. Evans. 1986. 'The c-erb-A gene encodes a thyroid hormone receptor', *Nature*, 324: 641-6.

Weiss, R. E., C. Korcarz, O. Chassande, K. Cua, P. M. Sadow, E. Koo, J. Samarut, and R. Lang. 2002. 'Thyroid hormone and cardiac function in mice deficient in thyroid hormone receptor-alpha or -beta: an echocardiograph study', *Am J Physiol Endocrinol Metab*, 283: E428-35.

Weiss, R. E., Y. Murata, K. Cua, Y. Hayashi, H. Seo, and S. Refetoff. 1998. 'Thyroid hormone action on liver, heart, and energy expenditure in thyroid hormone receptor beta-deficient mice', *Endocrinology*, 139: 4945-52.

Wettschureck, N., H. Rutten, A. Zywietz, D. Gehring, T. M. Wilkie, J. Chen, K. R. Chien, and S. Offermanns. 2001. 'Absence of pressure overload induced myocardial hypertrophy after conditional inactivation of Galphaq/Galpha11 in cardiomyocytes', *Nat Med*, 7: 1236-40.

Wiersinga, W. M. 2010. 'The role of thyroid hormone nuclear receptors in the heart: evidence from pharmacological approaches', *Heart Fail Rev*, 15: 121-4.

Wiersinga, W. M., L. Duntas, V. Fadeyev, B. Nygaard, and M. P. Vanderpump. 2012. '2012 ETA Guidelines: The Use of L-T4 + L-T3 in the Treatment of Hypothyroidism', *Eur Thyroid J*, 1: 55-71.

Wikstrom, L., C. Johansson, C. Salto, C. Barlow, A. Campos Barros, F. Baas, D. Forrest, P. Thoren, and B. Vennstrom. 1998. 'Abnormal heart rate and body temperature in mice lacking thyroid hormone receptor alpha 1', *EMBO J*, 17: 455-61.

Wilcoxon, J. S., G. J. Nadolski, J. Samarut, O. Chassande, and E. E. Redei. 2007. 'Behavioral inhibition and impaired spatial learning and memory in hypothyroid mice lacking thyroid hormone receptor alpha', *Behav Brain Res*, 177: 109-16.

Williams, G. R., A. M. Zavacki, J. W. Harney, and G. A. Brent. 1994. 'Thyroid hormone receptor binds with unique properties to response elements that contain hexamer domains in an inverted palindrome arrangement', *Endocrinology*, 134: 1888-96.

Wolff, J. 1960. 'Thyroidal iodine transport. I. Cardiac glycosides and the role of potassium', *Biochim Biophys Acta*, 38: 316-24.

Wood, W. M., J. M. Dowding, T. M. Bright, M. T. McDermott, B. R. Haugen, D. F. Gordon, and E. C. Ridgway. 1996. 'Thyroid hormone receptor beta2 promoter activity in pituitary cells is regulated by Pit-1', *The Journal of biological chemistry*, 271: 24213-20.

Wrutniak-Cabello, C., F. Casas, and G. Cabello. 2001. 'Thyroid hormone action in mitochondria', *Journal of Molecular Endocrinology*, 26: 67-77.

Wu, Y., and R. J. Koenig. 2000. 'Gene regulation by thyroid hormone', *Trends Endocrinol Metab*, 11: 207-11.

Wu, Y., Y. Z. Yang, and R. J. Koenig. 1998. 'Protein-protein interaction domains and the heterodimerization of thyroid hormone receptor variant alpha2 with retinoid X receptors', *Mol Endocrinol*, 12: 1542-50.

Xu, L., C. K. Glass, and M. G. Rosenfeld. 1999. 'Coactivator and corepressor complexes in nuclear receptor function', *Curr Opin Genet Dev*, 9: 140-7.

Yaoita, Y., Y. Shi, and D. Brown. 1990. 'Xenopus laevis alpha and beta thyroid hormone receptors', *Proc Natl Acad Sci U S A*, 87: 8684.

Ye, B., L. Li, H. Xu, Y. Chen, and F. Li. 2019. 'Opposing roles of TCF7/LEF1 and TCF7L2 in cyclin D2 and Bmp4 expression and cardiomyocyte cell cycle control during late heart development', *Lab Invest*, 99: 807-18.

Yen, P. M. 2001. 'Physiological and molecular basis of thyroid hormone action', *Physiol Rev*, 81: 1097-142.

———. 2015. 'Classical nuclear hormone receptor activity as a mediator of complex biological responses: A look at health and disease', *Best Pract Res Clin Endocrinol Metab*, 29: 517-28.

Yen, P. M., E. C. Wilcox, Y. Hayashi, S. Refetoff, and W. W. Chin. 1995. 'Studies on the repression of basal transcription (silencing) by artificial and natural human thyroid hormone receptor-beta mutants', *Endocrinology*, 136: 2845-51.

Yokoyama, N., and A. Taurog. 1988. 'Porcine thyroid peroxidase: relationship between the native enzyme and an active, highly purified tryptic fragment', *Mol Endocrinol*, 2: 838-44.

Yoneda, K., N. Takasu, S. Higa, C. Oshiro, Y. Oshiro, M. Shimabukuro, and T. Asahi. 1998. 'Direct effects of thyroid hormones on rat coronary artery: nongenomic effects of triiodothyronine and thyroxine', *Thyroid*, 8: 609-13.

Yoshida, A., S. Taniguchi, I. Hisatome, I. E. Royaux, E. D. Green, L. D. Kohn, and K. Suzuki. 2002. 'Pendrin is an iodide-specific apical porter responsible for iodide efflux from thyroid cells', *J Clin Endocrinol Metab*, 87: 3356-61.

Zhou, M. D., H. M. Sucov, R. M. Evans, and K. R. Chien. 1995. 'Retinoid-dependent pathways suppress myocardial cell hypertrophy', *Proc Natl Acad Sci U S A*, 92: 7391-5.

Zhu, X., and S. Y. Cheng. 2010. 'New insights into regulation of lipid metabolism by thyroid hormone', *Current opinion in endocrinology, diabetes, and obesity*, 17: 408-13.

List of Figures

List of Tables

Acknowledgements

First, and foremost, I would like to express my deepest gratitude to my supervisor Prof. Dr. Lars Möller. Thank you for providing me with this fascinating topic and your constant support and advice during my work. Your experience, immense enthusiasm and knowledge in the scientific field of endocrinology were a constant inspiration and motivation for me. Thank you for always taking time to discuss my projects and guiding me through my PhD time.

I would also like to express my gratitude to Prof. Dr. Dr. Dagmar Führer-Sakel for the opportunity to perform my studies in the clinic for endocrinology and all possibilities during this time.

A very special thank you goes to Sebastian for introducing me to the practical work in the endo lab, for always being there with helpful advice and proofreading many abstratcs, manuscripts and my PhD thesis. Thank you for always taking time for scientific discussions, which resulted in new ideas and approaches for my studies and were continuously encouraging.

Furthermore, I would like to take this oppurtunity thank the whole endo team. Thank you to Nina, Irina, Eva and Karina for taking this journey together, always lifting each other up and enjoying our time together, at and off work, and especially during our business travels. Thank you to Helena for the fruitful discussions and great time in the office. Thanks to Julius for supporting me in my mouse studies and lab work, Steffi for always having helpful advice around the lab and Kathrin for the assistance in the hypertrophy study.

I would like to thank our cooperation partners from the Institute for Pathophysiology. Thank you to Prof. Dr. Dr. h.c. Gerd Heusch, for the permission to perform experiments in the Pathophysiology lab and for helpful advices on this project and to Prof. Dr. Petra Kleinbongard for the scientific discussions and input. Thanks to Sandra for introducing me to one of my favorite methods and Astrid for performing blood pressure measurements and the shared time in the myograph lab.

Furthermore, I want to thank Prof. Dr. Kristina Lorenz for the cooperation in our hypertrophy study. I enjoyed and appreciate our work together and am very grateful for the support during and after our projects. Thank you for always taking time for our measurements, your scientific input

and making this cooperation such a positive part of my studies. Thanks to Conny for assistance in this project and the nice conversations we had during the echocardiography sessions.

I want to appreciate all employees at the MFZ and IG1 animal facility for always finding a solution when I needed more space, a quite room and being so helpful and supportive.

Thanks to the IMCES facility for the oppurtinuity to perform my microscopy studies.

I would also like to thank Dr. Helmut Fuchs, Dr. Valerie Gailus-Durner and Prof. Dr. Dr. h.c. Martin Hrabe de Angelis from the German Mouse Clinic for the mouse phenotyping and thereby providing basal data for this study.

I would also like to thank my best friend Johanna, thank you for always being there, visiting me wherever I've been moving and your wonderful love. Thanks to Jelli and Marion for including me into your weekly girls nights and becoming more than colleagues.

A special thank you goes to G and my magical weirdos Jude, Nessa, Muzi, Jules and Wout. Thank you for being the magic in my life. Thanks to Jude for reading this entire thing, you are an absolute gem.

Last but not least I want to express my gratitude for my family, especially my parents, for their unconditional love and support, always backing me up in my decisions and encouraging me to do what I love.

A very special thank you goes to my second half Marcel. Thank you for being at my side throughout this whole journey. Your permanent support helped me reach this goal. I aapreaciate our discussions after work and our journeys into worlds far away.

'To the people who look at the stars and wish.'

'To the stars who listen - and the dreams that are answered.'

- S.J. Maas

Publications

Hönes Georg Sebastian, Geist Daniela, Möller Lars Christian. **Noncanonical Action of Thyroid Hormone Receptors α and β**. Experimental and Clinical Endocrinology & Diabetes. *Accepted (2020).*

Geist Daniela, Hönes Georg Sebastian, Gassen Janina, Kerp Helena, Kleinbongard Petra, Heusch Gerd, Führer Dagmar, Moeller Lars Christian. **Rapid vasodilation is a physiological effect of noncanonical TRα action.** *Submitted.*

Gassen Janina, Kerp Helena, Lieder Helmut Raphael, Geist Daniela, Hönes Georg Sebastian, Heusch Gerd, Kleinbongard Petra, Möller Lars Christian, Führer Dagmar. **Lack of canonical thyroid hormone receptor alpha signalling is cardioprotective.** *In preparation.*

Geist Daniela, Hönes Georg Sebastian, Führer Dagmar, Lorenz Kristina, Moeller Lars Christian. **T_3-mediated cardiac hypertrophy is a physiological effect of noncanonical thyroid hormone receptor α action.** *In preparation.*

Geist Daniela, Hönes Georg Sebastian, Führer Dagmar, Moeller Lars Christian. **TRα is essential in heart rate and body temperature regulation during thyroid dysfunctions**. *In preparytion.*

Curriculum Vitae

"Der Lebenslauf ist in der Online-Version aus Gründen des Datenschutzes nicht enthalten."

Congress Contributions

Grants and awards

2019	Travel grant by ETA for the 42nd Annual Meeting of the European Thyroid Association in Budapest
2019	Travel grant by DGE for the 2nd International meeting of the Priority Program SPP1629 in Berlin
2019	Travel grant by DGE for the 62nd German Congress for Endocrinology in Göttingen
2019	**Von Basedow Award 2019** – Deutsche Gesellschaft für Endokrinologie (DGE)
2018	Travel grant by ETA for the 41st Annual Meeting of the European Thyroid Association in Newcastle
2018	**"Theo Visser ETA Young Investigators' Award" 2018** (basic science)
2018	Travel grant by DGE for the Thyroid Trans Act Conference in Berlin
2017	**„Best Oral Presentation"**, Annual retreat Graduate School of Biomedical Science in Bonn
2017	Travel grant by DGE for the Thyroid Trans Act Konferenz in Berlin
2016	Travel grant by DGE for the 32. Arbeitstagung Experimentelle Schilddrüsenforschung, Ratzeburg/Lübeck

Oral presentations

10/2019	Geist D., Hönes S., Führer D., Lorenz K., Moeller L. C., T_3-mediated cardiac hypertrophy is a physiological effect of noncanonical thyroid hormone receptor α action, *21st annual YARE meeting (Young Active Reserach in Endocrinology), Essen*
09/2019	Geist D., Hönes S., Führer D., Lorenz K., Moeller L. C., T_3-mediated cardiac hypertrophy is a physiological effect of noncanonical thyroid hormone receptor α action, *42nd Annual Meeting of the European Thyroid Association, Budapest, Hungary*
07/2019	Thyroid hormone receptor α action in the cardiovascular system, *Medical research centre seminar, UK Essen*

06/2019 Geist D., Hönes S., Gassen J., Kerp H., Kleinbongard P., Heusch G., Führer D., Moeller L. C., Rapid vasodilation is a physiological effect of noncanonical TRα action, *2nd International meeting of the Priority Program SPP1629 in Berlin*

03/2019 Geist D., Hönes S., Gassen J., Kerp H., Kleinbongard P., Heusch G., Führer D., Moeller L. C., Rapid vasodilation is a physiological effect of noncanonical TRα action, *62nd German Congress for Endocrinology, Göttingen*

09/2018 Geist D., Hönes S., Gassen J., Kerp H., Kleinbongard P., Heusch G., Führer D., Moeller L. C., Rapid vasodilation is a physiological effect of noncanonical TRα action, *41st Annual Meeting of the European Thyroid Association, Newcastle, United-Kingdom (Young investigator's session)*

09/2018 Geist D., Hönes S., Gassen J., Kerp H., Kleinbongard P., Heusch G., Führer D., Moeller L. C., Rapid vasodilation is a physiological effect of noncanonical TRα action, *13th International Workshop on Resistance to Thyroid Hormone, Doorn, Netherlands*

06/2018 Geist D., Hönes S., Fuchs H., Gailus-Durner V., Hrabe de Angelis M., Führer D., Moeller L. C., Phenotyping of TRα and TRβ mutant mice, *SPP1629 6th Annual meeting, Berlin*

12/2017 Geist D., Hönes S., Führer D., Moeller L. C., Noncanonical thyroid hormone action mediated by TRα, *Annual retreat Graduate School of Biomedical Science, Bonn*

06/2017 Geist D., Hönes S., Fuchs H., Gailus-Durner V., Hrabe de Angelis M., Führer D., Moeller L. C., Noncanonical thyroid hormone action mediated by thyroid hormone receptor α and β, *SPP1629 5th Annual meeting, Bremen*

12/2016 Groeben M., Hönes S., Geist D., Führer D., Moeller L. C., Investigation of molecular characteristics of TRαΔ1, *32. Arbeitstagung Experimentelle Schilddrüsenforschung, Ratzeburg/Lübeck*

12/2016 Geist D., Hönes S., Führer D., Moeller L. C., Noncanonical Thyroid Hormone action in Vascular Smooth Muscle cells, *Annual retreat Graduate School of Biomedical Science, Aachen*

Poster presentations

12/2019 Geist D., Hönes S., Führer D., Lorenz K., Moeller L. C., T_3-mediated cardiac hypertrophy is a physiological effect of noncanonical thyroid hormone receptor α action

18. Forschungstag der Medizinischen Fakultät in Essen

12/2018 Geist D., Hönes S., Gassen J., Kerp H., Kleinbongard P., Führer D., Moeller L. C., Rapid vasodilation is a physiological effect of noncanonical TRα action

17. Forschungstag der Medizinischen Fakultät in Essen

Annual retreat Graduate School of Biomedical Science in Münster

12/2016 Geist D., Hönes S., Führer D., Moeller L. C., Noncanonical Thyroid Hormone action in Vascular Smooth Muscle cells

15. Forschungstag der Medizinischen Fakultät in Essen

Eidesstattliche Erklärungen

Erklärung I:

Hiermit erkläre ich, gem. § 7 Abs. (2) d) + f) der Promotionsordnung der Fakultät für Biologie zur Erlangung des Dr. rer. nat., dass ich die vorliegende Dissertation selbständig verfasst und mich keiner anderen als der angegebenen Hilfsmittel bedient, bei der Abfassung der Dissertation nur die angegebenen Hilfsmittel benutzt und alle wörtlich oder inhaltlich übernommenen Stellen als solche gekennzeichnet habe.

Essen, den _____ _____

Daniela Geist

Erklärung II:

Hiermit erkläre ich, gem. § 7 Abs. (2) e) + g) der Promotionsordnung der Fakultät für Biologie zur Erlangung des Dr. rer. nat., dass ich keine anderen Promotionen bzw. Promotionsversuche in der Vergangenheit durchgeführt habe und dass diese Arbeit von keiner anderen Fakultät/Fachbereich abgelehnt worden ist.

Essen, den _____ _____

Daniela Geist

Erklärung III:

Hiermit erkläre ich, gem. § 6 Abs. (2) g) der Promotionsordnung der Fakultät für Biologie zur Erlangung des Dr. rer. nat., dass ich das Arbeitsgebiet, dem das Thema **„Canonical and noncanonical action of thyroid hormone receptor α in the cardiovascular system“** zuzuordnen ist, in Forschung und Lehre vertrete und den Antrag von **Daniela Geist** befürworte.

Essen, den _____ _____

Prof. Dr. Lars Möller